UNIVERSITÉ DE STRASBOURG

ÉCOLE DOCTORALE DES SCIENCES DE LA VIE ET DE LA SANTÉ

(ED 414)

Institut des Neurosciences Cellulaires et Intégratives
(CNRS UPR3212)

THÈSE

présentée par

Coralie GIANESINI

Soutenue le **26 juin 2015**

pour obtenir le grade de : **Docteur de l'Université de Strasbourg**

Discipline/ Spécialité : Sciences de la Vie / Neurosciences

Synthesis and role of melatonin in the retina of rodents

THÈSE dirigée par :

Virginie LAURENT-GYDE	MCF, Institut des Neurosciences Cellulaires et Intégratives, Strasbourg
David HICKS	DR, Institut des Neurosciences Cellulaires et Intégratives, Strasbourg
Gianluca TOSINI	PI, Morehouse School of Medicine, Atlanta, GA

RAPPORTEURS EXTERNE :

Pierre VOISIN	DR, Laboratoire Signalisation et Transport Ioniques Membranaires, Poitiers
Ralph JOCKERS	DR, Institut Cochin, Paris

RAPPORTEUR INTERNE :

Valérie SIMONNEAUX	DR, Institut des Neurosciences Cellulaires et Intégratives, Strasbourg

Savoir s'étonner à propos est le premier pas fait sur la route de la découverte.

Louis Pasteur

REMERCIEMENTS

Pour commencer, je voudrai remercier les membres du jury pour évaluer ce travail: **Dr Pierre Voisin, Dr Ralph Jockers et Dr Valérie Simonneaux**.

Merci à **Virginie et David** pour m'avoir accueilli dans leur équipe à Strasbourg pendant mon stage de M1. Notre aventure a ensuite continué pendant mon stage de M2. Je vous remercie de m'avoir fait confiance pour poursuivre en thèse, et d'avoir tout fait pour que cela se concrétise. Je remercie tout particulièrement Virginie pour sa disponibilité, son aide et son enseignement dans la réalisation des expériences ainsi que sa réacitivité dans la relecture de mes documents écrits et de la thèse. David je voudrai te remercier pour ton expertise scientifique, pour les connaissances que tu m'as apportées tout particulièrement sur l'anatomie et la physiologie de la rétine, et pour tes nombreuses relectures de l'article. Je vous exprime toute ma gratitude pour m'avoir donné l'oportunité de réaliser une partie de la thèse dans un autre laboratoire. Cette année aux Etats-Unis a été très enrichissante, une formidable expérience. Thank you **Dr Tosini** for accepting me in your lab and for your disponibility. Thank you also to make me feel well in USA: to meet me when I arrived in Atlanta, to give me advice for my new life, to help me find a car (that finally I didn't buy!)...

Thank you to all people in Atlanta who make that this aventure was so nice. **Sharon** for our scientific (and not scientific) conversations. I will see you soon in Paris! **Raiden** to make merry office! **Ward** for our morning discussion, your kindness and to help me find a new appartment! **Ken and Susumu** for your help and advice for my experiments. And **Susana**, for the Mexican/American Thanksgiving, to make me discover American vision of the "Medieval time" and other original American habits! Thank you also very much for your very precious technic help.

Bien sûr, il y a eu également le soutien des membres du 1er étage de l'INCI à Strasbourg. Merci à **Daniel Clesse** pour avoir passé du temps à tenter de détecter la mélatonine dans les rétines d'Arvicanthis. A **Christiane** pour la formation à la technique de dosage enzymatique. C'était très agréable de travailler à tes cotés. Merci à **Marie-Pierre et Paul Klosen** pour leur aide technique en immunohistochimie et hybridation. Je voudrais tout autant remercier **Marie Paule** pour ses conseils techniques en co-immunoprécipitation, ses retours intéressant sur mes présentations et pour sa gentillesse. **Patrick** pour sa bienveillance et pour m'avoir donné les connaissances de biologie animale nécessaire pour donner mes cours de TP/TD. Et aussi **Paul et Valérie**, les spécialistes de la mélatonine, toujours entousiasmés par mes résultats.

Un grand merci à toute **l'équipe des animaliers** et plus particulièrement à **Daniel** pour son travail quotidien auprès des Arvicanthis.

A tout ce beau monde il faut ajouter les étudiants de l'INCI, des personnes toutes plus enrichissante les unes que les autres, et qui ont fait de mes années de thèse des années très agréable! A commencer par **Cathy et Adrien** (Adrien je te mets dans la catégorie étudiants de l'INCI!), pour leur gentillesse, leur canapé, et pour m'avoir sensibilisé à l'écologie et à l'opéra (pour Cathy!). Ma petite **Edith**, ma compagne de thèse, qui m'a fait découvrir les meubles en cartons et avec qui j'ai beaucoup ri! A bientôt à San Francisco! **Ouafaa**, ma petite maman bienveillante, merci pour ton soutien tout au long de la thèse, pour tes conseils et pour l'aide à l'impression de mon manuscript. **Marie Audrey**, merci pour tes conseils concernant la vie américaine et les post doc! **Christina, Jo, Firuzeh, Hanan**, I wish you all the best for your projects!

Et bien sûr, il y a **les doctoneuros**! A commencer par **Antoine**, merci pour ton aide précieuse sur l'utilisation des logiciels (et oui grâce à toi je maîtrise Illustrator) et du microscope confocal, mais aussi pour tes conseils et ta compagnie. **Joseph** pour m'avoir fait découvrir le théâtre d'impro et pour m'avoir montré ce qu'était un vrai CV! **Annie** pour les contacts à Atlanta! **Popo, Alex, Leati, Vy, Florimond, JBS, Fred** pour les nombreuses soirées et tous les autres doctoneuros pour leur joie de vivre!

En dehors du labo, il y a tous les amis qui ont été là en support, en première ligne des râleries de la thèse. D'abords les copains de la fac à Nancy: **Mathieu**, le 2ème thésard de la bande, bien placé pour comprendre les hauts et les bas de la thèse! **Julie et Toto**, merci de m'avoir aidé à déménager à Strasbourg (il y a bien longtemps déjà…quand vous n'étiez pas encore en mission couches culottes !), et merci de toujours me donner votre avis quand je vous fais part de mes doutes (post-doc ou pas post-doc?). **Jess**, j'espère que nous n'en auront jamais fini de nos discussions interminables, par tous les moyens possible (téléphone, skype...). Et puis il y a les copines d'enfance : **Isa et Camille**. Des amies de longue date, c'est précieux, et je vous souhaite tout le bonheur que vous méritez. **Céline**, ton positif et tes encouragements incessants rendent toutes mes envies réalisables, et c'est très agréable! Nos discussions (à 1h du matin pour toi!) pendant mon année aux Etats Unis m'ont été d'une grande aide! Ainsi que votre visite (et oui **François** je te mets aussi!)! J'ajoute **Sophie, Mathieu, Batch et Fama**, merci pour vos messages d'encouragement et pour les agréables moments passés ensemble.

Thank you also to my roomates in Atlanta: **Dani, Paolo, Rob and Deede** who were my little familly during one year!

La fin sera réservée à ma famille, qui a toujours été présente. Pour **mes parents, mon frère, ma sœur** : merci de m'avoir épaulée pendant toutes ces années d'étude. Merci particulièrement à ma sœur et ma mère pour m'avoir soutenue pendant mes examens et mon année aux Etats-Unis, notamment pour les skype hebdomadaires qui me faisaient le plus grand bien. Pour **mes grands-parents** adorés, qui m'ont donné le goût de la curiosité, de l'effort, et qui ont joué un grand rôle dans ma scolarité (Mamy pour les maths et Papy pour le Français et la Philo). Merci pour votre écoute, votre disponibilité, et le petit "cocon" que vous m'avez toujours créé. Merci à **Jean-Marc et Doudou** pour leurs précieux conseils professionels. Et merci au reste de ma famille proche pour les bons moments passés ensemble, **Annick et Regis**, sans oublier les cousins: **Maxime, Hugo, Justine, Juliette, Valentin**. Merci aussi à ma belle-famille **CHATENDEAU** pour leur aide et leur soutien à toute épreuve. Et merci à tous ceux qui ont fait le voyage à Strasbourg pour m'encourager en ce 26 juin: **ma grand mère, Marie Claude et Fafi, Sylvie, Daniel et Colette**.

Bien évidemment le meilleur pour la fin : merci **Sully** pour m'avoir encouragé durant toutes ces années. Tout d'abords pendant les périodes d'exams à la fac, puis tout au long de la thèse. Merci de m'avoir soutenu dans mon idée d'aller aux Etats Unis et pour avoir tout fait pour que je me sente bien pendant cette année à l'étranger. Merci d'avoir sacrifié de ton sommeil pour que nous puissions nous voir tous les soirs malgré la distance et le décalage horaire. Merci également pour ta présence pendant la rédaction de la thèse, tu as rendu ce moment plus agréable, sans oublier ton aide qui a été très precieuse. Je suis heureuse d'avoir passé tous ces moments à tes côtés et je pense que cela est très prometeur pour la suite...

Merci à vous, qui peut-être lirez ce travail. Si vous lui trouvez une quelconque utilité, alors il prendra tout son sens.

RÉSUMÉ EN FRANÇAIS

Introduction

Les pathologies de l'œil conduisent à la cécité chez des centaines de millions de personnes dans le monde, représentant un enjeu colossal de société et de santé. Parmi elles, les rétinites pigmentaires qui concernent des mutations génétiques diverses provoquent la dégénérescence des photorécepteurs. L'essentiel des études concernant la rétinite pigmentaire porte sur les bâtonnets, et plus précisément sur les mutations de gènes spécifiques tels la rhodopsine ou la périphérine qui sont responsables de la malvoyance. De même, un défaut dans les récepteurs impliqués dans la phagocytose des photorécepteurs provoque la rétinite pigmentaire. En effet ces cellules se renouvellent continuellement tout au long de la vie, afin de se réparer suite aux lésions oxydatives importantes. Les rétinites pigmentaires touchent surtout une population jeune ; tandis que les personnes âgées sont très affectées par la dégénérescence maculaire liée à l'âge (DMLA), due à une inflammation chronique de la choroïde qui se répercute sur la santé de la macula. Dans tous les cas l'essentiel des informations expérimentales concernent les bâtonnets. Or ce sont les cônes qui déterminent la vision en pleine lumière, sont responsables de la discrimination des couleurs, et assurent une haute acuité visuelle chez l'homme.

Les enjeux cliniques des pathologies rétiniennes dépendent donc directement des cônes : la dégénérescence des cônes au niveau de la macula est centrale à la DMLA, et la disparition secondaire des cônes conduit au handicap visuel lors de la rétinite pigmentaire. La prévention de la perte des cônes constitue donc un objectif essentiel dans la mise en place de traitement, et la compréhension de leur physiologie est une étape incontournable.

Un facteur potentiellement important dans le fonctionnement et la santé rétinienne est la mélatonine, hormone « donneuse de temps » de l'organisme *(Pévet et al., 2006)*. En effet, cette indole-amine est également synthétisée dans la rétine, en plus de sa production principale dans la glande pinéale. Dans ce deuxième cas, la mélatonine est distribuée dans la circulation sanguine pour influencer sa physiologie générale : notamment la régulation du cycle éveil/sommeil *(Skene & Arendt, 2007)*, la reproduction *(Simonneaux, 2011)*, ou encore l'homéostasie du glucose *(Tosini et al., 2014)*.

Or la mélatonine rétinienne semble synthétisée pour agir dans ce tissu, où elle est impliquée dans différents aspects telles que l'activité électrique neuronale *(Sengupta et al., 2011)*, la phagocytose des photorécepteurs *(Besharse & Dunis, 1983)*, l'adaptation à l'obscurité *(Besharse & Dunis, 1983)*, ou la sensibilité à la lumière *(Baba et al., 2009, 2013)*. Une étude a montré que la mélatonine pourrait être impliquée dans la survie des photorécepteurs, cellules responsables de la vision, chez des souris âgées *(Baba et al., 2009)*. En effet, les récepteurs de la mélatonine, MT_1 et MT_2, couplés à des protéines G, activent différentes voies de signalisation dans la rétine. MT_1 a été détecté dans les photorécepteurs (cônes et bâtonnets), la couche nucléaire interne (INL) et la couche des cellules ganglionnaires (GCL) de la rétine de souris *(Sengupta et al., 2011)*. Une étude récente a montré que la mélatonine module la sensibilité visuelle de la rétine via l'hétérodimère MT1/MT2 présent dans les photorécepteurs et la voie de signalisation PLC/PKC *(Baba et al., 2013)*.

La mélatonine est synthétisée à partir du tryptophane grâce à l'action de quatre enzymes dont la pénultième : l'ArylAlkylamine-N-AcetylTransferase (AA-NAT) et la dernière : l'HydroxyIndol-O-MethylTransferase (HIOMT). Il est admis que la synthèse de mélatonine a lieu pendant la nuit *(Pévet et al., 2006)*. Cependant les études se sont focalisées sur l'AA-NAT, considérée comme l'enzyme responsable du rythme de synthèse de la mélatonine, et plus précisément sur l'ARNm *aa-nat*. En revanche, l'HIOMT, enzyme limitante de la synthèse de l'hormone, a été très peu étudiée.

Nous avons donc entrepris l'étude exhaustive de la synthèse de la mélatonine afin par la suite d'identifier des rôles potentiels de cette hormone dans la physiologie des photorécepteurs chez des mammifères tel que l'Homme.

But du projet

-Où et quand est produite la mélatonine dans la rétine?

-Quel est le rôle de la mélatonine dans la rétine?

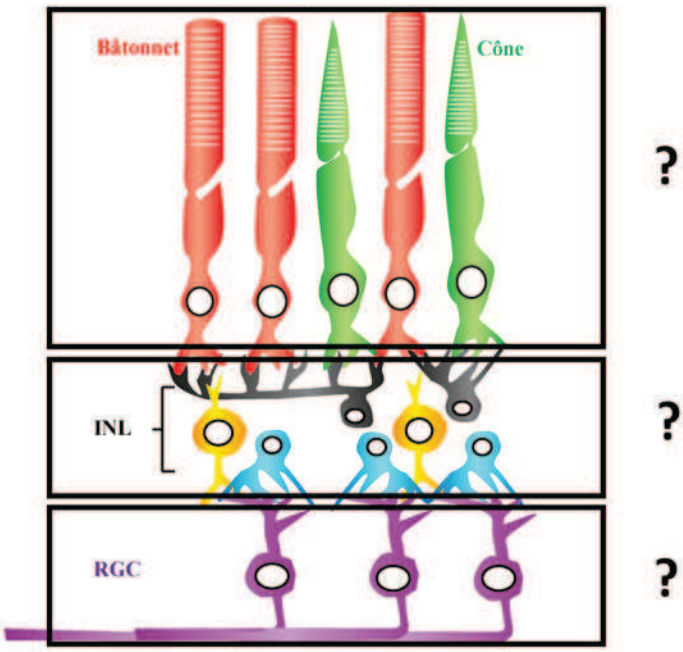

Figure 1. Quel est le lieu de production et d'action de la mélatonine dans la rétine?

Travaux réalisés

1ère partie : la voie de synthèse de la mélatonine dans la rétine

Cette étude a été réalisée chez le rongeur diurne *Arvicanthis ansorgei* qui présente l'avantage d'avoir une rétine ressemblante à la rétine centrale humaine, très riche en photorécepteurs de type cône (33 % contre 2-4 % pour les rats et souris), cellules potentiellement impliquées dans la synthèse de la mélatonine. Dans le but de caractériser le profil d'expression de la mélatonine dans la rétine, nous avons entrepris une analyse qualitative et quantitative de l'expression spatiale et temporelle des deux enzymes AA-NAT et HIOMT.

Figure 2. *Arvicanthis ansorgei* femelle adulte.

Animal élevé dans le Chronobiotron, animalerie, de l'Institut des Neurosciences Cellulaires et Intégratives Strasbourg.

Nos premiers travaux montrent que l'expression de l'ARNm *aa-nat* est observée majoritairement dans les cônes, la GCL et faiblement dans l'INL. Ces résultats montrent une nouvelle régulation de l'*aa-nat* avec une présence de l'ARNm dans les cones la nuit et dans les cellules ganglionnaires le jour.

La protéine AA-NAT a été localisée par immunohistochimie dans les photorécepteurs, ainsi que dans l'INL et la GCL. Cependant, la protéine HIOMT est faiblement exprimée dans les photorecepteurs ainsi que dans la GCL. A l'aide de doubles marquages immunohistochimiques nous avons identifié les populations cellulaires contenant de l'AA-NAT et de l'HIOMT. Les enzymes sont exprimées par les cônes, les cellules ganglionnaires et probablement les cellules amacrines déplacées (qui constituent 40 % du GCL), suggérant une production de la mélatonine dans ces types cellulaires.

Concernant l'expression et l'activité temporelle des enzymes, nos résultats obtenus par de multiples approches techniques montrent que : i) l'ARNm *aa-nat* est rythmique avec un pic en milieu de nuit dans les cônes et un pic en milieu de jour dans la GCL ; ii) la protéine AA-NAT présente une augmentation en fin de nuit, mais est exprimée pour la majorité de la période de 24 heures y compris de jour ; iii) L'AA-NAT est active durant les 24 heures avec une légère augmentation en fin de nuit mais l'enzyme est faiblement active comparé à ce qui est connu chez le primate ou le poulet ; iv) l'activité de l'HIOMT est présente mais faible tout au long des 24 heures, avec une légère augmentation en fin de jour et de nuit ; v) le dosage de la mélatonine montre une présence faible et constitutive de l'hormone avec une faible augmentation en fin de jour et de nuit, conformément au profil de l'activité des enzymes.

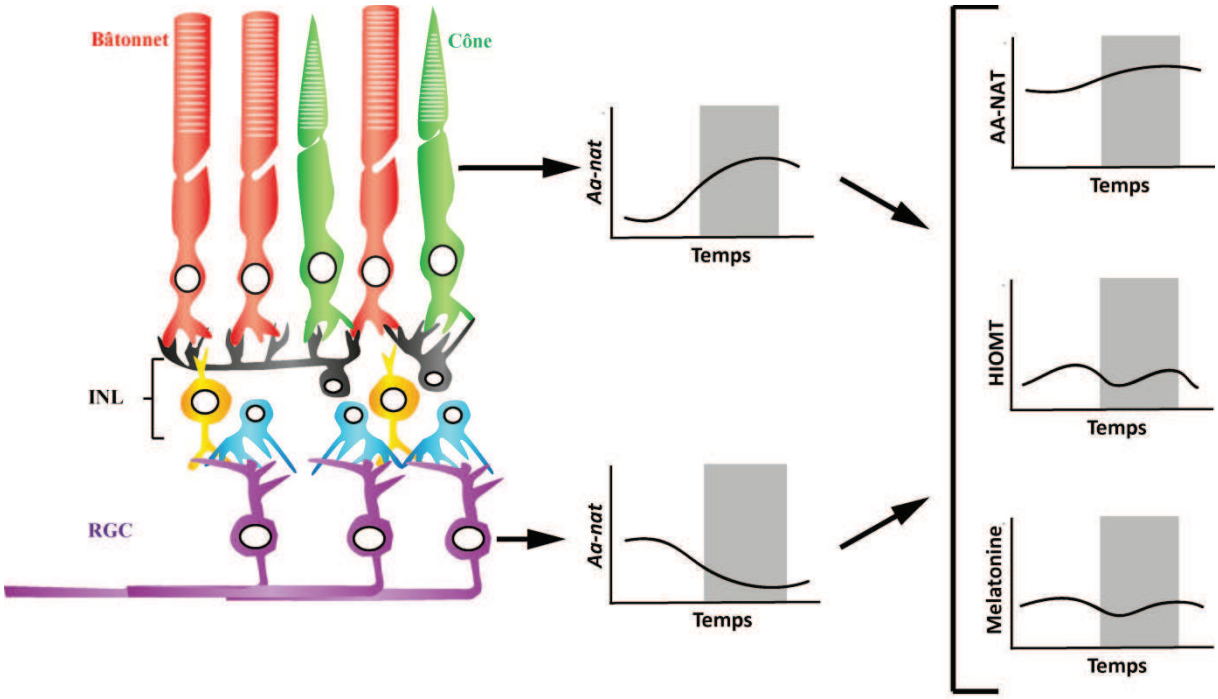

Figure 3. Modèle de synthèse de la mélatonine dans la rétine d'*Arvicanthis ansorgei*.

La mélatonine est produite dans les cônes la nuit et dans la GCL le jour. L'expression de l'AA-NAT au cours des 24 heures serait le résultat de l'intégration de l'AA-NAT des cônes la nuit et de l'AA-NAT de la GCL le jour. La même hypothèse peut être proposée pour l'HIOMT. Le niveau constitutif de mélatonine dans la rétine serait composé de l'addition de la mélatonine des cônes et de la GCL.

Nous avons localisé le récepteur MT_1 dans les bâtonnets, l'INL (probablement les cellules amacrines) et la GCL (et plus précisément dans les cellules ganglionnaires et les cellules amacrines déplacées). La présence des récepteurs nous permet de penser à un rôle de la mélatonine dans la rétine d'*Arvicanthis ansorgei* même en présence de faible quantité d'hormone.

Ces résultats suggèrent que la régulation de la synthèse de la mélatonine dans la rétine du rongeur diurne *Arvicanthis ansorgei* est remarquable à plusieurs égards : i) la protéine AA-NAT est présente tout au long de la période des 24 heures. Le système semble différent du modèle actuellement accepté pour la glande pinéale où l'AA-NAT présente un pic important de nuit. ii) La quantité élevée de protéine AA-NAT comparée à celle de l'HIOMT, suggèrent un autre rôle de l'AA-NAT que celui de production de la mélatonine. En effet, il a déjà été proposé que l'AA-NAT puisse jouer un rôle de détoxification au niveau des photorécepteurs durant le jour. iii) Nos résultats montrent une faible production de mélatonine de jour comme de nuit chez *Arvicanthis ansorgei*, ces résultats différent du profil de mélatonine obtenu chez les souris de souche C3H, montrant un pic de mélatonine durant la nuit et un niveau de l'hormone plus élevée.

La régulation de la synthèse de la mélatonine dans la rétine du rongeur diurne semble être très différente comparée au mécanisme accepté dans la glande pinéale et la rétine de rongeur nocturne.

L'ensemble de ces expériences permet d'avoir des informations concernant la localisation et l'expression des enzymes de synthèse de la mélatonine chez un modèle animal de la vision humaine. Nous avons démontré pour la première fois, la régulation fine de la synthèse de la

mélatonine chez un mammifère en montrant un maximum d'expression de l'ARNm *aa-nat* la nuit dans les cônes et un maximum durant le jour par les cellules de la GCL. Ces résultats suggèrent l'existence de deux sources de production de mélatonine avec un cycle d'expression opposé. Cette régulation est en accord avec les résultats publiés dans la rétine de poulet *(Garbarino-Pico et al., 2004; Valdez et al., 2012)*.

Nous avons ensuite voulu analyser les aspects physiologiques de l'action de la mélatonine dans la rétine, pour pondérer le potentiel de cette molécule dans le traitement des pathologies rétiniennes.

2ème partie : le rôle de la mélatonine sur la survie des photorécepteurs dans la rétine

Cette étude a été réalisée à l'aide de souris synthétisant de la mélatonine (C3H/$f^{+/+}$) et ceci en l'absence de récepteurs MT_1 et MT_2 fonctionnels (C3H/$f^{+/+}MT_2^{-/-}$ et C3H/$f^{+/+}MT_1^{-/-}$).

Figure 2. Souris C3H femelle adulte.

Animal en captivité à Morehouse School of Medicine à Atlanta.

Les résultats récents de l'équipe ont montré une diminution de la viabilité des photorécepteurs de 20% avec l'âge chez les souris C3H/$f^{+/+}MT_2^{-/-}$ et C3H/$f^{+/+}MT_1^{-/-}$ comparée aux C3H/$f^{+/+}$, suggérant un rôle de la mélatonine dans la viabilité des photorécepteurs qui passe par les récepteurs MT_1 et MT_2 *(Baba et al., 2009)*.

Nous avons montré une perte de 30% des cônes avec l'âge chez les souris C3H/$f^{+/+}MT_2^{-/-}$ et C3H/$f^{+/+}MT_1^{-/-}$ comparée aux C3H/$f^{+/+}$. Les cônes rouge/vert sont touchés mais nous ne sommes pas parvenus à montrer une atteinte des cônes bleus. La rétine de souris étant composée de 2 à 4% de cônes, nous pouvons donc dire que les 2 types de photorécepteurs, les bâtonnets et les cônes, sont affectés avec l'âge chez les souris mutées pour les récepteurs à la mélatonine.

Notre travail a ensuite consisté à comprendre par quel mécanisme la mélatonine contrôle la viabilité des photorécepteurs avec l'âge. Nous avons émis l'hypothèse que la voie de survie cellulaire, impliquant la protéine AKT (serine/thréonine kinase) et le facteur de transcription FOXO1, serait impliquée. En effet, les protéines AKT et FOXO1 sont connus pour jouer un rôle majeur dans la survie cellulaire *(Brunet et al., 1999)*; AKT et FOXO1 ont été localisés dans les photorécepteurs *(Reiter et al., 2003; Jomary et al., 2006; Li et al., 2007)*; la forme phosphorylée d'AKT présente un pic d'expression la nuit dans la rétine de poulet *(Ko et al., 2009)*; finalement, une étude a démontré que la mélatonine active AKT dans les cellules de Muller *(Jiang et al., 2012)*.

Nos résultats montrent que l'activation de la voie de survie cellulaire (AKT et FOXO1) n'est plus rythmique chez les souris C3H/$f^{+/+}MT_2^{-/-}$ et C3H/$f^{+/+}MT_1^{-/-}$ comparée aux souris C3H/$f^{+/+}$. Nous

proposons donc qu'une dérégulation du rythme d'activation de la voie de survie cellulaire pourrait conduire à une augmentation de la mort des photorécepteurs avec l'âge.

Afin de savoir si la voie de survie cellulaire est activée dans les photorécepteurs, et plus précisément dans les cônes et/ou les bâtonnets, nous avons réalisé des marquages immunohistochimiques contre AKT et FOXO1. Les deux protéines ont été localisées dans les cônes et les bâtonnets.

Ces résultats indiquent que la voie de survie cellulaire (AKT-FOXO1) pourrait être impliquée dans le mécanisme par lequel la mélatonine protège les photorécepteurs avec l'âge. Nos résultats étant similaires pour les souris C3H/$f^{+/+}MT_2^{-/-}$ et C3H/$f^{+/+}MT_1^{-/-}$, nous pouvons émettre l'hypothèse que ce phénomène implique l'hétérodimère MT_1/MT_2, connu pour être localisé et fonctionnel dans les photorécepteurs.

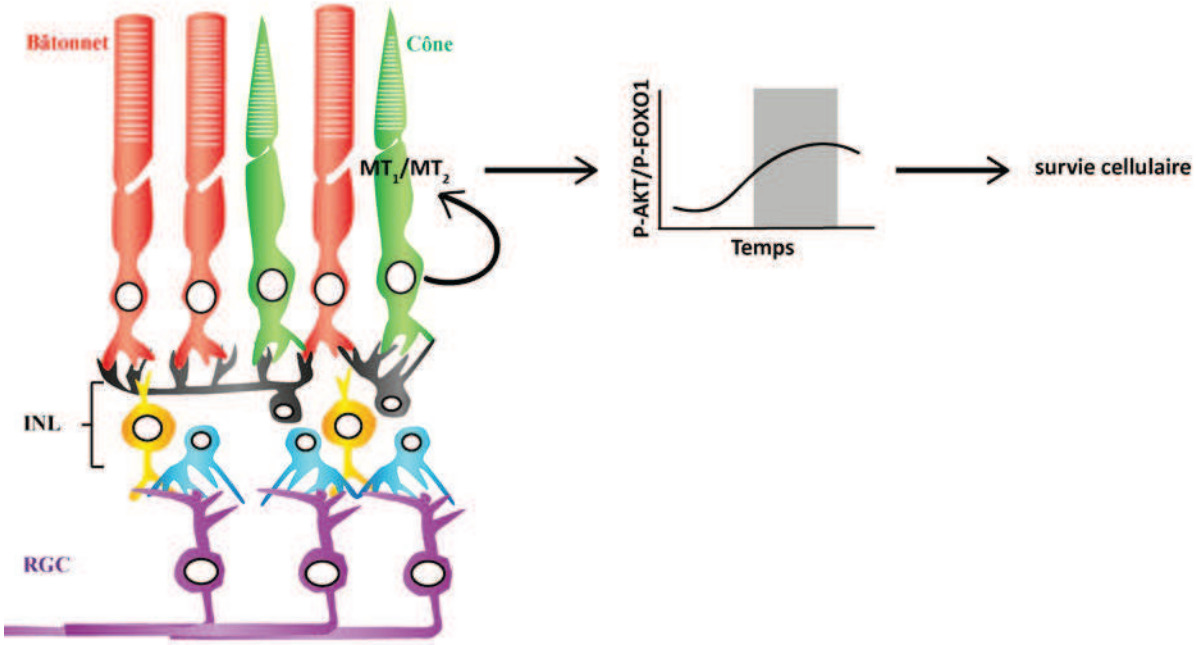

Figure 5. Modèle d'action de la mélatonine dans la rétine des souris C3H

Nous proposons que la mélatonine produite dans les cônes puisse agir comme un messager autocrine en activant ces récepteurs MT1 et MT_2 localisés dans les mêmes cellules. La mélatonine peut moduler l'activation rythmique de la voie de signalisation AKT/FOXO1 et stimuler la survie des cônes avec l'âge.

Ces résultats sont en accord avec une étude publiée en 2009, où les auteurs montrent que la voie de survie cellulaire (PI3/AKT) contribue à la modulation circadienne de l'ouverture des canaux calcium voltage dépendents *(Ko et al., 2009)*. Cette étude combinée avec notre travail suggère que la voie de survie cellulaire est une sortie de l'horloge circadienne dans les photorécepteurs, en aval de la mélatonine. Nous proposons que la rythmicité dans les cônes est importante pour maintenir une bonne physiologie de ces cellules.

Conclusion

L'ensemble de ces études a permis de mettre en évidence une nouvelle régulation de la synthèse de la mélatonine dans la rétine d'un mammifère diurne, de connaitre les sites d'action de l'hormone et de proposer un rôle de la mélatonine dans la survie de la rétine.

Notre travail montre l'importance d'étudier la rétine en considérant les différentes couches de façon indépendante et de ne plus considérer la rétine comme un tissu homogène. Notre travail est cohérent avec l'existence de plusieurs horloges dans la rétine comme l'a décrit récemment notre équipe *(Jaeger et al., 2015)*. Les deux sources de mélatonine avec une régulation en cycle opposé pourraient être contrôlée par une horloge circadienne pour synchroniser différents phénomènes dans la rétine et optimiser la physiologie du tissu.

Chez une espèce de rongeur diurne, l'AA-NAT semble avoir un autre rôle que celui de production de la mélatonine, notamment un rôle de détoxification des cônes, cellules exposées à de forts stress oxydatifs durant la période de lumière.

La présence de mélatonine en faible quantité mais de façon constante pourrait être adaptée au besoin physiologique d'*Arvicanthis ansorgei*. Il nous faudra identifier les rôles de l'hormone chez cette espèce.

Ce travail montre également l'importance d'étudier la mélatonine chez une espèce riche en cônes. En effet, la mélatonine semble contribuer au maintien d'une bonne physiologie des cônes avec l'âge. Dans la rétine humaine, les cônes sont les cellules responsables de la haute acuité visuelle et de la discrimination des couleurs. Dans de nombreuses maladies rétiniennes, la perte de vision est le résultat de la dégénérescence des cônes et une étude a montré que la mélatonine ralentit la progression de la DMLA *(Yi et al., 2005)*.

Chez la souris, rongeur nocturne, la mélatonine est rythmique et présente en plus forte quantité. Dans la rétine de cet animal, nous avons montré que la mélatonine protège les photorécepteurs de la dégénérescence avec l'âge. Ces résultats montent que la mélatonine par l'intermédiaire de ses récepteurs permet de maintenir une bonne physiologie rétinienne au cours du temps.

COMMUNICATIONS AND PUBLICATIONS

This work was financially supported by the Association Berthe Fouassier (Fondation de France), Société Francophone du Diabète, Retina France and the grant EY022216.

Posters

Tosini G, Gianesini C, Hiragaki S, Laurent V, Hicks D. Cones viability is affected by removal of melatonin signaling. ARVO Annual meeting - May 2015 - Denver - Colorado - USA.

Gianesini C, Hicks D, Laurent V. Novel regulation of the melatonin pathway in the retina of the diurnal rodent *Arvicanthis ansorgei*. Gordon Conference: Pineal Melatonin: Comparative Approaches to Human Health and Disease - January 2014 - Galveston - Texas - USA.

Publications

Gianesini C, Clesse D, Tosini G, Hicks D, Laurent V. Unique regulation of the melatonin synthetic pathway in the retina of diurnal female *Arvicanthis ansorgei* (Rodentia). *Endocrynology.* ***In press***.

Gianesini C, Hiragaki S, Contreras-Alcantara S, Laurent V, Hicks D, Tosini G. Cones viability is affected by removal of melatonin signaling. ***In preparation***.

TABLE OF CONTENT

TABLE OF ILLUSTRATIONS

Article I

Article II

ABBREVIATIONS

4P-PDOT: cis-4-phenyl-2-propionamidotetralin
IIK7: N-butanoyl 2-[9-methoxy-*6H*-isoindolo [2.1-*a*]indol-11-yl]ethanamine

-A-

aa: amino-acid
AA-NAT: arylalkylamine N-acetyltransferase
AAAD: acide L-amino aromatic decarboxylase
AC: adenylyl cyclase
AcCoA: acetylcoenzymeA
Adc1: adenylyl cylclase 1 gene
AFMK: N-acetyl-N-formyl-5-methoxykynuramine
AKT: serine/threonine protein kinase
AMK: N-acetyl-5-methoxykynuramine
AMD: age macular degeneration
ANOVA: analysis of variance
AP1: activating protein 1
APS: ammonium persulfate
Arvicanthis: *arvicanthis ansorgei*
ATP: adenosine triphosphate

-B-

BCIP: 5-bromo-4-chloro-3'-indolyphosphate p-toluidine
BET: ethidium bromide
BMAL1: brain and muscle ARNt-like protein
bp: base pairs
BSA: bovine serum albumine

-C-

CAM: calmoduline protein
cAMP: adenosine monophosphate cyclique
CCB: cone cell body
CCG: clock controlled gene
cGMP: cyclic guanosine 3', 5'-monophosphate
CCB: cone cell body
CIS: cone inner segment
CLOCK: circadian locomotor output cycles kaput
COS: cone outer segment
CRE(M): cAMP responsive element (modulator)
(P)-CREB: (phosphorylated)-cAMP regulatory element-binding protein
CRY: cryptochrome
CRX: cone-rod homeobox protein
CsnK: caseine kinase
CT: circadian time

-D-

(k)Da: (kilo) dalton
DAB: 3, 3-diaminobenzidine
DAG: diacylglycerol
DAPI: 4',6'-diamidino-2-phénylindole
DBP: D element-binding protein
DD: dark/dark
DEPC: diethylpyrocarbonate
DMPC: dimethylpyrocarbonate
(c)DNA: (complementary) deoxyribonucleic acid
dNTP: deoxynucleotide
DOPAC: 3,4-dihydroxyphenylacetic acid
DTT: dithiothreitol

-E-

E4BP4: E4 promoter binding protein 4
EDTA: ethylenediaminetetraacetic acid
ELISA: enzyme-linked immunosorbent assay
ERG: electroretinogram
ERK: extracellular signal-regulated kinase

-F-

FasL: Fas liguand
FOXO: forkhead-related family of mammalian transcription factor

-G-

$G_{(s)}$: (stimulatory) G protein
$G_{(i)}$: (inhibitory) G protein
GABA: acide γ-aminobutyrique
GC(L): ganglion cell (layer)
GDP: guanosine diphosphate
GPCR: G protein coupled receptors
GTP: guanosine triphosphate

-H-

HIOMT: hydroxyindole-*O*-methyltransferase
HPLC: high-performance liquid chromatography
HRP: horseradish peroxidase

-I-

ICER: inducible cAMP early repressor
IEG: immediate early gene
IML: intermediolateral cells of the spinal cord
INL: inner nuclear layer

IOP: intraocular pressure
IP3: inositol triphosphate
IPL: inner plexiform layer
IS: inner segment
ISH: *in situ* hybridization

-K-

kb: kilobase
KO: knock out

-L-

LD: light/dark
LL: light/light
LW: long wavenlength

-M-

MOPS: 3-(N-morpholino) propanesulfonic acid
mRNA: messenger ribonucleic acid
MT_1: melatonin receptor 1
MT_2: melatonin receptor 2
MT_3: melatonin receptor 3
MUPP1: multi-PDZ domain protein 1

-N-

NA: noradrenergic
NAS: N-acetylserotonin
NBT: nitro-blue tetrazolium chloride
nd: not determined

-O-

OD: optical density
ONL: outer nuclear layer
OPL: outer plexiform layer
OS: outer segment

-P-

(Un)P: (un)phosphorylated
PAF: paraformaldehyde
PACAP: pituitary adenylate cyclase activating paptide
PB(S): phosphate buffer (saline)
(RT)PCR: reverse transcriptase polymerase chain reaction
PDE: phosphodiesterase
PDK1: phosphoinositide-dependent kinase-1
PER: period
PI3K: phosphatidylinositol 3 kinase
PIP2/3: phosphoinositide-phosphates 2/3
PIRE: pineal regulatory element
PKA/C: protein kinase A/C
PLC: phospholipase C
PNA: peanut agglutinine
PNPP: p-nitrophenyl phosphate
PR: photoreceptor
PT: pars tuberalis
PVDF: polyvinylidene fluoride
PVN: paraventricular nucleus

-R-

RCB: rod cell body
REV-ERB: reverse viral erythroblastis oncogene product
(ip)RGC: (intrinsically photosensitive) retinal ganglion cells
RGS20: regulator of G protein signaling 20
(m)RNA: (messenger) ribonucleic acid
RORγ: retinoic acid receptor-related orphan nuclear receptor γ
ROS: rod outer segment
RPE: retinal pigmentary epithelium
RRE: ROR/REV-ERB response element

-S-

SAM: S-adenosyl-L-methionine
SCG: superior cervical ganglia
SCN: suprachiasmatic nuclei
SDS: sodium dodecyl sulphate
SEM: standard error of the mean
Ser: serine
sGC: soluble guanylyl cyclase
SSC: standard sodium citrate
SW: short wavelength

-T-

TBI: tris buffer imidazole
TBS: tris Buffer Saline
TEMED: tétra-methyl-éthylènediamine
Thr: threonine
Tm: melting temperature

-U-

U: unit
up: ultra pure

-V-

V: volt

-W-

WT: wild type

-Z-

ZT: zeitgeber time

INTRODUCTION

I. THE RETINA

I.A. The structure of the retina

In Vertebrates, the eye is the entry for light into the body and allows organisms to collect information such as color, form, distance to enable them to interact with their environment. The retina, a neurosensorial tissue, lining the posterior wall of the eye, is the most crucial ocular structure and gets direct stimulation from the outside world **(Figure 1)**.

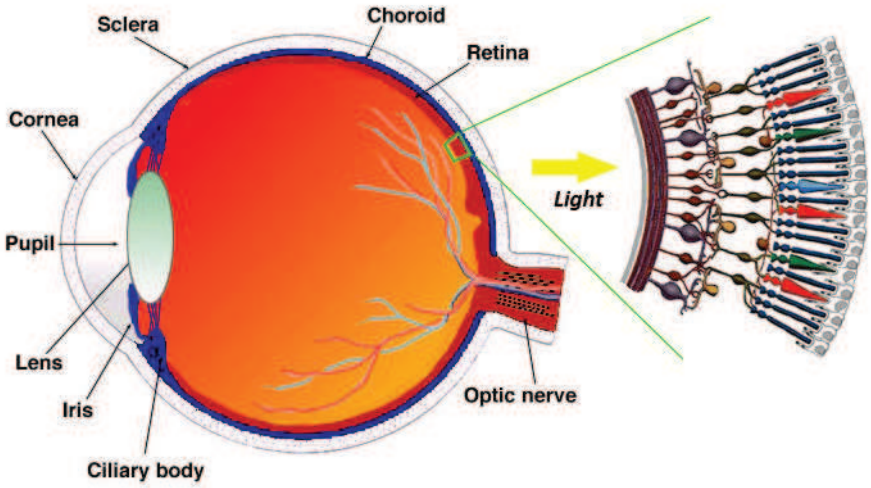

Figure 1. Drawing of a transversal section of human eye.

Light rays enter the eye through the cornea and are refracted twice with help of the lens to finally be focused on the retina. *From (Kolb, 2005)*.

The retina is a thin tissue (500 µm in human and 200 µm in mice) irrigated by two vascular systems. First, the choroid circulation, localized in the choroid, "feed" the outer retina. Second, the vessels from the retina bloodstream irrigate the internal retina.

As first described by Santiago Ramón y Cajal, the retina is composed of **three layers of cell bodies and two layers of synapses (Figure 2)**.

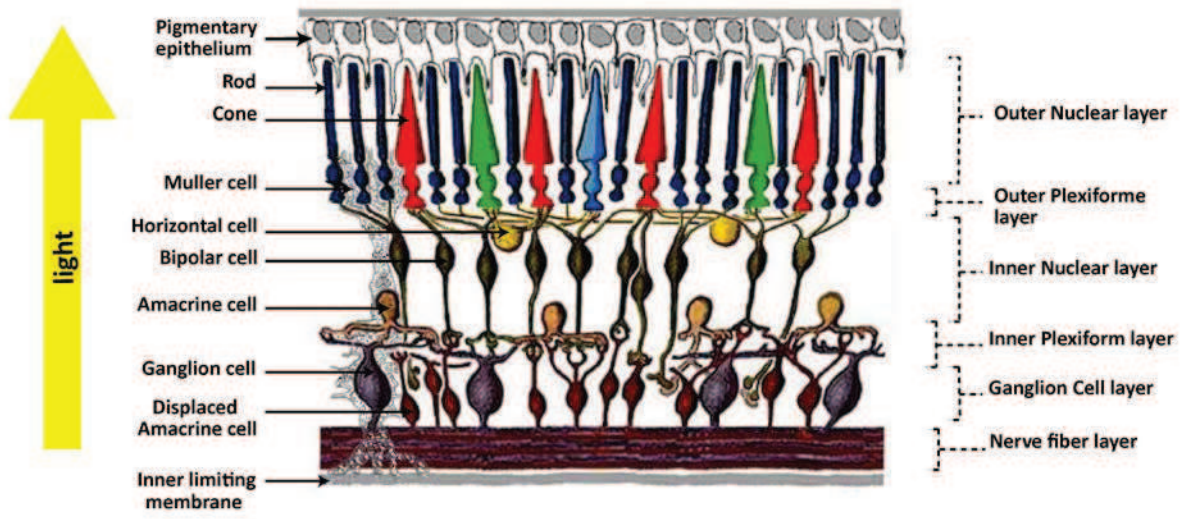

Figure 2. Diagram of the retina organization.

Names of the different cell-types are presented on the left and those of the layers on the right. *From (Kolb, 2005).*

I.A.1. The layers

I.A.1.1. The outer retina

The most external layer of the retina is the **photoreceptors layer** containing two types of **photoreceptors (PR)**: the **cones** and the **rods**. Both cells are photosensitive and have visual function. The photoreceptor layer is constituted of *(Kolb, 2005)*:

- **The outer segment of photoreceptors (OS)** filled with stacks of membranes containing the visual pigments and involved in the phototransduction process

- **The inner segment of photoreceptors (IS)** is attached to the OS by a cilia connector. IS contains the apparatus necessary for protein synthesis and ATP formation (mitochondria, Golgi apparatus, ribosomes).

- **The outer nuclear layer (ONL)** contains the nucleus and the axon extending to a synaptic terminal where neurotransmission to bipolar and horizontal cells occurs **(Figure 2)**.

The most external plexiform layer is the **outer plexiform layer (OPL)** containing the synapses of PR. In this layer the transmission of photic information from photoreceptors to bipolar cells takes place as well as a modulation of its transmission by horizontals cells *(la Cour & Ehinger, 2005)* **(Figure 2)**.

I.A.1.2. The inner retina

The most inner nuclear layer is the **ganglion cells layer (GCL)** containing the nuclei of the ganglion cells and those of displaced amacrine cells (60 % of the layer in mice retina, *(Jeon et al., 1998)*) **(Figure 2)**. The **ganglion cells (RGC)** transfer light information from the retina to the central brain. The long axons of the RGC are in the internal part of the GCL and merge together to become the optic nerve after crossing the retina at the optic papilla *(Kolb, 2005)* **(Figure 1, Figure 2)**. One-three % of the RGC represent the **intrinsically photosensitive retinal ganglion cells (ipRGC)** which contain the

photopigment melanopsin. These cells have photoadaptative functions other than image visual function. They integrate and distribute non visual information from all retinal photopigments (ie. cone, rod and ipRGC photopigments) to the brain. They project to the **suprachiasmatic nuclei (SCN)** and the intergeniculate leaflet to entrain the circadian clock **(see II.B to have information about the circadian clock)**. These cells also project to the olivary pretectal nucleus to start the pupillary light reflex and to the posterior thalamic nucleus to influence nociception *(Do & Yau, 2010)*.

The **inner plexiform layer (IPL)** is localized between the INL and the GCL and contains the synapses of the bipolar, amacrine and ganglion cells **(Figure 2)**. Information from bipolar cells are modulated by amacrine cells and transferred to the ganglion cells *(la Cour & Ehinger, 2005)*.

The **inner nuclear layer (INL)** contains the cell bodies of the **bipolar, horizontal and amacrine cells**. Bipolar cells relay information between PR and RGC. Horizontal and amacrine cells are respectively localized in the external and internal part of the INL. They combine and modify the PR synaptic signal prior to final transmission to RGC. These changes allow adjustment of sensitivity for bright and dim light vision. They also permit shaping of visual responses by processes such as lateral inhibition which increase contrast and sharpness of the image. INL also contains the nuclei of **Muller cells**, the main glial cells of the retina, from which axons span the entire retina *(Kolb, 2005)* **(Figure 2)**.

I.A.2. The cells: focus on cones and rods

Both PRs of the outer retina detect photons. However, they can be distinguished by their structure, physiology and respective roles.

I.A.2.1. Rod versus cone structures

First, whereas rods OS (ROS) are slim cylindrical structures, cones OS (COS) are shorter and more conical with a wider base and tapering shape **(Figure 3)**. Second, ROS are filled entirely with closed discs of double membranes enveloped by a separate plasma membrane, whereas COS are composed of successive folds in a single plasma membrane, and thus are open to the extracellular space on one face **(Figure 3)**. Third, rods synapses are known as spherules (small round enlargement of the axon) and are different from those of cones called pedicles (large, conical and flat) **(Figure 3)**.

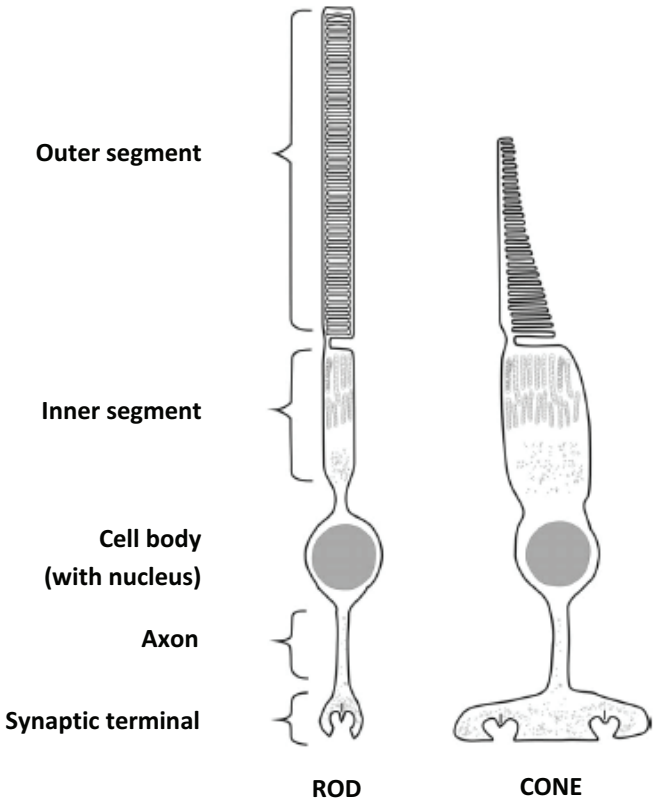

Figure 3. Schematic representation of rod and cone.

Both types of PR contain an outer segment, an inner segment, a cell body, an axon and a synaptic terminal From *(la Cour & Ehinger, 2005)*.

I.A.2.2. Rod versus cone distributions

Cones cell bodies (CCB) lie along the scleral border of the ONL with rods cells bodies (RCB) making up the remainder of the ONL between and below the cone cell bodies.

Rods and cones also have different lateral distributions depending on the species considered. In the human retina, rods are distributed all over the retina except for a small spot totally devoid of rods where 100 % of the PRs are cones: the foveola. In a radius of 1 mm around the foveola, the fovea contains 50 % of cones, while over the entire retina cones average 5 % of total PRs *(Curcio et al., 1991)*. In rats and mice, cones represent 2-3 % of PRs *(Szél & Rohlich, 1992; Jeon et al., 1998)* and are distributed over the entire retina.

I.A.2.3. Rod versus cone pigments

Rods contain a unique photopigment in OS called rhodopsin. Rhodopsin is sensitive to one wavelength range only, with peak intensity around 500 nm. Cones contain photopigments named opsins and can further be subdivided depending on the structure of these opsins. Three classes of mammalian cone opsins are named by acronyms roughly reflecting their spectral sensitivity maxima: the blue cones or short wavelength light (SW cones) (437 nm); the green cones or medium wavelength light (MW cones) (533 nm); the red cones or long wavelength light (LW cones) (564 nm) **(Figure 4)**.

Most non primate mammals are dichromates, containing rods, MW and SW sensitive cones in their retina. There is a large literature on asymmetrical cone opsin expression in mammals *(Peichl, 2005)*. In mice, an opposing dorso-ventral gradient of MW sensitive cone opsin (more abundant in dorsal

retina) and SW sensitive cone opsin (more abundant in ventral retina) has been reported *(Szel et al., 1992)*. It was subsequently described that both opsins can be found in the same cone in different proportions and regions of the retina *(Röhlich et al., 1994; Lukáts et al., 2005)*. Human and platyrrhine (New World) monkeys possess all three types of cone opsins *(Nathans et al., 1986; Jacobs, 1998)*.

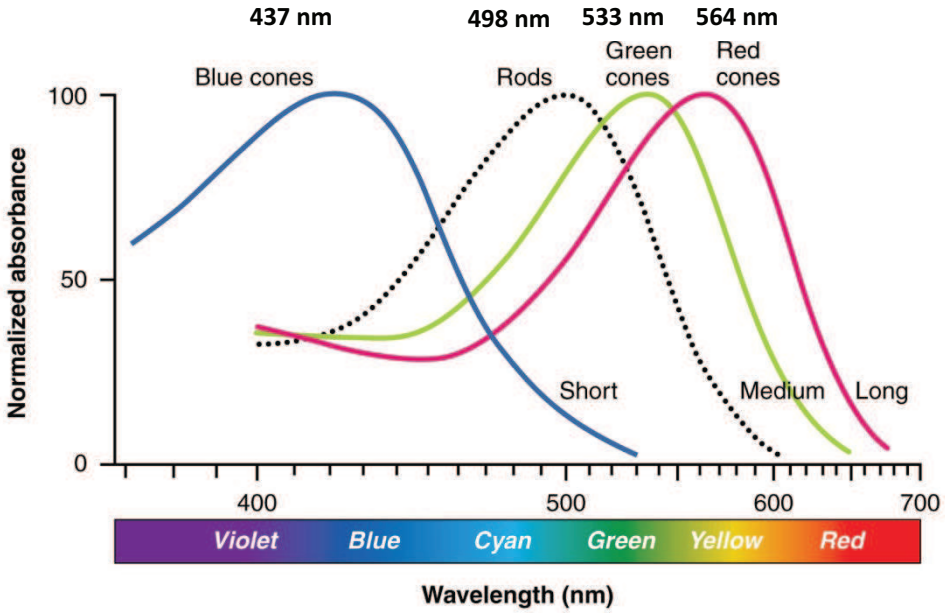

Figure 4. Absorption spectra of visual pigments in humans.

Rhodopsin, the visual pigment of rods has a maximum sensitivity around 498 nm. SW opsin, the visual pigment of blue cones has a maximum absorption peak around 437 nm, MW for green cones has a peak at 533 nm and LW opsin for red cones has a maximum at 564 nm. *From Openstax college, Human Anatomy and Physiology. Web site: http://cnx.org/content/col11496/1.6/.*

I.A.2.4. Rod versus cone connections

Rod and cone pathways are strictly separated: rods connect to rod bipolar cells and cones to cones bipolar cells. Cone bipolar cells form synapses with RGC whereas rod bipolar cells do not directly contact RGC but feed into cone bipolar cells via a population of amacrine cells. The wiring connection systems of rods and cones with RGC are different in the peripheral and central retina. Indeed, in the periphery, there is high convergence of the rods onto their postsynaptic neurons: one RGC carries information of a large number of photoreceptors **(Figure 5, left panel)**. At the opposite, in the cone rich fovea, a low convergence of cone is found: one cone cell is connected to one bipolar cell itself contacting one RGC **(Figure 5, right panel)**.

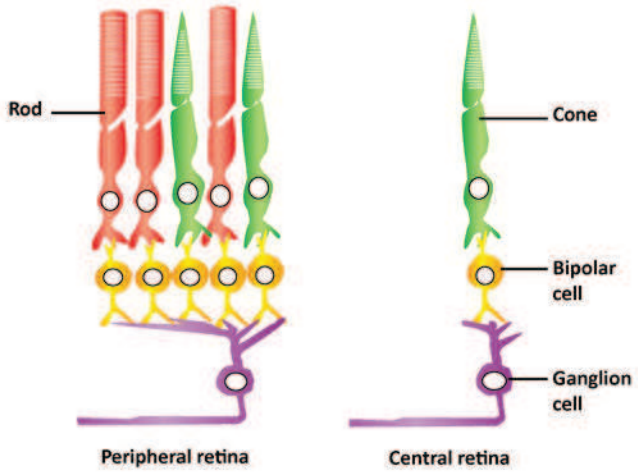

Figure 5. Connectivity of rod and cone in the peripheral and the central retina of human respectively.

I.A.2.5. Rod versus cone roles

Rods are very sensitive to light (they can be activated by one photon) *(Cicerone, 1976; Rodieck & Rushton, 1976)* and are responsible for the scotopic vision (in low light intensity) *(Sugita & Tasaki, 1988)*. Rods allow a grey nuance vision and they are sensible to contrast and movement perception. Therefore cones are the ones responsible for high visual acuity. They are less sensitive to light and are responsible for color discrimination in photopic condition (high level of light) *(Sugita & Tasaki, 1988)*.

I.B. The retinal pigmentary epithelium

The distal part of the OS is in close proximity with the retinal pigmentary epithelium (RPE) composed by one layer of epithelial cells.

First, for an optimal visual cycle, rods and cones need the RPE to recycle the trans-retinal produced after photon absorption. Indeed the RPE expresses the enzyme necessary for 11-cis retinal recycling which is sent back to the OS *(la Cour & Ehinger, 2005)*.

The highly pigmented cells of the RPE can absorb photons that OS didn't capture and thereby prevent photons accumulation in OS and avoid phototoxicity *(Strauss, 2005)*.

The RPE is also part of the blood-retinal barrier and allow the transfer of water, ions, metabolites (Vitamin A) between blood vessel of the choroid and the under retinal space (extracellular space between the membrane of OS and the RPE) *(Strauss, 2005)*.

Finally, one of the RPE major functions is the phagocytosis of PRs. Indeed PRs continually produce new membranous discs. Meanwhile discs from the distal extremity of the OS are phagocytized by RPE. The recycling of photoreceptors' disks by RPE is necessary to avoid oxidative stress in OS caused by light. A dysfunction in photoreceptors phagocytosis leads to their degeneration *(Strauss, 2005)*.

I.C. Visual function of the retina

Light coming in the internal retina crosses directly the tissue to be treated by OS of photoreceptors and to a lesser extent by ipRGC. Besides, Muller cells are important in this process because they drive

light information avoiding diffusion phenomena, reflection, refraction which could lead to a loss or distortion of light information *(Franze et al., 2007)*.

The phototransduction occurs in the OS which contains the visual pigments. These molecules are composed of opsin or rhodopsin (G protein coupled receptor) bound to a chromophore derived from vitamin A and known as the retinal. The **Figure 6** illustrates phototransduction in rods. The phenomenon begins by the absorption of a photon by retinal which changes its conformation from the 11-cis form to all-trans retinal. This change triggers conformational changes in the rhodopsin resulting in the activation of the G protein transducine located in the cytosol. This leads to bound guanosine diphosphate (GDP) exchange into guanosine triphosphate (GTP) and dissociation of the transducine α subunit. The α-subunit-GTP complex activates phosphodiesterase (PDE) that hydrolyses cyclic guanosine monophosphate (cGMP) to 5'-GMP, lowers the concentration of intracellular cGMP which in turn leads to closure of the sodium channels within the plasma membrane. Closure of the sodium channels causes hyperpolarization of the cell due to the ongoing potassium current.

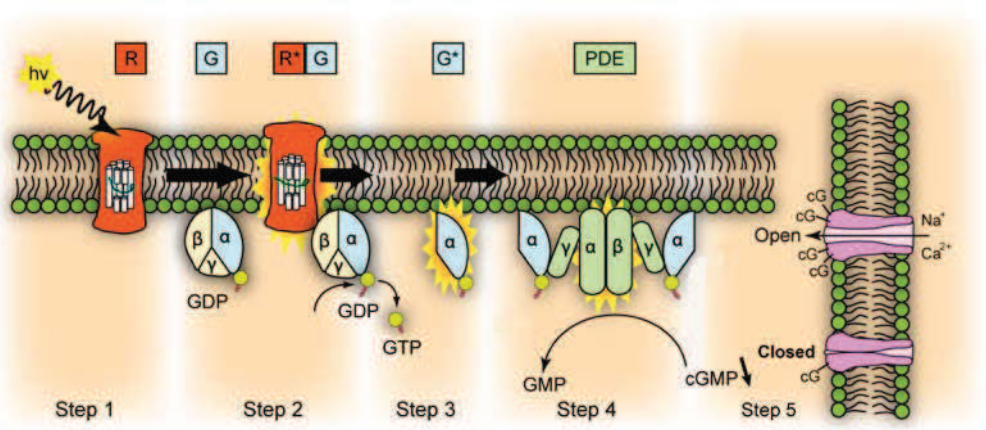

Figure 6. Schematic representation of the activation of vertebrate rod phototransduction.

Step 1: a photon (hv) is absorbed by the retinal bound to the rhodospin (R). **Step 2:** the activated rhodopsin (R*) binds the G protein heterotrimere (G). **Step 3:** activated G protein (G*) catalyzes the exchange of GDP for GTP, which produces the active Gα*-GTP. **Step 4:** Two Gα*-GTP bind to PDE γ subunits, thereby releasing the inhibition on the catalytic α and β subunits. This leads to activated PDE, which in turn catalyzes the hydrolysis of cGMP. **Step 5:** The subsequent decrease of the free cytoplasmic cGMP concentration leads to the closure of the cGMP-gated channels on the plasma membrane which blocks the influx of cations into the OS, and results in hyperpolarization of the cell. *From (Fu, 2010)*.

The reaction is stopped by phosphorylation of the visual pigment followed by its binding to arrestin. This eventually leads to the trans-retinal transformation into the 11-cis-retinal.

Hyperpolarization of the photoreceptor results in a decrease of the glutamate neurotransmitter release in the OPL. The effect of glutamate is to close a glutamate-activated Na^+ channel at the synaptic contact between PRs and bipolar cells. Therefore, during a light stimulus, lowered release of glutamate reduces the number of closed glutamate activated Na^+ channels, leading to bipolar cells depolarization. This increases the level of transmitter release onto the RGC which depolarize and produce an action potential relayed to the cortical visual processing area via the optic nerve.

Additionally to this pathway of light signal transduction (PR-bipolar cell-RGC), photoreceptor signal is modulated by horizontal and amacrine cells prior to final transmission to RGC.

In addition to its visual function, retina is also involved in non visual function, including different neuronal pathway. The major retinal non visual function is the photo-entrainment of biological event as described below.

II. THE CLOCK

II.A. Introduction to the Chronobiology

II.A.1. Definition

A number of biological functions display daily and seasonal variations in a way to anticipate and adapt to the upcoming cyclic changes in environmental conditions like light, temperature, food availability.

Indeed, every day we experience rhythms of our physiological functions and behaviors, which follow the 24 hours light-dark cycle due to the rotation of Earth around its axis. A biological rhythm can be defined as a periodically repeated sequence of biological functions, described by parameters like period (duration of one sequence) and amplitude **(Figure 7)**. For instance, we are active during the day, while we sleep during the night. Our body temperature drops every night and most of our hormones are secreted at particular times of the nycthemeron (period of 24 consecutive hours), for instance melatonin is released from the pineal gland during the night.

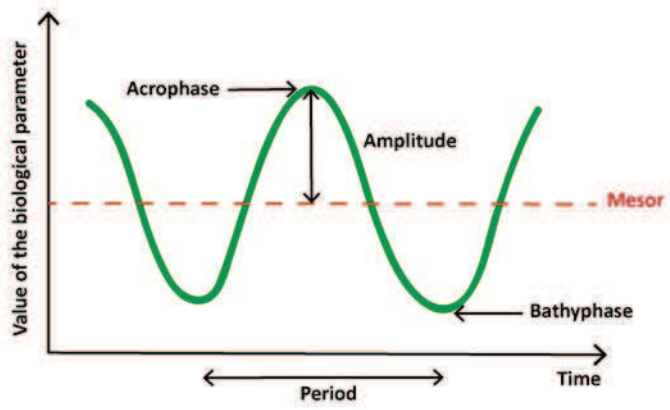

Figure 7. Parameters used to describe a biological rhythm.

The period is the time elapsed for one complete oscillation or cycle. Mesor (midline-estimating statistic of rhythm) is the average value around which the variable oscillates. Acrophase and batiphase are the time at which the peak and the trough of a rhythm occur respectively. Amplitude is the difference between the peak (or trough) and the mesor of a rhythm.

For many years it was believed that the daily rhythms observed in behavior or physiological functions were imposed by rhythms in the physical environment to which organisms responded passively. It was the demonstration that plants and animals are not passive responders but rather that they have accurate endogenous time-measuring systems or biological clock that generated new interest in the study of biological rhythms.

The chronobiology focuses on biological rhythm tightly coupled to some external environmental cycle and especially rhythms with periods close to those of the astronomical day **(circadian)**, or the alternation of seasons (circannual).

II.A.2. Properties of a circadian clock

- A clock distributes an **output**, assessed as a biological rhythm. This rhythm reflects the oscillation of the controlling entity.

- A regular oscillation is the fundamental requirement for any clock. Since circadian rhythms persist in constant environmental conditions, oscillations must be **self-sustained**. In absence of external cues, the endogenous period of a circadian clock is around, but never exactly 24 hours. The circadian rhythm occurring without any environmental cue is called "free-run".

- To adjust its endogenous period to the light/dark cycle, a clock must be able to synchronize to environmental cues. In other words, clock must possess a **setting mechanism** linking the internal oscillations to the apparent astronomical oscillations of the sun. The synchronizing agents capable of resetting the clock are called Zeitgebers, from german "Zeit" and "geber", meaning "time" and "giver", respectively *(Aschoff, 1954)*. In **Figure 8**, the **light/dark (LD)** cycle (12 hours light/12 hours dark) is a Zeitgeber entraining the clock.

Note: by convention, under regular LD cycle, Zeitgeber 0 (ZT0) refers to the light onset, while **Zeitgeber time** 12 (ZT12) refers to the light offset. In free-run condition, eg. **constant darkness (DD)** (12 hours dark/12 hours dark) or **constant light (LL)** (12 hours light/12 hours light), the onset of activity of nocturnal organisms defines **Circadian Time** 12 (CT12).

- Moreover, in order for a clock to work accurately, the oscillations must not vary with the inevitable temperature daily variation. A clock must thus be **temperature-compensated**.

These fundamental principles can be represented as a simple model, first developed by Arnold Eskin *(Eskin, 1979)* **(Figure 8)**.

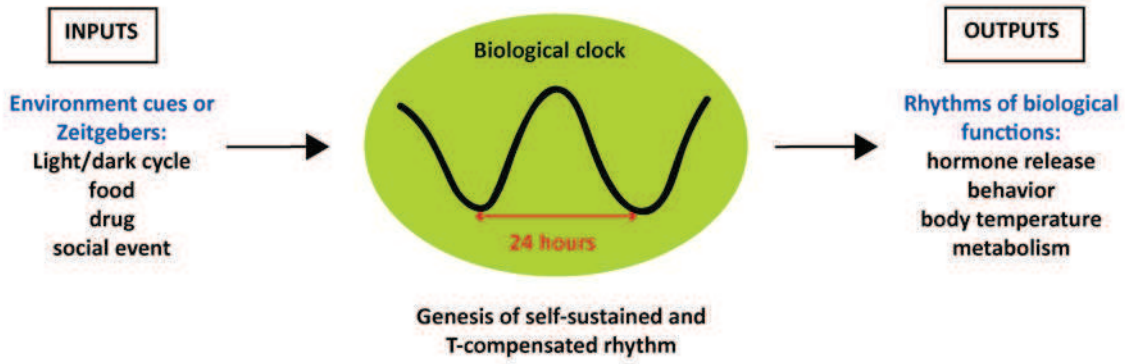

Figure 8. Representation of the fundamental properties of a circadian clock.

II.B. The master clock

II.B.1. Localization

Pittendrigh was the first to develop the idea of a multi-oscillating system including several oscillators synchronized by a master clock. This system is capable of generating endogenous rhythm and imposing this rhythm to the organism *(Pittendrigh, 1960)*. In mammals, the master clock is localized in the SCN of the hypothalamus. The SCN are synchronized to environmental changes in the

light/dark cycle by direct innervation from the retina via the retino-hypothalamic tract **(see III.A.1.2)**. In turn, the SCN coordinates the rhythmic activities of innumerable subordinate clocks. Indeed, many secondary clocks or oscillators are found in the brain and peripheral tissues (such as the skin, liver, hearth, kidney, muscle, adipose tissue). Circadian signals from the SCN are transmitted by nervous fibers to the brain and the peripheral targets to synchronize secondary clocks *(Pevet & Challet, 2011)*.

II.B.2. Molecular mechanisms

The SCN clock is a strong autonomous oscillator cycling with a period of about 24 hours. At the cellular level, circadian rhythm are generated by interlocked positive and negative transcriptional/translational feedback loops, which involve several specific clock genes and proteins *(Takahashi et al., 2008)*.

In mammals, the core mechanism consists of two transcription factors **(Figure 9)**: circadian locomotor output cycles kaput (**CLOCK**) and brain and muscle ARNt-like protein 1 (**BMAL1**). CLOCK/BMAL1 heterodimeres activate the transcription of other clock genes (**positive loop**), including three *Period* (***Per1, Per2, Per3***) and two *Cryptocrome* (***Cry1, Cry2***) genes. The PER/CRY protein complex translocates to the nucleus where they inhibit their own transcription and thereby CLOCK/BMAL1 induced transactivation (**negative loop**). The timing of nuclear entry is balanced by regulatory **kinases** that phosphorylate the PER and CRY protein, leading to their degradation. Inactivation of PER/CRY repressor complexes is considered as the critical step for allowing a new cycle of autoregulation to restart.

Adding to the robustness of the system, CLOCK/BMAL1 also drives transcription of nuclear receptors: the retinoic acid receptor-related orphan receptor γ (**RORγ**) and the reverse viral erythroblastis oncogene product α (**REV-ERBα**). In turn, REV-ERBα and RORγ inhibit and activate, respectively, the rhythmic transcription of *Bmal1*.

Finally the transcription factors involved in the clock mechanism control the expression of numerous clock controlled genes (**CCGs**), which constitute outputs of the molecular clock, involved in a large variety of biological processes (see Clock-related gene expression in **Figure 9**).

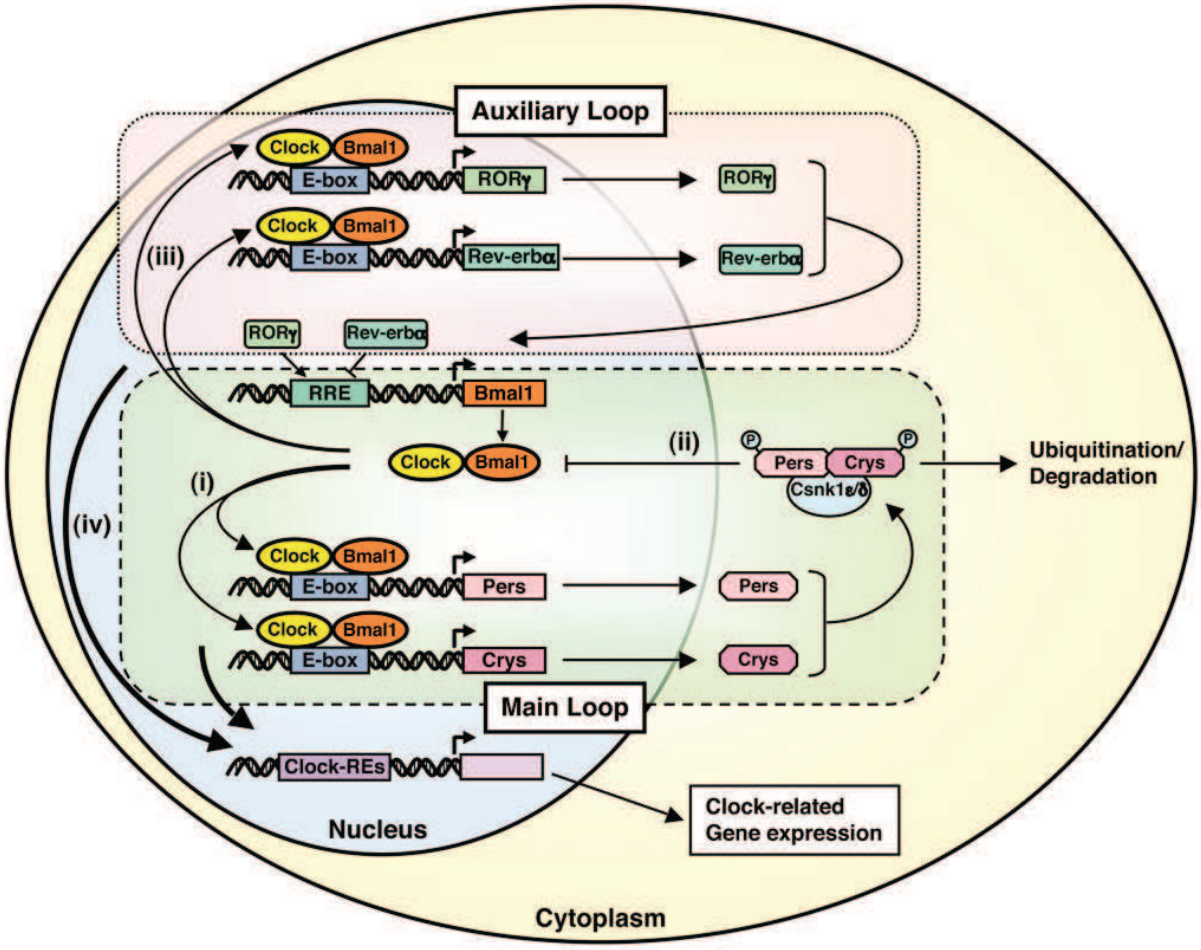

Figure 9. The circadian CLOCK system is regulated by a self-oscillating transcriptional loop.

Main loop: **(i)** the heterodimer CLOCK/BMAL1 binds to E-box[1] elements located in the promoter region of essential clock transcription factors Pers and Crys and stimulates their expression. PERS, CRYS form a complex with the caseine kinase 1ε and δ and **(ii)** repress the transcriptional activity of the CLOCK/BMAL1 heterodimer by inhibiting its binding to the E-box response elements located in their own promoters. **Auxiliary loop**: **(iii)** CLOCK/BMAL1 also stimulates expression of other CLOCK-related proteins, such as REV-ERBα and RORγ, which create an auxiliary loop that helps stabilizing the main regulatory loop. **Output of the clock**: **(iv)** these CLOCK transcription factors control numerous "downstream" CLOCK-responsive genes to influence a variety of biologic activities. Bmal1: brain-muscle-arnt-like protein 1, Clock: circadian locomotor output cycle kaput, Crys: cryptochromes, Csnk1ε/δ: caseine kinase 1ε/δ, P: phosphate residue on the phosphorylated molecules, Pers: periods, RORγ: retinoic acid receptor-related orphan nuclear receptor γ, REV-ERBα: reverse viral erythroblastis oncogene product α *(Nader et al., 2012)*.

[1] The E-box element contains a canonical sequence of DNA (usually CANNTG, with N = any base), able to bind the helix-loop-helix structural motif of dimerized transcription factors.

Another auxilliary loop includes D-site of albumine promoter-binding protein (**DBP**) and E4 promoter binding protein 4 (**E4BP4**). The transcriptional activator DBP (expression controlled by an E-box) and inhibitor E4BP4 (expression controlled by RRE in *Bmal1* promoter) **(Figure 9)** synergistically regulate the expression of D-box-containing genes, including *Per*. This additional loop contributes to stabilize and fine-tune the PER/CRY feedback loop *(Yamajuku et al., 2011; Silver & Kriegsfeld, 2014)*.

Hundreds of clock modifiers have now been identified through a genome-wide screen, some of which directly or indirectly associate with known clock components *(Silver & Kriegsfeld, 2014)*.

To summarize, it is now admitted that many levels of loops regulation are important for the proper functioning of the circadian clock, including transcriptional, post-transcriptional and post-translational mechanisms. All together, these regulations provide robust oscillations. Indeed more and more kinases and phosphatases are discovered as regulator of the clock. Most display a nutrient and metabolic factors dependent activity, providing then a way for metabolism to affect the core clock mechanism *(Silver & Kriegsfeld, 2014)*.

II.C. Retinal clock

II.C.1. Identification

The first secondary clock discovered was the retinal clock *(Besharse & Iuvone, 1983)*. *Xenopus laevis* cultured retina displayed a circadian rhythm of the arylalkylamine N-acetyltransferase (AA-NAT) enzyme activity (output of the clock) with a peak at night. This rhythm is maintained in DD with a period around 25 hours and is entrained by a phase reversed LD cycle. In mammals, the existence of a retinal clock was demonstrated in 1996. Indeed golden hamster cultured retina exhibit a circadian rhythm of melatonin (output of the clock) with a peak at night in LD cycle, DD and phase reversed LD cycle *(Tosini & Menaker, 1996)* **(Figure 10)**.

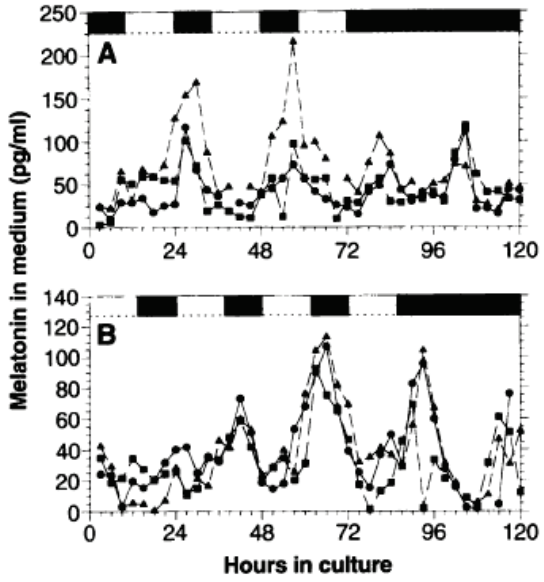

Figure 10. Entrainment by light of retinal melatonin synthesis in vitro.

A and B: in hamster retina melatonin rhythm follows the LD cycle imposed on the tissue and persists in DD *(Tosini & Menaker, 1996)*.

In cultured hamster retina melatonin rhythm is also temperature compensated *(Tosini & Menaker, 1998)*. Thus **the retinal clock presents all the parameters of an independent circadian clock**.

The presence of the retinal clock was then demonstrated in other mammalian species including rat *(Sakamoto et al., 2004; Buonfiglio et al., 2014)* and mice *(Tosini & Menaker, 1998; Ruan et al., 2008)*.

II.C.2. Cellular localization

As the retina is a highly heterogeneous tissue, several studies have focused on the cellular types expressing the retinal clock. Although circadian clock molecules (mRNA and protein) have been localized in mammalian retina, the cellular localization of the clock appears contradictory.

In mice, the clock could be localized in different cell types of the inner retina (horizontal, bipolar, amacrine cells, RGCs) *(Ruan et al., 2006)*. Another study found expression of the core circadian clock proteins in most retinal neurons of the mouse retina, including cone photoreceptors *(Liu et al., 2012)*. However interpretation of these studies is complicated by the fact that the authors used techniques with widely differing detection limits (eg. *in situ* hybridization vs. RT-PCR, laser micro-dissection to isolate cellular layers followed by RT-PCR, single cell PCR or immunohistochemistry), and different methods for assessing the independence of cell populations (pharmacology vs. physical lesions or genetic lesions) *(McMahon et al., 2014)*. Recently, one study reported that each layer of the mouse retina harbors a self-sustained oscillator *(Jaeger et al., 2015)*.

II.C.3. Functions

The circadian clock system in the retina is essential to ensure the physiology of the tissue. Retinal clock allows the anticipation of photopic and scotopic normal cycle. Indeed, visual conditions alternate with the day/night cycle. Another important circadian clock function resides in the ability to act as the gate for sensory information. This function is a fundamental property of sensory organs in a wide variety of species because retinal clock receives light information and send the photic message to the SCN.

Several studies have identified retinal processes under the control of the retinal circadian clock:

- The rod disk shedding *(Teirstein et al., 1980)*.

- Melatonin release *(Besharse & Iuvone, 1983; Tosini & Menaker, 1996, 1998)*.

- The expression of opsin and rhodopsin genes *(Von Schantz et al., 1999)*.

- The rods and cones coupling intensity via the gap junctions *(Ribelayga et al., 2008; Ribelayga & Mangel, 2010).* Gap junctions are present between cells to allow the transfer of ions and small molecules such as cAMP, cGMP. These junctions are composed of connexin oligomers. Their permeability is modulated by connexins phosphorylation performed by protein kinases. In photoreceptors, besides rods-rods and cones-cones coupling, cones and rods can also be coupled.

- Electrical activity of bipolar cells as seen with electroretinogam (ERG) b wave amplitude *(Storch et al., 2007)*.

Some retinal rhythms are under the SCN influence. Indeed a lesion of SCN leads to the loss of some mRNA rhythmicity in the retina (*Per2, Dbp*) when other mRNA are still rhythmic (*aa-nat*). These data suggest that retinal rhythms can be under control of the master clock as well as the retinal clock *(Sakamoto et al., 2000)*. Some retinal rhythms are also under the influence of ocular oscillators such as in the RPE *(Baba et al., 2010)* (eg. in case of the disk shedding) and the cornea *(Yoo et al., 2005)*.

III. MELATONIN: A ZEITGEBER IN THE BODY

III.A. Central production by the pineal gland

The pineal gland is an impaired structure with a pyramidal form. This gland is localized in the rostral part of the superior colliculi near the third ventricle in all mammals except rodent *(Møller & Baeres, 2002)*. Indeed in rodents the pineal gland is localized at the intersection between both cerebral hemispheres and the cerebellum. The mammal pineal gland is composed by pinealocytes (90 % of cells) and glial cells.

III.A.1. Melatonin synthesis

III.A.1.1. Melatonin identification and characteristics

In 1917, McCord and Allen reported that the pineal gland contained a biologically active substance by showing that bovine pineal extracts applied to frog skin could produce a skin lightning response. Many years later, Aaron Lerner used the amphibian skin lightning response as a bioassay to monitor the isolation of the active pineal principle. Lerner identified the substance as N-acetyl-5-methoxytryptamine and termed it melatonin for its bleaching effect on the skin (melanophores) of the amphibian *(Lerner et al., 1960)*.

Melatonin is synthesized from the essential amino acid tryptophane, which is first converted into 5-hydroxytryptophan before its decarboxylation into serotonin **(Figure 11)**. The conversion of serotonin to melatonin involves two major enzymatic steps. The first is N-acetylation by **AANAT** to yield N-acetylserotonin (**NAS**). The second step is the transfer of a methyl group to the N-acetylserotonin to yield melatonin through the action of hydroxyindole-O-methyltransferase (**HIOMT**).

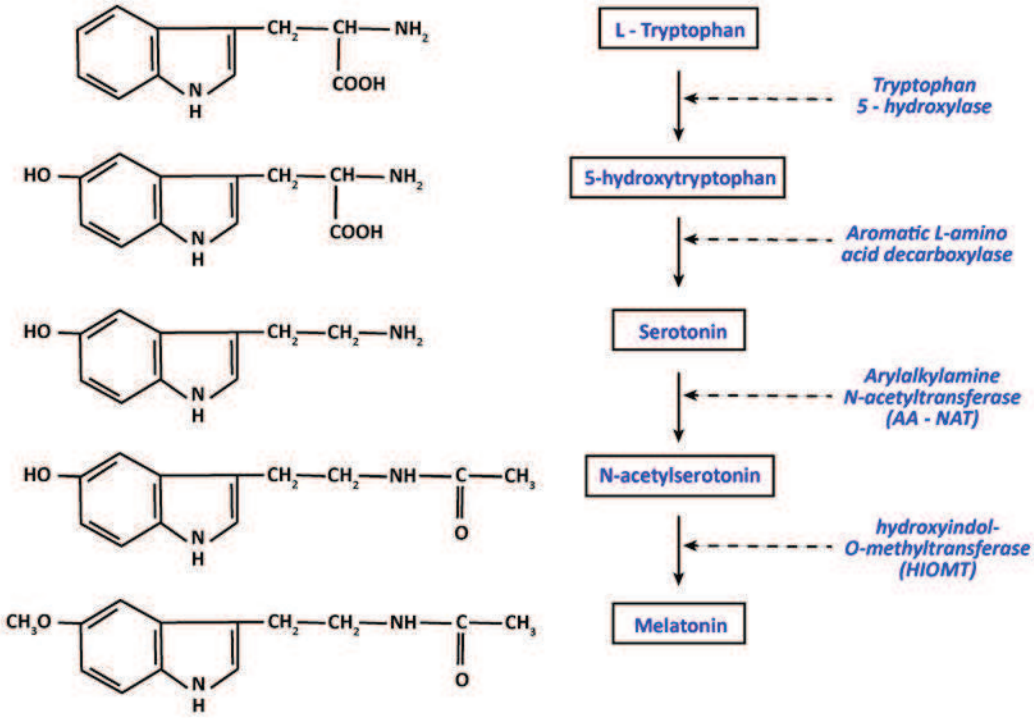

Figure 11. Melatonin synthesis.

Melatonin synthesis starts with the circulating amino acid tryptophan up-take and its subsequent 5-hydroxylation by tryptophane hydroxylase. 5-hydroxytryptophan is then converted to serotonin by the action of an aromatic L-amino acid decarboxylase. Serotonin is acetylated by AA-NAT to N-acetylserotonin, which is subsequently O-methylated and converted to melatonin by HIOMT. *Modified from (Konturek et al., 2006)*.

Melatonin is an amphiphile compound [composed of a hydrophobic element (indole nuclei) and a hydrophilic moiety (long carbon chain)] and diffuses across cell membranes as well as cell layers. The hormone rapidly disappears from the blood, with a half-life of approximately 30 min *(Cardinali et al., 1972; Waldhauser et al., 1984)*.

In human bloodstream, melatonin is converted to **6-hydroxymelatonin** by the liver, which clears 92 to 97 % of circulating melatonin *(Tetsuo et al., 1980; Young et al., 1985)*. Then 6-hydroxymelatonin is metabolized and excreted into the urine as the sulfate metabolite (50 to 80 %) and glucuronide (5 to 30 %) *(Ma et al., 2008).* The most abundant metabolite in mouse urine is the glucuronide (75-88 %) *(Kennaway et al., 2002; Ma et al., 2008)*.

In the brain, the primary cleavage product is N-acetyl-N-formyl-5-methoxykynuramine (**AFMK**), which is deformylated to N-acetyl-5-methoxykynuramine (**AMK**) *(Hardeland R, 2005)*.

III.A.1.2. Melatonin synthesis is driven through multisynaptic neuronal pathways

The major production of melatonin occurs in the pineal gland under the control of a multisynaptic neuronal pathway *(Larsen et al., 1998)*.

The light information is received by the retina which sends a message to the main circadian clock in the SCN via the **retinal-hypothalamic tract** *(Gillette & Mitchell, 2002; Hannibal, 2002)* **(Figure 12)**.

The **hypothalamo-pineal tract** relays the message from the SCN to the pineal gland. This pathway includes the paraventricular nucleus (**PVN**) which innerves the intermediolateral cells of the spinal cord (**IML**). The IML projects onto the superior cervical ganglia (**SCG**) and the SCG sends noradrenergic (**NA**) fibers *(Kappers, 1960)* to the pineal gland. This pathway is specifically activated at night and releases NA into the pineal perivascular space leading to melatonin synthesis. The implantation of this pathway starts after birth to be effective after 3 weeks *(Kappers, 1960)* **(Figure 12).**

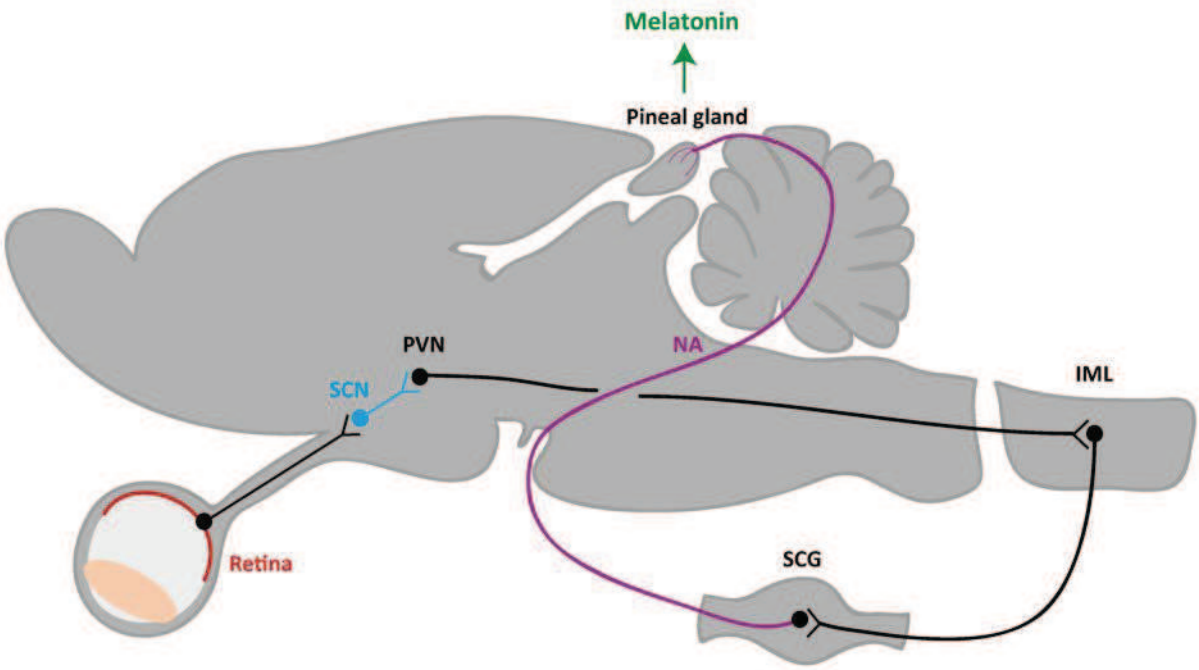

Figure 12. Diagram of the retinal-hypothalamic tract and the hypothalamo-pineal tract.

The light information arrives to the SCN via the retinal-hypothalamic tract. SCN controls melatonin synthesis by the pineal gland via the hypothalamo-pineal tract. SCN: suprachiasmatic nucleus; PVN: paraventricular nucleus; IML: intermediolateral cells of the spinal cord; SCG: superior cervical ganglia; NA: noradrenergic. *Modified from (Simonneaux, 2011)*.

III.A.1.3. Regulation of melatonin synthesis

In the pineal gland, the circadian change in melatonin synthesis is under the control of adrenergic receptors *(Deguchi & Axelrod, 1972a)*. Nocturnal NA activation of these receptors leads to activation of different signaling pathways.

First, the **β_1-adrenergic receptor** is positively coupled to the adenylyl cyclase (**AC**) via a G stimulatory protein (G_s) and leads to an increase in the cyclic adenosine 3',5'-monophosphate (**cAMP**) level within the cell *(Strada et al., 1972)*. Then, cAMP activates protein kinase A (**PKA)** *(Fontana & Lovenberg, 1971)*.

Secondly, the **α1-adrenergic receptor** is coupled to the phospholipase C (PLC) and to a calcium channel. Activated α1-adrenergic receptors increase the level of intracellular Ca^{2+} and protein kinase

C (PKC) *(Ho et al., 1988)*. During the night, the activation of AC is potentiated in presence of the Ca^{2+}/calmoduline (Ca^{2+}/CAM) complex *(Tzavara et al., 1996)*. This "cross-talk" causes a large and rapid increase in cAMP *(Vanecek et al., 1985)*.

The activation of cAMP/PKA pathway induces the phosphorylation of cyclic AMP-responsive element-binding protein (**CREB**) which binds the cyclic AMP-responsive element (CRE) *(Foulkes & Sassone-Corsi, 1996)* and induces the transcription of cAMP dependent genes such as *aa-nat*.

Phosphorylated CREB (P-CREB) can also bind the promoter of the CRE modulator (CREM) gene and induce the transcription of inducible cAMP early repressor (*Icer*). **ICER** is a powerful repressor of cAMP induced transcription *(Stehle et al., 1993)* and modulates cAMP response.

III.A.1.4. Characterization of the 2 main enzymes of melatonin synthesis

III.A.1.4.1. AA-NAT

III.A.1.4.1.1. *Aa-nat* gene

The *aa-nat* gene has been isolated in most studied mammals such as rat *(Borjigin et al., 1995)*, sheep *(Coon et al., 1995)*, human *(Coon et al., 1996)*, monkey *(Klein et al., 1997)*, mice *(Roseboom et al., 1998)*, chicken *(Bernard et al., 1997)* and fish *(Bégay et al., 1998)*.

The gene has been localized in the human 17q25 chromosome *(Coon et al., 1996)*, in the rat 10q32.3 chromosone *(Yoshimura et al., 1997)* and in the mice 11th chromosome in position E1.3-2.3 *(Roseboom et al., 1998)*.

The portion of *aa-nat* gene encoding the mRNA transcript is approximately 2.5 kilobases (kb) in human, 1.9 kb in sheep and 3.8 kb in chicken *(Klein et al., 1997)*. The gene is composed of 3 introns and 4 exons in human *(Coon et al., 1996; Klein et al., 1996)*.

III.A.1.4.1.2. *Aa-nat* mRNA

Northern blot analysis of *aa-nat* gene expression, revealed one band of *aa-nat* mRNA. Therefore *aa-nat* gene transcription codes for only one transcript in rat, sheep, human, monkey, chicken *(Klein et al., 1997)*. On the contrary, in some fishes, several bands were observed suggesting alternate splicing of the RNA leading to different possible AA-NAT isoforms (3 in trout, 2 in pike, 1 in Zebra-striped fish) *(Falcón, 1999)*.
Aa-nat mRNA presents a significant variation between day and night, with a 150 fold increase at night in rat, chicken, monkey and pike pineal gland *(Klein et al., 1997)*. At the opposite, in trout and ungulates, *aa-nat* mRNA is weakly increased at night *(Klein et al., 1997; Falcón, 1999; Stehle et al., 2001; Ganguly et al., 2002)*.

III.A.1.4.1.3. *Aa-nat* gene promoter

The *aa-nat* gene promoter (2160 base pairs (bp)) contains different sites for transcription factor binding **(Figure 13)**:

-CRE: binds P-CREB induced by cAMP *(Baler et al., 1997; Burke et al., 1999)*.

-Activating protein 1 (AP1): binds transcription factor from immediate early gene (IEG) *(Karin & Smeal, 1992)*.

-E box: binds the complex CLOCK/BMAL1, suggesting that clock genes can act on *aa-nat* transcription *(Chen & Baler, 2000)*.

-Pineal regulatory element (PIRE): binds a specific transcription factor of cones and rods (CRX), only expressed in the pineal gland and the retina *(Li et al., 1998)*.

Figure 13. *Aa-nat* gene promoter.

III.A.1.4.1.4. AA-NAT protein

The AA-NAT protein presents strong sequence homology between mammals, birds and fishes. Indeed, the homology between human AA-NAT and monkey's is of 97 %, 84 % for sheep, 90 % for rat, 76 % for chicken and 76 % for trout *(Klein et al., 1997)*.

In Vertebrates, AA-NAT has a molecular weight of 23 kilo-daltons (kDa). The protein is globular and composed of 8 β sheets and 5 α helixes *(Hickman, Klein, et al., 1999; Hickman, Namboodiri, et al., 1999; Craft & Zhan-Poe, 2000)*. The protein structure is constituted by a **catalytic core** with the enzymatic activity and **lateral parts** where phosphorylations occur **(Figure 14)**.

The catalytic core is very preserved in the superfamily of acetyltransferases *(Modis & Wierenga, 1998; Dyda et al., 2000)* and contains the binding site of acetylcoenzymeA (AcCoA), a histidine-rich catalytic domain and the binding site of arylalkylamine **(Figure 14)**.

In vertebrates, acquisition of the flanking regulatory regions represents a pivotal change in AA-NAT biology. C- and N- terminal regulatory regions contain a **PKA site (Figure 14)**. cAMP is able to control rapid AA-NAT activation/inactivation and protection/degradation switching by phosphorylating the Serine (Ser) and Threonine (Thr) residues in the PKA site *(Klein et al., 2002; Zheng et al., 2003)*. The N-terminal PKA site (Thr31 phosphorylation site) is located within a sequence that is converted to a **14-3-3** binding motif upon phosphorylation. Recent attention has focused on the PKA Ser205 phosphorylation site because its phosphorylation occurs in parallel with Thr31 phosphorylation, promoting binding to 14-3-3. This suggests that dual phosphorylation of Thr31 and Ser205 is required for activation of AA-NAT *(Zheng et al., 2005)*. The N-terminal region contains also an ubiquitination site, critical for proteosomal proteolysis *(Klein et al., 1997; Ganguly et al., 2002)*.

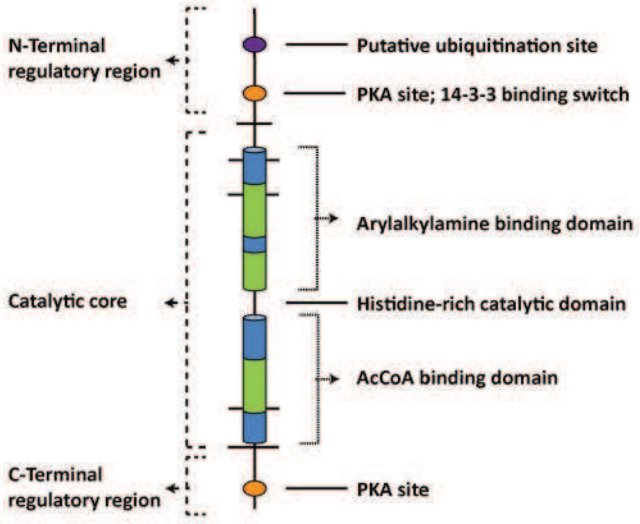

Figure 14. Schematic representation of vertebrate AA-NAT.

The central catalytic core is flanked by regulatory regions, each of which has a PKA site. The N-terminal PKA site is located within a sequence that is converted to a binding motif upon phosphorylation. *Modified from (Klein et al., 2002).*

In vivo, dark dependent phosphorylation of AA-NAT and binding to 14-3-3 occur as a function of environmental lighting *(Ganguly et al., 2001, 2005; Aitken, 2002, 2006; Pozdeyev et al., 2006)*. Biochemical studies of the 14-3-3 ζ isoform argue that one AA-NAT binds to a single 14-3-3 dimer *(Klein et al., 2002)*. However, structural studies indicate that two AA-NAT can bind to a single 14-3-3 ζ dimer, each contacting 14-3-3 via the N-terminal PKA/14-3-3 motif *(Klein et al., 2002)*. The stoechiometry of AA-NAT/14-3-3 complexes is still unclear. Binding of AA-NAT to 14-3-3 activates the enzyme by favoring an optimal configuration, in which affinity for arylalkylamine is increased. It also shields AA-NAT from proteins involved in dephosphorylation and degradation *(Klein et al., 2002)*.

Several studies in different species showed strong correlation between the level of AA-NAT protein and enzyme activity. Both exhibited variations between day and night with an increase at night which amplitude changes between species suggesting different regulation of AA-NAT *(Klein et al., 1997)*.

In rat, in optimal conditions of substrate (0.1 µmol tryptamine), co-factor (4 nmol AcCoA), temperature (37 °C) and pH (6.8), NAS is produced in low amount during the day (0.1 nmol/pineal gland/hour) but increases at night to reach a maximum of 10 nmol/pineal gland/hour *(Deguchi & Axelrod, 1972a; Parfitt et al., 1975)*.

III.A.1.4.2. HIOMT

In the pineal gland, HIOMT is involved in the last step of all methoxyindoles production including melatonin *(Axelrod & Weissbach, 1961)*.

III.A.1.4.2.1. *Hiomt* gene

The first *hiomt* cDNA has been cloned in the pineal gland of bovine *(Ishida et al., 1987)*, then chicken *(Voisin et al., 1992)*, human *(Donohue et al., 1993)* and rat *(Gauer & Craft, 1996)*.

Contrary to *aa-nat*, the rat *hiomt* sequence presents a weak homology to the ones of other species: 65 % with bovine, 63 % with human, 59 % with chicken *(Gauer & Craft, 1996)* **(Figure 15)**. Rat cDNA presents a coding region of 1.1 kb. In human *hiomt* has been localized in the pseudo-autosomal region of the X chromosome *(Rodriguez et al., 1994)*.

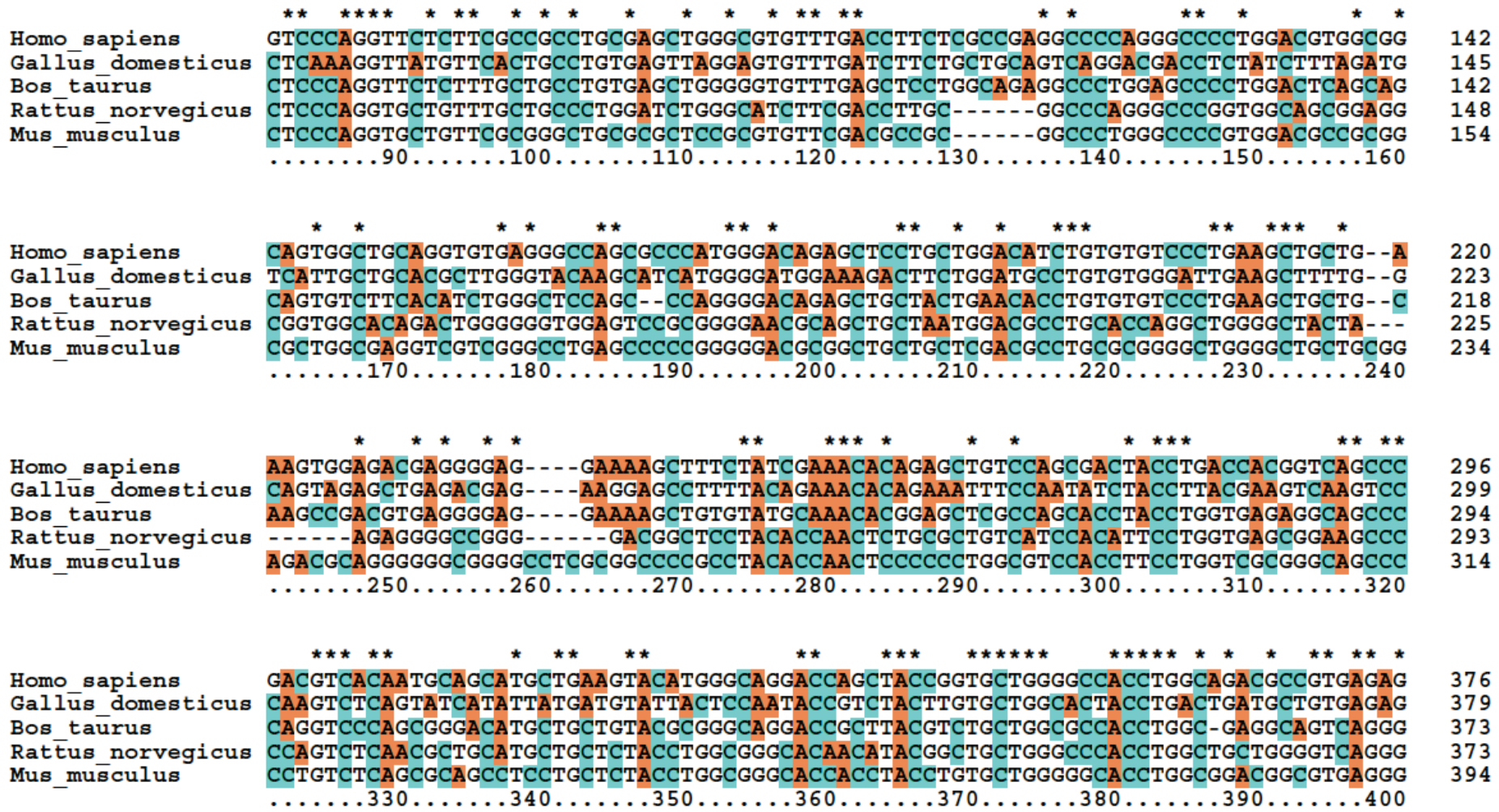

Figure 15. Alignment of coding sequences comparing HIOMT from human, chicken, bovine, rat, mouse.

Identical residues are marked by stars. (81-400 residues). A: orange; C: blue.

III.A.1.4.2.2. *Hiomt* mRNA

In the rat, contrasting to human's, *hiomt* gene only codes for one transcript *(Gauer & Craft, 1996)*. *Hiomt* mRNA exhibits a day/night rhythm with low amplitude. Indeed rat *hiomt* expression is 2 fold higher at night *(Ribelayga, Garidou, et al., 1999; Ribelayga, Gauer, et al., 1999)*.

III.A.1.4.2.3. *Hiomt* gene promoter

In human, *hiomt* promoter is composed of two regions: only one is functional in the retina (promoter A with a CCAATTAG sequence which binds only retinal transcription factor) and one including the CRE and AP1 sites *(Rodriguez et al., 1994).* In human and chicken a PIRE site has been localized in the *hiomt* promoter as in *aa-nat* gene (indicating pineal gland and retina specificity **as described in III.A.1.4.1.3**) *(Li et al., 1998; Bernard et al., 2001)*.

III.A.1.4.2.4. HIOMT protein

The protein has a molecular weight of 39 kDa for the monomer and is composed by two domains. The C-terminal domain is typical of other S-adenosyl-L-methionine (SAM)-dependent O-methyltransferases. The N-terminal domain intertwines several helixes with another monomer to form the physiologically active dimer *(Botros et al., 2013)*.

As the *hiomt* cDNA homology between species is very low, the amino acid sequence is also very heterogeneous between species. Indeed, rat HIOMT has 66 % homology with bovine, 69 % with chicken and 60 % with human HIOMTs *(Nakane et al., 1983)*. HIOMT protein, contrary to AA-NAT is very stable with a half life superior to 24 hours *(Bernard et al., 1993, 1995; Bernard & Klein, 1996)*.

In optimal conditions of substrate (0.1 µmol NAS), co-factor (0.2 µmol SAM) temperature (37 °C) and pH (7.9), HIOMT activity changes between 0.7 nmole/pineal gland/hour during the day to 2 nmol/pineal gland/hour during the night *(Ribelayga et al., 1997, 1998; Ribelayga, Garidou, et al., 1999; Ribelayga, Gauer, et al., 1999)*. The weak increase of HIOMT activity at night and its long half life demonstrate a different dynamic of HIOMT metabolism compared with the one of AA-NAT *(Ribelayga, Gauer, et al., 1999)*. This suggests that HIOMT may not be involved in the short term regulation (day/night) of melatonin synthesis. Indeed as the enzyme activity exhibits low daily variation, it probably cannot control daily rhythm.

Affinity studies in vivo with the different substrates of HIOMT demonstrated that the enzyme preferentially methoxyls NAS (50-80 %), then 5-hydroxytryptophol (15-30 %), serotonin (around 10 %) and finally 5-hydroxy-tryptophane and 5-hydroxyindole acetic acid (less than 5 %) *(Axelrod & Weissbach, 1961; Cardinali & Wurtman, 1972; Morton, 1986, 1987)*.

III.A.1.5. Summary of melatonin synthesis in rodent

In rat, the mechanisms involved in the induction of **melatonin synthesis** have been described as **transcription dependent mechanisms** resulting in high *aa-nat* mRNA variation between day and night *(Klein & Weller, 1970; Borjigin et al., 1995; Roseboom et al., 1996)*. Indeed, *aa-nat* mRNA is highly synthesized at night in response to the NA stimulation *(Klein et al., 1997)* **(Figure 16)**.

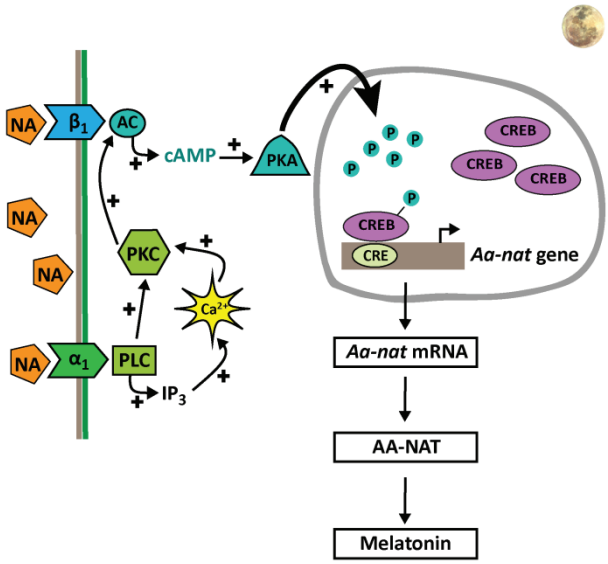

Figure 16. Melatonin synthesis initiation in rat.

The signaling pathway mainly involved is NA/β1/cAMP/PKA/P-CREB. NA binding to α1 increases the potency of the β1 pathway activation via Ca^{2+} and PKC. This leads to increase AC level and consequently cAMP level. AC: adenylyl cyclase; NA: norepinephrine; cAMP: cyclic adenosine 3',5'-monophosphate; PKA: protein kinase A; CREB: cyclic AMP-responsive element-binding protein; P-CREB: phosphorylated-CREB; PKC: protein kinase C; β1: β1 noradrenergic receptor; α1: α1 noradrenergic receptor. *Modified from (Stehle et al., 2001)*.

In an opposite way, the **decrease in melatonin synthesis** depends on **post-translational mechanism**. Indeed, the level of AA-NAT protein and its activity decrease more quickly than *aa-nat* mRNA's *(Stehle et al., 2001)* **(Figure 17)**.

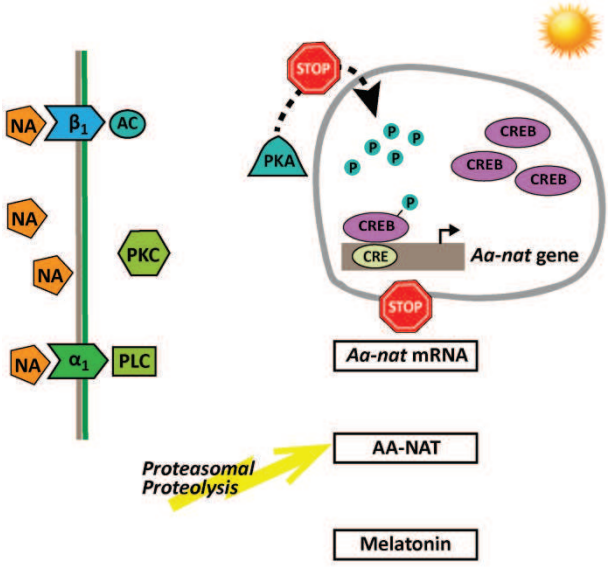

Figure 17. Melatonin synthesis inhibition in rat.

At the end of the night, NA release is inhibited by the circadian clock or the light arrival, resulting immediately in a decrease of cAMP level and the inhibition of AA-NAT protection by PKA. AA-NAT is then degraded by the proteasome. Moreover, the transcription of *aa-nat* is stopped because CREB is no longer phosphorylated. Abbreviation as in Figure 16. *Modified from (Stehle et al., 2001)*.

In ungulate, monkey and human, melatonin **synthesis** appears not to be controlled at the transcriptional level (*aa-nat* mRNA exhibits no day/night difference) but rather by the **post-translational regulation** of AA-NAT (the protein and activity of AA-NAT present day/night differences). During the night, NA activates AC via β1 receptor and increases cAMP level, which in turn activates PKA. Thus phosphorylated AA-NAT is protected from the proteasomal proteolysis *(Klein et al., 1997; Craft et al., 1999)*. The **inhibition** of melatonin synthesis is also under **post-translational control** in these species. Indeed, during the day, AA-NAT protein is not phosphorylated and is catabolized by the proteasome *(Stehle et al., 2001)*.

III.A.2. Melatonin function in the body

III.A.2.1. Melatonin receptors structure

The first pharmacological characterization of a functional mammalian melatonin receptor *(Dubocovich, 1983)* and the cloning of the first human melatonin receptor *(Reppert et al., 1994)* came 25 and 36 years respectively after melatonin discovery. Demonstration that melatonin receptors are coupled to a G protein took place in 1987 in *Xenopus laevis* dermal melanophores *(White et al., 1987)*.

In mammals, two G protein coupled receptors (GPCR) have been identified and termed **MT_1 and MT_2** (ortholog of Mel_{1a} and Mel_{1b} respectively for non mammalian) (and also named MTNR1A and MTNR1B respectively referring to human genes *(Bouatia-Naji et al., 2009)*). These receptors present a general structure consisting of seven transmembrane α-helical segments connected by alternating intracellular and extracellular loops. The amino terminus is located on the extracellular side whereas the carboxyl terminus is in the intracellular side **(Figure 18)**.

The human MT_1 and MT_2 melatonin receptors encode proteins of 350 and 362 amino acids, respectively. The amino acid homology for the human MT_1 and MT_2 receptors is approximately 60 % overall and 73 % within the trans-membrane domains. The amino terminus of the MT_1 melatonin receptor contains two consensus sites for N-terminal asparagine-linked glycosylation **(Figure 18)**, whereas that of the MT_2 shows only one site.

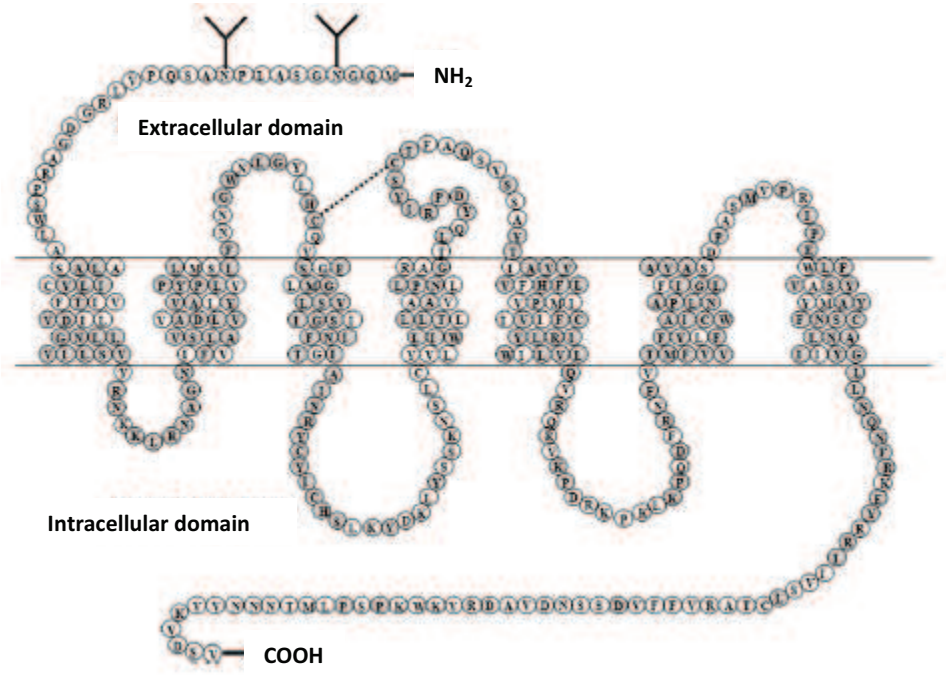

Figure 18. Membrane topology of the human MT_1 (hMT_1) melatonin receptor.

Gray circles denote identical amino acids in the hMT_1 and hMT_2 melatonin receptors. Both glycosylation sites on the hMT_1 receptor are denoted (Y) in the N terminus. *From (Dubocovich et al., 2010). Adapted from (Reppert & Weaver, 1995).*

Molecular analysis of genomic clones have demonstrated that the human MT_1 and MT_2 melatonin receptors genes contain two exons separated by a 13 kb intron *(Reppert et al., 1995; Slaugenhaupt et*

al., 1995; Roca et al., 1996). The melatonin receptors show distinct chromosomal localizations. The human MT_1 receptor gene is localized in the 4q35.1 chromosome locus while it is in the chromosome 8 of the mouse *(Slaugenhaupt et al., 1995; Roca et al., 1996)*. The human MT_2 melatonin receptor resides on 11q21-22 chromosome, while mouse MT_2 resides on chromosome 9 *(Reppert et al., 1995).*

A recent study has demonstrated strikingly similar overall profiles between recombinant human and mouse MT_1 and MT_2 receptors *(Devavry et al., 2012)* suggesting that selective ligands for mouse MT_1 and MT_2 could also have high affinity for human receptors. The first competitive melatonin antagonist discovered was the **luzindole** *(Dubocovich, 1988)* which is an **antagonist for MT_1/MT_2 heteromers** *(Baba et al., 2013)* **and MT_2 homomers**. Another selective **antagonist** which has been identified, the cis-4-phenyl-2-propionamidotetralin (**4P-PDOT**) presents higher affinity for **MT_2 receptor** in hamster (100 fold higher affinity for MT_2 *(Devavry et al., 2012))*, mouse (22 fold *(Baba et al., 2013)*), human (300 fold *(Dubocovich et al., 1997)*). 4P-PDOT is also an antagonist of **MT_1/MT_2 heteromers** *(Baba et al., 2013).* The N-butanoyl 2-[9-methoxy-*6H*-isoindolo[2.1-*a*]indol-11-yl]ethanamine (**IIK7**) has been identified as a selective **agonist for MT_2 receptors** in mouse (1000 fold higher affinity for MT_2 versus MT_1 receptor *(Baba et al., 2013)*) and in human (90 fold higher affinity for MT_2 *(Sugden et al., 1999)*). Low doses of IIK7 only activate MT_2 receptors but **high doses of IIK7 activate MT_2 and MT_1** *(Baba et al., 2013).* These results indicate that despite a high overall conservation of pharmacological properties between species, there might exist some important differences in MT_1 and MT_2 selective compounds between human and mouse *(Tosini et al., 2014).* More studies will be necessary to identify MT_1 selective agonists and antagonists.

MT_1 and MT_2 are considered high affinity melatonin receptors (ligands with picomolar binding affinity *(Dubocovich, 1995)*). Besides, there is another receptor with lower melatonin affinity (nanomolar range) which has been designated **MT_3** melatonin receptor. However this receptor is the homologue of a human quinone reductase 2 *(Nosjean et al., 2000)*, an enzyme suspected to be the molecular target of anti-malarian drugs such as chloroquin or paraquine *(Vella et al., 2005)*. Another endogenous MT_3 ligand is NAS (ligand with same affinity as that of melatonin *(Dubocovich et al., 2010)*).

In mammals, an **orphan receptor GPR50** (ortholog of Mel_{1c} for non mammalian) was identified as a melatonin related receptor because it has 45 % identity *(Reppert et al., 1996; Dufourny et al., 2008)* with the melatonin receptor family. However GPR50 is encoded by a gene located on the X chromosome and does not bind melatonin *(Drew et al., 1998)*. GPR50 can heterodimerize with MT_1 and MT_2 receptors, leading to a suppression of MT_1 but not MT_2 affinity for melatonin *(Levoye et al., 2006)*. This orphan receptor may also be important in regulating energy metabolism *(Ivanova et al., 2008)*.

III.A.2.2. Melatonin receptor signaling pathways

MT_1 and MT_2 are coupled to an inhibitory G protein (G_i) which stimulate **cAMP pathway** inhibition and **ERK1/2 pathway** activation *(Guillaume et al., 2008)* **(Figure 19)**. MT_1 has also been shown to couple to the G_q protein which stimulate **PLC pathway** *(Brydon et al., 1999; Tosini et al., 2014)* **(Figure 19)**. Furthermore, inhibition of the **guanylyl cyclase pathway** was shown to be MT_2 specific *(Jockers et al., 1997; Petit et al., 1999)* **(Figure 19)**.

Melatonin can also increase the activation of phosphatidylinositol 3 kinase (PI3K) and serine/threonine protein kinase (AKT). Melatonin can thus stimulate the survival pathway *(Ha et al., 2006; Faria et al., 2013)*.

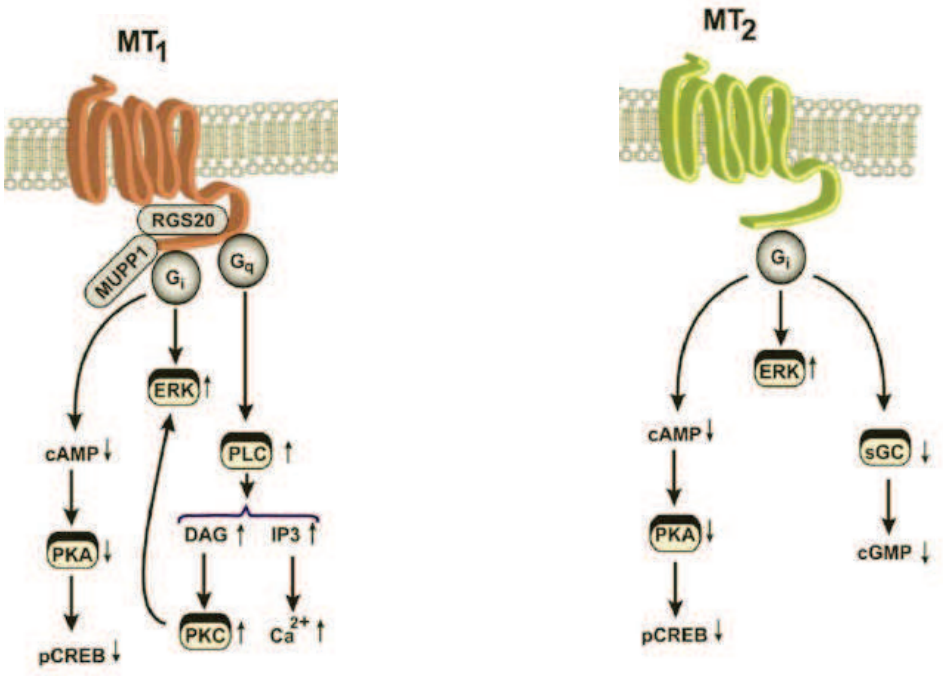

Figure 19. Principal melatonin-receptor signaling pathways.

Depending on the type of melatonin receptor complexes present in cells (MT_1 homomers, MT_2 homomers) the depicted signaling pathways are activated upon melatonin stimulation. DAG: diacylglycerol; ERK: extracellular signal-regulated kinase; IP3: inositol triphosphate; MUPP1: multi-PDZ domain protein 1; pCREB: phosphorylated-cAMP-response element-binding protein; PLC: phospholipase C; PKA: protein kinase A; PKC: protein kinase C; RGS20: regulator of G protein signaling 20; sGC: soluble guanylyl cyclase; cGMP: cyclic guanosine 3', 5'-monophosphate *(Tosini et al., 2014)*.

Depending on the cellular background, the species and receptor types, only 15-40 % of the MT_1 and MT_2 receptors are in the uncoupled state (not coupled to a G protein). Affinities for ligands are similar for MT_1 and MT_2 when receptors are uncoupled to G protein. However, these affinities are three to tenfold higher for MT_1 versus MT_2 when receptors are coupled to the G protein *(Legros et al., 2014)*. These results suggest that the differences in binding affinities of MT_1 and MT_2 receptors are not due to intrinsic affinity differences between the binding sites of the receptors, but rather to the formation of different complexes between agonist/receptor/G protein. These complexes bind melatonin ligands with different affinities *(Tosini et al., 2014)*.

Indeed, MT_1 and MT_2 form different receptor signaling complexes. Multi-PDZ domain protein 1 (MUPP1) binds to G_i protein and promotes interaction between G_i and MT_1 receptor. This leads to promote G_i mediated signaling of MT_1 *(Guillaume et al., 2008)*. In addition, MT_1 receptor binds to G_i protein and the regulator of G-protein signalling 20 (RGS20). $MT_1/G_i/RGS20$ complex is asymmetric between the different protomers of receptor dimers. The concept of asymmetry in receptor dimers suggests that each protomer fulfils its specific task. *(Maurice et al., 2010)* **(Figure 19)**.

III.A.2.3. Melatonin synchronizes annual/daily rhythms

Because the duration of nocturnal melatonin secretion is directly proportional to the length of the night, melatonin provides a signal for seasonal change **(Figure 20)**. Melatonin is, indeed, the critical parameter for photoperiod integration and the induction of particular physiological responses, such as those observed in seasonal breeders *(Karsch et al., 1988; Pitrosky et al., 1991; Cardinali & Pévet, 1998; Malpaux et al., 1999)*. The *pars tuberalis* of the pituitary gland which expresses a very high density of melatonin receptors *(von Gall et al., 2002)* interprets this rhythmic melatonin signal and generates a precise cycle of circadian genes expression to **synchronize reproduction with the seasons** *(Duncan, 2007)*.

Pineal melatonin thus serves as the internal signal that relays day length and displays **chronobiotic properties**. In rats kept in DD condition, peripheral administration of exogenous melatonin at the beginning of the night is able to synchronize the free-running locomotor activity *(Redman et al., 1983)* and to advance endogenous melatonin secretion *(Bothorel et al., 2002)*. However, these synchronizing effects of melatonin require doses 100 to 1000 fold higher than the physiological nighttime level. Nevertheless, this chronobiotic property of melatonin is used in humans, in blind people, during jet-lag or shift work to help them synchronize their free-running sleep-wake activity with the day/night cycle *(Claustrat et al., 1996; Skene & Arendt, 2007)*. It is believed that melatonin synchronizes circadian function by feedback onto the SCN **(Figure 20)**. Indeed, both melatonin receptors are expressed in the SCN *(Reppert, 1997)*. Furthermore, the circadian rhythm of SCN electrical activity is phase shifted by melatonin *(McArthur et al., 1991)* suggesting that melatonin entrain circadian function by acting onto SCN. To support this, one study has demonstrated that melatonin does not entrain the free running locomotor activity of species without melatonin receptors in the SCN *(Bonnefond et al., 1993)*.

Melatonin is also able to regulate vascular tone through activation of MT_1 (constriction) and MT_2 receptors (dilation) in arterial beds *(Masana et al., 2002).* Melatonin receptors are also involved in the regulation of glucose metabolism *(Tosini et al., 2014)* **(Figure 20)**.

In pregnant female rodents, maternal melatonin readily crosses the placental barrier and is proposed to synchronize fetal oscillators in individuals and among the litter with the cycling environment, at a time when the fetus has no functional SCN and cannot synthesize its own melatonin *(Simonneaux, 2011)* **(Figure 20)**.

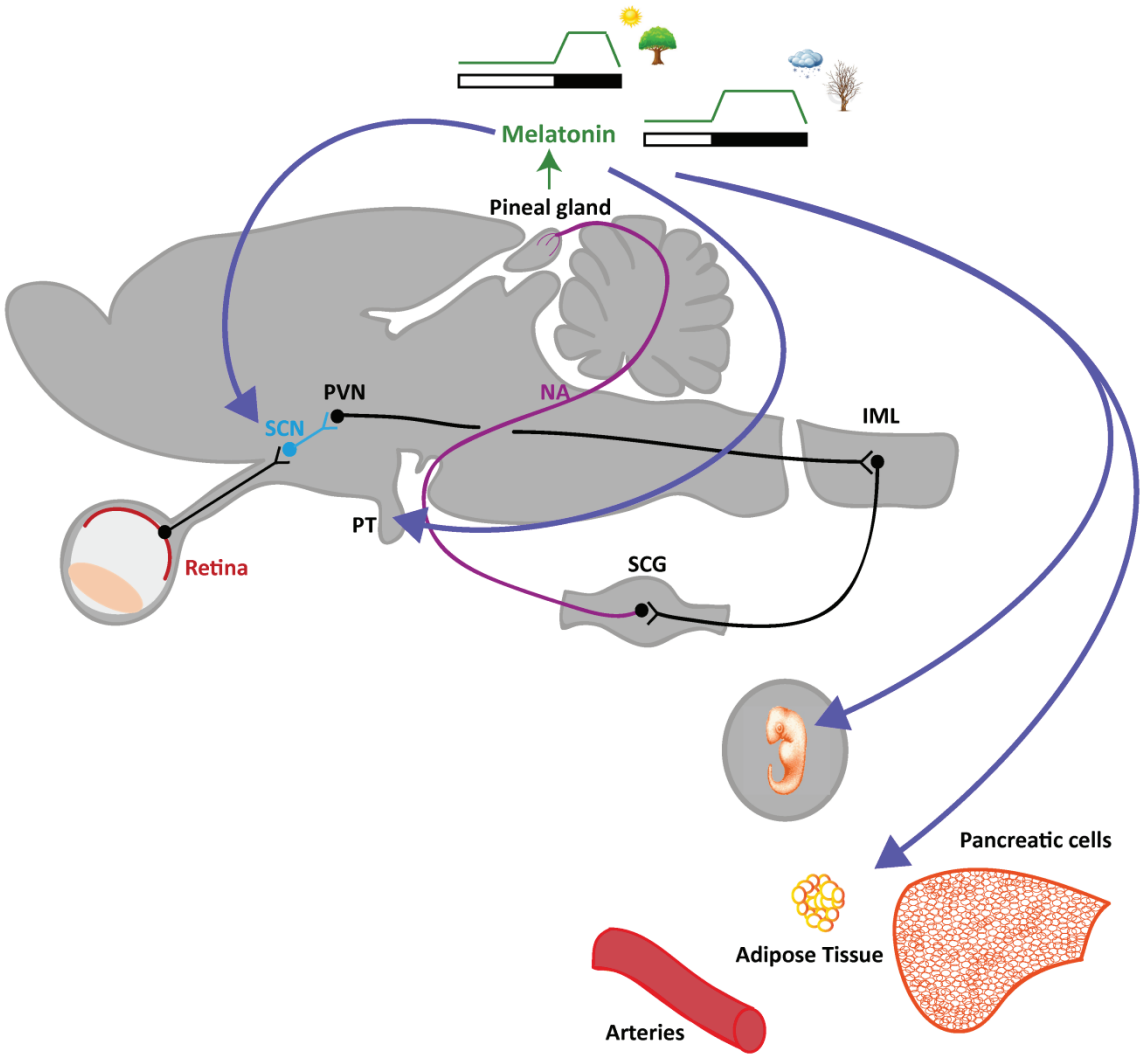

Figure 20. Diagram showing melatonin function in the body.

Melatonin synthesis is controlled by the SCN via multisynaptic neuronal pathways. This leads to the melatonin release in the bloodstream and the increase in circulating melatonin matches the length of the night. Melatonin feed backs onto the SCN which expresses melatonin receptors to synchronize circadian functions. Maternal melatonin synchronizes fetal oscillators. The expression of MT_1 and MT_2 melatonin receptors has also been reported in human pancreatic tissue to modulate glucose homeostasis. Melatonin also modulates adipocyte function via activation of MT_1 and MT_2. The hormone regulates the cardiovascular system by activating the receptors localized in arteries. Finally, melatonin synchronizes seasonal function such as reproduction. SCN: suprachiasmatic nucleus; PVN: paraventricular nucleus; IML: intermediolateral cells of the spinal cord; SCG: superior cervical ganglia; NA: noradrenergic; PT: *pars tuberalis*. White bar: light; black bar: night. *Modified from (Dubocovich et al., 2010; Simonneaux, 2011).*

In addition to its action mediated by MT_1 and MT_2 receptors, melatonin can also act as an antioxidant *(Hardeland R, 2005)*. Melatonin is able to down-regulate prooxidant enzymes (such as oxyde nitric synthase) and up-regulate antioxidant enzyme (such as superoxyde dismutase) *(Hardeland R, 2005)*. Melatonin can also acts directly as a free-radical scavenger by interacting with several reactive oxygen and nitrogen species *(Hardeland R, 2005)*. Oxido-reductive properties of the quinone

reductase (MT_3 receptors homologue) could explain the antioxidant role of melatonin when the hormone binds to MT_3 *(Vella et al., 2005)*.

Melatonin can have neuroprotective effects in central nervous system disease such as amyotrophic lateral sclerosis, Parkinson's disease and Alzheimer's disease. Indeed oxidative stress is implicated in the pathogenesis of these diseases *(Kaur 2008)*. Results from *in vitro* and *in vivo* investigations have demonstrated that melatonin protects mammalian cells from the toxic effects of ionizing radiation used in radiotherapy *(Vijayalaxmi et al., 2004)*. However it is important to note that these effects were observed with pharmacological melatonin concentration.

III.B. Melatonin is also produced by other structures

As described previously, AA-NAT and HIOMT are necessary to produce melatonin. Both enzymes were found in other structures that the pineal gland suggesting melatonin production in these sites.

AA-NAT is strongly expressed in the retina **(see Table 1 below for more details)**. The acetyl transferase is also expressed in other structures of the nervous system such as hippocampus, cerebellum, olfactive bulb, *pars tuberalis*, grey matter of the spinal cord and in peripheral tissue: eye (Harderian gland, ciliary body, aqueous humor, lens), testis, ovary, intestine *(Martin et al., 1992; Menendez-Pelaez & Reiter, 1993; Borjigin et al., 1995; Niki et al., 1998; Sakamoto & Ishida, 1998a; Uz & Manev, 1999; Fleming et al., 1999; Hamada et al., 1999; Djeridane et al., 2000; Stefulj et al., 2001; Uz et al., 2002; Alarma-Estrany & Pintor, 2007)*.

HIOMT has been detected in the retina, Harderian gland, ciliary body, aqueous humor, lens, duodenum, testis, ovaries but in low amount compared to its production in the pineal gland *(Cardinali & Wurtman, 1972; Pévet et al., 1980; Martin et al., 1992; Nowak et al., 1993; Itoh et al., 1997; Stefulj et al., 2001; Alarma-Estrany & Pintor, 2007)*.

Melatonin itself has been detected in the digestive tract of several species and appears to be synthetized by enterochromaffin cells of the intestine *(Martin et al., 1998)*. In ocular tissues, melatonin is produced in aqueous humor and Harderian gland *(Martin et al., 1992; Djeridane et al., 1998; Chiquet et al., 2006)*. Finally melatonin is synthesized in the retina as described below.

IV. MELATONIN: A SECOND MAJOR FOYER OF PRODUCTION IN THE RETINA

IV.A. Melatonin production in the retina

IV.A.1. Expression of AA-NAT and HIOMT enzymes in the retina

Numerous studies have revealed the presence of melatonin in the retina **(see Table 2 below for more details)**. Since the level of melatonin in the retina does not decrease following pinealectomy *(Hamm & Menaker, 1980; Yu et al., 1981; Reiter et al., 1983)* it has been postulated that the retinal hormone is not synthesized in the pineal gland but in the retina. This suggestion has thereafter been supported by the discovery of the enzymes necessary for melatonin formation in retinas *(Wiechmann, 1986)*. Indeed, as in the pineal gland, melatonin is synthesized from serotonin by AA-

NAT and HIOMT. AA-NAT, known as the key hormone of the melatonin rhythmic production has been well studied during the last 30 years. However, information about its localization and expression in the retina are still contradictory. HIOMT, the ultimate enzyme of melatonin synthesis has been poorly studied and information is missing. I propose a review on qualitative and quantitative circadian expression of AA-NAT and HIOMT in Vertebrate retinas **(Table 1)**.

	Rat/Mouse	Monkey	Chicken	Trout	Other
***Aa-nat* mRNA**	**Rat:** *(Niki et al., 1998):* CCB +++ at ZT17, 0 at ZT5. *(Liu et al., 2004):* ONL +++ at ZT20, + at ZT8; INL, GCL ++ at all ZT. *(Sakamoto & Ishida, 1998a):* N>D ~3x. **Mouse:** *(Sakamoto & Ishida, 1998b):* N>D ~2x.	*(Coon et al., 2002):* time of day not specified. ONL +++; INL ++; GCL +. N=D.	*(Bernard et al., 1997):* ONL+++ at ZT18, ++ at ZT6; INL and GCL + at all ZT. N>D ~4x. *(Garbarino-Pico et al., 2004):* PR +++ at ZT22, + at ZT3; GCL +++ at ZT3, 0 at ZT22. Under DD: PR, N>D ~3x; RGC, D>N ~6x.	*(Besseau et al., 2006):* ONL, vitreal-most INL, GCL +++ at night; ONL +, other layers 0 at day. N>D ~5x.	**Human:** *(Coon et al., 1996):* whole retina +++. **Bovine:** *(Craft et al., 1999):* whole retina +++. **Ovine:** *(Privat et al., 1999):* N=D.
AA-NAT protein	Nd	*(Coon et al., 2002):* N>D ~5x.	*(Iuvone et al., 2002):* N>D ~4.5x.	*(Besseau et al., 2006):* D>N ~2.5x.	nd
AA-NAT activity	**Rat:** *(Nowak et al., 1989):* 300 pmol/retina/h. N>D ~6x.	*(Coon et al., 2002):* ~25000 pmol/mg prot/h. N>D ~5x.	*(Valdez et al., 2012):* ~1000 pmol/mg prot/h in PR; 400 pmol/mg prot/h in RGC. In PR, N>D ~2x; in RGC D>N ~1.5x. *(Iuvone et al., 2002):* ~24000 pmol/mg prot/h. N>D ~18x. *(Bernard et al., 1997):* N>D ~8x. *(Hamm & Menaker, 1980):* ~15000 pmol/mg prot/h. N>D ~15x. *(Garbarino-Pico et al., 2004):* under DD: ~2000 pmol/mg prot/h in PR; ~800 pmol/mg prot/h in RGC. In PR, N>D ~6x; in RGC, D>N ~2x. *(Nowak et al., 1989):* 800 pmol/mg retinal tissue/h. N>D ~8x.	*(Besseau et al., 2006):* ~2800 pmol/mg prot/h. D>N ~4x.	***Xenopus laevis*:** *(Iuvone & Besharse, 1983):* ~24000 pmol/mg prot/h. N>D ~6x. **Rabbit:** *(Nowak et al., 1989):* 40 pmol/mg retinal tissue/h. N>D ~8x. **Mongolian gerbil:** *(Olcese & Møller, 1989):* 7000 pmol/mg prot/h. N>D ~1.8x.

	Rat/Mouse	Monkey	Chicken	Trout	Other
***Hiomt* mRNA**	**Rat:** *(Gauer & Craft, 1996):* +, N=D.	*(Coon et al., 2002):* +/-, N=D.	*(Wiechmann & Craft, 1993):* IS, ONL, OPL.	*(Besseau et al., 2006):* ONL +, vitreal-most INL, GCL +/-. N=D.	**Human:** *(Bernard et al., 1995):* +/-. *(Rodriguez et al., 1994):* +.
HIOMT protein	**Rat:** *(Wiechmann et al., 1985):* ONL, IS +++; INL, GCL +.	nd	*(Voisin et al., 2012):* ONL +++, GCL ++.	nd	**Bovine:** *(Wiechmann et al., 1985):* ONL, IPL +/-. *(Kuwano et al., 1983):* 0. **Lizard:** *(Wiechmann et al., 1985):* CCB, CIS. **Human:** *(Wiechmann et al., 1985):* ONL, IS. *(Bernard et al., 1995):* 0.
HIOMT activity	**Rat:** *(Gauer & Craft, 1996):* ~20 pmol/mgprot/h. N=D. *(Bernard et al., 1995):* ~200 pmol/mgprot/h. *(Nowak et al., 1989):* ~20 pmol/retina/h. N=D.	nd	**Hen:** *(Nowak et al., 1989):* ~20 pmol/mg retinal tissue/h. N=D.	nd	**Human:** *(Bernard et al., 1995):* 0. **Bovine:** *(Bernard et al., 1995):* 0. **Rabbit:** *(Nowak et al., 1989):* 5 pmol/mg retinal tissue/h. N=D.

Table 1. Species comparison of the melatonin synthetic pathway within the retina.

Compilation of published data underlines variations in the enzyme expression and activity of most studied Vertebrate retinas. The relative change in gene or protein expression between night and day is indicated using blue color. Activity values were expressed in pmol/h/mg prot to allow comparison between species. ONL: outer nuclear layer; INL: inner nuclear layer; GCL: ganglion cell layer; CCB: cone cell body; CIS: cone inner segment; PR: photoreceptor; RGC: ganglion cell; prot: protein; DD: dark/dark; D: day values; N: night values; nd: not determined. Staining intensity or expression level are represented as follows: +++: strong; ++: moderate; +: weak; +/-: very weak; 0: absent.

IV.A.2. Regulation of AA-NAT in the retina

Most of the cellular and molecular mechanisms controlling AA-NAT expression and activity have been described in the retina of chicken and rat.

In rat, ***aa-nat* mRNA** expression shows marked day-night variations that persist in DD condition (Sakamoto & Ishida, 1998a) suggesting that the rhythm is driven by an endogenous **circadian clock**. **The changes in mRNA expression are followed by variations in AA-NAT activity and then in melatonin levels in rat retina (Table 1 and Table 2)**.

The **AA-NAT activity** rhythm is abolished in the retina of rats maintained in constant **light** condition (LL) *(Nowak et al., 1989)*. Moreover light exposure in the middle of the night induces a decrease in retinal AA-NAT activity in rat, chicken, carp, rabbit, Mongolian gerbil *(Nowak et al., 1989; Olcese & Møller, 1989; Fukuhara et al., 2001)*. *In vitro* study reports that exposure to light at night can decrease AA-NAT activity by half within 5 min, and completely decrease AA-NAT activity to the daytime level within 10 min whereas *aa-nat* mRNA expression is not affected by light *(Fukuhara et al., 2001)*. A pretreatment of the retina with lactacystin, a specific inhibitor of proteasome degradation, prevented the reduction of AA-NAT activity following light exposure, showing that the decrease of AA-NAT is due to the action of the **protasomal proteolysis** *(Fukuhara et al., 2001).* In conclusion, light plays an important role in AA-NAT regulation **(Figure 21)**.

As described previously, photoreceptors depolarize in darkness. **Photoreceptors depolarization** leads to **Ca^{2+}** influx through dihydropyridine-sensitive voltage-gated channels, followed by activation of Ca^{2+}/CaM-stimulated adenylyl cyclase 1 (**AC1**) and a consequent increase in **cAMP** level **(Figure 21)**. As shown in the pineal gland, the increase in intracellular cAMP leads to the activation of **PKA**, which phosphorylates the CREB transcription factor. **P-CREB** binds to the **CRE element** localized on the *aa-nat* promoter which leads to the activation of ***aa-nat* gene transcription** *(Baler et al., 1997)*. Indeed in the rat retina *in vitro* study indicates that melatonin synthesis can be activated by exposure to darkness during the day *(Tosini & Fukuhara, 2003)*. Exposure to darkness in the presence of a specific inhibitor of PKA prevent the melatonin increase following dark exposure showing that **cAMP signaling cascade mediates melatonin synthesis after darkness exposure** *(Tosini & Fukuhara, 2003)*.

Besides its photic regulation, **AC1/cAMP/PKA pathway is also modulated by the circadian clock (Figure 21)**. Indeed AC1 and cAMP exhibited a circadian rhythm with a peak at night which is maintained in DD condition *(Ivanova & Iuvone, 2003; Fukuhara et al., 2004; Chaurasia et al., 2006).* The promoter of adenylyl cylclase 1 gene (*Adc1*) contains an E box. E-boxes are believed to be key regulatory elements of the circadian clock and the molecular components by which the circadian clock directly controls and regulates clock controlled genes *(Jin et al., 1999)*. This indicated that the circadian oscillator directly controls the transcription of *Adc1* by the action of the BMAL1/CLOCK complex *(Fukuhara et al., 2004)*. Similar rhythms of *Adc1* and AC1 were observed *(Chaurasia et al., 2006)*. AC1 daily variation induces cAMP and PKA rhythms. These changes appear to be causally related to **control AA-NAT activity** *(Ivanova & Iuvone, 2003)*. Indeed light mediated suppression of AA-NAT activity (as described above) is reversed by Ca^{2+} channel agonist and cAMP agonist *(Ivanova & Iuvone, 2003)*.

In addition, the promoter region of *aa-nat* contains an E-box *(Chen & Baler, 2000)*. ***Aa-nat* gene** transcription could be under the direct control of the **circadian clock** by the action of the

BMAL1/CLOCK complex. Studies have demonstrated that *aa-nat* transcription in rat photoreceptors can be activated by the BMAL1/CLOCK complex *(Chen & Baler, 2000)* **(Figure 21)**.

In conclusion, **a dynamic interplay of circadian oscillator and light exist in the regulation of AA-NAT** (mRNA and activity) **(Figure 21)**.

HIOMT regulation in the retina is not documented.

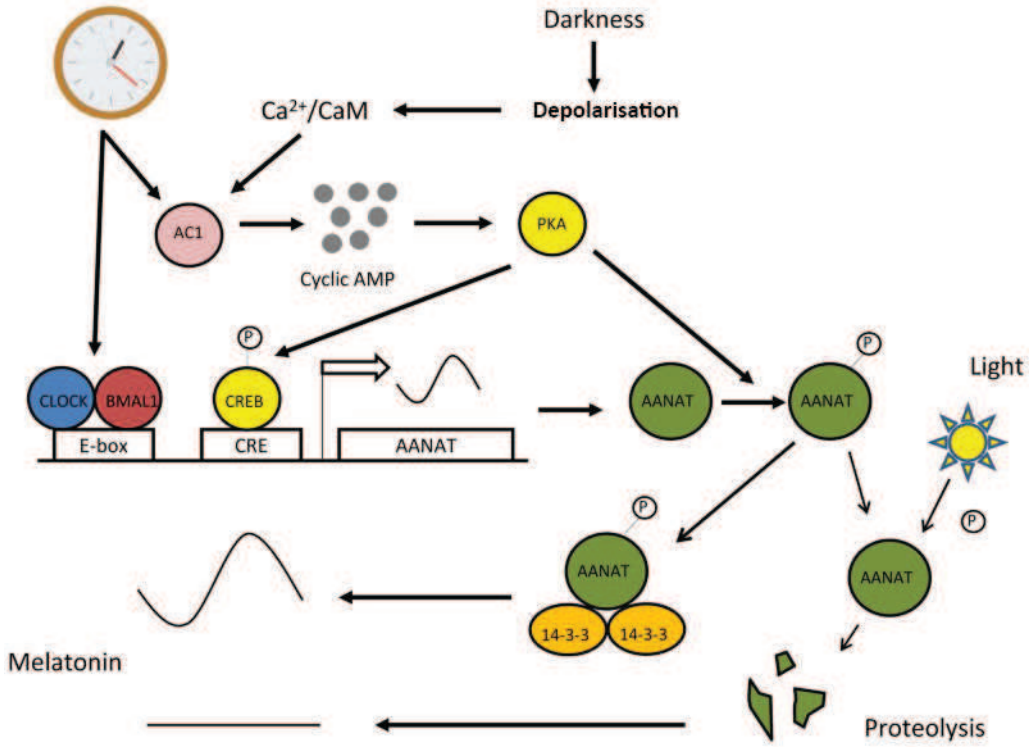

Figure 21. Regulation of retinal melatonin level by light and the circadian clock.

At night, cyclic AMP levels are elevated, activating PKA, which induces *aanat* gene transcription and phosphorylates AANAT protein. P-AANAT associates with 14-3-3 proteins. The activated enzyme thus stabilized increases conversion of serotonin to *N*-acetylserotonin which is ultimately followed by melatonin formation. Light exposure decreases cAMP levels resulting in dephosphorylation of AANAT and its subsequent degradation by proteasomal degradation. The circadian clock controls melatonin levels by directly regulating *Aanat* transcription and by gating the cyclic AMP signaling cascade. AC1: adenylyl cyclase 1; cyclic AMP: cyclic adenosine 3',5'-monophosphate; PKA: protein kinase A; CREB: cyclic AMP-responsive element-binding protein; CRE: cyclic AMP-responsive element; Ca^{2+}/CaM: complex Ca^{2+}/calmoduline; P: phosphorylated *(Tosini et al., 2012)*.

If the **initiation of melatonin synthesis** in the retina depends on **transcriptional regulation**, **post-translational regulation** has also been described in rat and chicken. As described in the pineal gland, AA-NAT is phosphorylated at night by PKA. In the chicken, P-AA-NAT forms a dimer with the 14-3-3 chaperone protein. In this complex, AA-NAT is active and protected from dephosphorylation and degradation *(Pozdeyev et al., 2006)* and thereby allows the synthesis of melatonin **(Figure 21)**.

The **inhibition of melatonin synthesis** depends also on **transcriptional and post-translational regulation.** At the transcriptional level, during the day, hyperpolarization of photoreceptors decrease the level of $Ca^{2+}$and cAMP leading to a decrease in P-CREB and a decrease of *aa-nat* transcription. *Aa-*

nat transcription is also regulated by the circadian clock **(Figure 21)**. At the translational level, AA-NAT is no more phosphorylated by PKA during the day and cannot bind 14-3-3 leading to its degradation by the proteasome *(Pozdeyev et al., 2006)* **(Figure 21)**.

IV.A.3. Melatonin production in the retina

Due to the low level of melatonin in the retina, few studies have analyzed the hormone in this tissue. A review of qualitative and quantitative circadian expression of melatonin in Vertebrates is presented in **Table 2**.

	Rat/Mouse	Monkey	Chicken	Trout	Other
Melatonin	**Mouse:** ~ 60 pg/mg prot. N>D ~3x. **Rat:** *(Grota et al., 1982):* ONL, INL. Peak at the beginning of the day ~3x; and beginning of the night ~4x. *(Pang et al., 1980; Yu et al., 1981):* ~150 pg/retina. N>D ~2x. *(Reiter et al., 1983):* ~ 60 pg/retina. D>N ~2x (peak at the beginning of the day). *(do Carmo Buonfiglio et al., 2011):* ~1000 pg/retina. N>D ~5x.	nd	**Chick:** *(Hamm & Menaker, 1980):* ~1000 pg/mg prot. N>D ~4x. *(Reppert & Sagar, 1983):* ~1000 pg/retina. N>D ~4x. *(Garbarino-Pico et al., 2004):* under DD: ~40000 pg/mg prot in PR; ~4000 pg/mg prot in RGC; +/- in INL. N>D in PR ~13x; D>N in RGC ~7x. *(Contin et al., 2006):* under DD: ~1000 pg/mg prot in RGC. D>N ~5x.	**Sea bass:** *(García-Allegue et al., 2001):* D>N in autumn and winter; N=D in summer and spring.	**Golden Hamster:** *(Faillace et al., 1995):* D>N. **Bovine:***(Hall et al., 1985):* 3000 pg/retina.

Table 2. Species comparison of melatonin concentration within the retina.

Compilation of published data underlines variations in the retinal melatonin synthesis of most studied Vertebrates. Relative change between night and day are presented in blue color. Melatonin concentration was expressed in pg/mg prot or pg/retina to allow comparison between species. +/-: very weak levels; ONL: outer nuclear layer; INL: inner nuclear layer; PR: photoreceptor; RGC: ganglion cell; DD: dark/dark; D: day values; N: night values; nd: not determined.

IV.B. Melatonin: a key of retinal physio-pathology?

IV.B.1. Melatonin receptors and their signaling

MT_1 and MT_2 melatonin receptors are expressed in the retina of many species. **Table 3** compares the distribution and level of both receptors expression in the retina of Vertebrates.

No specific antibody is yet available to localize MT_2 receptor in rodent. Therefore, the lack of information regarding MT_2 is great as illustrated in **Table 3**.

Nonetheless, MT_1 has also been detected in the rat RPE *(Fujieda et al., 1999)*.

	Rat/Mouse	Monkey	Chicken	Trout	Other
***MT_1 (Mel_{1a})* mRNA**	**Mouse:** *(Baba et al., 2009):* ONL, INL +++, GCL +. **Young rat:** *(Fujieda et al., 1999):* GC, amacrine cells, horizontal cells +++.	nd	**Chick:** *(Natesan & Cassone, 2002):* IS, INL, GCL. D>N.	nd	**Xenopus:** *(Wiechmann & Smith, 2001):* retina, RPE.
MT_1 (Mel_{1a})	**Rat:** *(Fujieda et al., 1999):* OPL, IPL +++. *(Sheng et al., 2015):* ipRGC. **Young rat:** *(Fujieda et al., 1999):* OPL, horizontal cells +++, IPL +. **Mouse:** *(Sengupta et al., 2011):* COS, ROS +++, RGC ++, OPL +.	*(Scher et al., 2003):* amacrine cells.	**Chick:** *(Rada & Wiechmann, 2006):* IS, ONL, OPL, horizontal and amacrine cells, IPL, GCL. Peak at evening.	**Carp**: *(Huang et al., 2005):* OPL, horizontal cells.	**Human:** *(Meyer et al., 2002):* GCL, IS +++. *(Savaskan et al., 2002):* IS +++, GCL ++, amacrine cells and IPL +. *(Scher et al., 2002):* RIS, horizontal cells, amacrine cells, IPL, RGC. **Guinea pig**: *(Fujieda et al., 2000):* GCL +++, amacrine cells, IPL, OPL ++. ***Xenopus laevis:*** *(Wiechmann et al., 2004):* OPL (horizontal cells that ramify OPL).
***MT_2 (Mel_{1b})* mRNA**	**Mouse:** *(Baba et al., 2013):* ONL, INL.	nd	**Chick:** *(Natesan, 2002):* IS, ONL, INL, GCL.	nd	***Xenopus laevis*:** *(Wiechmann & Smith, 2001):* RPE, IS, INL, GCL. D>N.
MT_2 (Mel_{1b})	**Rat:** *(Zhao et al., 2010):* RGC. *(Sheng et al., 2015):* ipRGC.	nd	**Chick:** *(Rada & Wiechmann, 2006):* Peak at evening.	nd	**Human:** *(Savaskan et al., 2007)*: IS, OPL, bipolar cells, IPL, RGC. ***Xenopus laevis*:** *(Wiechmann et al., 2004):* RPE, IS, OPL (horizontal cells that ramify in OPL), GCL.
MT_1/MT_2	**Mouse:** *(Baba et al., 2013):* PR.	nd	nd	nd	nd

Table 3. Species comparison of melatonin receptors expression within the retina.

Data show retinal melatonin receptors localization and expression in most studied Vertebrates. Relative changes between night and day are indicated by blue color. ONL: outer nuclear layer; OPL: outer plexiform layer; INL: inner nuclear layer; GCL: ganglion cell layer; CCB: cone cell body; CIS: cone inner segment; COS: cone outer segment; RIS: rod inner segment; ROS: rod outer segment; PR: photoreceptor; RGC: ganglion cell; RPE: retinal pigmentary epithelium; D: day values; N: night values; nd: not determined. Staining intensity is represented as follows: +++: strong; ++: moderate; +: weak; +/-: very weak; 0: absent.

As previously described in the pineal gland, **MT_1 and MT_2** are coupled to a **G_i (Figure 22)** in chick retinal cell culture *(Iuvone & Gan, 1994)* as well as in rat and human retinal pigment epithelial cells *(Nash & Osborne, 1995).*

The widely observed co-expression of MT_1 and MT_2 (in mouse, chicken and human) and the potential of both receptors to form heteromeric complexes *in vitro* are particularly interesting. A recent study reports for the first time the presence of the heterodimer in the mouse retina where they are responsible for the melatonin dependant increase in light sensitivity at night *(Baba et al., 2013)*. **MT_1/MT_2 heteromer** is coupled to the **G_i/cAMP pathway** and a **G_q/PLC pathway** *(Baba et al., 2013)*. Studies on mouse MT_1/MT_2 heteromers indicate a significant amplification of G_q/PLC pathway activation in cells co-expressing both receptors types with improved amplitude and EC50 values as compared to cells expressing MT_1 alone (tenfold difference) *(Baba et al., 2013)*. MT_2 receptor alone was not able to activate G_q/PLC pathway and MT_1/MT_2 cannot activated the pathway when MT_2 is inactive. The authors propose that in MT_1/MT_2 heteromer, **MT_2 can be considered as a positive allosteric regulator of MT_1 receptor in respect to the G_q/PLC activation** *(Baba et al., 2013)* **(Figure 22)**.

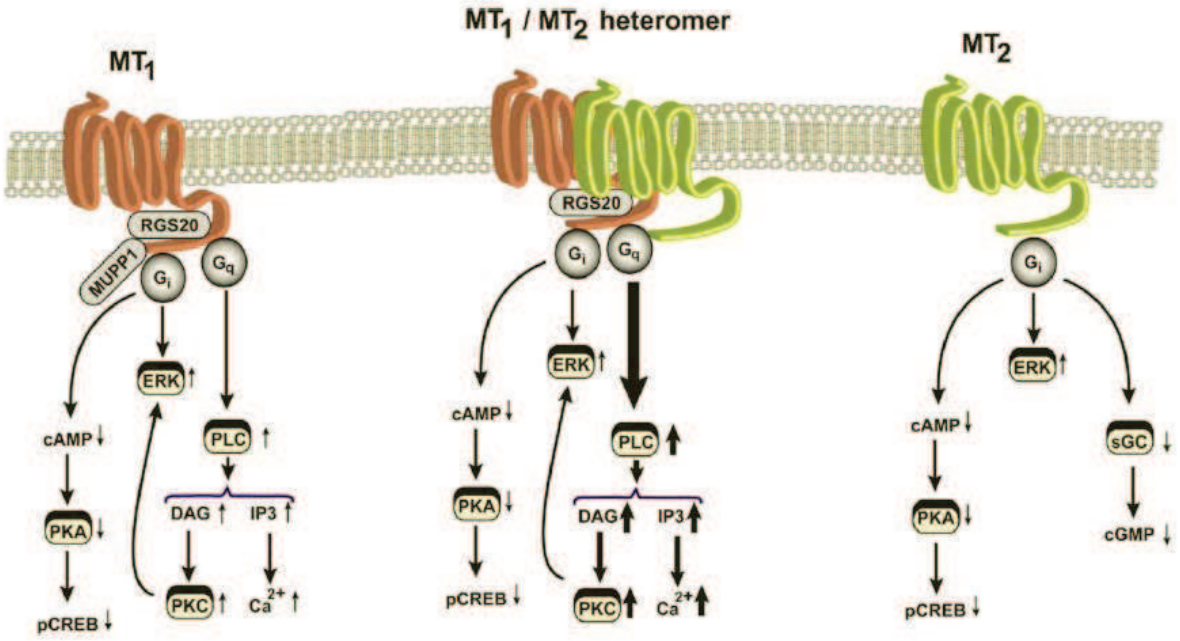

Figure 22. Melatonin receptor signaling in the retina.

Depending on the cells, different types of melatonin receptor complexes are present (MT_1 homomers, MT_2 homomers, MT_1/MT_2 heteromers) and different signaling pathways are activated upon melatonin stimulation. Thickness of the arrows represents the potency and efficiency of the pathway activation. DAG: diacylglycerol; ERK: extracellular signal-regulated kinase; IP3: inositol triphosphate; MUPP1: multi-PDZ domain protein 1; pCREB: phosphorylated-cAMP-response element-binding protein; PLC: phospholipase C; PKA: protein kinase A; PKC: protein kinase C; RGS20: regulator of G protein signaling 20; sGC: soluble guanylyl cyclase *(Tosini et al., 2014)*.

The propensity of MT_1/MT_2 heteromer and MT_1 homomer formation is similar, whereas MT_2 homomer formation is 3-4 fold lower, suggesting that the MT_2 receptor preferentially exists as heteromeric complexes with MT_1 or as monomers *(Ayoub et al., 2004)*.

IV.B.2. Melatonin in retinal physiology

IV.B.2.1. Interaction between dopamine and melatonin

Several studies have shown that melatonin and dopamine play opposing function in the regulation of retinal physiology *(Green & Besharse, 2004; Tosini et al., 2008)*. They are considered to act in opposite manner: melatonin is produced at night *(Tosini & Menaker, 1996, 1998)* whereas dopamine peaks during the day **(Table 4)**. Dopamine is thus a humoral signal of light and thereby controls light adaptive physiology whereas melatonin regulates dark adaptive effect.

Melatonin inhibits the release of dopamine through melatonin receptors *(Dubocovich, 1983; Boatright et al., 1994; Ribelayga et al., 2004)* and dopamine inhibits the synthesis of melatonin by acting on D2-like dopamine receptors *(Zawilska & Iuvone, 1992; Nguyen-legros et al., 1996; Tosini & Dirden, 2000)*. Dopamine is synthesized from a unique cell population within the INL which are amacrine cells *(Witkovsky, 2004)*. The circadian rhythm of dopamine release is dependent on melatonin *(Dubocovich, 1983)*. Indeed dopamine is no longer rhythmic in mice that are genetically incapable of synthesizing melatonin *(Nir et al., 2000; Doyle et al., 2002; Pozdeyev et al., 2008)*. Moreover daily injections of melatonin induce a circadian rhythm of dopamine release in retinas of mice that are unable to synthesize melatonin *(Doyle et al., 2002)*. On the contrary, the circadian rhythm of *aa-nat* mRNA is maintained when the dopamine rhythm is abolished *(Sakamoto et al., 2006)*, probably because *aa-nat* gene is directly controlled by the circadian clock via CLOCK/BMAL1 and the E box. These results suggest that the circadian regulation of dopamine depends on melatonin but melatonin rhythm is independent of the dopamine presence.

Dopamine has different roles in the retina. The hormone regulates protein phosphorylation in photoreceptors *(Pozdeyev et al., 2008)* and modulates the response of ipRGCs to light *(Van Hook et al., 2012)*. Moreover, dopamine modulates the rhythm of genes coding for melanopsin and PACAP *(Sakamoto et al., 2005)*, controls the expression of *Adcy1* (gene coding for AC) *(Jackson et al., 2011)* and influences the phagocytosis of PRs *(Masri et al., 1996)* as well as their coupling via gap junctions *(Ribelayga et al., 2008)*. Dopamine sensitizes the bipolar cells of rods to light via GABA *(Herrmann et al., 2011)*. Finally, dopamine may play a role on the surviving of PR in a murine model of retinal degeneration (rd mouse) *(Ogilvie & Speck, 2002)* and on the ocular refraction in a primate model of myopia *(Iuvone et al., 1991)*.

In conclusion, melatonin modulates dopamine release to control retinal circadian rhythms and essential retinal functions.

	Rat/Mouse	Monkey	Chicken	Trout	Other
Dopamine	**Rat:** *(Melamed et al., 1984):* ~200pg/mg wet weight. D>N ~2x. *(Gibson, 1988):* ~3000 pg/mg prot. D>N ~1.5x. *(Pozdeyev & Lavrikova, 2000):* ~30 pmol/retina. D>N ~1.5x. **Mouse BALB/c:** *(Nir et al., 2000):* ~700 pg/retina. D=N.	*(Boelen et al., 1998):* ~6 pmol/10 min/retina. D>N ~2x.	*(Zawilska & Iuvone, 1992):* ~2000 pg/mg prot. D>N ~2x.	**Cichlid fish:** *(Wulle et al., 1990):* ~2000 pg/retina. D>N ~1.5x.	**Rabbit:** *(Nowak & Zurawska, 1989):*~300pg/mg wet tissue. D>N ~1.5x. **Human:** *(Di Paolo et al., 1987):* ~3000 pg/mg prot. D>N ~2.5x.

Table 4. Species comparison of dopamine expression within the retina.

Dopamine expression in the retina of most studied Vertebrates. The relative changes between night and day is written in blue color. D: day values; N: night values.

IV.B.2.2. Regulation of clock genes

As an output of the circadian clock, melatonin may have feedback on the molecular clockwork. Indeed studies report that melatonin influences the amplitude and phase of clock gene transcripts such as *Per1* and *Cry1* in the mouse retina *(Dinet & Korf, 2007; Dinet et al., 2007)*. A recent study in the retina of melatonin proficient mice demonstrated that melatonin signaling (via MT_1 and MT_2) may be important for the regulation of clock genes expression in the INL or GCL but not in PR *(Hiragaki et al., 2014)*.

IV.B.2.3. ERG/light sensitivity

In *Xenopus laevis*, melatonin acting through melatonin receptors, directly stimulates the responsiveness of rod photoreceptor to light *(Wiechmann et al., 2003)*. Melatonin is proposed to act as an autocrine and/or paracrine signal by binding to its receptors in PRs and other retinal cells in order to increase visual sensitivity. Administration of exogenous melatonin in *Xenopus laevis* and in the carp increases the amplitude of the scotopic ERG *(Wiechmann et al., 2003; Ping et al., 2008)*.

However in chickens and pigeons, administration of exogenous melatonin during the day reduces the amplitude of the b waves (activation of the bipolar cells) *(Lu et al., 1995)*. In humans, oral administration of melatonin during the day decreases the amplitude of the cone ERG. Authors suggest that naturally increasing melatonin in the evening may decrease the impact of the cone system (day vision) in order to better promote the rod system (night vision) and by doing so, ensuring that the most suitable visual function is enhanced according to the time of the day *(Gagné et al., 2009)*.

Constant administration of melatonin abolishes circadian rhythms of a-waves (activation of PR) and b-waves implicit times (time to peak) as well as b-wave amplitude circadian rhythm *(McGoogan & Cassone, 1999)*. Melatonin proficient mice exhibit daily rhythms in the scotopic and photopic ERG and removals of melatonin receptors inhibit ERG daily rhythm *(Baba et al., 2009, 2013)*. Administration of exogenous melatonin during the day increase the amplitude of a and b waves and lowers the scotopic threshold response to nocturnal levels *(Baba et al., 2009, 2013)*. Removal of MT_1 and MT_2 receptor abolished these effects *(Baba et al., 2009, 2013)*.

In conclusion, melatonin seems to modulate ERG and visual sensitivity circadian rhythms, in a species dependent manner. The precise mechanisms by which melatonin mediates these functions is unknown.

IV.B.2.4. Photoreceptors phagocytosis

As described before, photoreceptor OS are continuously renewed by the assembly of new membrane disks at the base of the OS and by displacement of older disks at the top of them. These old disks are shed from the apical part of the OS and collected by the RPE. This phenomenon exhibits a daily rhythm with a peak at the beginning of the day *(LaVail, 1976; Besharse & Hollyfield, 1979)*. The daily rhythm is maintained in DD, indicating that PRs phagocytosis is under the control of a circadian clock *(Bobu & Hicks, 2009)*.

Earlier studies suggested a role of melatonin in the regulation of PR phagocytosis. Indeed exogenous melatonin activates the disk shedding in *Xenopus laevis* retina *(Besharse & Dunis, 1983)* and increase

shedding of large phagosomes frequency in rat RPE cells *(White & Fisher, 1989)*. However Grace et al., questioned the contribution of melatonin in the regulation of disk shedding in mice comparing the circadian regulation of disk shedding in melatonin proficient mice and melatonin deficient mice *(Grace et al., 1999)*. This study reported that PRs phagocytosis was rhythmic in both strains and was not affected by administration of exogenous melatonin, suggesting that other circadian output than melatonin can be important to synchronize disk shedding. However recently, our team has recorded a 3 hours phase shifting in PRs phagocytosis rhythm in the retina of C3H mice knockout (KO) for MT_1 or MT_2 receptors *(personal communication)*. These results suggest that melatonin is involved in the synchronization of PRs phagocytosis via MT_1 and MT_2.

IV.B.2.5. Cell viability

Melatonin has been shown to delay PR degeneration in rd mutant mice *(Liang et al., 2001)*. Recently, studies in melatonin proficient MT_1 KO mice, demonstrated a significant decrease in cell number of the ONL and GCL during aging compared to wild type mice *(Baba et al., 2009; Alcantara-Contreras et al., 2011)*. These studies suggest that melatonin increase viability of PR and cells from the GCL during time course.

However, albino rats injected with melatonin and exposed to bright light exhibited an increase in PR cell death compared to vehicle treated controls *(Wiechmann & O'Steen, 1992)*. Moreover, administration of a melatonin receptor antagonist at night (luzindole) reduces light-induced PR degeneration of rats exposed to bright light on the following day *(Sugawara et al., 1998)*. These results suggest that melatonin increases the susceptibility of the retina to light damage. It may be critical that melatonin levels are low during the daytime in rat to avoid melatonin potentiated light-induced oxidative damage in the retina *(Tosini et al., 2012)*.

IV.B.2.6. Summary of melatonin functions in the retina

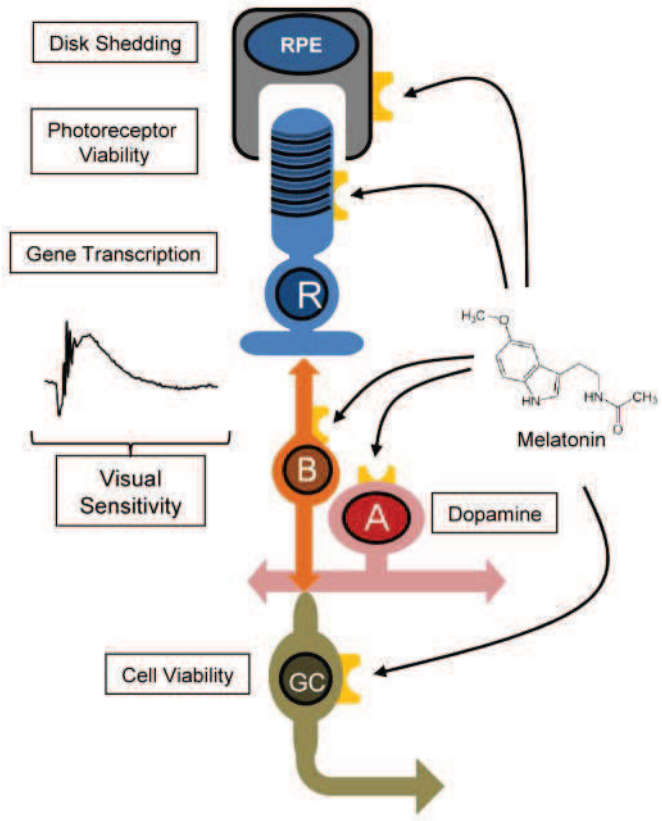

Figure 23. Melatonin functions in retinal physiology.

Melatonin receptors are expressed in many retinal cell types. Activation of these receptors may modulate several functions such as: disk shedding, retinal cell viability; visual sensitivity; dopamine levels and metabolism. RPE: retinal pigmented epithelium; R: rod photoreceptor; B: bipolar cell; A: amacrine cell; GC: ganglion cell *(Tosini et al., 2012)*.

IV.B.3. Melatonin in retinal pathology

IV.B.3.1. AMD

A series of studies has involved melatonin in the pathogenesis of age related macular degeneration (AMD). AMD accounts for 8.7 % of all blindness and is predicted to affect 196 million people by 2020. It is more prevalent in European than in Asian and African populations *(Wong et al., 2014)*. AMD is a degenerative disease that damages the RPE and PRs. The degenerescence of cones in the macula leads to the loss of central vision affecting daily tasks and having severe consequences on quality of life *(Coleman et al., 2010)*.

We know that melatonin decreases during aging *(Pulido & Clifford, 1986; Tosini et al., 2006)* and one study has reported that melatonin production decreases in AMD patients with respect to age-matched controls *(Rosen et al., 2009)*. These data suggest that a deficiency in melatonin may play a role in the modulation of AMD. In patients with AMD, daytime levels of melatonin were significantly higher *(Schmid-Kubista et al., 2009)*, suggesting that the daily rhythm of melatonin may be disrupted in these patients. Finally one study reported that daily administration of melatonin (3 mg) at bedtime may protect the retina and delay the progression of AMD *(Yi et al., 2005)*.

IV.B.3.2. Glaucoma

Melatonin has been implicated in the modulation of intraocular pressure (IOP) *(Samples et al., 1988; Pintor et al., 2001; Wiechmann & Wirsig-Wiechmann, 2001; Alarma-Estrany et al., 2008)* and it has

been suggested that melatonin may be useful in the treatment of glaucoma *(Lundmark et al., 2007; Belforte et al., 2010)*. Glaucoma is an important cause of irreversible blindness. It is an optic neuropathy characterized by RGCs death. In glaucoma, elevated IOP and oxidative stress have been implicated in RGCs death. Intraocular hypertension and vascular insufficiency in the optic nerve are suggested as main risks factors for glaucoma *(Park et al., 2012)*.

In rabbits, topical application of melatonin or melatonin analogue leads to a reduction in IOP, whereas luzindole (MT_1 and MT_2 antagonist) abolishes the effect of both compounds suggesting a role of melatonin via MT_1 and MT_2 in the regulation of IOP *(Pintor et al., 2001)*. Melatonin analogue also reduces IOP in glaucomatous monkey eye *(Serle et al., 2004)*. In humans, administration of oral melatonin causes a small but significant decrease in the IOP of individuals kept in bright light to suppress endogenous melatonin *(Samples et al., 1988)*.

In C3H MT_1 KO mice, IOP was higher than in the wild type mice during the night but not during the day *(Alcantara-Contreras et al., 2011)*. As seen previously, C3H MT_1 KO mice also showed a significant decrease in the GCL cell number during the course of aging, suggesting that even a small nocturnal increase of IOP may have an effect on RGC viability. Administration of melatonin in WT mice reduces IOP at night but not during the day suggesting a role for melatonin in the modulation of nocturnal IOP *(Tosini et al., 2012)*.

IV.B.4. Antioxydant role of melatonin in the retina

Studies demonstrate that melatonin can act as an antioxydant in PR. Indeed melatonin reduces the light-induced oxidative processes in PR at picomolar and low nanomolar concentrations *(Marchiafava & Longoni, 1999)*. On the contrary, melatonin exhibits potent prooxidant effects at micromolar concentration, ie. above the physiological melatonin concentration *(Marchiafava & Longoni, 1999).* Guajardo et al., have described that melatonin (milimolar concentration) decreases lipid peroxydation of polyunsaturated fatty *(Guajardo et al., 2003)*. The neurohormone (milimolar concentration) also reduces NO-induced lipid peroxydation in rat retinal homogenates *(Siu et al., 1999)*. Finally, in the guinea pig retina, melatonin reduces retinal oxydative damage during ischemia reperfusion injury (tissue damage occuring when blood returns to the tissue after a period of ischemia) *(Celebi et al., 2002)*. Melatonin may also have protective effects on RPE cells *(Osborne et al., 1998; Liang et al., 2004; Fu et al., 2012)*. Indeed melatonin decreases ischemia induced apoptosis in human RPE cells *(Osborne et al., 1998)* and protects RPE cells against hydrogen peroxide (H_2O_2) induced cell death *(Liang et al., 2004)*.

V. ANIMAL MODEL TO STUDY MELATONIN IN THE RETINA

V.A. Relevant model to study melatonin synthesis

In order to study the molecular mechanisms regulating diurnality and nocturnality as well as the physiology and surviving of cones (cells which permit high acuity and chromatic eyesight in human), a breeding colony of a diurnal rodent species *Arvicanthis ansorgei* Thomas 1910 was initiated in Strasbourg in 1998. Funder animals were trapped in the southern and central part of Mali **(Figure**

24). This West African species ranges from Senegal to Niger and Burkina Faso in subtropical or tropical scrubland.

Figure 24. *Arvicanthis ansorgei* female adult.

Animal in captivity at the Chronobiotron facility, Institute of Cellular and Integrative Neuroscience (INCI) in Strasbourg.

Arvicanthis ansorgei, as most diurnal rodents, exhibits bimodal locomotor activity, with increased activity at dawn and dusk *(Katona & Smale, 1997; García-Allegue et al., 1999; Weinert et al., 2007; Cuesta et al., 2009)*. Others parameters such as body temperature or corticosterone secretion are bimodal in diurnal rodents *(Verhagen et al., 2004; Cuesta et al., 2009)*. This is consistent with the tight relationships between activity, corticosterone and temperature *(Refinetti & Menaker, 1992; Challet et al., 1995; Coleman et al., 1998)*. The bimodality of *Arvicanthis* is also observed in the field *(Sicard B., unpublished data)*, and could be a response to environmental pressure (eg. high temperature and/or high pressure of predation around midday) that would persist even in laboratory conditions.

However, many physiological and metabolic parameters exhibit a unimodal rhythm in *Arvicanthis ansorgei*. Indeed SCN clock genes oscillation as well as rhythms of different cerebral neurotransmitters display a unimodal rhythm *(Caldelas et al., 2003; Cuesta et al., 2009)*. For instance, *aa-nat* mRNA rhythm, AA-NAT activity and melatonin in the pineal gland of *Arvicanthis ansorgei* exhibit a unique peak at night *(Garidou et al., 2002)*.

These results suggest that, despite a partial bimodality, *Arvicanthis ansorgei* has a diurnal physiology, with a circadian organization close to that in humans.

Importantly, *Arvicanthis ansorgei* can be successfully bred in captivity (5-7 young per litter). The gestation and weaning times are similar to other laboratory-housed rodents (21 days and 1 month respectively) and their estimated lifespan is approximately 2.5-3 years *(communication from animal keepers at INCI)*.

Cytogenetic and molecular analyses have demonstrated the monophylum of this genus with estimated time of divergence from other Muridae divisions ranging from 4 to 13 million years *(Ducroz et al., 1998)*. The phylogenetic match to laboratory mice and rats is crucial to optimize exploitation of existing databanks, available antibodies and probes. So far, many *Arvicanthis* homologues of neurotransmitters and visual pigment genes have been cloned successfully based on

murine sequences. Moreover, all tested antibodies, raised against either mouse or rat sequences of retinal proteins fully cross-reacted with *Arvicanthis ansorgei* antigens *(Bobu et al., 2006, 2008)*.

An initial characterization of *Arvicanthis ansorgei* retina performed in our group *(Bobu et al., 2006)* revealed that this species possesses 33 % of cones, which is approximately 10 times more than the mouse and rat number of cones. Moreover, cones are arranged in two regularly aligned cell layers at the scleral surface of the ONL, distributed uniformly across the entire retina and easy to distinguish from rods by their position and nuclear morphology. The easy identification of both rods and cones will be important to discriminate cellular localization of melatonin synthesis. Indeed one study shows *aa-nat* mRNA in the cones of rat, suggesting that melatonin synthesis takes place in these cells *(Niki et al., 1998)*. Finally the retina of *Arvicanthis ansorgei* (33 % cones vs 2-4 % in rats and mice) seems closer to the cone rich central retina of human (foveola).

To conclude, *Arvicanthis ansorgei* appears to be the relevant model to study melatonin synthesis in the retina of a diurnal mammal in order to get closer to the human retinal biology.

V.B. Relevant model to study melatonin function

To study melatonin function in mice has long been a problem since some strains such as C57BL/6 do not synthesize melatonin *(Ebihara et al., 1986; Goto et al., 1989)* including in the retina *(Tosini & Menaker, 1998)* because of mutations in *aa-nat (Roseboom et al., 1998)* and *hiomt* genes *(Kasahara et al., 2010)*. Contradiction persists, especially about melatonin rhythm generation in these species *(Conti & Maestroni, 1996; Vivien-Roels et al., 1998).* Some studies suggest that these mice can produce melatonin in some tissues *(Conti et al., 2000)* but the level of circulating melatonin is lower *(Gómez-Corvera et al., 2009)*. Although the amounts of melatonin produced in these mice are small (6 fold less in pineal gland; 1.5 fold less in plasma compared to melatonin proficient mice), we cannot exclude the possibility that these melatonin levels are sufficient to activate melatonin receptors *(Gómez-Corvera et al., 2009)*.

The melatonin production in presence of *aa-nat* gene mutation can be explained because other enzymes can bring a N-acetylation to yield N-acetylserotonin *(Slominski et al., 2003)* or because an alternative splicing of *aa-nat* can allow the production of a functional enzyme in tissues where the splicing occurs *(Gómez-Corvera et al., 2009)*. However melatonin production in presence of *hiomt* mutation is not documented.

The use of melatonin receptor KO mice is essential to understand the functions of melatonin. As only CBA and C3H mice are considered melatonin-proficient mice, Reppert laboratory developed melatonin receptor KO mice in one of these strains: C3H/$MT_2^{-/-}$ and C3H/$MT_1^{-/-}$ *(Roca et al., 1996; Jin et al., 2003)*. However these mice are homozygous for the rd1 mutation (*Pde6b*^{rd1} gene encoding the β subunit of cGMP-PDE) which induce the death of rods (98 % rods are gone in the central retina at 17 postnatal days, all rods are gone at 63 postnatal days) associated with a slower death of cones *(Carter-Dawson et al., 1979; Jiménez et al., 1996)*. Fortunately, C3H wild type mice at the rd locus namely C3H/$f^{+/+}$ were made available by Michael Menaker team *(Foster et al., 1991)*. C3H/$MT_2^{-/-}$ and C3H/$MT_1^{-/-}$ were then backcrossed with C3H/$f^{+/+}$ mice to produce C3H/$f^{+/+}MT_2^{-/-}$ and C3H/$f^{+/+}MT_1^{-/-}$ *(Baba et al., 2009)*.

AIMS OF MY PROJECT

The aim of my PhD project is to provide new insights of the **synthesis and role of melatonin in rodent retina.**

The retina is the second major melatonin production site. The local retinal production of melatonin is thought to exert local modulatory effects in this tissue.

Although melatonin synthesis in the pineal gland is fully described, the hormone production in the retina is less documented and controversies persist regarding the localization and the regulation of its synthesis. Indeed protein localization and expression of the penultimate enzyme of melatonin synthesis, AA-NAT, have not been described in mammals (except monkey) **(see Introduction Table 1)**. And more importantly, information about the ultimate enzyme of melatonin synthesis, HIOMT, are very limited **(see Introduction Table 1)**. As the retina is a multi-cellular organ, it is necessary to identify the cells producing melatonin to better assess its role in the retina.

Furthermore retinal circadian melatonin expression varies greatly between species. Indeed, in some cases melatonin exhibits a nocturnal peak, sometimes a diurnal peak, depending on species **(see Introduction Table 2)**. AA-NAT expression displays a nocturnal peak in a majority of Vertebrates, whereas some studies report a peak of expression during the day or no circadian rhythm **(see Introduction Table 1)**. Nonetheless, HIOMT temporal expression is poorly documented. Thus, the study of melatonin expression in the retina is necessary to better understand melatonin regulation and function in this tissue.

In the first part of my thesis (Chapter I), **melatonin temporal and spatial expressions** were characterized. For that purpose I studied AA-NAT and HIOMT mRNAs and proteins as well as their enzymatic activities in the diurnal rodent *Arvicanthis ansorgei* retina. Melatonin expression was also assessed. In addition, dopamine, which is through to act in opposing manner than that of melatonin, was measured. The results in *Arvicanthis ansorgei* retina were confronted with results in others species. Melatonin receptors MT_1 were also examined for their localization in the diurnal rodent retina.

Melatonin receptors are localized in different nuclear layers suggesting that melatonin could be involved in different retina functions **(see Introduction IV.B.1)**. Indeed several studies describe alternately beneficial and deleterious melatonin effects on the retina **(see Introduction IV.B.2, 3, 4)**. So it is important to carry a complete study of melatonin in the retina to better understand its role in the retina physiopathology and the associate mechanisms. Melatonin has been described to modulate photoreceptors viability during the course of aging **(see Introduction IV.B.2.5)** but the mechanisms by which melatonin exerts this effect is unknown. Photoreceptor viability and more particularly cones are crucial for vision in human. It is thus important to know if melatonin modulates cones viability.

The second part of my thesis (Chapter II) focuses on the following question: **Does melatonin modulates cones viability during the course of aging?** To address this question we counted cones number in C3H/$f^{+/+}$, C3H/$f^{+/+}MT_2^{-/-}$ and C3H/$f^{+/+}MT_1^{-/-}$ mice retinas at 3 and 18 months of age. To understand the **mechanism involved in this melatonin function**, we characterized expression and localization of the survival signaling pathway in the retina of the same animal models.

Organization of the manuscript

The details of the used methods are reported in the chapter **Materials and Methods**.

The **Results** section is divided in 2 parts:

- **Chapter I** includes Article I and enclosed experiments linked to this paper.

- **Chapter II** presents Article II.

Both result parts are finally confronted in the general **Discussion**, in which short and long term perspectives are presented.

MATERIALS AND METHODS

I. ANIMALS

I.A. *Arvicanthis ansorgei* and *Rattus norvegicus*

I.A.1. Animal care and handling

Sudanian unstriped Grass rats, *Arvicanthis ansorgei,* were raised in our animal facilities (Chronobiotron) from individuals captured in southern Mali in 1998 *(Challet et al., 2002)*. Albino Wistar rats were supplied by our own colony in the Chronobiotron. *Arvicanthis ansorgei* and *rattus norvegicus* were maintained in LD condition, with 200–300 lux during light phase and < 5 lux during the dark phase at room temperature of 22 ± 1 °C with food and water *ad libitum*. For DD experiment, animals were kept 4 days in DD condition prior to experimentation. Each experiment involved young (3 to 6 months old) adult females.

Animal treatment and experimentation were in agreement with institutional and national guidelines, and adhered to the Association for Research in Vision and Ophthalmology Guidelines for Use of Animals, and to the European Communities Council Directive of 24 November 1986 (86/609/EEC) and the Animal Use and Care Committee from Strasbourg. The experimental procedures were covered by an authorization to perform small animal experimentation (CREMEAS, AL/24/31/02/13).

Animals were anesthetized by isoflurane inhalation and immediately decapitated every 4 hours over a nychthemeron. ZT0 is defined as the beginning of the day, when lights are on (7 AM in summer and 8 AM in winter) in LD condition. Animals were sacrificed at ZT3, 7, 11, 15, 19, 23. CT0 is defined as the beginning of the subjective day in DD condition. Animals were sacrificed at CT3, 7, 11, 15, 19, 23 **(Figure 25).**

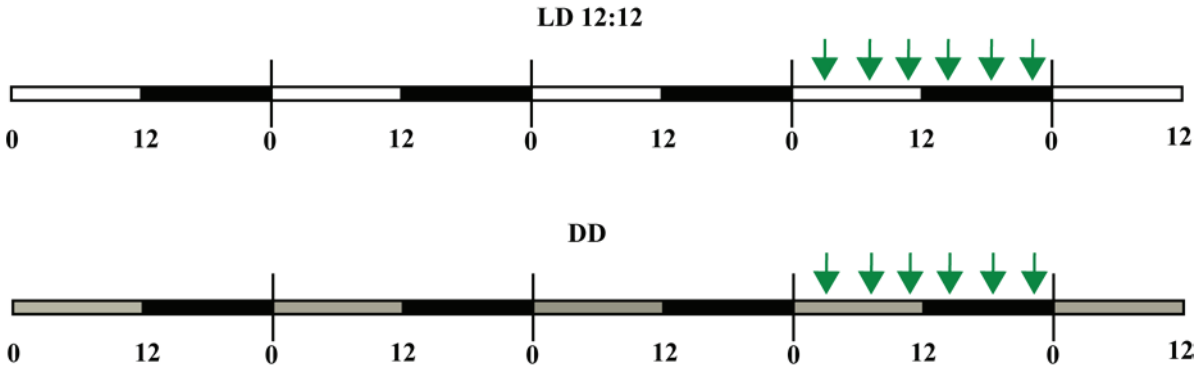

Figure 25. Experimental design for *Arvicanthis ansorgei* and rat sacrifice.

Periods of darkness and light are indicated by black and white bars respectively. Grey bars represent the subjective day in DD condition. 0 is defined as the beginning of the day or subjective day in LD and DD conditions respectively. Green arrow indicates time of sacrifice.

I.A.2. Sample preparation

For immunostaining and *in situ* hybridization studies on retinal section: eyes were collected and fixed in 4 % paraformaldehyde (PAF) (Sigma Aldrich) for 6 hours at 4 °C. Prior to cryoprotection, eye balls were dissected into two halves at the level of the optic nerve, removing cornea, lens and aqueous humor. Both halves were then incubated successively in 10 %, 20 %, 30 % sucrose diluted in phosphate buffered saline (PBS). Each semi-globe was individually included in Tissue-Tek ®OCT™ compound and frozen in liquid nitrogen before being kept at -80 °C. Using a cryostat (Leica CM3050 S), frozen sections (10 µm thick) were mounted on SuperFrost*Plus slides (Menzel-Gläser, Braunschweig, Germany) and stored at -20 °C until use.

For immunostaining on pineal gland, cortex and *pars tuberalis* section: the brains were collected and fixed in 4 % PAF during 12 hours. After a cryoprotection in 10, 20, 30 % sucrose solution, the brains were frozen at -60 °C in isopentane and stored at -80 °C. Using a cryostat, frozen sections (12 µm thick) were mounted on SuperFrost*Plus slides and stored at -20 °C until use.

For immunostaining on whole-mounts retina: eyeballs were collected and fixed in 4 % PAF for 6 hours. Fixed eyeballs were treated for antigenic reactivation in Tris-EDTA buffer (10 mM Tris (hydroxymethyl)aminomethane (Tris); 1 mM EDTA; pH 8) for 1 hour at 95 °C and 2 hours at room temperature. The samples were rinsed in PBS and retinas were carefully dissected under a binocular.

Regarding all other experiments: each eye was collected, the cornea was slit with a scalpel blade, lens and vitreous discarded and the retina collected and snap frozen individually in sterile Eppendorf® tubes in liquid nitrogen.

I.B. C3H/$f^{+/+}$, C3H/$f^{+/+}MT_1^{-/-}$ and C3H/$f^{+/+}MT_2^{-/-}$ mice

I.B.1. Animal care and handling

C3H/$MT_1^{-/-}$ and C3H/$MT_2^{-/-}$ mice homozygous for the *rd1* mutation, generously donated by Dr. Reppert and Weaver (University of Massachusetts Medical School), were back-crossed with C3H/$f^{+/+}$ mice in which the *rd1* mutation has been removed to produce C3H/$f^{+/+}MT_1^{-/-}$ and C3H/$f^{+/+}MT_2^{-/-}$. The genotypes were determined according to the protocols previously described *(Lem et al., 1992; Liu et al., 1997)*. Mice were housed in a temperature-controlled environment (22 ± 1 °C) and had access to water and food *ad libitum*. Animals were kept under LD condition. Light intensity was between 200-300 lux during the light phase and < 5 lux during the dark phase.

All the experimental procedures were carried out in accordance with Association for Assessment of Laboratory Animal Care policies and approved by the Morehouse School of Medicine Animal Care and Use Committee.

Animals were euthanized with CO_2 at different ZT: ZT1, 4, 7, 10, 13, 16, 19, 22 **(Figure 26)**.

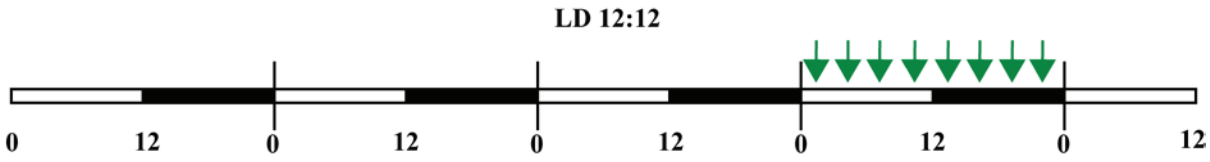

Figure 26. Experimental design for mice sacrifice.

Periods of darkness and light are indicated by black and white bars respectively. 0 is defined as the beginning of the day. Green arrow indicates time of sacrifice.

I.B.2. Sample preparation

Immunofluorescence on retinal section: eyes were immediately removed from sacrificed animals and fixed with 4 % PAF in PBS during 12 hours. Subsequent to fixation, eyeballs were rinsed in PBS, transferred to sucrose 30 % overnight and embedded (Tissue-Tek™ CRYO-OCT Compound, Fisher Healthcare). Cryostat sections (12 µm thick) were mounted on SuperFrost*Plus slides (VWR) and stored at -20 °C until ready for use.

AKT pan immunofluorescence on retinal section: after fixation the eyes were incubated in a retrieval solution (10 mM sodium citrate; pH 6) overnight at 4 °C. Then they were immersed in boiling retrieval solution 3 min and immediately placed in 30 % cold sucrose before being embedded in Tissue-Tek™ CRYO-OCT Compound. Cryostat sections (12 µm thick) were mounted on SuperFrost*Plus slides (VWR) and stored at -20 °C until ready for use.

Toluidine blue staining on retinal section: before eye nucleation the superior cornea was marked with a hot needle. After 1 hour fixation in 4 % PAF, the anterior segment was removed, except for the superior cornea, and the eyes were fixed overnight at 4 °C. After dehydration through a graded ethanol series, eyecups were embedded in Durcopan (Fluka, Hatfield, PA), cut in 1.5 µm thick sections, mounted on SuperFrost*Plus slides (VWR) and stored at -20 °C until ready for use.

For AKT and FOXO1 detection by western blot: each eye was collected, the cornea was slit with a scalpel blade, lens and vitreous discarded and the retina collected and snap frozen individually in sterile Eppendorf® tubes in liquid nitrogen.

II. mRNA LOCALIZATION

II.A. cDNA cloning and probe preparation

Digoxigenin-labeled riboprobes with alkaline phosphatase detection were used.

II.A.1. Plasmid preparation with *aa-nat* insert

A plasmid (pBK-CMV) (Stratagene®) containing the 1311 bp rat *aa-nat* DNA **(Figure 27)**, was cut by EcoRI and XhoI to get the *aa-nat* DNA. *Aa-nat* DNA was extracted (Zymoclean gel DNA recovery kit) and end converted by a T4 polymerase before *aa-nat* insert ligation into the blunt Pst-blue plasmid vector. Transformation in competent cells (NovablueSingles™) was then performed. The plasmid was sequenced (LGC genomics). We selected the clones 1 (antisense) and 6 (sense) with formaldehyde-

MOPS agarose gel electrophoresis and Kpn1 digestion. The plasmid was linearized with BamH1 and analysed by formaldehyde-MOPS agarose gel electrophoresis.

```
   1 tcagcaggat tgggtcaggg cctgactacc aagccctgct ggcatcatac tgcctggggt
  61 aacatgggag gcagggccag ggggattaga atctctgagc catcacatgc tgtcaggggg
 121 aatgcgggct acagcttcct cgcaggcagg agtctcaggt tctcctcatt cctgcaccca
 181 gtaacagccc cagtgtgacc agctctgtgg tggggacacc tggactcctt cttacagttc
 241 tggtgctaag ggaccacttc caaagctggg gaaccccagg gaggggtcag tggccagata
 301 cccatgttga gcatccaccc cctgaaacct gaggccctgc atctgcctct tgggacctca
 361 gagttcctag gctgccagcg gcgccacaca ctccctgcca gtgagttccg ctgcctcacg
 421 ccggaggatg ccaccagtgc gtttgagatt gagcgcgaag cctttatctc agtctcgggt
 481 acctgccccc tccacttgga tgagatccgg cacttcctca ccctgtgtcc agagctgtca
 541 ctgggctggt tcgaggaggg gtgtcttgtg gccttcatca tcggttcact ttgggacaag
 601 gagagactta ctcaggagtc gctgacacta cacaggcctg gaggccgcac ggcccacctg
 661 cacgtactgg ccgtgcaccg aaccttccgg cagcagggca agggctccgt cctgctgtgg
 721 cgataccttc accacctggg gagtcagccg gcggtgcgcc gggctgtgct catgtgcgag
 781 aacgccctgg tgcccttcta tgagaaattt ggtttccagg ccatgggccc gtgcgccatc
 841 accatgggat ctctcacctt cactgagctg caatgttcct tacggtgcca caccttcctg
 901 aggaggaaca gtggctgctg acccaagctg cgcacttggc catggcgagg gtgggagtga
 961 caagcttggg ggctcctgtc cacttcccag gtcacatcct tctctgccca actagagctg
1021 gctagcatga agggagacag cagttcccaa gtggagtaga gaggtaaggg tcaataaaga
1081 ggacaggaga tggcttccct tcagcacagg ctgctgtctg tccccagtgg accgcttgcc
1141 ttctgaacag tgcacaaagg caagaccagg acgtggaaac gggagcagcg ggaggtttgt
1201 ccccacactt cctcctctcc ctgctctgtt tctgggctcc agtgcggtgc cctggttctt
1261 gggagcctca ctctaggcca ggctgacatc ccttcctggc tcctaagtct gggaatgagg
1321 ggcagccagg agccggggac ttgtgaatgg tggcatcatt ggggtacaga catgacacag
1381 ggccacacca aagtacactc aggcaccaat gtgctggctc acctgcctcc ctagttcccc
1441 ttctatcctg gtccccctac cagccccagt actgacacta ataaagcagc tatgttccc
```

Figure 27. *Rattus norvegicus aa-nat* mRNA.

Reference sequence in NCBI: DQ075321.1. 5'-3'. 1499 base pairs (bp). *Aa-nat* probe is presented in red (1300 bp).

II.A.2. Plasmid preparation with *hiomt* insert

A plasmid (pBluescript) containing rat *hiomt* DNA sequence *(Gauer & Craft, 1996)* was used for *hiomt* cDNA amplification by PCR (dNTP; plasmid; Taq polymerase; primer 1 (254-273); primer 2 (1400-1423)) at Tm = 55 °C. PCR products were analyzed on a formaldehyde-MOPS agarose gel. A 1200 bp *hiomt* cDNA **(Figure 28)** was extracted (Zymoclean gel DNA recovery kit) from the gel and was processed for end conversion. The *hiomt* insert was ligated in the pSTblue-1 plasmid (pSTblue-1 perfectly blunt cloning kit, Novagen) before tansformation in competent cells (NovablueSingles™). The plasmid was then sequenced (LGC Genomics). Sma1 digestion of the plasmid was achieved for *hiomt* insert sense and antisense orientations. The plasmid was linearized with BamH1. This step was checked by formaldehyde-MOPS agarose gel electrophoresis.

```
   1 ctgaggctag gataggcaag atggcacccg gccgggaggg cgagcttgac cgcgacttcc
  61 gagtccttat gagcctcgcc cacggcttca tggtctccca ggtgctgttt gctgccctgg
 121 atctgggcat cttcgacctt gcggcccagg gcccggtggc agcggaggcg gtggcacaga
 181 ctgggggtg gagtccgcgg ggaacgcagc tgctaatgga cgcctgcacc aggctggggc
 241 tactaagagg ggccggggac ggctcctaca ccaactctgc gctgtcatcc acattcctgg
 301 tgagcggaag cccccagtct caacgctgca tgctgctcta cctggcgggc acaacatacg
 361 gctgctgggc ccacctggct gctggggtca gggaagggcg gaaccagtac tccagggccg
 421 tgggcatctc cgctgaggac ccctttcgg ccatctacag gtcagagcct gagcgcctgc
 481 tgttcatgag gggcctgcag gagacatgga gtctatgcgg gggacgggtc ctcacagcct
 541 ttgacctctc acgcttccgg gtcatctgtg accttggcgg cgggtctggg gcgctggcac
 601 aggaggccgc ccgcctctat cccggtagct ccgtgtgtgt ctttgatctc cctgatgtca
 661 tcgccgctgc ccgcacccac ttcctgtcgc caggggcaag acccagtgtg aggtttgtcg
 721 ctggtgactt cttccgttcc cgcctccccc gcgctgacct cttcattctt gcccgggtcc
 781 tgcacgactg ggctgatggt gcctgcgtgg agttgctggg gcggctgcac agggcctgca
 841 ggccaggtgg tgcactactg ctggtggagg cagtgctggc caagggcggg gctgggccgc
 901 tgcggtcgct cctgctgtca ctcaacatga tgctgcaggc tgaggggtgg gagcgccagg
 961 ccagcgacta ccgcaacctg gccactcgtg caggcttccc ccgcctgcag ctgcggcgtc
1021 ctggtgggcc ataccatgcc atgctggccc ggcggggacc ccgccctggg atcatcacag
1081 gagtgggaag taacactacg gggacaggaa gttttgtcac aggtataaga cgtgatgtcc
1141 ctggggcaag aagtgacgct gcagggacag gaagtggcac tggaaacaca ggaagtggca
1201 tcatgctaca gggagagacg ttggaatcag aggtcagcgc cccacaagca ggaagtgacg
1261 ttggcggggc aggaaatgaa cccagaagtg gcaccctcaa gcaaggagac tggaagtgac
1321 tggggagtga gggcagggaa tcctgggcaa gaaatgatgt cccggatggg aatggaggag
1381 ttttggccag gaagtgacgc cataaccaaa acctgtgact tgggatagga agtgacatca
1441 tgggtgggaa tttatgactt ctggacagtt acattacagc tgagagtcag tgagttttag
1501 gcaggaagtg atgtcacagt aatggtgggg taggggacaa taaacgca
```

Figure 28. *Ratus norvegicus hiomt* mRNA.

Reference sequence in NCBI: NM_144759.2. 5'-3'. 1548 bp. *Hiomt* probe is presented in red (1169 bp).

II.A.3. Phenol/chloroform extraction

Hundred µL of linearized plasmid were mixed with 100 µL phenol/chloroform and centrifuged (10000 rpm, 5 min, room temperature). After centrifugation, the aqueous phase was isolated. This step was realized twice. One equal volume of chloroform was added to the supernatant. This solution was then mixed thoroughly and centrifuged (10000 rpm, 5 min, room temperature). Supernatant was saved to which, 1/10 of its volume in NaAcetate 3 M pH 7 and 2.5 volume of ethanol 100 % were added for overnight precipitation at -20 °C. Next day, the sample was centrifuged 45 min (10000 rpm, 4 °C) and the supernatant was discarded. The pellet was washed several times with ethanol 70 % and dissolved in ultra pure (up) H_2O to obtain the plasmid at a 0.5 µg/ µL concentration.

II.A.4. Probe synthesis

Transcription step was performed with 1.5 µg plasmid at 37 °C for 2 hours and in the following buffer: 2 µL NTP RNA labeling mix 10X; 4 µL of transcription buffer 5X; 1 µL RNA polymerase Sp6; H_2O up to a total volume of 20 µL. Then 1 µL RNase-free DNase (1 U/µL) was added to the transcription mix (15 min, 37 °C). Precipitation was then conducted overnight at -20 °C by adding 3 µL Yeast tRNA (10 mg/mL), 3 µL LiCl 4 M and 70 µL cold ethanol 100 % to the sample. Next day, the solution was centrifuged 1 hour (13400 rpm, 4 °C). Once the supernatant discarded, the pellet was washed several

times with ethanol 70 % and dissolved in H_2O up with 0.04 % diethyl pyrocarbonate (DEPC) (Sigma). These transcripts were incubated 30 min at 37 °C. The probe was kept at -20 °C until use.

II.A.5. Northern blotting of the probes

One µL RNA probe was denatured 10 min at 90 °C with 7 µL RNA denaturation buffer **(Table 5)**. Denatured samples were separated onto a formaldehyde-MOPS agarose gel for a 5 hours run in migration buffer at 50 mA (**buffers composition are reported in Table 5**). The gel was washed in 10X standard sodium citrate (SSC) and transferred to nitrocellulose membrane. The membrane was washed in A-DIG buffer, incubated 30 min in blocking buffer (DIG nucleic acid detection kit blocking reagent, Roche) and 1 hour with the primary antibody anti-digoxigenin (anti-digoxigenin-AP Fab fragments; reference number: 11093274910, Roche), 1:20000. The membrane was washed in A-DIG and AP buffers before detection in nitro-blue tetrazolium chloride (NBT) 0.66 % and 5-bromo-4-chloro-3'-indolyphosphate p-toluidine (BCIP) 0.33 %.

	Composition	pH
Denaturation buffer	64 % deionized formamide; 8.3 % formaldehyde; 0.64X MOPS; 64 µg/mL ethidium bromide (BET)	
1.4 % formaldehyde-MOPS agarose gel	1.4 % Agarose; 1X MOPS; 6.3 % formaldehyde	
Migration buffer	1X MOPS; 6.3 % formaldehyde	
A-DIG buffer 1X	100 mM Tris; 150 mM NaCl; 5 mM $MgCl_2$	7.5
AP buffer 1X	100 mM Tris; 100 mM NaCl; 5 mM $MgCl_2$	9.5
SSC 10X	1.5 M NaCl; 150 mM Na Citrate	7

Table 5. Northern blot buffers.

II.B. *In situ* hybridization

Hiomt and *aa-nat* mRNA *in situ* hybridizations were respectively performed on rat and *Arvicanthis ansorgei* retinal sections.

Frozen sections were post-fixed for 20 min with 4 % formalin in 100 mM PB and washed in PBS before dehydration and rehydration through a sequence of 70, 95, 100, 95, 70 % ethanol. After washing in PBS, sections were digested with 0.5 µg/mL proteinase K (Roche, Meylan, France) at 37 °C during 30 min for *aa-nat.* For *hiomt* conditions sections were digested with 0.25 µg/mL proteinase K for 20 min. Retinal sections were quickly washed with cold PBS, post-fixed 5 min with 2 % formalin in 100 mM PB on ice and washed with 0.02 % dimethylpyrocarbonate (DMPC) in cold PBS. Sections were acetylated twice for 10 min in 100 mM triethanolamine and 0.25 % acetic anhydride. Sections were washed with 0.02 % DMPC in PBS, followed by wash in 5X SSC; 0.05 % Tween20; 0.02 % DMPC. *Aa-nat* and *hiomt* probes were denatured for 5 min in 90 °C. Hybridization was performed at 54 °C for *aa-nat* and at 60 °C for *hiomt* during 40 hours with 200 ng/mL labeled sense or antisense probes in hybridization buffer (**buffer composition are reported in Table 6**). Stringency rinses were performed for 6 times 10 min each in 0.1X SSC; 0.05 % Tween20 at 72 °C. Sections were washed in NTE buffer before treated with RNAse (AMRESCO) diluted at 3 µg/mL in NTE buffer at 37 °C 30 min regarding *aa-nat* or 20 min with RNAse at 5 µg/mL for *hiomt*. After washing in NTE buffer, samples

were incubated 1 hour in blocking buffer. Then sections were incubated overnight at room temperature with alkaline phosphatase-labeled anti-digoxigenin antibodies (reference number: 11 093274910, Roche) diluted at 1:5000 in blocking buffer. Sections were rinsed with 0.05 % Tween20 in A-DIG buffer and then in AP buffer. The detection was performed with NBT 0.66 % and BCI 0.33 % during 26 hours for *hiomt* and 2 hours for *aa-nat*. Sections were covered with Crystalmount solution (Sigma Aldrich) and were mounted with a coverslip and Eukitt (ChemLab). Images were obtained by a microscope (Leica DMRB) coupled to a camera video capture (Olympus DP-50) linked to a dedicated computer containing image analysis software (Viewfinder 3.0.1, Pixera).

Semi-quantification of *Aa-nat* mRNA transcripts is representative of the subjective mean staining within the photoreceptor (ONL and IS), INL and GCL from 4 retinal sections of each of 3 different retinas (ie. from 3 different animals) for each time point.

Quantification of *aa-nat* mRNA transcripts by densitometric measures of hybridization signal is representative of the mean of staining from 4 distinct areas in photoreceptor (ONL and IS) of 3 retinas (ie. from 3 different animals) at each time point.

	Composition	pH
Hybridization buffer	50 % formamide; 5X SSC; 5X Denhardt's solution; 0.1 % Tween20; 0.04 % DEPC; 1 mg/ml salmon sperm DNA	
NTE buffer 1X	10 mM Tris; 400 mM Nacl; 2.5 mM EDTA	7.5
A-DIG buffer 1X	100 mM Tris; 150 mM NaCl; 5 mM $MgCl_2$	7.5
Blocking buffer	Roche blocking reagent dissolved at 0.5 % in A-DIG buffer; 0.05 % Tween20	
AP buffer 1X	100 mM Tris; 100 mM NaCl; 5 mM $MgCl_2$	9.5
PBS 1X	137 mM NaCl; 2.7 mM KCl; 8 mM Na_2HPO_4; 1.5 mM KH_2PO_4	7.4
PB 1X	162 mM Na_2HPO_4; 38 mM NaH_2PO_4	7.4

Table 6. *In situ* hybridization buffers.

II.C. Immunofluorescence following *in situ* hybridization

Ten µm retina slices hybridized with *hiomt* probe were washed in PBS and incubated in blocking buffer (1 % bovine serum albumine (BSA); 0.1 % Tween20; 0.1 % sodium azide in PBS) for 1 hour. The slides were then incubated simultaneously with an antibody against cone-arrestin diluted 1:1000 **(for antibodies description, see Table 9)** overnight. Next, following 5 washes in PBS, sections were incubated 2 hours with secondary antibody Alexa488 or 594 (goat anti-rabbit antibody; Invitrogen) diluted at 1:500 in blocking buffer. Cell nuclei were visualized with 4',6'-diamidino-2-phénylindole (DAPI) diluted 1:500. After a final wash in PBS, slides were mounted with PBS/glycerol (1:1) and observed as described for *in situ* hybridization. To overlap *hiomt* mRNA staining and the cone arrestin staining, we modified the color read out for *hiomt* mRNA to obtain a white staining. Indeed we could visualize both staining on the merged pictures **(see Figure 33)**.

III. PROTEIN LOCALIZATION

III.A. Immunohistochemistry with peroxidase methods

AA-NAT, HIOMT and MT_1 immunohistochemistry analysis were performed on *Arvicanthis ansorgei* retinal, pineal gland, cortex and *pars tuberalis* sections.

Antigenic reactivation was performed prior to immunohistochemistry. For that purpose sections were incubated in Tris-EDTA buffer **(buffer composition is reported in Table 7**) for 1 hour at 95 °C and 2 hours at room temperature. Then, sections were rinsed in PBS and permeabilized with 0.1 % Triton X-100 (in PBS) for 5 min. To destroy endogenous peroxidase activity, sections were incubated 30 min in endogenous peroxydase blocking buffer. Sections were rinsed in PBS and saturated in blocking buffer for 1 hour. Samples were then incubated overnight at 4 °C with one of the following primary antibodies diluted in the blocking buffer: anti AA-NAT 3314, diluted 1:1000; anti HIOMT 1478, 1:250; anti MT_1, 1:400 **(Table 9)**. After incubation in primary antiserum solution, sections were washed 5 x 10 min in PBS and incubated for 2 hours in biotinylated donkey anti-rabbit secondary antibody (reference number: 711-066-152, Jackson Laboratory, Bar Harbor, ME) diluted at 1:2000 in blocking buffer. Sections were then washed 40 min in PBS, and incubated for 2 hours in Avidin/Biotin complex coupled to horseradish peroxidase (Vectastain ABC kit, Vector Laboratories) diluted 1:500 in 0.5 % Tween20; 0.2 % fish serum in Tris buffer saline (TBS). Finally, sections were washed in TBS and then in Tris buffer imidazole (TBI). Detection of AA-NAT, HIOMT and MT_1 was conducted using 3,3-diaminobenzidine (DAB) (0.5 mg/mL; Sigma) with H_2O_2 (0.003 %) in TBI for 5 min, 10 min and 15 min respectively. Reaction was stopped in TBS and sections were dehydrated in graded ethanol and toluene baths before mounting and observation under a microscope (Nikon Optiphot 2). Images were obtained by CCD camera video capture linked to a dedicated computer containing image analysis software (Nikon BIA).

	Composition	pH
Tris-EDTA buffer	10 mM Tris; 1 mM EDTA	8
Endogenous peroxydase blocking buffer	0.1 % NaN3; 0.3 % H_2O_2 in PBS	
Blocking buffer	3 % BSA; 0.05 % Tween-20; 0.1 % Triton X-100; 0.1 % sodium azide in PBS	
TBS	25 mM Tris; 150 mM NaCl	7.6
TBI	50 mM Tris; 10 mM Imidazole	7.6

Table 7: Buffers used for immunohistochemistry with peroxidase methods.

III.B. Immunofluorescence on retinal whole-mounts

Immunofluorescence experiment was performed on *Arvicanthis ansorgei* retina whole-mounts to test AA-NAT/phosducine, AA-NAT/Brn3, HIOMT/phosducine, HIOMT/Brn3, MT_1/RET-P3, MT_1/Brn3 co-localizations.

Fixed retinas were permeabilized with 0.3 % Triton X-100 for 1 hour and blocked with 3 % BSA; 0.1 % Tween20; 0.1 % NaN3 in PBS for 48 hours. Then retinas were immersed in two distinct primary

antibodies diluted in blocking buffer for 48 hours at 4 °C under gentle agitation. Antibodies used were: AA-NAT 3314, 1:500 dilution; HIOMT 1478, 1:250; MT_1, 1:400; Brn3, 1:200; anti phosducin, 1:400; RET-P3, 1:50 **(Table 9)**. After extensive wash in PBS, samples were incubated overnight in corresponding secondary antibody: goat anti-rabbit IgG-Alexa488 or -Alexa594 diluted 1:500 (Invitrogen) for AA-NAT, HIOMT and MT_1; donkey anti-goat IgG-Alexa488 for Brn3; rabbit anti-mouse IgG-Alexa594 for anti-phosducin and RET-P3. Retinas were finally thoroughly washed in PBS and flattened onto microscope slides with mounting medium (Prolong, Invitrogen) before their observation using a confocal microscope (Leica).

III.C. Immunofluorescence on retinal section

III.C.1. Phosphorylated-AKT, phosphorylated-FOXO1, FOXO1

P-Akt, P-FOXO1, FOXO1 immunofluorescence determination were performed on retinal sections of C3H/$f^{+/+}$, C3H/$f^{+/+}MT_1^{-/-}$ and C3H/$f^{+/+}MT_2^{-/-}$ mice.

Retinas were permeabilized with 0.1 % Triton X-100 for 5 min and the endogenous peroxidase activity was quenched with 1 % H_20_2 in PBS during 1 hour. Retinas were then incubated in blocking buffer (BSA 1 % in PBS) 1 hour and in primary antibody overnight at 4 °C. The primary antibodies were as follows: P-AKT (Ser473), 1:200 dilution; P-FOXO1 (Ser256), 1:500; FOXO1, 1:200 **(Table 9)**. After extensive wash in PBS, retinas were incubated 1 hour in HRP conjugate secondary antibody (Tyramide Signal Amplification Kit #12; Life technologies), 1:100. Retinas were washed once more in PBS, incubated 10 min with labeled tyramide (Tyramide Signal Amplification Kit #12; Life technologies), 1:100; washed thoroughly in PBS and mounted with Prolong medium (Life technologies) before examination with confocal microscope (Zeiss LSM700).

III.C.2. AKT pan, peanut agglutinine, red/green cones, blue cones

AKT pan, peanut agglutinine (PNA), red/green opsin and blue opsin immunofluorescence experiments were performed on retinal sections of C3H/$f^{+/+}$, C3H/$f^{+/+}MT_1^{-/-}$ and C3H/$f^{+/+}MT_2^{-/-}$ mice.

The sections were permeabilized with 0.1 % Triton X-100 (in PBS) for 5 min and then saturated with blocking buffer (3 % BSA, 0.05 % Tween20, 0.1 % Triton X-100, 0.1 % sodium azide in PBS) during 2 hours. A set of sections was incubated with rhodamine coupled to PNA (in order to stain the cone matrix sheaths), 1:500 for 2 hours. Others sections were incubated with primary antibody diluted in blocking buffer: red/green opsin, 1:1000; blue opsin, 1:500; AKT pan, 1:50 **(Table 9)** overnight at 4 °C. Secondary antibody incubation was performed at room temperature for 2 hours with Alexa488 conjugated goat anti-rabbit or Alexa568 conjugated goat anti-mouse, 1:500 (Invitrogen). Retinas were washed thoroughly in PBS, mounted with Prolong medium and observed with a confocal microscope (Zeiss LSM700).

III.C.3. Cones counting

PNA, red/green opsin and blue opsin positive cells were counted on retinal sections of C3H/$f^{+/+}$, C3H/$f^{+/+}MT_1^{-/-}$ and C3H/$f^{+/+}MT_2^{-/-}$ mice.

Pictures were done of the central, middle and peripheral areas of the retina (six regions in total) **(Figure 29)**. The number of positive PNA cells in cone matrix sheath (at the level of cones segment) and opsin cells in OS were counted in a 140 µm length area for each region of the retina.

The number of cones in the retina represents the average of the six values and was determined for each animal.

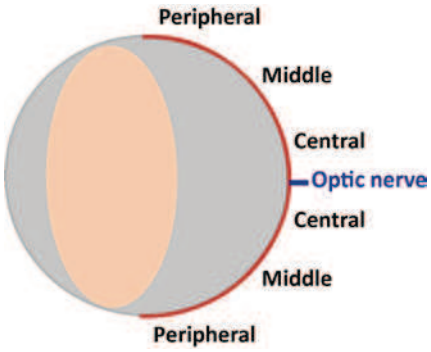

Figure 29. The 6 regions of the retina for cones counting.

III.D. Outer nuclear layer cell counting

ONL cells were counted on retinal sections of C3H/$f^{+/+}$, C3H/$f^{+/+}MT_1^{-/-}$ and C3H/$f^{+/+}MT_2^{-/-}$ mice.

Retinal sections were stained with toluidine blue. Photoreceptor nuclei were counted in a 10 µm microscopic field that was centered at 300 µm above the edge of the optic nerve head. For each sample, we counted the number of photoreceptor cells in 10 different locations within each of three adjacent sections. The number of nuclei in the ONL was counted using the Image-Pro Plus 3.0 software. The data obtained from the different adjacent sections were combined. Measurements were made by observers who were blinded to the genotype and age of the samples.

IV. WESTERN BLOT

IV.A. AA-NAT detection

AA-NAT western blot analysis was performed on *Arvicanthis ansorgei* retina.

Each retina was subjected to ultrasonication in 200 µL of cold lysis buffer **(buffers composition is reported in Table 8)**. Samples were centrifuged for 20 min at 13000 rpm and supernatants were collected. Protein content in the extracts was determined using the Lowry method *(Lowry et al., 1951)*, with BSA as standard (ascending concentrations 0.125, 0.250, 0.500, 0.750 and 1 mg/mL). Retinal proteins (24 µg/ per sample) were mixed with Laemmli buffer (BioRad laboratories, Hercules, Ca, USA) containing 5 % β-mercaptoethanol (Sigma Aldrich) and boiled for 5 min. Samples were separated once loaded onto SDS-polyacrylamide gels (4-10 %) and a run in electrophoresis buffer 1 hour at 100 V. After transfer to polyvinylidene fluoride (PVDF) membranes (immobilon-P, Millipore) in transfer buffer, membrane strips were blocked in 0.2 % Tween20; 5 % fat-free milk in TBS for 1 hour. Then membranes were incubated overnight at 4 °C with the primary antibody diluted in blocking buffer: AA-NAT 3314, diluted 1:15000; AA-NAT 3305, 1:30000; AA-NAT 3352, 1:14000; 14-3-

3, 1:1000 **(Table 9)**. The following day, membranes were rinsed in TBS 0.2 % Tween20 and incubated with the secondary antibody (goat anti rabbit, HRP; reference number: 111-035-144, Jackson) diluted at 1:200000 in TBS 0.2 % Tween20 with 0.25 % fish gelatin for 2 hours. The signal was developed by chemoluminescence (kit Amersham^{TM}, GE Healthcare) and revealed by autoradiography (CL-XPosure films, Thermo Scientific). Analyses of immunoblots were performed on 3 to 5 retinas from different animals at each time point. Normalization was done against ACTIN protein detected on the same membrane.

	Composition	pH
Lysis buffer	20 mM Tris; 150 mM NaCl; 1 mM EDTA; 1 % Triton X-100; 0.2 % Sodium dodecyl sulphate (SDS); 1 mM DTT; 4 % protease inhibitor cocktail (Roche, Mannheim, Germany); 1 % phosphatase inhibitor cocktail (Sigma Aldrich)	7.6
10 % acrylamide running gel	10 % acrylamide/0.1 % bis acrylamide; 0.37 M Tris; 0.1 % SDS; 0.1 % ammonium persulfate (APS); 0.1 % TEMED	8.8
4.5 % acrylamide Stacking gel	4 % acrylamide/0.1 % bis acrylamide; 0.12 M Tris; 0.1 % SDS; 0.1 % APS; 0.1 % TEMED	6.8
Electrophoresis buffer	250 mM Tris; 750 mM glycine; 1.5 % SDS	
Transfer buffer	25 mM Tris; 192 mM glycine; 20 % methanol	

Table 8. Western blot buffers.

IV.B. AKT and FOXO1 detection

AKT and FOXO1 western blot analysis was performed on C3H/$f^{+/+}$, C3H/$f^{+/+}MT_1^{-/-}$ and C3H/$f^{+/+}MT_2^{-/-}$ mice.

Retinas were sonicated in cell extraction buffer (Life technologies) and briefly centrifuged. The protein contents of the supernatants were determined by Micro BCA Protein Assay Kit (Thermo Fisher Scientific, Rockford, IL). Proteins (10 µg/lane) were separated as described previously and transferred to Immobilon-P transfer membrane (Millipore, Billerica, Massachusetts, MA). Membranes were briefly washed with TBS 0.1 % Tween20, blocked for 1 hour at room temperature in TBS 0.1 % Tween20 containing 5 % nonfat milk powder or BSA. Membranes were washed with TBS 0.1 % Tween, and then incubated with specific primary antibodies: P-AKT_{Ser473}, P-AKT_{Thr308} , AKT pan, P-$FOXO1_{Ser256}$, FOXO1 **(Table 9)** diluted 1:5000 - 1:80000 in TBS 0.1 % Tween20 containing 1 % nonfat milk or BSA for 16 hours at 4 °C. Membranes were then washed 4 times for 10 min with TBS 0.1 % Tween20 previous incubation with HRP-conjugated donkey anti-rabbit IgG or anti-mouse IgG diluted 1:1000-1:5000 (Cell signaling technology) in TBS 0.1 % Tween20 containing 1 % nonfat milk. Membranes were finally washed 4 times for 10 min with TBS 0.1 % Tween20. SuperSignal West Femto Chemiluminescent Substrate (Thermo Scientific) was used to detect the antigen.

V. ENZYMATIC ASSAYS

Enzymatic assays were performed on *Arvicanthis ansorgei* retina.

Analysis of retinal HIOMT and AA-NAT enzymatic activities were performed as previously described in pineal gland *(Ribelayga et al., 1997)* adapted from *(Axelrod & Weissbach, 1961)* for HIOMT and

(Garidou et al., 2001) adapted from *(Deguchi & Axelrod, 1972b; Namboodiri et al., 1979)* for AA-NAT, with some modifications. Enzymatic activities were determined within the 24 hours following sacrifice of the animals. Individual left eyeballs were sonicated in 100 µL of PB (0.05 M; pH 8.25) for HIOMT activity determination. Right eyeballs were sonicated in 80 µL of acetyl-CoA 0.35 mM (Sigma) in PB (0.05 M; pH 6.8) for AA-NAT activity determination. For HIOMT activity assay, 50 µL of the tissue homogenate was incubated for 30 min at 37 °C with 1 mM N-acetylserotonin (Sigma, Saint Quentin Fallavier, France) as substrate and 43.8 µM *S*-adenosyl-l-[^{14}C]methionine (SAM; 59.3 mCi/mmol; NEN-Dupont, Le Blanc Mesnil, France) in a final volume of 100 µL. For AA-NAT activity assay, 40 µL of tissue homogenate was incubated for 20 min at 37 °C in the presence of 80 mM tryptamine (Sigma) as a substrate and 192 µM [^{14}C] acetyl-CoA (47 mCi/mmol; NEN-Dupont, Zaventem, Belgium) in a final volume of 80 µL. The reaction was stopped on ice for AA-NAT activity assay and by the addition of 200 µL of cold sodium borate buffer (12.5 mM $Na_2B_4O_7$, $10H_2O$; pH 10) for HIOMT activity assay. Newly synthesized melatonin or N-acetyltryptamine was assessed after extraction in 1 mL of water-saturated chloroform. Radioactivity determination was done after evaporation of the organic solvent. HIOMT and AA-NAT activities are expressed as picomoles/mg proteins/hour.

VI. HPLC

HPLC measurement was performed on *Arvicanthis ansorgei* retina.

Each frozen retina was homogenized by ultrasonication in 100 µL of cold mobile phase (1 % methanol (V/V); 50 mM citric acid; 40 mM Na_2HPO_4; 0.8 mM EDTA and 0.3 mM Octan Sulfonic Acid dissolved in H_20), 0.22 µm filtered and degassed under vacuum plus ultrasonication (final pH is 3.3)). The samples were centrifuged (13000 rpm for 30 min) and supernatants were analyzed for dopamine and 3,4-dihydroxyphenylacetic acid (DOPAC) with an HPLC system using an amperometric electrochemical detector (HPLC-ED; Decade II Antec, Leyden, Netherlands). The electrochemical flowcell VT-03 was an Ag/AgCl (filled with saturated KCl) versus glassy carbon electrode configuration. For detection, the working potential was set at 0.6 V between working electrode and auxiliary electrode. The range of sensitivity was 2 nA (full scale on the chromatogram) with an offset of 50 % to avoid peak saturation, and the electrochemical signal was smoothed with a filter set at 0.005Hz. The temperature of the oven, which included the cell detection and the column, was maintained at 34 °C. The HPLC-ED system was also composed of a high pressure pump (515, Waters, Milford USA, Japan) and an autosampler (Triathlon, Spark, Emmen, Netherlands), which allowed sample cooling at 4 °C. Each 20 µL sample was injected on a 100 mm length 3 mm internal diameter C18 column (Kinetex C18- and XB-C18, 2.6 µ, 100 A, Phenomenex, Torrance, CA, USA) equipped with a guard column. For isocratic separation, the flow rate was kept at 0.8 mL/min. Standard solutions (prepared in 10 mM HCl) of dopamine and DOPAC (Sigma Aldrich, Saint-Quentin Fallavier, France) were stored at 4 °C and protected from light. These were diluted in the same solution as used for the samples in order to obtain a 3 points standard curve for each standard. Values were expressed using the acquisition software Azur v4.5 (Datalys, St Martin d'Hères, France). The results are presented in pg/µL.

VII. ELISA

Melatonin quantification by ELISA was performed on *Arvicanthis ansorgei* and C3H/f$^{+/+}$ retina.

In order to assess melatonin content in the mouse retinas, we used a melatonin ELISA kit (RE54021, IBL international GMBH) following the protocol described in the manual instruction. Briefly, retinas were sonicated in Ammonium acetate buffer with protease inhibitor. The protein concentration was determined for each retina by Bradford protein assay. Retinas, standards and controls were extracted with 100 % methanol and pipetted into distinct wells of the microtiter plate (in duplicates). Biotinylated melatonin and melatonin antiserum (rabbit, polyclonal) were added into each well. The plate was incubated during 17 hours at 4 °C. The incubation solution was then discarded and wash buffer was added to each well. After adding of enzyme conjugate, the plate was incubated 2 hours at room temperature. After discarding the incubation solution and washing each well, the substrate solution (p-nitrophenyl phosphate (PNPP)) was added. The plate was incubated 40 min at room temperature. The substrate reaction was stopped by adding the PNPP stop solution. The optical density (OD) was measured with a photometer at 405 nm. The obtained OD of the standards is plotted against their concentration. The concentration of the samples can be read directly from the standard curve. The results are presented in pg melatonin/mg protein.

VIII. STATISTICAL ANALYSIS

Data are given as the mean ± standard error of the mean (SEM) of n = 3-5 animals. In order to compare changes of mRNA, protein, enzyme, hormone levels, we performed one-way analysis of variance (ANOVA) followed by post-hoc comparisons. Holm-Sidak test was used for post-hoc comparisons exept for the western blot P-AKT and P-FOXO1 (Article II) where Tukey test was used. These analyses were achieved with the Sigma plot software (Jandel Scientific, Chicago, IL, US). p values above 0.05 were considered non significant.

Antibody anti-	Antigen	Type	Known distribution	Source, references
cone-arrestin	Synthetic peptide of cone arrestin	Rabbit PAB	Cone arrestin (OS)	Generous gift of Dr. Craft, Doheny Eye Inst. USC, Los Angeles, USA
Phosducine	Nd	Mouse MAB	Rods	*(Bobu et al., 2008)*
AA-NAT 3314	aa 25-200 of rat AA-NAT	Rabbit PAB		Generous gift of Dr D.C Klein, National Institute of Child Health and Human Development (Bethesda, Maryland, USA)
AA-NAT 3352	aa 22-37p of rat AA-NAT. Detect only the phosphorylated form of AA-NAT	Rabbit PAB		Generous gift of Dr D.C Klein, National Institute of Child Health and Human Development (Bethesda, Maryland, USA) *(Pozdeyev et al., 2006)*
AA-NAT 3305	aa 1-24 of rat AA-NAT. Detect only the phosphorylated form of AA-NAT	Rabbit PAB		Generous gift of Dr D.C Klein, National Institute of Child Health and Human Development (Bethesda, Maryland, USA)
14-3-3zeta	Recombinant fusion protein of aa 51-150 of mouse 14-3-3 zeta	Mouse PAB		Abcam, 52875
HIOMT 1478	rat HIOMT	Rabbit PAB		Generous gift of Dr T.Bourgeron, Institut Pasteur (Paris, France)
MT_1	aa 218-236 C-terminal of mouse MT_1	Rabbit PAB	OS, INL, GCL	*(Sengupta et al., 2011)*
Brn3	Synthetic sequence of aa 397-410 C-terminal of human Brn3b	Goat PAB	RGC	Santa Cruz, #sc-6026 *(Xiang et al., 1993; Poché et al., 2008)*
RETP3	Rat retinal homogenate	Mouse MAB	Rods CB	*(Barnstable, 1980)*
P-AKT_{Ser473} (D9E)	Synthetic P-peptide of aa Ser473 of human AKT	Rabbit MAB	OS	Cell Signaling, #4060 *(Jomary et al., 2006)*
P-AKT_{Thr308} (C31E5E)	Synthetic P-peptide of aa Thr308 of human AKT	Rabbit MAB		Cell Signaling, #2965
AKT pan (40D4)	Synthetic peptide of C-terminal aa of human AKT (detects P- and UnP-AKT)	Mouse MAB		Cell Signaling, #2920
P-$FOXO1_{Ser256}$	Synthetic P-peptide of aa Ser256 of human FOXO1	Rabbit PAB	OS, GCL	Cell Signaling, #9461 *(Jomary et al., 2006)*
FOXO1 (C29H4)	GST fusion protein of C-terminal human FOXO1 aa (detects P- and UnP-FOXO1)	Rabbit MAB		Cell Signaling, #2880
Red/green opsin	Recombinant human red/green opsin	Rabbit PAB	Cone opsin (OS)	Chemicon, AB5405
Blue opsin	Recombinant human blue opsin	Rabbit PAB	Cone opsin (OS)	Chemicon, AB5407

Table 9. Primary antibodies.

aa: amino-acid; PAB: polyclonal antibody; MAB: monoclonal antibody; P-: phosphorylated; UnP-: unphosphorylated; nd: not determined.

RESULTS

CHAPTER I

MELATONIN SYNTHESIS IN THE RODENT RETINA

Article I

Unique regulation of the melatonin synthetic pathway in the retina of diurnal female *Arvicanthis ansorgei* (Rodentia)

Coralie Gianesini[1], Daniel Clesse[2], Gianluca Tosini[3], David Hicks[1] and Virginie Laurent[1]

[1] CNRS UPR 3212, Institute for Cellular and Integrative Neurosciences, 5 rue Blaise Pascal, F-67084, Strasbourg, France

[2] CNRS UMR 7364, Laboratoire de Neurosciences Cognitives et Adaptatives, Université de Strasbourg, Faculté de Psychologie, 12 rue Goethe, F-67000 Strasbourg

[3] Department of Pharmacology and Toxicology, Morehouse School of Medicine, 720 Westview Drive, Atlanta, GA 30110, United States

Corresponding author: Virginie Laurent, CNRS UPR 3212, Institute for Cellular and Integrative Neurosciences, 5 rue Blaise Pascal, F-67084, Strasbourg, France. gydelaurent@inci-cnrs.unistra.fr

Abstract

Knowledge about melatonin synthesis and its potential roles within the retina remains fragmented, especially in mammals where studies have focused on the penultimate enzyme of melatonin synthesis Arylalkylamine N-acetyltransferase (AA-NAT), whereas the final enzyme necessary for melatonin production is Hydroxyindole-O-methytransferase (HIOMT). We explored multiple parameters of the melatonin synthetic pathway in the cone-rich retina of a diurnal rodent, *Arvicanthis ansorgei*, the cones being previously implicated as probable reservoirs of melatonin production. We analyzed the temporal and spatial expression of *Aa-nat* mRNA and AA-NAT protein, and enzymatic activity of AA-NAT, HIOMT, as well as the high-affinity melatonin receptor MT_1 and melatonin itself. We report that *Aa-nat* mRNA was localized principally to cones and ganglion cells (RGC) with opposing cyclic expression, being maximal in cones during the night, and maximal in RGC in the daytime. AA-NAT protein was also immunolocalized to these same populations, and was globally present and active throughout the 24 hour period. HIOMT immunolocalization largely mirrored that of AA-NAT, but expression levels and activity were extremely low and remained uniform throughout the 24 hour period. MT_1 showed a complementary expression pattern to the synthetic enzymes, present in rod photoreceptors, some inner retinal neurons and RGC. Surprisingly, melatonin levels were consistently low throughout the day-night cycle, in accordance with the low expression and activity levels of HIOMT. These data demonstrate that the melatonin synthetic pathway in diurnal rodents differs from that described for other tissues and species, the contrasting expression in photoreceptors and RGC suggesting distinct roles in these populations.

Introduction

Melatonin is a ubiquitous molecule retained throughout evolution from bacteria to humans acting as a substrate for multiple functions ranging from antioxidant properties to circadian clock output *(1,2)*. In mammals, melatonin is a neurohormone synthesized principally at night by the pineal gland *(3)*. Circadian regulation of this indolamine is controlled by a poly-synaptic pathway commencing with retinal photoreception, neural transmission to the hypothalamus and relays within the autonomic nervous system. Then transduction of the neural message into a biochemical output occurs within the pineal gland *(3,4)*. Melatonin, as a prominent output of the central circadian clock, modulates a wide array of physiological functions such as the sleep/wake cycle *(5)*, reproduction *(6,7)* and immune modulation *(8)*. Melatonin is also synthesized *de novo* in the vertebrate retina where it can exert local effects on photoreceptor phagocytosis *(9,10)*, neuronal electric activity *(11,12)*, dark adaptation *(13)* and light sensitivity *(14)*, by way of specific MT_1 and MT_2 receptors expressed in the eye *(15,16)*. In nocturnal rodents MT_1 receptors are localized in photoreceptors, inner nuclear layer (INL) and retinal ganglion cells (RGC) *(12)*. Furthermore, a melatonin-proficient mouse that lacks MT_1 displays reduced viability of photoreceptors and RGC during aging *(11)*. Nevertheless, our knowledge about melatonin synthesis, regulation and precise role(s) remains fragmented in mammalian retina. The available evidence shows that melatonin synthesis in nocturnal rodent retinas shares many classical features with that of the pineal gland, such as the biochemical substrates (tryptophan and serotonin) and enzymatic machinery (notably AA-NAT and HIOMT) *(17,18)*. AA-NAT, under the control of light, a retinal circadian clock and proteasome formation, represents the limiting enzyme of rhythmic melatonin secretion *(19)*. As in the pineal gland, within the retina *Aa-nat* mRNA is maximal in the middle of the night *(20,21)* when melatonin synthesis takes place.

Localization studies in the retina have revealed contrasting results: whereas one study detected *Aa-nat* mRNA exclusively within a subpopulation of photoreceptor cells that resemble cones in number and distribution *(22)*, another group reported a much wider expression pattern, throughout the photoreceptors and in the INL and RGC *(23)*. In chicken retina, *Aa-nat* mRNA is mainly detected in photoreceptors *(24)* and at a lower level in RGC *(25)*. Compared to rodents, primate retina show a very different spatial and temporal expression pattern of both *Aa-nat* and AA-NAT. Primate *Aa-nat* levels are virtually equal between night and day, while AA-NAT shows marked nightly increase *(26)*. In rodents, expression levels of *Aa-nat* vary greatly between night and day. These differences indicate that control of melatonin synthesis occurs at the level of transcription in rodents, while in primates this control is principally post-translational *(26)*. HIOMT is the true rate-limiting step of N-acetyl serotonin (NAS, the product of AA-NAT) conversion into melatonin *(27)*. HIOMT/*hiomt* biology is still poorly understood, partly because the level of *hiomt* gene expression is low and constitutive in rat retina *(28)*, partly because HIOMT has not been detected in non-human primate eyes *(26)*, and also because its sequence is extremely divergent between species *(29)*. Only chicken retinas express HIOMT protein in photoreceptors *(30)*. The aim of this study was therefore to characterize the retinal melatonin synthetic pathway as completely as possible, through analyzing the spatial and temporal expression patterns of *Aa-nat*, AA-NAT, *Hiomt* and HIOMT, as well as their relative activities.

Emphasis is made on the use of a diurnal rodent *Arvicanthis ansorgei (31)*: this species possesses a retina whose morphology has two great advantages: i) compared to nocturnal rats and mice with only 1-3% cones *(32,33)*, this population makes up 33% of total photoreceptors in *Arvicanthis (34)*. As available evidence suggests cones are an important site of melatonin production *(22)*, and cones are

essential to human eyesight, enabling high acuity chromatic vision *(35,36)*, this species constitutes a potentially valuable experimental model; ii) these cones are neatly arranged in two rows of cell bodies overlying the rods, a feature which facilitates discrimination between photoreceptor types *(34)*. Finally the photic niche of this species makes it simpler to extrapolate towards other diurnal species including humans. Our data indicate that the melatonin synthetic pathway in *Arvicanthis* differs in several respects from both nocturnal rodent and diurnal primate (and chicken) retinas, contrasting with the accepted models of melatonin regulation and functional effects.

Materials and methods

Animals

This study was conducted with young adult (3-6 month) female Sudanian Unstriped Grass Rats *Arvicanthis ansorgei*, raised in our animal facilities (Chronobiotron) under conditions of cyclic light (12 h white light, ~100 lux) and darkness (LD), as previously described *(34)*. In some experimental series, animals were maintained in constant darkness (DD) for 24 h prior to tissue collection, performed during the following 24 h, still under DD. Animals were anesthetized by isoflurane inhalation and immediately decapitated every 4 h over a period of 24 h. Zeitgeber Time 0 (ZT0) and circadian time (CT) 0 are defined as the beginning of the day (real or subjective), when lights are turned on (or expected to be turned on), 07:00 h. For immunohistochemistry and *in situ* hybridization studies, eyes were treated as detailed previously *(34)*. Regarding all other experiments, retinas were rapidly isolated by slitting the cornea with a scalpel blade, discarding the lens and vitreous and snap frozen individually in sterile Eppendorf® tubes in liquid nitrogen. Animal treatment and experimentation were in agreement with institutional and national guidelines, and adhered to the Association for Research in Vision and Ophthalmology Guidelines for Use of Animals, to the European Communities Council Directive of 24 November 1986 (86/609/EEC) and the Animal Use and Care Committee from Strasbourg. The experimental procedures were covered by European authorization to perform animal experimentation (CREMEAS, AL/24/31/02/13).

In situ hybridization

We used a previously published protocol *(37)* with some modifications. Sense and anti-sense riboprobes were transcribed from linearized plasmide (pBK-CMV phagemid) containing a 1311 base pairs rat *Aa-nat* cDNA (Stratagene®, La Jolla, CA, USA) in the presence of digoxygenin-labeled nucleotide (Roche, Meylan, France). Frozen retinal sections were post-fixed for 20 min with 4% formalin in 100 mM PBS before dehydration and rehydration through a sequence of 70%, 95%, 100%, 95%, 70% ethanol. Sections were digested by 0.5 µg/mL proteinase K (Roche, Meylan France) at 37°C for 30 min. Hybridization was performed at 54°C with 200 ng/mL labeled sense or antisense probes in 50% formamide, 5X Standard Sodium Citrate (SSC), 5X Denhardt's solution, 0.1% Tween20, 0.04% DEPC and 1 mg/mL salmon sperm DNA. Sections were treated with RNAseA (AMRESCO) at 3 µg/mL in NTE buffer (Tris 100 mM, Nacl 400 mM, EDTA 25mM) at 37°C 30 min. Alkaline phosphatase activity was detected after 2 h. Relative quantification of *Aa-nat* mRNA transcripts is representative of the subjective mean staining within the photoreceptor (outer nuclear layer or ONL), INL and ganglion cell layer (GCL) from four retinal sections of each of three different retinas (n=3) for each time point.

Immunohistochemistry

The protocol was adapted from published procedures *(38)*. For AA-NAT and HIOMT immunostaining, antigen retrieval was performed in Tris-EDTA buffer (Tris 10 mM, EDTA 1 mM, pH 8) for 1 h at 95°C followed by 2 h slow cooling at room temperature. Then retinas were permeabilized with Triton X-100 (0.1% in PBS) for 5 min, and sections were saturated in blocking buffer (3% BSA, 0.05% Tween-20, 0.1% Triton -X100 and 0.1% sodium azide in PBS) for 1 h. Retinas were incubated overnight at 4°C with different primary antibodies diluted in the blocking buffer: rabbit polyclonal cone arrestin (generous gift of Dr. C. Craft, Doheny Eye Institute, USC, Los Angeles, USA) and was used at 1/5000 dilution; rabbit polyclonal anti-rat AA-NAT 3314 was a generous gift from Dr D.C Klein, National Institute of Child Health and Human Development (Bethesda, Maryland, USA), 1/1000; rabbit polyclonal anti-rat HIOMT 1478 was a generous gift of Dr T. Bourgeron, Institut Pasteur (Paris, France), 1/250; rabbit polyclonal anti-mouse MT_1 *(12)*, 1/400. Sections were then incubated with the appropriate secondary antibody (Jackson Labs, Bar Harbor, ME; 711-066-152) and the Avidin/Biotin/horseradish peroxydase complex (Vectastain ABC kit, Vector Laboratories). Detection of AA-NAT, HIOMT and MT_1 signals was conducted using 3,3-diaminobenzidine (0.5 mg/mL, Sigma) with H_2O_2 (0,003%) in Tris Buffer Imidazole (TBI) for 5 min, 10 min and 15 min respectively. The sections were dehydrated in graded ethanol followed by toluene baths before mounting and observation under a microscope (Nikon Optiphot 2). Images were obtained by CCD camera video capture linked to a dedicated PC containing image analysis software (Nikon BIA).

Immunohistochemistry of whole-mounted retina

The protocol is according to published methods from our laboratory *(39)* with some modifications. Briefly, fixed retinas were treated for antigenic reactivation as described above. Samples were blocked with PBS buffer containing 3% BSA, 0.1%Tween-20, 0.1% NaN3 for 48 h. Then retinas were immersed in the primary antibody solution for 48 h at 4°C. Antibodies used were: AA-NAT 3314, 1/500 dilution; HIOMT 1478, 1/250; goat polyclonal anti-human Brn3 (Santa Cruz, CA; #sc-6026), 1/200; mouse monoclonal phosducin, 1/400 *(40)*, and mouse monoclonal RET-P3 *(41)*, 1/50. Brn3 expression is restricted to nuclei of RGC in *Arvicanthis (42)*; phosducin is specific to rod cytoplasm and provides a robust marker of rod IS; RET-P3 (of which the antigen is unknown) is specific to rod cell bodies and provides a reliable marker of this compartment. Samples were incubated overnight in corresponding secondary antibodies: goat anti-rabbit IgG-Alexa488 or -Alexa594 diluted 1/500 (Invitrogen) for AA-NAT and HIOMT, donkey anti-goat IgG-Alexa488 for Brn3, and rabbit anti-mouse IgG-Alexa488 or Alexa594 for anti-phosducin and RET-P3. Retinas were flattened onto microscope slides with mounting medium (Prolong, Invitrogen) and observed using a confocal microscope (Leica).

Western blotting

The protocol was adapted from a previous publication *(34)*: equal amounts of total protein (24 µg/lane) were separated by electrophoresis and transferred to polyvinyl difluoride (PVDF) membranes (Millipore; Immobilon-P). The membranes were blocked and incubated with anti-AA-NAT 3314 diluted 1/15000 in blocking buffer overnight at 4°C. Membranes were rinsed in TBS Tween-20 0.2% and incubated with the secondary antibody (goat anti rabbit-HRP, Jackson 111-035-144) diluted 1/200000 in TBS Tween 0.2% with 0.25% fish gelatin for 2 h. The signal was developed by chemoluminescence (kit Amersham™, GE Healthcare) and revealed by autoradiography (CL-XPosure films, Thermo Scientific). Analyses of immunoblots were performed on five retinas from different

animals at each time point. Normalization was achieved against actin protein detected on the same membrane.

Enzymatic assays

Analyses of HIOMT and AA-NAT enzyme activities were performed in *Arvicanthis ansorgei* retinas as previously described for pineal gland *(43,44)*. Individual left retinas were sonicated in 100 µL of phosphate buffer (0.05 M; pH 8.25) for determination of HIOMT activity. Right retinas were sonicated in phosphate buffer (0.05 M, pH 6.8) containing 0.35 mM acetyl-CoA (Sigma) for AA-NAT activity determination. HIOMT and AA-NAT activities are expressed as pmoles/mg protein/hour.

HPLC measurements

Each frozen retina was homogenized by ultrasonication in 100 µL of mobile phase [1% methanol (V/V), 50 mM citric acid, 40 mM Na_2HPO_4, 0.8 mM EDTA and 0.3 mM Octan Sulfonic Acid. The samples were centrifuged (13000 rpm -16100 g) for 30 min and supernatants were analyzed for dopamine and 3,4-dihydroxyphenylacetic acid (DOPAC) with an HPLC system using an amperometric electrochemical detector (HPLC-ED; Decade II Antec, Leyden, Netherlands). For the detection, the working potential was set at 0.6 V. The temperature of the column and cell detection was maintained at 34°C. Each 20 µL sample was injected on a 100 mm length, 3 mm internal diameter, C18 column (Kinetex C18- and XB-C18 -2.6µ 100A, Phenomenex, Torrance, CA, USA). For the isocratic separation, the flow rate was kept at 0.8 mL/min. Standard solutions of dopamine and DOPAC (Sigma Aldrich, Saint-Quentin Fallavier, France) were diluted in the same mobile phase in order to obtain a 3 points standard curve for each standard for the quantification of the samples.

Melatonin quantification by ELISA

Melatonin ELISA kit (RE54021, IBL international GMBH) was used to perform the melatonin immunoassay following the protocol described in the kit instructions. For comparative purposes we analyzed melatonin levels both in diurnal *Arvicanthis* but also nocturnal mouse retinas, the latter involving the melatonin-competent C3H strain *(11)*. Briefly, Retinas, standards and controls were individually extracted in ammonium acetate buffer with protease inhibitor. The protein concentration was determined for each retina by a Bradford protein assay. Samples were incubated during 17 h at 4°C with the melatonin antiserum (rabbit polyclonal). The optical density (OD) was measured at 405 nm. The obtained ODs of the standards are plotted against their concentration. The results are presented in pg melatonin/mg protein.

Statistical analysis

Data are given as the mean ± SEM of n = 3-5 animals. Statistical analysis was performed with one-way analysis of variance (ANOVA) using the Sigma plot software. The significant level was set at $p < 0.05$. When required, ANOVA were followed by post-hoc Holm-Sidak test.

Results

Aa-nat mRNA expression in cone photoreceptors and RGC of *Arvicanthis ansorgei* shows phase-inversed expression under cyclic light conditions

We performed *in situ* hybridization studies with digoxygenin-conjugated RNA probes. Since previous publications for nocturnal rodents report a nocturnal peak in *Aa-nat* RNA levels, we first examined retinal sections prepared at ZT19. Staining was observed uniquely within and lying directly above the two scleral-most rows of cells of the outer nuclear layer (ONL) **(Figures 1A, B)**, with no detectable signal elsewhere in the retina (lower ONL, INL and GCL respectively). At the middle of the day, ZT6, hybridization signal was no longer apparent in the ONL but was now detected strongly in the GCL, and weakly in the INL **(Figure 1C)**. These localizations are shown at higher magnification in **Figures 1D-H**. We used anti-cone arrestin antibody to identify the cell type expressing *Aa-nat* at ZT19 **(Figures 1D, E)**: *Aa-nat* transcripts were localized to the apical cytoplasm and inner segments (IS) of cones. As stated earlier, GCL was not labeled at ZT19 **(Figure 1F)**, but at ZT6 labeling was no longer detectable in cones **(Figure 1G)**, whereas positive signal was clearly seen in the GCL **(Figure 1H)**. Sense probe controls did not demonstrate any signal **(Figure 1I)**. Validation of the *Aa-nat* probe was performed with rat retina, and similar results were obtained (at ZT19 we observed scattered staining of individual cells located near the sclera margin, corresponding to cones: **Supplemental Figure 1**).We examined *Aa-nat* hybridization in sections taken across the entire 24 h period, and used a semi-quantitative scale to record expression levels and cellular localization **(Table 1)**. It was seen that expression within the cones was faint or undetectable throughout the day, but intense during the night; expression within the INL was always weak but could be seen at both night and day; and expression in the GCL was moderate to strong during the day but below detection levels at night.

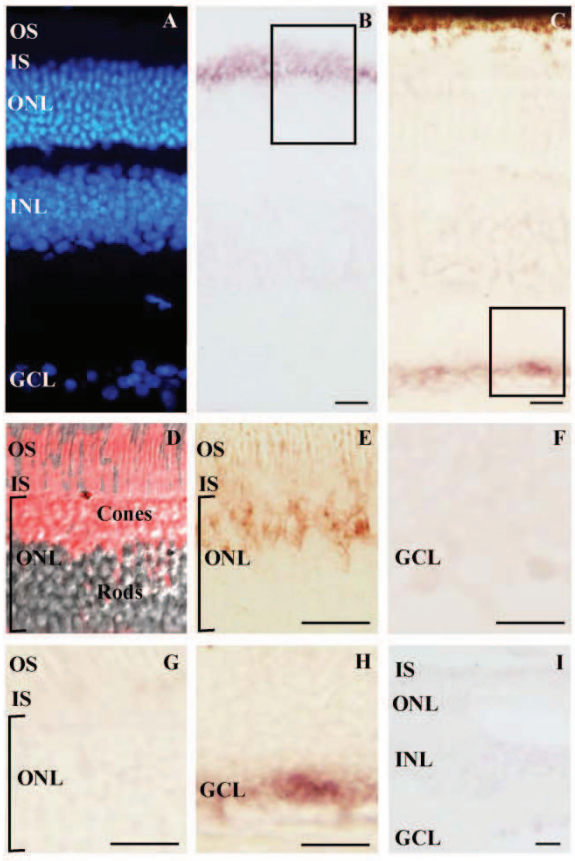

Figure 1: Aa-nat gene is expressed in the cones and ganglion cells of *Arvicanthis ansorgei* retina.

A) DAPI staining of a 10 µM section of *Arvicanthis ansorgei* retina indicates the area of interest: from top to bottom: OS: photoreceptor outer segments; IS: photoreceptor inner segments; ONL: outer nuclear layer; INL: inner nuclear layer; GCL: ganglion cell layer. **B)** *Aa-nat* antisense probe at ZT19 (night time) stains IS and the upper part of the ONL. **C)** *Aa-nat* antisense probe at ZT6 stains GCL. **D)** Immunostaining of *Arvicanthis ansorgei* retina with anti-cone arrestin (red) clearly showing ONL organization with cone cell bodies lying on top of rods. **E)** At ZT19, *Aa-nat* mRNA staining is restricted to the two uppermost cell body rows and IS. **F)** At ZT19 *Aa-nat* antisense probe does not stain GCL. **G, H)** At ZT6 *Aa-nat* antisense probe stains GCL (H) but not ONL (G). **I)** Use of *Aa-nat* sense probe at ZT19 does not stain any structures. Scale bar = 10 µm. Additional abbreviations: RPE: retinal pigmented epithelium.

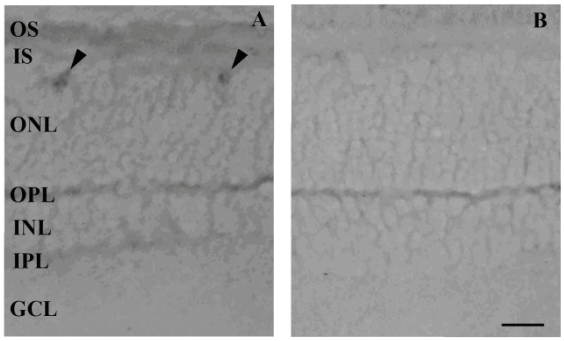

Supplemental Figure 1: *Aa-nat* gene is expressed in the cones of rat retina.

A) In ZT19 rat retina, hybridized *Aa-nat* anti sense probe is detected in some cells of the ONL (arrowheads), corresponding to the number and position of cones. **B)** *Aa-nat* sense probe shows no staining in the ONL. Abbreviations as in Figure 1.

	ZT3	ZT6	ZT7	ZT11	ZT15	ZT19	ZT23
Photoreceptor	+	0	0	+/-	++	+++	++
INL	+/-	+	0	+/-	0	0	+
GCL	+	++	+	+/-	0	0	0

Table 1: Semi-quantification of Aa-nat expression in the retina of *Arvicanthis ansorgei*.

Aa-nat gene displays an opposing cyclic expression in cone and ganglion cell layers of *Arvicanthis ansorgei* retina. n= 3 animals for each time point. +++: strong; ++: moderate; +: weak; +/-: very weak; 0: absent. ZT: Zeitgeber Time with ZT0 = light on.

AA-NAT is expressed in many cells of the *Arvicanthis ansorgei* retina

Immunohistochemistry was performed on transverse sections prepared from retinas fixed at different times in the LD cycle **(Figure 2)**. At ZT23, AA-NAT immunoreactivity was strong and widespread, seen in IS, cone cell bodies, throughout most of the INL and inner plexiform layer (IPL), and within a subset of cells in the GCL **(Figures 2A-C)**. The lower area of the ONL, corresponding to rod cell bodies, showed no staining above background levels **(Figures 2A, B)**, while the outer segments (OS) were devoid of label. In sections of retinas fixed in the daytime (ZT7), AA-NAT staining was overall weaker, albeit still detectable in the cone cell bodies and the majority of the INL, IPL and GCL. Rods, OS and horizontal cells were unstained **(Figure 2D)**. Positive controls with sections of pineal gland obtained at ZT23 showed generalized strong staining **(Figure 2E)** and negative controls using sections of cortex or omission of primary antibody only showed background label **(Figures 2F,G respectively)**.

The cone-specific localization of AA-NAT was confirmed by performing double label immunofluorescent staining on whole retina. Staining with a rod-specific antibody (anti-phosducin) filled the cytoplasm in rod IS, forming a meshwork pattern across the retinal surface (Figure 2H); the unstained interstices corresponded to the profiles of cone IS **(Figure 2H)**. AA-NAT staining also revealed a meshwork aspect of stained profiles **(Figure 2I)**. Merged images demonstrated that AA-NAT immunoreactivity co-localized with the dark spaces (cones) between phosducin-positive profiles **(Figure 2J)**. However not all cone profiles were immunostained, and weak AA-NAT immunostaining was also observed in rods. We did not assess markers for INL neurons, but as AA-NAT immunoreactivity was previously seen in the GCL, we performed similar double immunofluorescence studies at this level. Brn3 was localized in RGC nuclei **(Figures 2K, M)**, while AA-NAT staining was seen within the cytoplasm of these cells **(Figures 2L, M)**. AA-NAT was also detected in numerous Brn3-immunonegative cells **(Figure 2M)**.

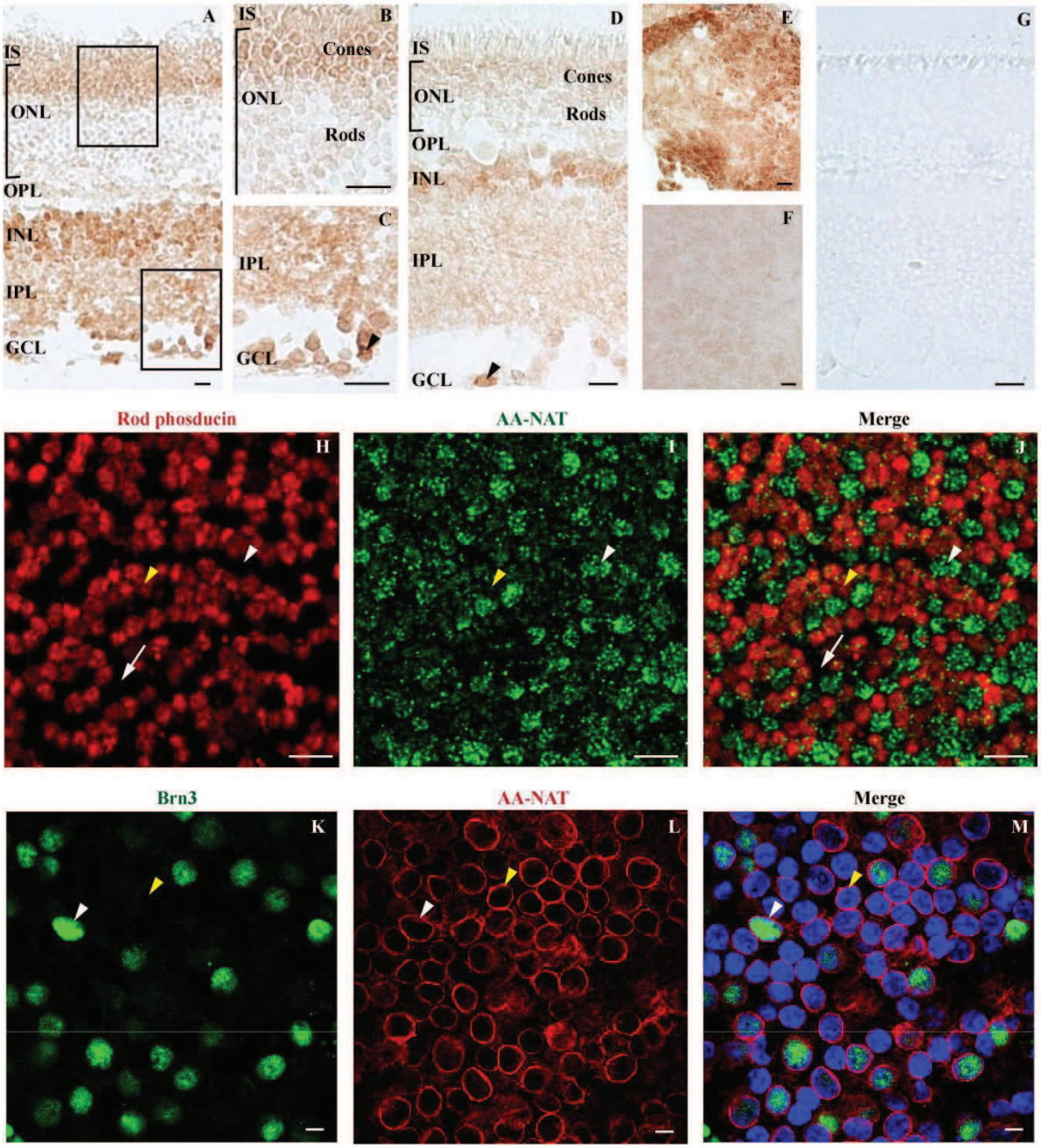

Figure 2: AA-NAT is localized in many cells in the retina of *A. ansorgei*.

Panels A) to G) represent analysis of AA-NAT localization by immunoperoxidase methods. **A)** At ZT23, AA-NAT staining was clearly visible in IS, upper ONL (cones), INL, IPL (inner plexiform layer) and GCL. The lower ONL (rods) is unlabelled. **B)** Enlargement of the ONL confirms that AA-NAT expression is restricted to cone cell bodies and IS. **C)** Enlargement of the IPL and GCL confirms expression in these areas. Black arrowhead indicates immunostained cell in GCL. **D)** Staining is likewise present at ZT7 although notably fainter at the level of the cones. Panels **E)** and **F)** are respectively positive and negative controls of AA-NAT detection at ZT23, in the pineal gland and cortex respectively of *Arvicanthis ansorgei*. **G)** Control without primary antibody. Scale bar for A-G = 20µm. **Panels H) to M)** fluorescence immunohistochemistry of whole mounted retinas at ZT23. **Panels H) to J)**: the optical section was fixed at the level of the IS. **H)** Rod IS are specifically stained with anti-phosducin antibody (yellow arrowhead), while cone IS are unstained and visible as dark profiles (white arrowhead). **I)** AA-NAT (green staining) is seen in numerous profiles. **J)** When both fields are merged, it can be seen that AA-NAT is weakly present in rod IS but strongly expressed in many (but not all) cone IS. An unstained cone IS is shown

by the white arrow in H and J. **K) to M)** optical sections fixed at the level of the GCL. **K)** Retinal ganglion cells (RGC) are stained with Brn3 antibody, visible within numerous nuclei (green staining). **L)** AA-NAT (red staining) is also detected in many cells as annular profiles corresponding to cytoplasm. **M)** Merged images show that AANAT is expressed in all Brn3-positive RGC (white arrowhead in K-M, as well as Brn3-negative cells (yellow arrowhead in K-M). Total cell nuclei are counter-stained with DAPI (blue). Scale bar for H-M = 5 µm. Abbreviations as in Figure 1.

To obtain information about the quantitative expression profile for AA-NAT protein in *Arvicanthis* retina, we performed western blotting analyses at similar time points across the 24 h period **(Figure 3A)**. Identical results were obtained using two different antibodies raised against AA-NAT. In both cases an intense immunoreactive band of the expected molecular weight for AA-NAT could be observed. There was considerable variation in immunoreactive intensity within sample groups (even though sibling animals were raised under identical housing conditions), and the only time point that gave reproducibly low expression was ZT3 **(Figure 3A)**. We observed that AA-NAT expression was high across the remainder of the day and early night, rising further at ZT19 and reaching a maximum at ZT23, around 10 fold higher levels than at ZT3 ($p > 0.05$, one-way ANOVA) **(Figure 3B)**. A similar profile of virtually continuous AA-NAT expression (except for CT3) was also observed in *Arvicanthis* raised under DD conditions **(Figure 3C-D)**. AA-NAT protein levels were elevated throughout the night with a peak at CT23, and showed intense expression in the middle of the day at CT7 ($p < 0.05$, one-way ANOVA) **(Figure 3D)**.To complete the characterization of AA-NAT temporal expression in *Arvivcanthis* retina, the enzymatic activity was assayed over the 24 h period. Values were weakly correlated with the expression levels in that the enzyme was constitutively active throughout the day and night cycle **(Figure 3E)**. There was no significant increase of activity at night ($p > 0.05$, one-way ANOVA).

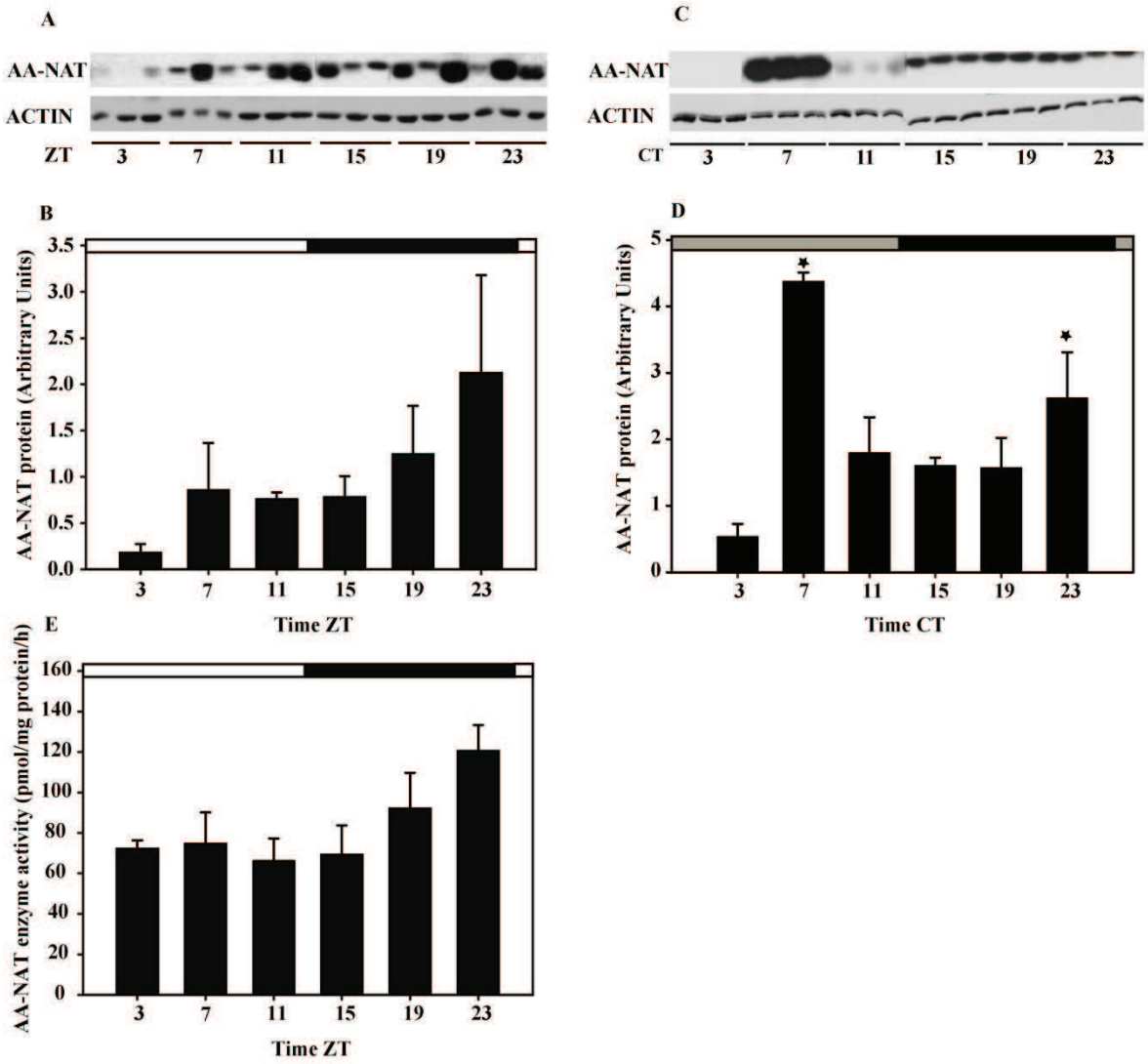

Figure 3: AA-NAT expression and activity are high at night but persist throughout daytime.

A) Western blotting analysis of AA-NAT expression in retinas from 3 different animals per time point reveals the presence of the protein AA-NAT throughout the 24 h. Data indicate that AA-NAT expression across 24 hours is overall higher at night but is also elevated at every point sampled in the daytime except ZT3. It is also evident that there was great variability between individuals within a sample time. **B)** Densitometric quantification of AA-NAT on western blots (n=5) confirms the general increase in the dark period as well as the substantial expression in late day, and the low expression at ZT3 ($p > 0.05$, one-way ANOVA).**C)** Western blotting analysis of AA-NAT expression in retinas (1 animal per time point, the same sample is repeated 3 times) reveals the presence of AA-NAT protein throughout the 24 h. Data indicate that AA-NAT expression is higher at CT7 but remains elevated at night. **D)** Densitometric quantification of AA-NAT protein as seen on western-blots (n = 3, three distinct experiments) demonstrates that the maximum of AA-NAT is at CT7 ($p < 0.001$, one-way ANOVA, Holm-Sidak test). The lowest expression is at CT3. Data are the mean values ± SEM of 3 animals analyzed in 3 independent experiments. **E)** AA-NAT activity is uniform throughout the day and early night, then increases slightly at ZT19 and peaks at ZT23 ($p > 0.05$, one-way ANOVA). Data are the mean values ± SEM of 4 animals. Light bar represents day time, black bar represents night-time, grey bar represents the subjective night.

HIOMT is expressed in photoreceptors, OPL and GCL in *Arvicanthis ansorgei* retina

Although we could not investigate *Hiomt* RNA expression in *Arvicanthis*, due to lack of cross-reactivity with an RNA probe specific for rat HIOMT (data not shown), we were able to perform immunohistochemical studies. Immunolabeled HIOMT was detected in IS, OPL, IPL and GCL at ZT23 **(Figure 4A)** but was not visible within the ONL or INL. HIOMT immunostaining was similar at ZT7 **(Figure 4B)**. Pineal gland and cortex were respectively used as positive and negative controls for HIOMT immunolabeling specificity **(Figures 4C, D)**. No signal was detected when the primary antibody was omitted **(Figure 4E)**. As for AA-NAT, to confirm HIOMT distribution we performed double label immunohistochemistry on whole mounted retina **(Figures 4F-K)**. As before, phosducin-positive profiles correspond to rod IS, while the black spaces represent cone IS **(Figure 4 F)**. HIOMT appeared as patchy staining **(Figure 4G)**. Merged images demonstrated that HIOMT was present throughout the IS layer, but more strongly in cones **(Figure 4H)**. At the level of the GCL, Brn3 staining was seen in RGC nuclei **(Figures 4I, K)**. HIOMT staining was localized in the cytoplasm of Brn3-immunopositive RGC **(Figures 4J, K)**, as well as many Brn3-immunonegative cells. In summary, use of multiple independent approaches indicated that within the *Arvicanthis* retina, despite phase-inversed expression of *Aa-nat* in cones (maximum at night) and GCL (maximum at day), AA-NAT and HIOMT are produced together in cones and RGC throughout the 24h period.

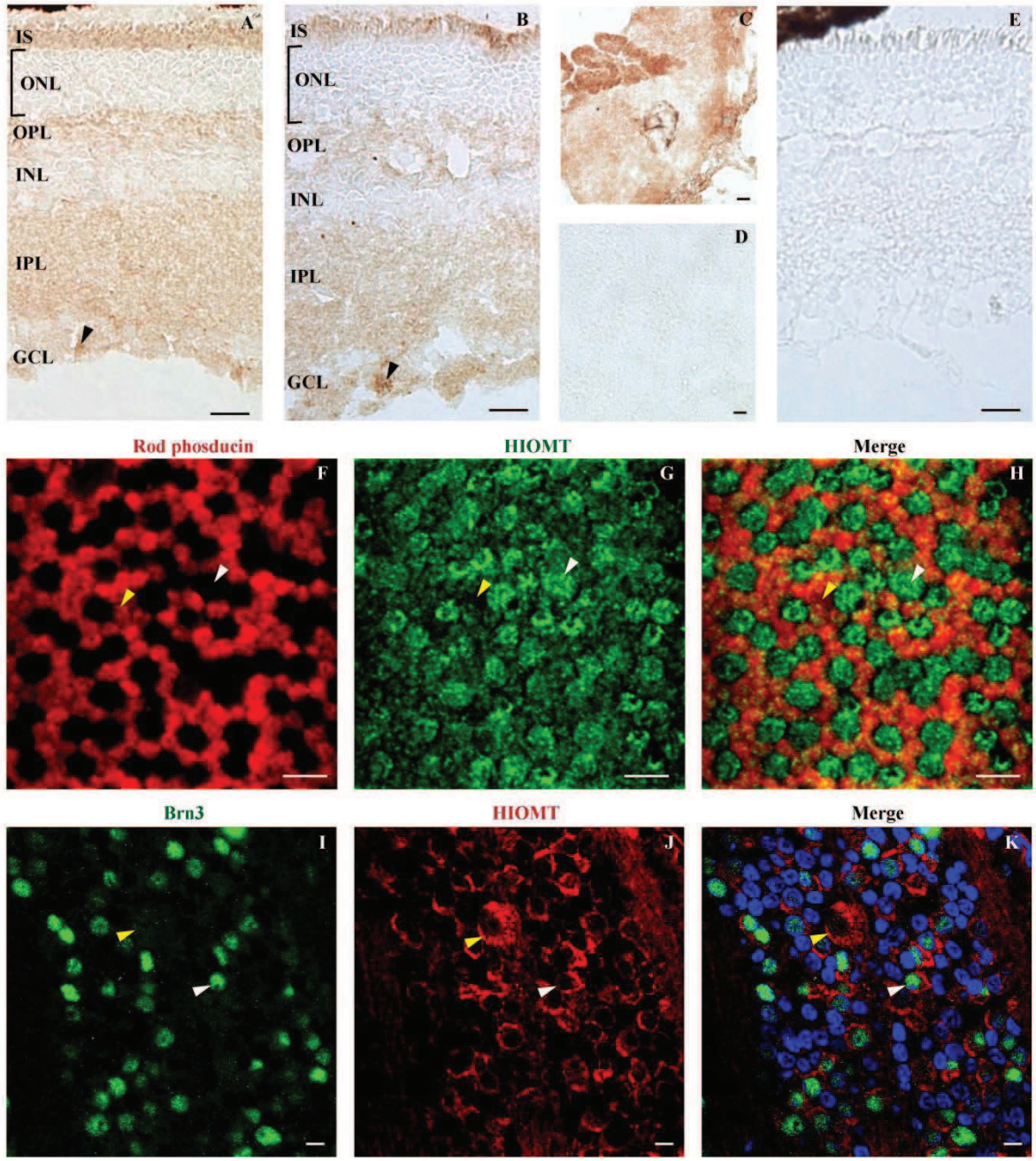

Figure 4: HIOMT is expressed in photoreceptors, synaptic layers and RGC in the retina of *Arvicanthis ansorgei.*

Panels A) to F) represent analysis of HIOMT localization using immunoperoxidase techniques. **A)** At ZT23, HIOMT staining can be seen in IS, OPL, IPL and GCL. **B)** Staining of similar intensity and distribution is also present at ZT7. Black arrowhead indicates immunostained cell in GCL. **C)** and **D)** are respectively positive and negative controls of HIOMT detection at ZT23 in sections of pineal gland and cortex of *Arvicanthis ansorgei*. **E)** Control without primary antibody. Scale bar for A-E = 20 µm. **Panels F) to K):** fluorescence immunohistochemistry of whole mounted retinas at ZT23. **Panels F) to H):** optical section fixed at the level of the IS. **F)** As in figure 3, rod IS are heavily stained by anti-phosducin antibody (yellow arrowhead), leaving unstained cone IS visible as black spaces (white arrowhead). **G)** HIOMT immunostaining is seen as circular profiles. **H)** Merged images reveal that HIOMT is mostly expressed in cone IS, with weaker staining in the surrounding rod IS. Panels **I) to K):** optical sections fixed at the level of the GCL. **I)** As in figure 3, RGC are

stained with Brn3 antibody, visible within numerous nuclei (green staining). **J)** HIOMT is visible as circular profiles corresponding to cell cytoplasm (red). **K)** Merged images indicate co-localization between HIOMT and Brn3-positive RGC (white arrowheads in I-K), as well as Brn3-negative profiles (yellow arrowheads in I-K). Scale bar for F-K = 5 µm. Abbreviations as in Figure 3.

Melatonin concentrations are constitutively low in the Arvicanthis ansorgei retina

HIOMT enzyme activity in *Arvicanthis ansorgei* retina was very low (fiftyfold less) compared to AA-NAT activity **(compare Figures 5A and 3E)**, but was detectable throughout the 24 h cycle at a roughly similar level. ELISA quantification of melatonin concentrations was similarly low and uniform across the day/night cycle **(Figure 5B)**. We also attempted to identify melatonin by HPLC. There was no spike in the elution profile corresponding to purified melatonin standard, even at high signal amplification (data not shown). Furthermore, we also assayed for NAS (the end product of AA-NAT) by HPLC, and as for melatonin there was no detectable peak (data not shown). For comparative purposes, we also quantified melatonin in retinas isolated from C3H melatonin-competent mice. In this case, there was a notable rhythm of melatonin concentration, peaking in the night at fourfold higher values than that of *Arvicanthis* **(Supplemental Figure 2)**. As retinal melatonin and dopamine synthesis are seen in anti-phase in many species, we measured dopamine expression in *Arvicanthis ansorgei*. Using HPLC we measured levels of dopamine and its major metabolite, dihydroxyphenyl acetic acid (DOPAC). Dopamine levels showed a significant increase at the middle of the day (ZT7) **(Figure 5C)**, and likewise DOPAC levels were maximal at ZT7, decreasing towards the end of the day and remaining low through the night **(Figure 5D)**.

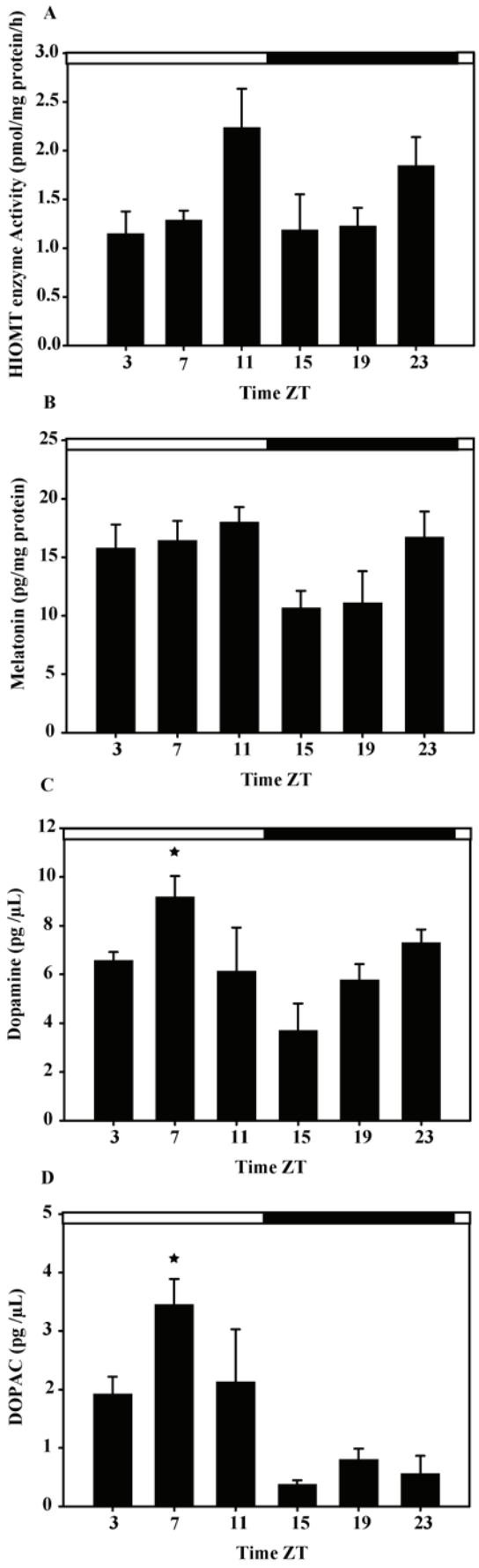

Figure 5: HIOMT activity and melatonin are present throughout 24 hours.

A) Daily profile of HIOMT enzymatic activity (n = 4 retinas per point) was obtained by radioactive assay performed on retinas of *Arvicanthis ansorgei* raised under 12h light/12h dark cycles. HIOMT enzyme activity appears constitutive with small increases at the end of the day (ZT11) and night (ZT23) periods ($p > 0.05$, one-way ANOVA). **B)** Melatonin concentrations were measured by ELISA in 5 *Arvicanthis* retinas for each time point. Melatonin is constitutively present at low levels ($p > 0.05$, one-way ANOVA). **Panels C) and D):** dopamine and dihydroxyphenyl acetic acid (DOPAC) were analyzed by HPLC (n = 4 retinas per time point). Dopamine concentrations were fairly uniform but exhibited a daytime peak at ZT7 ($p=0.035$, one-way ANOVA followed by Holm Sidak test); DOPAC levels were markedly higher during the day period, also peaking at ZT7 ($p=0.001$, one-way ANOVA followed by Holm Sidak test).

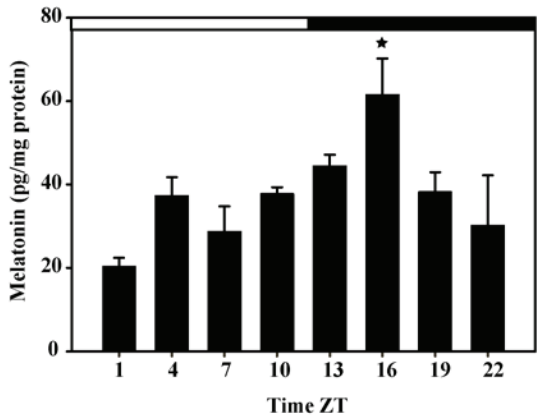

Supplemental Figure 2: Melatonin increases at night in the mouse retina.

Melatonin concentrations were measured by ELISA in 6 melatonin proficient mouse retinas for each time point. Melatonin levels rose gradually during the day and early night to peak at ZT16, threefold higher than the lowest level at ZT1 ($p = 0.05$, one-way ANOVA, Holm-Sidak test).

MT_1 receptors show a complementary distribution to AA-NAT/HIOMT in *Arvicanthis ansorgei* retina

An important component of melatonin action resides in the presence and function of its receptors MT_1 and MT_2. Although we were unable to perform immunolocalization studies of MT_2, using a specific MT_1 antibody we detected immunoreactivity in rod cell bodies, within selected cells of the INL (especially the innermost row corresponding to the position of amacrine cells) and strong labeling in most cells of the GCL, with no difference across the light/dark cycle **(Figures 6A, B)**. In an opposite pattern to AA-NAT, immunostaining was low in cone cells. Positive and negative controls, respectively *pars tuberalis* and cortex, showed strong immunostaining and absence of label respectively **(Figures 6C, D)**. Control retinas without primary antibody showed no labeling **(Figure 6E)**. Confirmation of MT_1 expression on rod cell bodies **(Figure 6G, H)** was provided by co-localization studies using RET-P3, a specific marker of this compartment **(Figures 6F, H)**. We also studied the cell-specific localization of MT_1 in the GCL: Brn3 **(Figure 6I)** and MT_1 immunostaining **(Figure 6J)** overlapped within many cells **(Figure 6K)**. As for AA-NAT and HIOMT, MT1 was also present in many Brn3-negative cells.

The totality of these data concerning the melatonin synthetic pathway in retina, along with those reported in the literature for other mammalian and non-mammalian species are summarized in **Table 2**.

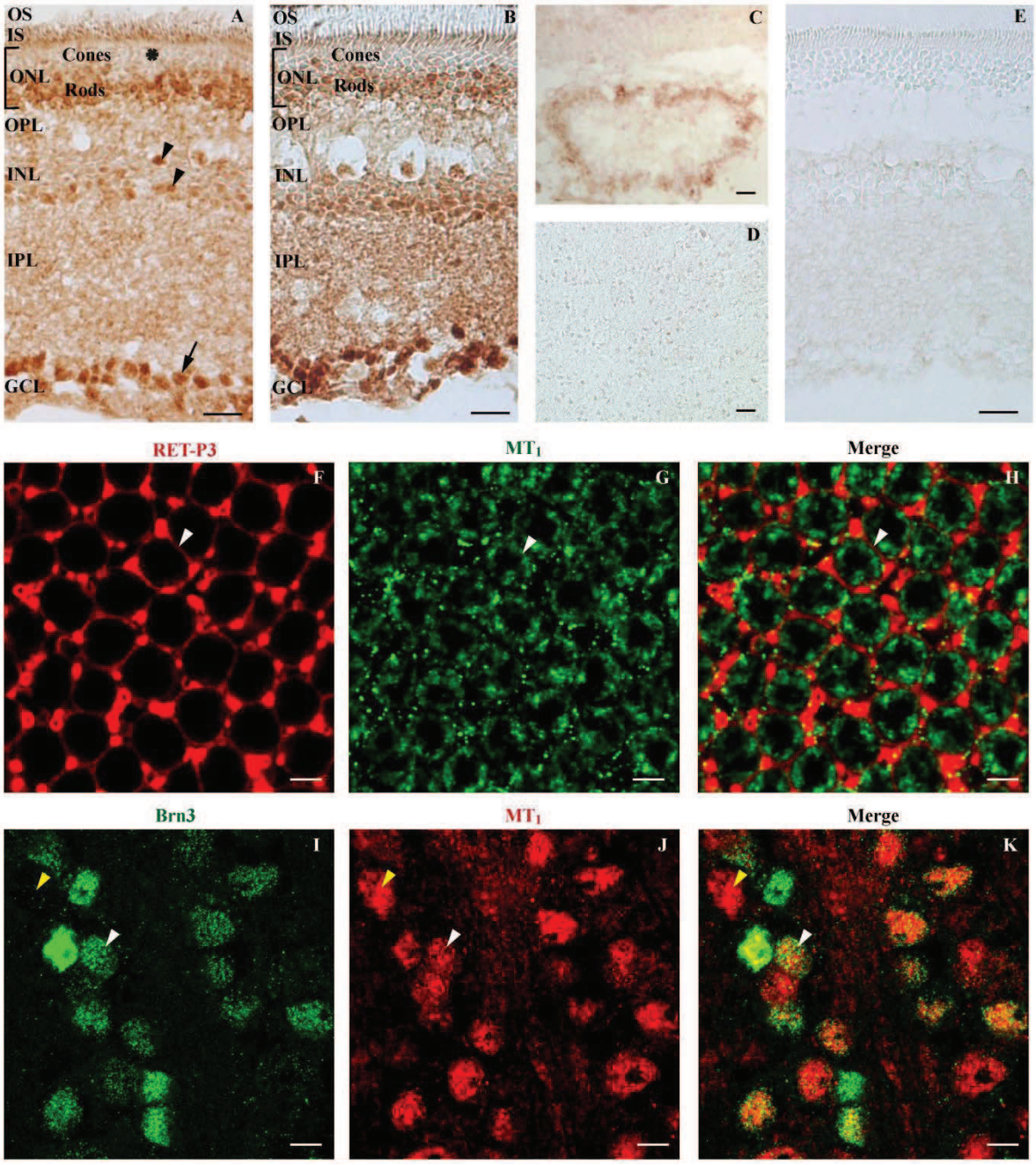

Figure 6: Melatonin receptor MT_1 is expressed in the rods, inner nuclear layer and ganglion cells in the retina of *A. ansorgei*.

Panels A) to E) represent analysis of MT_1 localization using immunoperoxidase techniques. **A)** Arrowheads point to specific MT_1 staining at ZT23 in the INL (upper arrowhead corresponding to horizontal cell; lower arrowhead corresponding to amacrine cell) Arrow points to MT_1 staining in GCL. Strong staining was also seen throughout the lower ONL (rod cell bodies), and more moderately in IS, OPL and IPL. Notably, MT_1 staining was weak in cone cell bodies (asterisk). **B)** MT_1 staining is also present at ZT7 during daytime, with similar distribution and intensity. **Panels C) and D)** are respectively positive and negative controls of MT_1 detection at ZT23 in sections of *pars tuberalis* and cortex of *Arvicanthis ansorgei*. **E)** Control without primary antibody. Scale bar for A-E = 20 µm. **Panels F) to K):** fluorescence immunochemistry of MT_1 expression at ZT23 in whole mounted retinas. **Panels F) to H):** optical section fixed at the level of the lower ONL (rod cell bodies). **F)** Rod cell bodies are outlined by RetP3 binding (staining in red, white arrowhead). **G)** The same field immunostained for MT_1 shows widespread binding (staining in green). **H)** Merged images reveal co-localization of MT_1 and rod cell

body plasma membranes. **Panels I) to K):** optical section fixed at the level of the GCL. **I)** As in Figure 3, RGC are stained with Brn3 antibody, visible within numerous nuclei (green staining). **J)** The same field immunostained for MT_1 shows widespread binding (in red). **K)** Merged images demonstrate co-localization between MT_1 and Brn3-positive RGC (white arrowhead in I-K). There are also Brn3-negative cells stained with MT_1 (yellow arrowhead in I-K) as for AA-NAT and HIOMT analysis. Scale bar for F-K = 5 µm. Abbreviations as in Figure 3.

	Arvicanthis	Rat/Mouse	Monkey	Chicken	Trout	Other
***Aa-nat* mRNA** Qualitative and quantitative expression during 24 h	CCB, CIS +++ at ZT19, GCL ++ at ZT6. In PR, N>D ~4x; in RGC: D>N by ISH. *(60):* N>D ~20x by qPCR.	**Rat:** *(22):* CCB +++ at ZT17, 0 at ZT5. *(23):* ONL +++ at ZT20, + at ZT8; INL, GCL ++ at all ZT. *(21):* N>D ~3x. **Mouse:** *(20):* N>D ~2x.	*(26):* time of day not specified. ONL +++; INL ++; GCL +. N=D.	*(24):* ONL+++ at ZT18, ++ at ZT6; INL and GCL + at all ZT. N>D ~4x. *(25):* PR +++ at ZT22, + at ZT3; GCL +++ at ZT3, 0 at ZT22. Under DD: PR, N>D ~3x; RGC, D>N ~6x.	*(48):* ONL, vitreal-most INL, GCL +++ at night; ONL +, other layers 0 at day. N>D ~5x.	**Human:** *(72):* whole retina +++. **Bovine:** *(73):* whole retina +++. **Ovine:** *(74):* N = D.
AA-NAT protein	CCB, CIS, INL, IPL, GCL +++ at ZT23; CCB, CIS +, INL, IPL, GCL ++ at ZT7. Present at all times except ZT3. N>D ~10x.	nd	*(26):* N>D ~5x.	*(47):* N>D ~4.5x.	*(48):* D>N ~2.5x.	nd
AA-NAT activity	~100 pmol/mg prot/h. Present at all times, small increase at night, ~1.5x.	**Rat:** *(75):* 300 pmol/retina/h. N >D ~6x.	*(26):* ~25000 pmol/mg prot/h. N>D ~5x.	*(50):* ~1000 pmol/mg prot/h in PR; 400 pmol/mg prot/h in RGC. In PR, N>D ~2x; in RGC D>N ~1.5x. *(47):* ~24000 pmol/mg prot/h. N>D ~18x. *(24):* N>D ~8x. *(76):* ~15000 pmol/mg prot/h. N>D ~15x. *(25):* under DD: ~2000 pmol/mg prot/h in PR; ~800 pmol/mg prot/h in RGC. In PR, N>D ~6x; in RGC, D>N ~2x. *(75):* 800 pmol/mg retinal tissue/h. N>D ~8x.	*(48):* ~2800 pmol/mg prot/h. D>N ~4x.	***Xenopus laevis*: *(77):*** ~24000 pmol/mg prot/h. N>D ~6x. **Rabbit:** *(75):* 40 pmol/mg retinal tissue/h. *N>D ~8x.* Mongolian gerbil: *(78):* 7000 pmol/mg protein/h. N>D ~1.8x.
***Hiomt* mRNA**		**Rat:** *(data not show):* CCB, CIS, GCL +, INL+/- at night; CCB 0, GCL +, INL+/- at day. *(28):* +, N=D.	*(26):* +/-, N=D.	*(54):* IS, ONL, OPL.	*(48):* ONL +, vitreal-most INL, GCL +/-. N=D.	**Human:** *(79):* +/- *(80):* +

	Arvicanthis	Rat/Mouse	Monkey	Chicken	Trout	Other
HIOMT protein	CIS, OPL, IPL, GCL +. N=D.	**Rat:** (53): ONL, IS +++; INL, GCL +.	nd	*(30):* ONL +++, GCL ++.	nd	**Bovine:** *(53):* ONL, IPL +/- (51): 0 **Lizard:** *(53):* CCB, CIS. Human: *(53):* ONL, IS. *(79):* 0
HIOMT activity	~2 pmol/mg prot/h. N=D.	**Rat:** *(28):* ~20 pmol/mg prot/h. N=D. *(79):* ~200 pmol/mg prot/h. *(75):* 20 pmol/retina/h. N=D.	nd	*(75):* ~20 pmol/mg retinal tissue/h. N=D.	nd	**Human:** *(79):* 0 **Bovine:** *(79):* 0 **Rabbit:** *(75):* 5 pmol/mg retinal tissue/h. N=D.
Melatonin	~18 pg/mg prot. N=D.	**Mouse:** ~60 pg/mg prot. N>D ~3x. **Rat:** *(81):* ONL, INL. N>D ~4x. *(61):* ~150 pg/retina. N>D ~2x. *(62):* ~1000 pg/retina. N>D ~5x. *(82):* 60 pg/retina. N>D ~2x.	nd	**Chick:** *(76):* ~1 ng/mg prot. N>D ~4x. *(63):* ~1000 pg/retina. N>D ~4x. *(25):* under DD: ~40000 pg/mg prot in PR; ~4000 pg/mg prot in RGC; +/- in INL. N>D in PR ~13x; D>N in RGC ~7x. *(45):* under DD: ~1000 pg/mg prot in RGC. D>N ~5x.	**Sea bass:** (83): D>N or N=D.	**Golden Hamster:** *(84):* D>N. **Bovine:** *(85):* 3000 pg/retina.
Dopamine	~10 pg/µL. D>N ~2x.	**Rat:** *(86):* ~200 pg/mg wet weight. D>N ~2x. *(87):* ~3000 pg/mg prot. D>N ~1.5x. *(88):* ~30 pmol/retina. D>N ~1.5x. **MouseBALB/c:** *(89):* ~700 pg/retina. D=N.	*(90):* ~6 pmol/10 min/retina. D>N ~2x.	*(68):* ~2000 pg/mg prot. D>N ~2x.	**Cichlid fish:** *(91):* ~2000 pg/retina. D>N ~1.5x.	**Rabbit:** *(92):*~300 pg/mg wet tissue. D>N ~1.5x. **Human:** *(93):* ~3000 pg/mg prot. D>N ~2.5x.

Table 2: Species comparison of the melatonin synthetic pathway within the retina.

Compilation of published data and those from the present study underline variations in the melatonin pathway of most studied vertebrates. We have indicated the relative change in gene or protein expression between night and day using italic. Activity values were all expressed in pmol/h/mg prot to allow comparison between species. Abbreviations as in figure 3. Additional abbreviations: CCB: cone cell body; CIS: cone inner segment; DD: dark/dark; D: day values; N: night values; n.d: not determined; PR: photoreceptors. Staining intensity is represented as follows: +++: strong; ++: moderate; +: weak; +/-: very weak; 0: absent.

Discussion

Vertebrate retina has long been known to synthesize melatonin thought to modulate various physiological processes within the eye. However, knowledge of the melatonin synthetic pathway has never been examined in a systematic fashion, is fragmentary in mammalian retina, and limited principally to nocturnal species (mouse and rat). Published studies have focused on the penultimate enzyme of melatonin synthesis, AA-NAT, whereas expression and activity of the final enzyme in the pathway, HIOMT, are still poorly understood. In the work reported here we performed systematic localization and expression of multiple components of the melatonin synthetic pathway in a diurnal rodent *Arvicanthis ansorgei*, arguably a closer model to human central cone-rich retina. In stark contrast to nocturnal rodent retina, *Aa-nat* mRNA expression showed differential phase expression in distinct cell populations, and AA-NAT was abundantly expressed throughout the 24 h light/dark cycle, although actual melatonin levels were low at all times.

Differential expression of AA-NAT, HIOMT and MT_1 suggests distinct roles in Arvicanthis ansorgei retina

Within the photoreceptors, *Aa-nat* expression was abundantly detected in cones exclusively during the night, whereas levels were below the detection limit in rods, consistent with data from rat retina *(22)* **(Supplemental Figure 1)**, as well as the other cell types in the retina. In contrast, *Aa-nat* expression appeared in RGC during the day, in phase opposition to that of cones. To the best of our knowledge, this is the first description of two phase-opposed sites of *Aa-nat* transcription in mammals, similar to the situation in chicken retina *(45)* **(Table 1)**. Immunodetection of AA-NAT has proved very problematic in previous studies, possibly because AA-NAT is strongly associated with the protein chaperone 14-3-3 *(46)* leading to inaccessibility of epitopes to antibodies directed against AA-NAT. We initially compared multiple immunohistochemical procedures, and optimal results for frozen sections were achieved using antigen retrieval techniques followed by immunoperoxidase protocols. To the best of our knowledge this is the first demonstration of AA-NAT protein localization in the retina, where it was clearly found in cones, many cells within the INL and in the majority of neurons within the GCL. Contrary to mRNA expression, protein was also highly expressed during the day, under both normal cyclic and constant darkness conditions (except for ZT3/CT3). To explain this profile, we propose that AA-NAT detected at night derives from cones, and is under strict light/circadian control similar to the scheme hypothesized by Tosini, Iuvone and colleagues. Previous studies in rat retina proposed that light decreases Ca^{2+} and cAMP levels leading to activation of proteasome proteolysis *(19)*. Studies in chicken demonstrated that during the day AA-NAT phosphorylation by PKA is decreased, leading to dissociation from the chaperone 14-3-3 and subsequent degradation by the proteasome *(46,47)*. AA-NAT detected during the day comes from the GCL, and constitutes an independent light-insensitive pool. Similar hypotheses have been advanced for trout retinas *(48)*, where AA-NAT expression is also detected during the day. This model is depicted in **Figure 7**. AA-NAT in the GCL co-localized with both Brn3-positive and -negative neurons, indicating that both RGC and possibly displaced amacrine cells [which constitute ~40% of neurons in the GCL *(33)* and are Brn3-immunonegative] synthesize AA-NAT. One previous study in rats employing a fluorescence-based *in situ* hybridization approach showed widespread distribution of *Aa-nat* mRNA throughout the retina *(23)*. Also, widespread *Aa-nat* distribution was seen in the macaque monkey retina *(26)*, and in cones and GCL of chicken retina *(49,50)* **(Table 2)**.

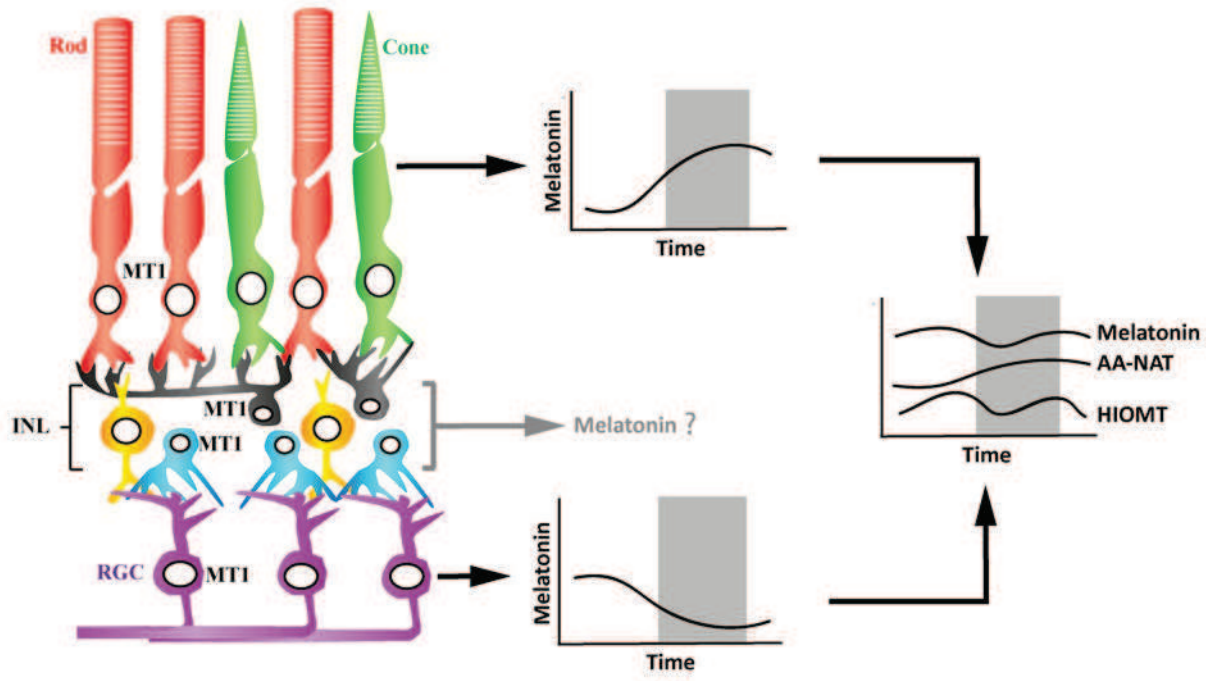

Figure 7: Model of melatonin synthesis in *Arvicanthis ansorgei* retina.

Middle upper scheme: melatonin is produced by cones at night. Lower middle diagram: melatonin is produced by RGCs during the day. Constitutive melatonin level in the retina may reflect the cumulative PRs and RGCs melatonin. Right scheme: similarly, AA-NAT expression throughout the 24 hours could result from integration of PR nocturnal AA-NAT and RGC daytime AA-NAT productions. The same hypothesis can be proposed for HIOMT.

HIOMT represents the ultimate step in melatonin production and is therefore crucial for understanding its synthetic pathway. Previous studies in rat retina have revealed very faint expression of *Hiomt* *(28)*, and it was virtually undetectable in bovine *(51)* and macaque retinas *(26)*. Although we were not successful in obtaining reliable *in situ* hybridization images, HIOMT immunoreactivity was detected in photoreceptor IS, the two synaptic layers and GCL. *In situ* hybridization studies have been hampered by the lack of specific probes due to the highly divergent *Hiomt* sequences as demonstrated between mouse strains *(52)*. Previous studies showed HIOMT immunoreactivity in IS of several mammalian [rat, bovine and human *(53)*] and non mammalian species [chicken *(30,54)* and lizard *(53)*] **(Table 2)**. Hence in *Arvicanthis*, HIOMT was expressed in two of the same compartments as AA-NAT, mainly cone IS and RGC. It has been stated that co-expression of these two enzymes leads to production of melatonin *(55)*, implicating cones and GCL as major foyers of melatonin synthesis in *Arvicanthis* retina.

MT_1 receptor distribution was complementary to that of the supposed sites of melatonin synthesis: within the ONL, MT_1 expression was high in rod cell bodies; within the INL it was limited to scattered cells lying along the vitreal-most border, possibly a sub-population of amacrine cells; and within the GCL it was strongly expressed by many Brn3 positive RGC. Receptor expression was below detection limits in cones, indicating that in this species cones might release melatonin which targets uniquely rods. A recent study proposes that melatonin increases light sensitivity in the retina of mice via MT_1/MT_2 heteromer, suggesting that melatonin could be involved in dark adaptation *(14)*. A

physiological role for melatonin is further supported by rod and RGC loss in MT1-deficient mice *(11)*, although it is not known if such effects occur in *Arvicanthis*.

AA-NAT and HIOMT expression indicates constitutive production of melatonin.

It is generally accepted in pineal gland and retina that AA-NAT is under strict circadian and light control resulting in highly predominant nocturnal activity *(56–58)*. *Aa-nat* transcripts display a marked nocturnal maximum in *Arvicanthis ansorgei* cones, consistent with the known regulation of *Aa-nat* in the pineal gland of rat *(59)* and retina of nocturnal rodents *(20,21)* primates *(26)* **(Table 2)**, as well as in the pineal gland of *Avicanthis ansorgei* itself *(57)*. Furthermore using quantitative PCR we previously demonstrated cyclic expression profiles of *Aa-nat* in the retina of *Arvicanthis ansorgei* maintained under different lighting regimens *(60)*. It is important to note that the day-to-night ratio in the retina is much lower than in the pineal gland, around fourfold as previously shown for rat, mouse *(20,21)*, chicken *(24)* and primates *(26)* **(Table 2)**.We also performed western blotting analyses of AA-NAT expression across the 24 h. Although there was much individual variation, the overall pattern displayed a nocturnal maximum but with sustained expression throughout most of the day. Coon et al. *(26)* showed a nocturnal peak of AA-NAT levels in monkey retina and Iuvone et al. *(47)* reported AA-NAT protein expression across 24 h in the chicken retina with a peak at night **(Table 2)**. Our analysis of HIOMT protein expression during 24 h was performed in DD condition and displays a constitutive pattern **(Supplemental Figure 3)**. This result is coherent with the HIOMT activity **(Figure 5A)** performed in LD condition.

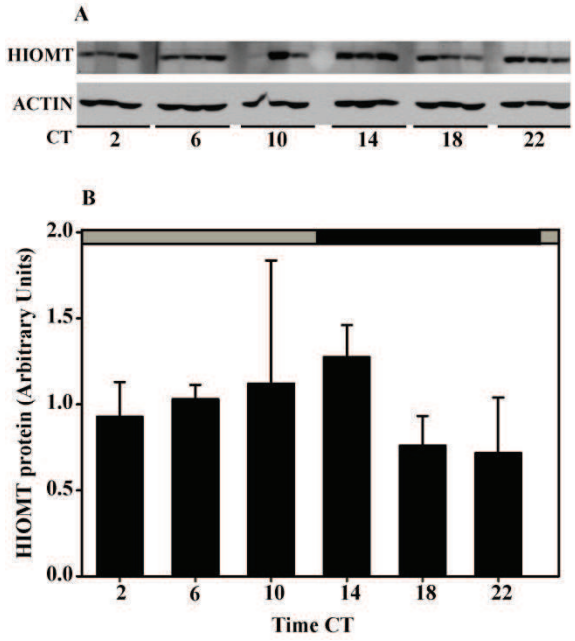

Supplemental Figure 3. HIOMT protein is expressed in *Arvicanthis ansorgei* retina.

A) Western blotting analysis of HIOMT expression in retinas from 3 different animals per time point reveals the presence of HIOMT protein throughout the 24 h. **B)** densitometric quantification of HIOMT (n=3 per time point) confirms the presence of HIOMT over the 24 h ($p > 0.05$, one-way ANOVA). White, black and grey bars represent day time, night-time, and the subjective night respectively. **C)** HIOMT peptide-antibody absorption control displays a reduced staining of *Arvicanthis* retina. Scale bar = 20 µm.

Different regulation and functions of the melatonin synthetic pathway in a diurnal rodent retina compared to other species

Taking together our observations and those reported in the literature, *Arvicanthis* shows similarities and differences to all described tissues. Some important data are missing, but within the Rodentia there are clear distinctions between nocturnal and diurnal species **(Table 2)**. Although only very low uniform levels of *Hiomt* have been reported in rat retina *(28)*, levels of melatonin are relatively high at night in both the rat *(61,62)* and mouse **(present study, Supplemental Figure 2)**. If cones are to be

considered a major source of retinal melatonin, as is known for chickens *(25,46)* and suggested by the strong expression of *Aa-nat* mRNA and AA-NAT protein in both nocturnal *(22)* and diurnal **(present study)** rodents, then *Arvicanthis* should exhibit relatively high values compared to the mouse. The contrary is true, and approximation to cone numbers indicates *Arvicanthis* has actually fifty-fold less melatonin than mouse retina **(Table 2)**. Although this study does not address the question directly, one possibility is that melatonin is exported towards the bloodstream. Given the level of melatonin production in *Arvicanthis* retina (10-15 pg/mg protein across the entire day/night cycle) compared to the pineal gland [estimates from published data give peak night values of 530 pg/mg protein, day values of 25 pg/mg protein: *(57)*], any retinal contribution to circulating melatonin would be minor, at least at night. Pinealectomy reduces the nocturnal plasma melatonin value by 80% in chicks, and bilateral enucleation further reduces the value by another 9% *(63)*. These results suggest that 9% of plasma melatonin originates from the eyes, hence retina which is the major melatonin production site in this organ. Combined with the widespread distribution of MT_1 receptors, these findings suggest that melatonin is synthesized in the retina principally for local purposes *(64)*.

As stated above, *Arvicanthis* pineal melatonin is strongly regulated in a cyclic manner, with the nocturnal peak being ~100 fold daytime levels *(57)*. The uniformly low values for retinal melatonin across the 24 h period indicate that circulating melatonin does not enter the retina, contrary to observations in the mouse *(65)*. It has been suggested that in primate retinas, in which HIOMT levels are also extremely low, that rather than synthesizing melatonin, AA-NAT plays a role in detoxification by acetylating arylalkylamines and preventing them depleting the photoreceptors of retinaldehyde *(58)*. Adding our immunolocalization data to this hypothesis suggests such reactions occur specifically in cones and that they are somehow preferentially vulnerable to depletion compared to rods. Primate retinas show large differences in day versus night levels of AA-NAT protein and activity *(26)*; this was not the case for *Arvicanthis*, which although showing AA-NAT predominantly at night also exhibits robust expression in the latter half of the day, whereas activity was unchanged across the 24 h period with a low increase at night **(Table 2)**. There is thus only weak correlation between AA-NAT expression levels and AA-NAT activity in *Arvicanthis*. It is noteworthy that AA-NAT actually generates NAS, which has been shown recently to exhibit pronounced intrinsic biological activity in the mouse. Notably, it binds to trkB receptors with high affinity, and can act as a ligand to trkB and thereby exert neuroprotective effects *(66,67)*. However, NAS was undetectable in *Arvicanthis* retina, at any time of day or night, even when extracts were prepared from pooled retinas (data not shown). So this does not seem to be a viable explanation for the role of AA-NAT in this species. In *Arvicanthis* retina, melatonin and dopamine production is not clearly opposed on a day/night basis **(Figure 5)**. These results differ from the previously described interplay between both compounds where dopamine inhibits AA-NAT activity, and melatonin in turn inhibits dopamine release, forming a mutual inhibition loop in retina of chicken and mammals *(68–70)*.

To summarize, although AA-NAT and HIOMT can be observed in *Arvicanthis* retina across most of the 24 h period, enzyme activity levels are actually low and melatonin itself is synthesized at correspondingly low levels. AA-NAT within photoreceptors (principally cones) may fulfill a detoxifying function, or even exert some neuroprotective effect. This is intriguing given that the retinas in this species are highly resistant to intense light damage *(71)*, and may represent an adaptation to exposure to potentially damaging light levels. Nevertheless the presence of MT_1 receptors indicates the low melatonin amounts are still functional and melatonin action may differ in photoreceptors

compared to inner retinal neurons: *Arvicanthis* exhibits a diurnal or bi-modal activity pattern *(31)* and is hence active in variable light intensities. Thus, melatonin may modulate the responsiveness of rod photoreceptors under dim lighting (dark adaptation).We also demonstrate that RGC contain all the machinery necessary to produce melatonin and respond to it. Published studies support a role for melatonin signaling through high affinity receptors in the survival of this cell-type *(11)*, and parallel studies demonstrate that MT_1 activation is necessary for cone survival during aging *(Gianesini et al., manuscript in preparation)*. In conclusion, our data describe a unique melatonin pathway in the retina of *Arvicanthis,* indicating distinct physiological adaptation of diurnal versus nocturnal rodents, and highlights the fine tuning of melatonin regulation in each layer of the retina.

Acknowledgments

The authors thank Dr D.C. Klein and Dr Bourgeron for the generous gift of antibodies. They also acknowledge the expert technical assistance of Susana Contreras-Alcantara and Perrine Spinnhirny. The authors are grateful for generous financial assistance from the Foundation of France (Berthe Fouassier Association), the Foundation for Medical Research, NIH grant EY022216 and Retina France.

References

1. **Tan DX, Hardeland R, Manchester LC, Paredes SD, Korkmaz A, Sainz RM, Mayo JC, Fuentes-Broto L, Reiter RJ.** The changing biological roles of melatonin during evolution: From an antioxidant to signals of darkness, sexual selection and fitness. *Biological Reviews* 2010;85:607–623.
2. **Pevet P, Challet E.** Melatonin: Both master clock output and internal time-giver in the circadian clocks network. *Journal of Physiology Paris* 2011;105(4-6):170–182.
3. **Klein DC, Moore RY.** Pineal N-Acetyltransferase and Hydroxyindole-O-Methyl-Transferase: control by the retinohypothalamic tract and the suprachiasmatic nucleus. *Brain research* 1979;174:245–262.
4. **Larsen PJ, Enquist LW, Card JP.** Characterization of the multisynaptic neuronal control of the rat pineal gland using viral transneuronal tracing. *European Journal of Neuroscience* 1998;10(1):128–145.
5. **Burke TM, Markwald RR, Chinoy ED, Snider J a, Bessman SC, Jung CM, Wright KP.** Combination of light and melatonin time cues for phase advancing the human circadian clock. *Sleep* 2013;36:1617–24.
6. **Simonneaux V.** Naughty melatonin: how mothers tick off their fetus. *Endocrinology* 2011;152(5):1734–8.
7. **Barrett P, Bolborea M.** Molecular pathways involved in seasonal body weight and reproductive responses governed by melatonin. *Journal of Pineal Research* 2012;52:376–388.
8. **Sande PH, Fernandez DC, Aldana Marcos HJ, Chianelli MS, Aisemberg J, Silberman DM, Sáenz DA, Rosenstein RE.** Therapeutic effect of melatonin in experimental uveitis. *The American journal of pathology* 2008;173(6):1702–1713.
9. **White MP, Fisher LJ.** Effects of exogenous melatonin on circadian disc shedding in the albino rat retina. *Vision research* 1989;29(2):167–179.
10. **Besharse JC, Dunis DA.** Methoxyindoles and Photoreceptors Metabolism: Activation of Rod Shedding. *Science* 1983;219(4590):1341–3.

11. **Baba K, Pozdeyev N, Mazzoni F, Contreras-Alcantara S, Liu C, Kasamatsu M, Martinez-Merlos T, Strettoi E, Iuvone PM, Tosini G.** Melatonin modulates visual function and cell viability in the mouse retina via the MT1 melatonin receptor. *Proceedings of the National Academy of Sciences of the United States of America* 2009;106(35):15043–8.
12. **Sengupta A, Baba K, Mazzoni F, Pozdeyev N V, Strettoi E, Iuvone PM, Tosini G.** Localization of melatonin receptor 1 in mouse retina and its role in the circadian regulation of the electroretinogram and dopamine levels. *PloS one* 2011;6(9):e24483.
13. **Wiechmann AF, Vrieze MJ, Dighe R, Hu Y.** Direct modulation of rod photoreceptor responsiveness through a Mel 1c melatonin receptor in transgenic Xenopus laevis retina. *Investigative Ophthalmology and Visual Science* 2003;44:4522–4531.
14. **Baba K, Benleulmi-Chaachoua A, Journé A-S, Kamal M, Guillaume J-L, Dussaud S, Gbahou F, Yettou K, Liu C, Contreras-Alcantara S, Jockers R, Tosini G.** Heteromeric MT1/MT2 Melatonin Receptors Modulate Photoreceptor Function. *Science Signaling* 2013;6(296):ra89.
15. **Alarma-Estrany P, Pintor J.** Melatonin receptors in the eye: Location, second messengers and role in ocular physiology. *Pharmacology and Therapeutics* 2007;113:507–522.
16. **Wiechmann AF, Summers J a.** Circadian rhythms in the eye: The physiological significance of melatonin receptors in ocular tissues. *Progress in Retinal and Eye Research* 2008;27:137–160.
17. **Tosini G, Menaker M.** Circadian rhythms in cultured mammalian retina. *Science (New York, N.Y.)* 1996;272(5260):419–21.
18. **Menaker M.** Commentary: what does melatonin do and how does it do it? *Journal of biological rhythms* 1997;12(6):532–534.
19. **Fukuhara C, Dirden JC, Tosini G.** Photic regulation of melatonin in rat retina and the role of proteasomal proteolysis. *Neuroreport* 2001;12(17):3833–7.
20. **Sakamoto K, Ishida N.** Molecular cloning of serotonin N-acetyltransferase gene from the mouse and its daily expression in the retina. *Neuroscience letters* 1998;250(3):181–4.
21. **Sakamoto K, Ishida N.** Circadian expression of serotonin N-acetyltransferase mRNA in the rat retina. *Neuroscience Letters* 1998;245(2):113–116.
22. **Niki T, Hamada T, Ohtomi M, Sakamoto K, Suzuki S, Kako K, Hosoya Y, Horikawa K, Ishida N.** The Localization of the Site of Arylalkylamine N -Acetyltransferase Circadian Expression in the Photoreceptor Cells of Mammalian Retina. *Biochemical and biophysical research communications* 1998;248(1):115–120.
23. **Liu C, Fukuhara C, Wessel JH, Iuvone PM, Tosini G.** Localization of Aa-nat mRNA in the rat retina by fluorescence in situ hybridization and laser capture microdissection. *Cell and tissue research* 2004;315(2):197–201.
24. **Bernard M, Iuvone PM, Cassone VM, Roseboom PH, Coon SL, Klein DC.** Avian melatonin synthesis: photic and circadian regulation of serotonin N-acetyltransferase mRNA in the chicken pineal gland and retina. *Journal of neurochemistry* 1997;68(1):213–24.
25. **Garbarino-Pico E, Carpentieri AR, Contin M a, Sarmiento MIK, Brocco M a, Panzetta P, Rosenstein RE, Caputto BL, Guido ME.** Retinal ganglion cells are autonomous circadian oscillators synthesizing N-acetylserotonin during the day. *The Journal of biological chemistry* 2004;279(49):51172–81.
26. **Coon SL, Del Olmo E, Young WS, Klein DC.** Melatonin synthesis enzymes in Macaca mulatta: focus on arylalkylamine N-acetyltransferase (EC 2.3.1.87). *The Journal of clinical endocrinology and metabolism* 2002;87(10):4699–706.
27. **Steinlechner S, King TS, Champney TH, Richardson BA, Reiter RJ.** Pharmacological studies on the regulation of n-acetyltransferase activity and melatonin content of the pineal gland of the syrian hamster. *Journal of Pineal Research* 1985;2(2):109–19.
28. **Gauer F, Craft CM.** Circadian regulation of hydroxyindole-O-methyltransferase mRNA levels in rat pineal and retina. *Brain research* 1996;737(1-2):99–109.
29. **Klein DC, Roseboom PH, Donohue SJ, Marrs BL.** Evolution of melatonin as a night signal: Contribution from a primitive photosynthetic organism. *Molecular and Cellular Neurosciences* 1992;3:181–183.

30. **Voisin P, Cailleau V, Naud N, Cantereau a, Bernard M.** Visual photoreceptor subtypes in the chicken retina: melatonin-synthesizing activity and in vitro differentiation. *Cell and tissue research* 2012;348(3):417–27.
31. **Challet E, Pitrosky B, Sicard B, Malan A, Pévet P.** Circadian organization in a diurnal rodent, Arvicanthis ansorgei Thomas 1910: chronotypes, responses to constant lighting conditions, and photoperiodic changes. *Journal of biological rhythms* 2002;17(1):52–64.
32. **Szél A, Rohlich P.** Two Cone Types of Rat Retina Detected by Anti-visual Pigment Antibodies. *Exp.Eye Res.* 1992;55(1):47–52.
33. **Jeon CJ, Strettoi E, Masland RH.** The major cell populations of the mouse retina. *The Journal of neuroscience : the official journal of the Society for Neuroscience* 1998;18(21):8936–46.
34. **Bobu C, Craft CM, Masson-pevet M, Hicks D.** Photoreceptor organization and rhythmic phagocytosis in the Nile rat Arvicanthis ansorgei: a novel diurnal rodent model for the study of cone pathophysiology. *Investigative ophthalmology & visual science* 2006;47(7):3109–3118.
35. **Harrison ER.** Visual acuity and the cone cell distribution of the retina. *The British journal of ophthalmology* 1953;37(9):538–542.
36. **Gowdy PD, Cicerone CM.** The spatial arrangemengt of L and M cones in the peripheral human retina. *Vision Res.* 1998;38(17):2575–89.
37. **Rasri K, Mason P, Govitrapong P, Pevet P, Klosen P.** Testosterone-driven seasonal regulation of vasopressin and galanin in the bed nucleus of the stria terminalis of the Djungarian hamster (Phodopus sungorus). *Neuroscience* 2008;157(1):174–187.
38. **Bartzen-Sprauer J, Klosen P, Ciofi P, Mikkelsen JD, Simonneaux V.** Photoperiodic co-regulation of kisseptin, neurokinin B and dynorphin in the hypothalamus of a seasonal rodent. *Journal of Neuroendocrinology* 2014;26(8):510–520.
39. **Mehdi MKIM, Sage-Ciocca D, Challet E, Malan A, Hicks D.** Oxygen-induced retinopathy induces short-term glial stress and long-term impairment of photoentrainment in mice. *Graefe's Archive for Clinical and Experimental Ophthalmology* 2014;252(4):595–608.
40. **Bobu C, Lahmam M, Vuillez P, Ouarour A, Hicks D.** Photoreceptor organisation and phenotypic characterization in retinas of two diurnal rodent species: potential use as experimental animal models for human vision research. *Vision research* 2008;48(3):424–32.
41. **Barnstable C.** Monoclonal antibodies which recognize different cell types in the rat retina. *Nature* 1980;286(5770):231–5.
42. **Karnas D, Hicks D, Mordel J, Pévet P, Meissl H.** Intrinsic Photosensitive Retinal Ganglion Cells in the Diurnal Rodent, Arvicanthis ansorgei. *PLoS ONE* 2013;8(8):e73343.
43. **Ribelayga C, Pevet P, Simonneaux V.** Adrenergic and peptidergic regulations of hydroxyindole- O -methyltransferase activity in rat pineal gland. *Brain Research* 1997;777(1-2):247–250.
44. **Garidou ML, Bartol I, Calgari C, Pévet P, Simonneaux V.** In vivo observation of a non-noradrenergic regulation of arylalkylamine N-acetyltransferase gene expression in the rat pineal complex. *Neuroscience* 2001;105(3):721–9.
45. **Contin MA, Verra DM, Guido ME.** An invertebrate-like phototransduction cascade mediates light detection in the chicken retinal ganglion cells. *The FASEB journal : official publication of the Federation of American Societies for Experimental Biology* 2006;20(14):2648–2650.
46. **Pozdeyev N, Taylor C, Haque R, Chaurasia SS, Visser A, Thazyeen A, Du Y, Fu H, Weller J, Klein DC, Iuvone PM.** Photic regulation of arylalkylamine N-acetyltransferase binding to 14-3-3 proteins in retinal photoreceptor cells. *The Journal of neuroscience : the official journal of the Society for Neuroscience* 2006;26(36):9153–9161.
47. **Iuvone PM, Brown AD, Haque R, Weller J, Zawilska JB, Chaurasia SS, Ma M, Klein DC.** Retinal Melatonin Production : Role of Proteasomal Proteolysis in Circadian and Photic Control of Arylalkylamine N -Acetyltransferase. *Investigative ophthalmology & visual science* 2002;43(2):564–572.

48. **Besseau L, Benyassi A, Møller M, Coon SL, Weller JL, Boeuf G, Klein DC, Falcón J.** Melatonin pathway: breaking the "high-at-night" rule in trout retina. *Experimental eye research* 2006;82(4):620–7.
49. **Grève P, Alonso-Gómez a, Bernard M, Ma M, Haque R, Klein DC, Iuvone PM.** Serotonin N-acetyltransferase mRNA levels in photoreceptor-enriched chicken retinal cell cultures: elevation by cyclic AMP. *Journal of neurochemistry* 1999;73:1894–1900.
50. **Valdez DJ, Garbarino-Pico E, Díaz NM, Silvestre DC, Guido ME.** Differential regulation of arylalkylamine N-acetyltransferase activity in chicken retinal ganglion cells by light and circadian clock. *Chronobiology international* 2012;29(8):1011–20.
51. **Kuwano R, Iwanaga T, Nakajima T, Masuda T, Takahashi Y.** Immunocytochemical demonstration of hydroxyindole O-methyltransferase (HIOMT), neuron-specific enolase (NSE) and S-100 protein in the bovine pineal gland. *Brain research* 1983;274(1):171–175.
52. **Kasahara T, Abe K, Mekada K, Yoshiki A, Kato T.** Genetic variation of melatonin productivity in laboratory mice under domestication. *Proceedings of the National Academy of Sciences of the United States of America* 2010;107(14):6412–7.
53. **Wiechmann AF, Bok D, Horwitz J.** Localization of hydroxyindole-O-methyltransferase in the mammalian pineal gland and retina. *Investigative Ophthalmology and Visual Science* 1985;26(3):253–265.
54. **Wiechmann AF, Craft CM.** Localization of mRNA encoding the indolamine synthesizing enzyme, hydroxyindole-O-methyltransferase, in chicken pineal gland and retina by in situ hybridization. *Neuroscience Letters* 1993;150(2):207–211.
55. **Simonneaux V, Ribelayga C.** Generation of the melatonin endocrine message in mammals: a review of the complex regulation of melatonin synthesis by norepinephrine, peptides, and other pineal transmitters. *Pharmacological reviews* 2003;55(2):325–395.
56. **Iuvone PM, Tosini G, Pozdeyev N, Haque R, Klein DC, Chaurasia SS.** Circadian clocks, clock networks, arylalkylamine N-acetyltransferase, and melatonin in the retina. *Progress in Retinal and Eye Research* 2005;24(4):433–456.
57. **Garidou M-L, Gauer F, Vivien-Roels B, Sicard B, Pevet P, Simonneaux V.** Pineal arylalkylamine N-acetyltransferase gene expression is highly stimulated at night in the diurnal rodent, Arvicanthis ansorgei. *European Journal of Neuroscience* 2002;15(10):1632–1640.
58. **Klein DC.** Arylalkylamine N-acetyltransferase: "The timezyme." *Journal of Biological Chemistry* 2007;282(7):4233–4237.
59. **Coon SL, Roseboom PH, Baler R, Weller JL, Namboodiri M a, Koonin E V, Klein DC.** Pineal serotonin N-acetyltransferase: expression cloning and molecular analysis. *Science (New York, N.Y.)* 1995;270(5242):1681–1683.
60. **Bobu C, Sandu C, Laurent V, Felder-Schmittbuhl M-P, Hicks D.** Prolonged light exposure induces widespread phase shifting in the circadian clock and visual pigment gene expression of the Arvicanthis ansorgei retina. *Molecular Vision* 2013;19:1060–1073.
61. **Pang SF, Yu HS, Suen HC, Brown GM.** Melatonin in the retina of rats: a diurnal rhythm. *J.Endocr* 1980;87(1):89–93.
62. **Do Carmo Buonfiglio D, Peliciari-Garcia RA, do Amaral FG, Peres R, Nogueira TCA, Afeche SC, Cipolla-Neto J.** Early-stage retinal melatonin synthesis impairment in streptozotocin-induced diabetic wistar rats. *Investigative ophthalmology & visual science* 2011;52(10):7416–22.
63. **Reppert SM, Sagar SM.** Characterization of the day-night variation of retinal melatonin content in the chick. *Investigative Ophthalmology and Visual Science* 1983;24:294–300.
64. **Vanecek J.** Cellular mechanisms of melatonin action. *Physiological reviews* 1998;78(3):687–721.
65. **Doyle SE, Grace MS, McIVOR W, Menaker M.** Circadian rhythms of dopamine in mouse retina: The role of melatonin. *Visual Neuroscience* 2002;19(05):593–601.
66. **Jang S-W, Liu X, Pradoldej S, Tosini G, Chang Q, Iuvone PM, Ye K.** N-acetylserotonin activates TrkB receptor in a circadian rhythm. *Proceedings of the National Academy of Sciences of the United States of America* 2010;107(8):3876–81.

67. **Sompol P, Liu X, Baba K, Paul KN, Tosini G, Iuvone PM, Ye K.** N-acetylserotonin promotes hippocampal neuroprogenitor cell proliferation in sleep-deprived mice. *Proceedings of the National Academy of Sciences of the United States of America* 2011;108(21):8844–9.
68. **Zawilska JB, Iuvone PM.** Melatonin synthesis in chicken retina: effect of kainic acid-induced lesions on the diurnal rhythm and D2-dopamine receptor-mediated regulation of serotonin N-acetyltransferase activity. *Neuroscience letters* 1992;135(1):71–74.
69. **Nguyen-legros J, Chanut E, Versaux-botteri C, Simon A, Trouvin J.** Dopamine Inhibits Melatonin Synthesis in Photoreceptor Cells Through a D -Like Receptor Subtype in the Rat Retina : Biochemical and Histochemical Evidence. *Journal of neurochemistry* 1996;67(6):2514–2520.
70. **Tosini G, Dirden JC.** Dopamine inhibits melatonin release in the mammalian retina: In vitro evidence. *Neuroscience Letters* 2000;286(2):119–122.
71. **Boudard DL, Acar N, Bretillon L, Hicks D.** Retinas of the diurnal rodent Arvicanthis ansorgei are highly resistant to experimentally induced stress and degeneration. *Investigative Ophthalmology and Visual Science* 2011;52(12):8686–8700.
72. **Coon SL, Mazuruk K, Bernard M, Roseboom PH, Klein DC, Rodriguez IR.** The human serotonin N-acetyltransferase (EC 2.3.1.87) gene (AANAT): structure, chromosomal localization, and tissue expression. *Genomics* 1996;34(1):76–84.
73. **Craft CM, Murage J, Brown B, Zhan-Poe X.** Bovine arylalkylamine N-acetyltransferase activity correlated with mRNA expression in pineal and retina. *Molecular Brain Research* 1999;65(1):44–51.
74. **Privat K, Ravault J-P, Chesneau D, M F.** Day / night variation of tryptophan hydroxylase and serotonin N-acetyltransferase mRNA levels in the ovine pineal gland and retina. *Journal of Pineal Research Pineal Research* 1999;26(4):193–203.
75. **Nowak JZ, Zurawska E, Zawilska J.** Melatonin and its generating system in vertebrate retina: circadian rhythm, effect of environmental lighting and interaction with dopamine. *Neurochemistry international* 1989;14(4):397–406.
76. **Hamm HE, Menaker M.** Retinal rhythms in chicks: circadian variation in melatonin and serotonin N-acetyltransferase activity. *Proceedings of the National Academy of Sciences of the United States of America* 1980;77(8):4998–5002.
77. **Iuvone PM, Besharse JC.** Regulation of indoleamine N-acetyltransferase activity in the retina: effects of light and dark, protein synthesis inhibitors and cyclic nucleotide analogs. *Brain research* 1983;273(1):111–119.
78. **Olcese J, Møller M.** Characterization of serotonin N-acetyltransferase activity in the retina of the Mongolian gerbil, Meriones unguiculates. *Neuroscience letters* 1989;102(2-3):235–240.
79. **Bernard M, Donohue SJ, Klein DC.** Human hydroxyindole-O-methyltransferase in pineal gland, retina and Y79 retinoblastoma cells. *Brain Research* 1995;696:37–48.
80. **Rodriguez I., Mazuruk K, Schoen T., Chader G.** Structural analysis of the human hydroxyindole-O-methyltransferase gene. *The Journal of biological chemistry* 1994;269(50):31969–77.
81. **Grota LJ, Holloway WR, Brown G.** 24-Hour Rhythm of Hypothalamic Melatonin Immunofluorescence Correlates with Serum and Retinal Melatonin Rhythms. *Neuroendocrinology* 1982;34(5):363–368.
82. **Reiter J, Richardson BA, Matthews SA, Lane SJ, Ferguson BN.** Rhythms in immunoreactive melatonin in the retina and hardarian gland of rats: persistence after pinealectomy. *Life Sciences* 1983;32(11):1229–36.
83. **García-Allegue R, Madrid J a, Sánchez-Vázquez FJ.** Melatonin rhythms in European sea bass plasma and eye: influence of seasonal photoperiod and water temperature. *Journal of pineal research* 2001;31(1):68–75.
84. **Faillace MP, Cutrera R, Sarmiento MI, Rosenstein RE.** Evidence for local synthesis of melatonin in golden hamster retina. *Neuroreport* 1995;6(15):2093–2095.

85. **Hall F, Tengerdy C, Morita M, Pautler E.** Determination of bovine retinal melatonin with HPLC-EC. *Current eye research* 1985;4(8):847–850.
86. **Melamed E, Frucht Y, Lemor M, Uzzan a, Rosenthal Y.** Dopamine turnover in rat retina: a 24-hour light-dependent rhythm. *Brain research* 1984;305:148–151.
87. **Gibson CJ.** Diurnal alterations in retinal tyrosine level and dopamine turnover in diabetic rats. *Brain research* 1988;454:60–66.
88. **Pozdeyev N V, Lavrikova E V.** Diurnal changes of tyrosine, dopamine, and dopamine metabolites content in the retina of rats maintained at different lighting conditions. *Journal of molecular neuroscience : MN* 2000;15:1–9.
89. **Nir I, Haque R, Iuvone PM.** Diurnal metabolism of dopamine in dystrophic retinas of homozygous and heterozygous retinal degeneration slow (rds) mice. *Brain Research* 2000;884((1-2)):13–22.
90. **Boelen MK, Boelen MG, Marshak DW.** Light-stimulated release of dopamine from the primate retina is blocked by 1-2-amino-4-phosphonobutyric acid (APB). *Visual neuroscience* 1998;15(1):97–103.
91. **Wulle I, Kirsch M, Wagner HJ.** Cyclic changes in dopamine and DOPAC content, and tyrosine hydroxylase activity in the retina of a cichlid fish. *Brain research* 1990;515:163–167.
92. **Nowak JZ, Zurawska E.** Dopamine in the rabbit retina and striatum: diurnal rhythm and effect of light stimulation. *Journal of neural transmission* 1989;75(3):201–212.
93. **Di Paolo T, Harnois C, Daigle M.** Assay of dopamine and its metabolites in human and rat retina. *Neuroscience letters* 1987;74:250–254.

Annexes

Aa-nat mRNA peaks at night in cone photoreceptors of *Arvicanthis ansorgei*

We quantified *Aa-nat* mRNA expression levels in the cones across the 24 hour period, by densitometric measures of hybridization signal. *Aa-nat* mRNA expression levels were relatively low and uniform during the daytime, then began to rise at early night to reach a peak of fourfold daytime levels at ZT19, decreasing again to twofold by ZT23 **(Figure 30)**. Z19 values were statistically significantly different from ZT7, 3, 11 and 23.

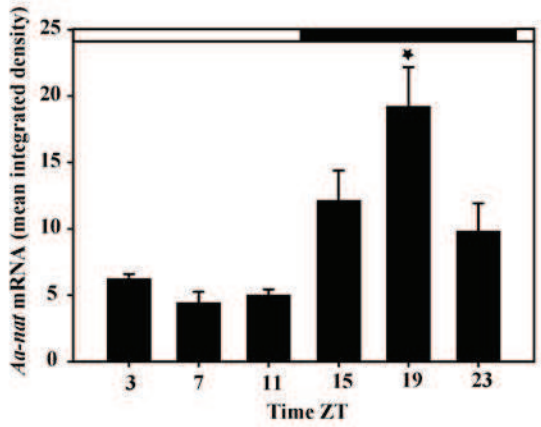

Figure 30. *Aa-nat* gene expression is higher at night in the cones of *Arvicanthis ansorgei's* retina.

Quantitative densitometric measures of hybridization signal at the level of cones cell bodies/IS across the 24 hour period. Expression of transcripts showed a statistically significant peak at ZT19 ($p < 0.001$, one-way ANOVA, Holm-Sidak test) ($n = 3$).

Expression of phosphorylated AA-NAT is high at night but persist throughout daytime

We studied the expression of the phosphorylated (P) form of AA-NAT across the 24 hours in an attempt to explain the presence of AA-NAT (protein and activity) during the day while it is generally accepted that AA-NAT is under strict circadian and light control resulting in highly predominant nocturnal activity. Indeed, during the night, chicken retinal AA-NAT is phosphorylated and forms a complex with the 14-3-3 protein, leading to a protection of AA-NAT from degradation *(Pozdeyev et al., 2006)*.

We performed western blotting analyses of *Arvicanthis* retinas collected every 4 hours across the 24 hours period to analyze P-AA-NAT protein (Figure 31**A**). We detected an immunoreactive band at the expected size of 26 kDa corresponding to AA-NAT. There was considerable variation in immunoreactive intensity within sample groups (even though animals were raised under identical conditions) (Figure 31**A**). We observed P-AA-NAT expression over the 24 hours, rising at ZT11 but reaching a maximum during the night (at ZT23) (Figure 31**B**). The unphosphorylated (UnP) form of AA-NAT was also detected by western blotting analyses (Figure 31**C**). UnP-AA-NAT was present over the 24 hours with a peak at ZT15, a slight decrease at ZT23 and a minimum at ZT11 (Figure 31**D**). Our results display a maximum level of AA-NAT expression (P and UnP) at night but expression persists throughout daytime **(Article I Figure 2B)**. The 14-3-3 protein was detected over the 24 hours in the retina of *Arvicanthis ansorgei* (Figure 31**E**) and exhibited the same profile as the one of P-AA-NAT. Indeed 14-3-3 data show a first rise at ZT7, followed by a decrease at ZT15, and a second increase at ZT23 (Figure 31**F**). These results suggest that 14-3-3 is present in the retina at the same time as P-AA-NAT allowing a possible interaction between both proteins.

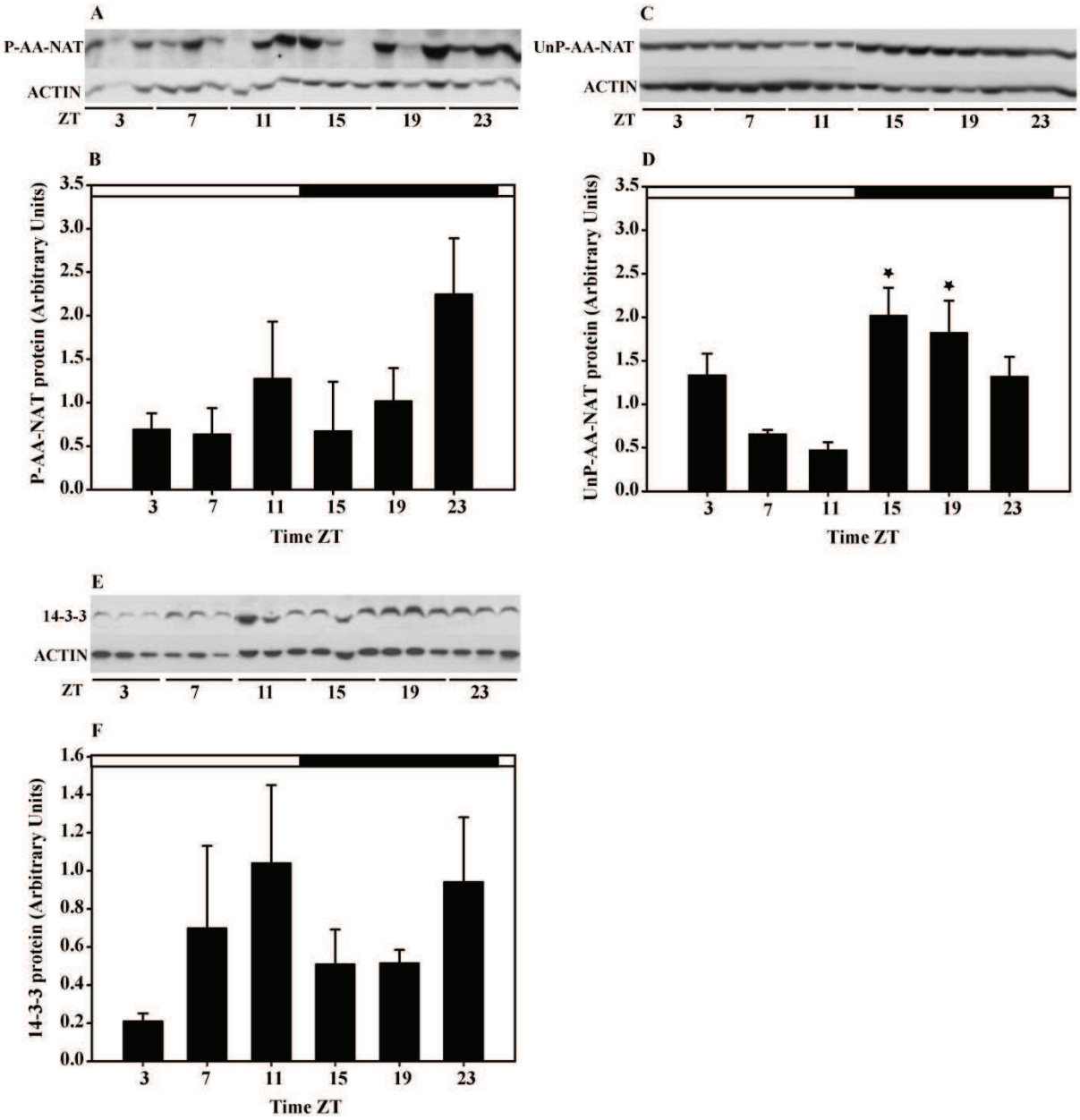

Figure 31. Phosphorylated AA-NAT and 14-3-3 expression exhibit the same profile.

A) Western blotting analysis of phosphorylated (P)-AA-NAT expression (antibody anti AA-NAT 3352) in retinas from 3 different animals per time point reveals the presence of P-AA-NAT protein throughout the 24 hours. Data indicate that AA-NAT expression across 24 hours is overall higher at the end of the night. It is also evident that there was great variability between individuals within sampling time. **B)** Densitometric quantification of P-AA-NAT in western blots (n = 3) confirms a constitutive expression with modest increases at the end of the night (ZT23) and day (ZT11) ($p > 0.05$, one-way ANOVA). **C)** Western blotting analysis of unphosphorylated (UnP)-AA-NAT (antibody anti AA-NAT 3305) expression in retinas from 3 different animals per time point. UnP-AA-NAT is present over the 24 hours. **D)** Densitometric quantification of UnP-AA-NAT in western blots (n = 3) underlines a peak at the beginning of the dark period ($p = 0.005$, one-way ANOVA, Holm-Sidak test). **E)** Western blotting analysis of 14-3-3 expression in retinas from 1 animal per time point (same sample repeated 3 times for each ZT) reveals the presence of the protein 14-3-3 throughout the 24 hours. **F)** Densitometric quantification of 14-3-3 in western blots (n = 3) confirms a constitutive expression with slight increases at the end of the night (ZT23) and day (ZT11) ($p > 0.05$, one-way ANOVA). Data are the mean values ± SEM of 3

animals analyzed in 3 independent experiments or per time point. Black bars represent night-time; light bars represent day-time.

AA-NAT expression peaks at day in DD condition

To assess whether both the circadian clock and the light control AA-NAT expression in *Arvicanthis* retina, we performed AA-NAT western blotting analyses across the 24 hours period with retinas from animal raised 4 days in DD. We observed an intense immunoreactive band at the expected molecular weight of AA-NAT **(Figure 32A)**. Moreover AA-NAT expression was the lowest at CT3, reached a peak at CT7 and slightly decreased over the subjective night. LD AA-NAT expression **(Article I, Figure 2B)** didn't exhibit the peak at CT7 suggesting that in LD condition, the light inhibits the peak of AA-NAT in the middle of the day. These results suggest that AA-NAT may be degraded during the day (in LD condition).

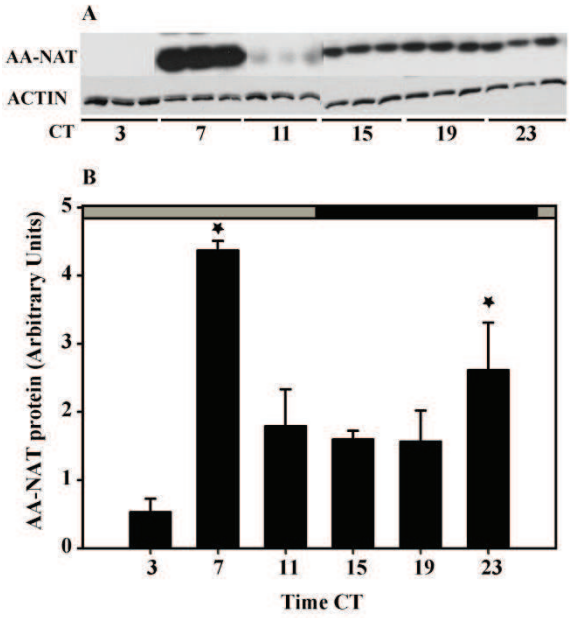

Figure 32. AA-NAT expression exhibits a peak at CT7 in DD.

A) Western blotting analysis of AA-NAT expression in retinas of 1 animal per time point (the same sample is repeated 3 times) reveals the presence of AA-NAT protein throughout the 24 hours. Data indicate that AA-NAT expression is higher at CT7 but remains elevated at night. **B)** Densitometric quantification in western blots (n = 3) confirms that the maximum of AA-NAT is at CT7 ($p < 0.001$, one-way ANOVA, Holm-Sidak test) as well as arising expression at night. The lowest expression is at CT3. Data are the mean values ± SEM of 3 animals analyzed in 3 independent experiments. Black bars represent subjective night; grey bars represent subjective day.

***Hiomt* is specifically expressed in cones and GCL of the rat retina**

We then studied the ultimate enzyme of the melatonin synthetic pathway: HIOMT. Precisely, we determined the cellular localization of *hiomt*. For that purpose, we used a digoxigenin-labeled riboprobe specific for rat tissue. The sequence of *hiomt* varies greatly between species, is expressed only at very low levels, so this riboprobe gave no signal in *Arvicanthis ansorgei* retina. We hence restricted our observations to rat retina, obtained across the 24 hours light/dark cycle. *In situ* hybridization of rat retinas collected at ZT19 displayed expression in rare loci along the scleral border of the ONL and weak expression in INL and GCL **(Figure 33B)**. This pattern suggested that staining was restricted to cones, since they represent < 2 % of total photoreceptors in the rat. To confirm this, we performed *in situ* hybridization for *hiomt* followed immediately with immunostaining against cone arrestin. Although the harsh treatment of sections reduced antibody efficacy, immunostaining was localized to rare cytoplasmic profiles (arrow) **(Figure 33D)**. *Hiomt* mRNA label (white label) was overlying immunostained cells **(Figure 33F)**. Expression of *hiomt* mRNA in cones was not visible during the day **(Figure 33C, H)**. On the other hand GCL expression is higher during the day **(Figure 33C, I)**. Weak staining was also observed in the INL during day and night **(Figure 33B, C)**.

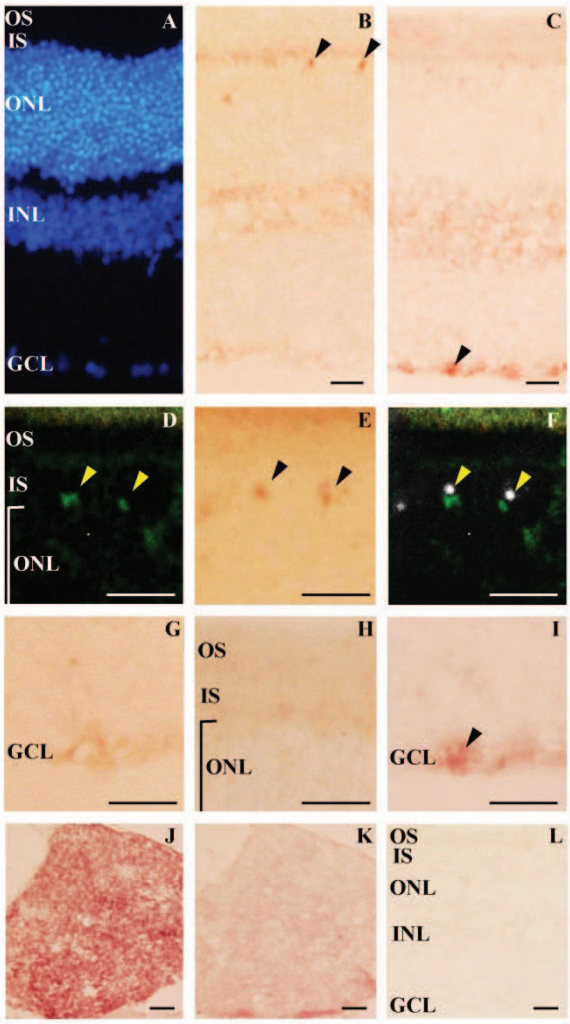

Figure 33. *Hiomt* gene is expressed in the cones and GCL of rat retina.

A) DAPI staining of a 10 µm rat retina section indicates the area of interest: from top to bottom: OS, IS, ONL, INL, GCL. **B)** *Hiomt* antisense probe labeling at ZT23 (night time) is detected in cells of the ONL and more weakly the INL and GCL. **C)** *Hiomt* staining with antisense probe at ZT7 (day time) appears mainly in the GCL and weakly in the INL. **D)** Immunostaining of rat retina with anti-cone arrestin (green) shows cone segment (arrow). **E)** Enlargement of ONL at ZT23 shows *hiomt* staining in 2 cells (arrow). **F)** Overlapping of *hiomt* and cone arrestin images reveal that *hiomt* staining (show in white) is restricted to the cones segment (arrow). **G)** Enlargement of GCL at ZT23 reveals a weak *hiomt* staining. **H)** Enlargement of ONL at ZT7 shows no *hiomt* staining. **I)** Enlargement of GCL at ZT7 reveals strong *hiomt* staining. **J)** Positive control with *hiomt* antisense probe in rat pineal gland at ZT23. **K) and L)** Use of *hiomt* sense probe at ZT23 on pineal gland and retina tissues respectively does not reveal labeling in any structures. Scale bar = 10 µm.

CHAPTER II

ROLE OF MELATONIN IN THE RODENT RETINA

Article II

Cone viability is affected by interruption of melatonin signaling

Gianesini Coralie[1, 2], Hiragaki Susumu[1], Susana Contreras-Alcantara[1], Laurent Virginie[2], Hicks David[2], Tosini Gianluca[1]

[1]Department of Pharmacology and Toxicology and Neuroscience Institute, Morehouse School of Medicine, 720 Westview Drive, Atlanta, GA, United States

[2]CNRS UPR 3212, Institute for Cellular and Integrative Neurosciences, 5 rue Blaise Pascal, F-67084, Strasbourg, France

Abstract

Previous studies have demonstrated that melatonin may play an important role in the modulation of photoreceptor viability during aging and studies in humans have involved melatonin in the pathogenesis of age-related macular degeneration. This hormone exerts its influence by binding to G-protein coupled receptors named melatonin receptor 1 (MT_1) and 2 (MT_2). MT_1 and MT_2 receptors activate a wide variety of signaling pathways including the AKT-FOXO1 cell survival pathway. In the photoreceptors they form MT_1/MT_2 heteromers.

Melatonin proficient mice (C3H/$f^{+/+}$) and melatonin proficient mice lacking MT_1 or MT_2 receptors ($MT_1^{-/-}$ and $MT_2^{-/-}$) were used in this study. Mice were sacrificed at the age of 3 and 18 months and photoreceptor viability was assessed by counting nuclei number in the outer nuclear layer and the number of cones. Cones were identified by immunohistochemistry using peanut agglutinin lectin, green/red and blue opsin antibodies. AKT and FOXO1 were assessed by western blotting and immunohistochemistry.

The nuclei number in the outer nuclear layer was significantly reduced in $MT_1^{-/-}$ and $MT_2^{-/-}$ mice at 18 months of age ($P < 0.05$) with respect to 3 months old animals. Furthermore in 18 month old $MT_1^{-/-}$ and $MT_2^{-/-}$ mice the number of cones was significantly reduced ($P < 0.05$) with respect to young (3 months) $MT_1^{-/-}$ and $MT_2^{-/-}$ mice or age matched C3H/$f^{+/+}$. No difference in the number of cones in young C3H/$f^{+/+}$, $MT_1^{-/-}$ and $MT_2^{-/-}$ mice ($P > 0.1$) or between young and old C3H/$f^{+/+}$mice ($P > 0.1$) was observed. The red/green cones showed a more pronounced decline than the blue cones. In C3H/$f^{+/+}$ the activation of AKT-FOXO1 pathway showed a daily rhythm ($P < 0.05$) with peak values at ZT22. No rhythmicity in the AKT-FOXO1 activation was observed in $MT_1^{-/-}$ and $MT_2^{-/-}$ ($P > 0.05$). AKT/FOXO1 was localized in rods and cones.

Our data indicate that interruption of melatonin signaling via MT_1 and MT_2 receptors induces a significant reduction in the number of cells in the outer nuclear layer during aging, especially red/green cones. Our data also suggest that the AKT-FOXO1 survival pathway may be involved in the mechanism by which melatonin protects photoreceptors. Finally, melatonin action on photoreceptor viability seems to be mediated by MT_1/MT_2 heteromers.

Introduction

Retinal melatonin is synthesized by photoreceptors of many vertebrate species via a well-defined biosynthetic pathway *(Klein et al., 1997; Iuvone et al., 2005)*. The amount of melatonin produced by the retina is much smaller than that produced by the pineal gland and retinal melatonin is thought to act as a local neuromodulator within the eye *(Cahill & Besharse, 1989)*. Melatonin synthesis in the retina, as in the pineal gland, occurs primarily during the night in darkness, and thus melatonin levels are high during the night and low during the day *(reviewed in Tosini et al., 2012)*. Melatonin synthesis is controlled by a circadian clock located within the photoreceptors *(Zawilska & Iuvone, 1992; Cahill & Besharse, 1993; Tosini & Menaker, 1998; Tosini et al., 2007)*. Transcriptional and post-translational mechanisms ensure that melatonin levels are maintained at extremely low levels in the presence of light *(Fukuhara et al., 2001, 2004)*. Such tight control of retinal melatonin levels suggests that high melatonin levels during the light-phase may be deleterious for the photoreceptor cells *(Wiechmann & O'Steen, 1992)*.

Melatonin exerts its influence by binding to G protein-coupled receptors (GPCRs) named melatonin receptor type 1 (MT_1) and type 2 (MT_2). Both receptors are present in the vertebrate retina and activate a wide variety of signaling pathways *(Fujieda et al., 1999; Scher et al., 2002; Savaskan et al., 2007; Baba et al., 2013)*. The co-localization of MT_1 and MT_2 receptors suggests they may form heteromeric complexes, as demonstrated previously *in vitro (Ayoub et al., 2002, 2004)* and recently confirmed in photoreceptors *in vivo (Baba et al., 2013)*.

Melatonin modulates the sensitivity of photoreceptors and second-order neurons at night when photopic input is low *(Wiechmann et al., 1988)*. In some species, melatonin can affect glutamatergic transmission from cones to cone-driven bipolar cells *(Huang et al., 2005)* and may potentiate responses of ON bipolar cells to rod signals *(Ping et al., 2008)*. In *Xenopus laevis,* melatonin directly stimulates the responsiveness of rod photoreceptors *(Wiechmann et al., 2003)*. Administration of exogenous melatonin in fishes and amphibians can increase the amplitude of the a- and b-wave of the scotopic electroretinogram *(Wiechmann et al., 2003; Ping et al., 2008)*. In mice, administration of exogenous melatonin increases the amplitudes of a- and b- waves and lowers the scotopic threshold response (ie. visual sensitivity) to levels observed at night under controlled conditions; removal of MT_1 and/or MT_2 receptors abolishes these effects *(Baba et al., 2009, 2013)*. Finally, several studies have shown that melatonin plays a key role in the regulation of retinal circadian rhythms *(Hiragaki et al., 2014; McMahon et al., 2014 for recent review)*.

Earlier studies have demonstrated that melatonin can exert both beneficial and detrimental effects on photoreceptors: on one hand it may play an important role in protecting them from oxidative stress *(Marchiafava & Longoni, 1999)*, preventing apoptosis *(Liang et al., 2001)* and also promotes photoreceptor viability during aging *(Baba et al., 2009)*; on the other hand it can also sensitize photoreceptors to light-induced damage *(Sugawara et al., 1998)*. Some studies have implicated melatonin in the pathogenesis of age-related macular degeneration (AMD). AMD is a slow and progressive disease of the macula, ie. the central part of the retina where cone density is maximal, and constitutes the leading cause of irreversible visual loss in the western world *(Coleman et al., 2008)*. Yi et al., (2005) reported that daily administration of melatonin (3 mg) may protect the retina and delay the progression of AMD *(Yi et al., 2005)* while, Rosen et al. (2009) described that

production of melatonin is decreased in AMD patients with respect to age-matched controls *(Rosen et al., 2009)*. These findings suggest that a deficiency in melatonin may play a role in the progression of AMD.

To gather more insight into the role of melatonin during aging, we investigated the effect of MT_1 and MT_2 deletion on the viability of cone photoreceptors and the potential role therein of the survival pathway involving a serine/threonine protein kinase (AKT) and the Forkhead-related family of mammalian transcription factor (FOXO1) *(Brunet et al., 1999)*.

Materials and methods

Animals

C3H/$f^{+/+}$, C3H/$f^{+/+}MT_1^{-/-}$ and C3H/$f^{+/+}MT_2^{-/-}$ mice were used in this study *(see Baba et al., 2009, 2013 for details)*. All the experimental procedures were carried out in accordance with Association for Assessment of Laboratory Animal Care policies and approved by the Morehouse School of Medicine Animal Care and Use Committee.

Outer nuclear layer cell counting

Mice were euthanized and before eye nucleation the superior cornea was marked with a hot needle. After 1 hour fixation in 4 % paraformaldehyde (PAF) (Sigma-Aldrich), the anterior segment was removed, except for the superior cornea, and the eyes were fixed overnight at 4 °C. After dehydration through a graded ethanol series, eyecups were embedded in Durcopan (Fluka, Hatfield, PA), cut in 1.5 µm thick sections, and stained with toluidine blue. Photoreceptor nuclei were counted in a 10 µm microscopic field that was centered at 300 µm above the edge of the optic nerve head. For each sample, we counted the number of photoreceptor cells in 10 different locations within each of three adjacent sections. The number of nuclei in the outer nuclear layer (ONL) was counted using the Image-Pro Plus 3.0 software. The data obtained from the different adjacent sections were combined and the mean ± SEM was calculated. Measurements were made by observers who were blinded to the genotype and age of the samples.

Immunohistochemical analysis of phosphorylated-AKT, phosphorylated-FOXO1 and FOXO1

After sacrifice, eyes were collected and fixed with 4 % PAF in PBS during 12 hours. Subsequent to fixation, the eyeballs were rinsed in PBS, transferred to sucrose 30 % overnight and embedded (Tissue-Tek™ CRYO-OCT Compound, Fisher Healthcare). Cryostat sections (12 µm thick) were mounted on SuperFrost*Plus slides (VWR) and stored at -20 °C until ready for use.

The retinas sections were permeabilized with 0.1 % Triton X-100 for 5 min and the endogenous peroxidase activity was quenched with PBS + 1 % H_20_2 during 1 hour. Retinas were incubated in blocking buffer 1 hour (1 % BSA in PBS) and in primary antibody overnight at 4 °C. The primary antibodies were as follows: monoclonal anti-rabbit phosphorylated (P) AKT (Ser473) (Cell Signaling, #4060), dilution 1:200; polyclonal anti-rabbit P-FOXO1 (Ser256) (Cell Signaling, #9461), 1:500; monoclonal anti-rabbit FOXO1 (detects P and unphosphorylated (UnP) FOXO1) (Cell Signaling, #2880), 1:200. After extensive wash in PBS, retinas were incubated 1 hour in HRP conjugated secondary antibody (Tyramide Signal Amplification Kit #12, Life technologies), dilution 1:100. Retinal

sections were again washed thoroughly and incubated 10 min with labeled tyramide (Tyramide Signal Amplification Kit #12, Life technologies), dilution 1:100. After several washes, retinal sections were mounted with mounting medium (Prolong, Life technologies) before being examined with a confocal microscope (Zeiss LSM700).

Immunofluorescence analysis of AKT pan, red/green opsin, blue opsin and peanut agglutinin

The samples were treated as described before. For AKT pan staining, after fixation the eyes were incubated in a retrieval solution (10 mM sodium citrate, pH 6) overnight at 4 °C. The eyes were immersed in boiling retrieval solution 3 min and immediately placed in cold sucrose 30 %.

The sections were permeabilized with Triton X-100 (0.1 % in PBS) for 5 min and then saturated with blocking buffer (3 % BSA, 0.05 % Tween-20, 0.1 % Triton X-100, 0.1 % sodium azide in PBS) during 2 hours. Sections were incubated 2 hours with rhodamine labeled peanut agglutinin [PNA; a lectin from the plant *Arachis hypogaea*, which binds galactose-galactosamine disaccharide and labels the cone matrix sheath but not rod photoreceptors (RL-1072, Vector Laboratories)], dilution 1:500; or overnight with primary antibody diluted in blocking buffer: polyclonal anti-rabbit red/green opsin (AB5405, Millipore), dilution 1:1000; polyclonal anti-rabbit blue opsin (AB5407, Millipore), 1:500; monoclonal anti-mouse AKT pan (detects P- and UnP-AKT) (#2920, Cell Signaling), 1:50. Secondary antibody incubation was performed at room temperature for 2 hours with Alexa488 conjugated goat anti-rabbit or Alexa568 conjugated goat anti-mouse (Invitrogen), dilution 1:500. Retinas were washed thoroughly, mounted with Prolong medium (Life technologies) and observed with a confocal microscope (Zeiss LSM 700).

Pictures were done of the central, middle and peripheral sections of the retina (six regions in total). The number of cones was counted at the level of OS for PNA and opsins in a 140 µm length area for each region of the retina. The number of cones in the retina represents the average of the six values and was determined for each animal.

Western blotting

Retinas were sonicated in cell extraction buffer (Life technologies) and briefly centrifuged. The protein contents of the supernatants were determined by Micro BCA Protein Assay Kit (Thermo Fisher Scientific, Rockford, IL). Proteins (10 µg/lane) were separated according to the method of Laemmli and transferred to Immobilon-P transfer membrane (Millipore, Billerica, Massachusetts, MA). Membranes were briefly washed with Tris-buffered saline (TBS; 20 mM Tris-HCl, pH 7.6; 150 mM NaCl) containing 0.1 % Tween20 (TBS-Tween). Then membranes were blocked for 1 hour in TBS-Tween containing 5 % nonfat milk powder or BSA at room temperature. Membranes were washed with TBS-Tween, and then incubated 16 hours at 4 °C with primary antibodies: P-AKT (Ser473), P-AKT (Thr308) (Cell signaling #2965), AKT pan, P-FOXO1 (Ser256), FOXO1, diluted 1:5000-1:80000 in TBS-Tween containing 1 % nonfat milk or BSA. Membranes were then washed 4 times for 10 min with TBS-Tween previous incubation with HRP conjugated donkey anti-rabbit IgG or anti-mouse IgG diluted 1:1000-1:5000 (Cell signaling technology) in TBS-Tween containing 1 % nonfat milk. Membranes were finally washed 4 times for 10 min with TBS-Tween. Super Signal West FemtoChemiluminescent Substrate (Thermo Scientific) was used to detect the antigen.

Statistical analysis

Data are given as the mean ± SEM of n = 3-6 animals. Statistical analysis was performed with one-way analysis of variance (ANOVA) using the Sigma plot software. The significant level was set at $p < 0.05$. For cell counting, ANOVA were followed by post-hoc Holm-Sidak test. For Western-blotting, ANOVA were follow by post-hoc Tukey test.

Results

Effect of MT_1 and MT_2 deletion on photoreceptor cell viability during aging

The ONL cell number was quantified by light microscopy observation of C3H/$f^{+/+}$, C3H/$f^{+/+}MT_1^{-/-}$ and C3H/$f^{+/+}MT_2^{-/-}$ mouse retinas at 3 and 18 months **(Figure 1)**. No significant differences were observed among young (3 months of age) C3H/$f^{+/+}$, C3H/$f^{+/+}MT_1^{-/-}$ and C3H/$f^{+/+}MT_2^{-/-}$ mice ($P > 0.05$, one-way ANOVA; **Figure 1A**), whereas in older C3H/$f^{+/+}MT_1^{-/-}$ and C3H/$f^{+/+}MT_2^{-/-}$ mice (18 months of age) we observed a significant reduction in the number of photoreceptors with respect to C3H/$f^{+/+}$ at the same age ($P < 0.05$, one-way ANOVA, Holm-Sidak test; **Figure 1B**). We also observed a small, but significant, reduction in the ONL cell number of older C3H/$f^{+/+}$ (18 months) with respect to the number of cells of young C3H/$f^{+/+}$ (3 months) ($P < 0.05$, one-way ANOVA, Holm-Sidak test; **Figure 1A, B**).

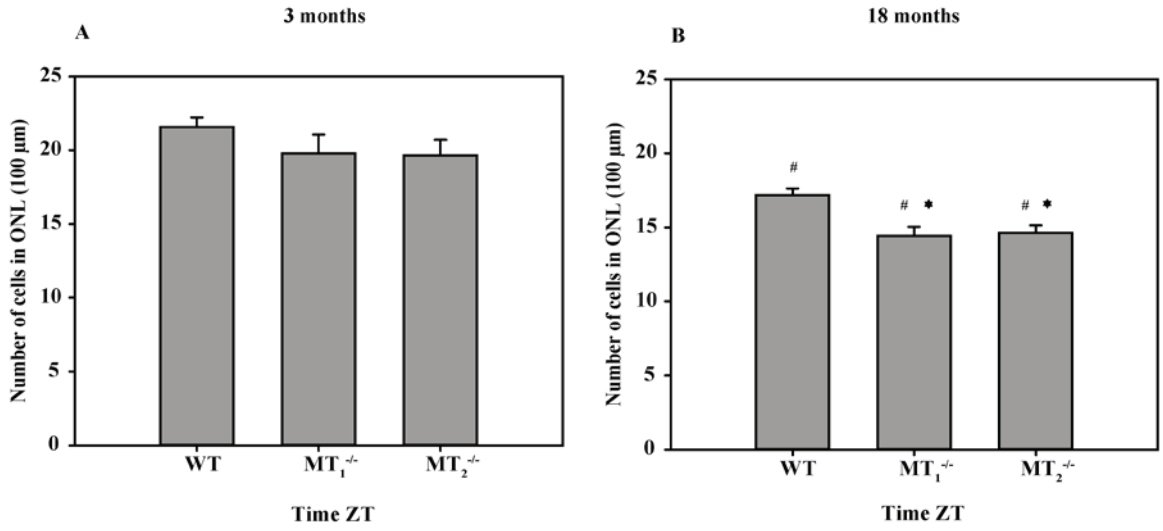

Figure 1. MT_1 and MT_2 deletion reduce photoreceptor cell viability during aging.

Number of cell nuclei in the ONL of C3H/$f^{+/+}$, C3H/$f^{+/+}MT_1^{-/-}$ and C3H/$f^{+/+}MT_2^{-/-}$ mice at 3 **(A)** and 18 months **(B)** of age in the central retina. A significant change in the ONL cell number occurs between C3H/$f^{+/+}MT_1^{-/-}$, C3H/$f^{+/+}MT_2^{-/-}$ and C3H/$f^{+/+}$ at 18 months of age (*, $P < 0.05$). The number of cells in each genotype is also affected by aging (#, $P < 0.05$). Each bar represents the mean ± SEM; n = 4-6. * and # $P < 0.05$, one-way ANOVA, followed by Holm-Sidak test. WT: C3H/$f^{+/+}$; $MT_1^{-/-}$: C3H/$f^{+/+}MT_1^{-/-}$; $MT_2^{-/-}$: C3H/$f^{+/+}MT_2^{-/-}$; ONL: outer nuclear layer.

Blocking melatonin signaling affects cone viability during aging

Retinal sections obtained from C3H/$f^{+/+}$, C3H/$f^{+/+}MT_1^{-/-}$ and C3H/$f^{+/+}MT_2^{-/-}$ mice at 3 and 18 months of age **(Figure 2A, B)** were labeled with PNA to identify cones. No differences were observed in 3 months old mice of the different genotypes ($P > 0.05$, one-way ANOVA; **Figure 2C**), whereas at 18 months, C3H/$f^{+/+}MT_1^{-/-}$ and C3H/$f^{+/+}MT_2^{-/-}$ mice showed a significant decrease (about 30 %) in the number of PNA-labeled cones in the retina with respect to C3H/$f^{+/+}$ at the same age ($P < 0.05$, one-way ANOVA, Holm-Sidak test; **Figure 2D**). Each region of the retina (peripheral, middle, central) exhibited a significant decrease in the number of PNA-positive cells for C3H/$f^{+/+}MT_1^{-/-}$ mice ($P < 0.05$, one-way ANOVA, Holm-Sidak test; **Table 1**), while only peripheral and central retina of C3H/$f^{+/+}MT_2^{-/-}$ mice showed significant decreases ($P < 0.05$, one-way ANOVA, Holm-Sidak test; **Table 1**). To explore possible differences in cone sub-populations, we labeled red/green (medium/long wavelength opsin) **(Figure 2E, F)** and blue cones (short-wavelength opsin) **(Figure 2I, J)** with specific antibodies. No significant differences were observed between the 3 genotypes at 3 months of age for either red/green ($P > 0.05$, one-way ANOVA; **Figure 2G**) or blue cones ($P > 0.05$, one-way ANOVA; **Figure 2K**). On the other hand there was a significant reduction (27-30 %) in the number of red/green cones in the entire retina of C3H/$f^{+/+}MT_1^{-/-}$ and C3H/$f^{+/+}MT_2^{-/-}$ mice with respect to C3H/$f^{+/+}$ at the same age ($P < 0.05$, one-way ANOVA, Holm-Sidak test; **Figure 2H**). As shown in Table 1 there was a significant reduction in the number of red/green cones in the middle retina of C3H/$f^{+/+}MT_1^{-/-}$ and C3H/$f^{+/+}MT_2^{-/-}$ mice, and in the peripheral retina of C3H/$f^{+/+}MT_2^{-/-}$ mice ($P < 0.05$, one-way ANOVA, Holm-Sidak test; **Table 1**). The number of blue cones was not different among the different parts of retina, for all genotypes and ages ($P > 0.05$, one-way ANOVA; **Figure 2L; Table 1**).

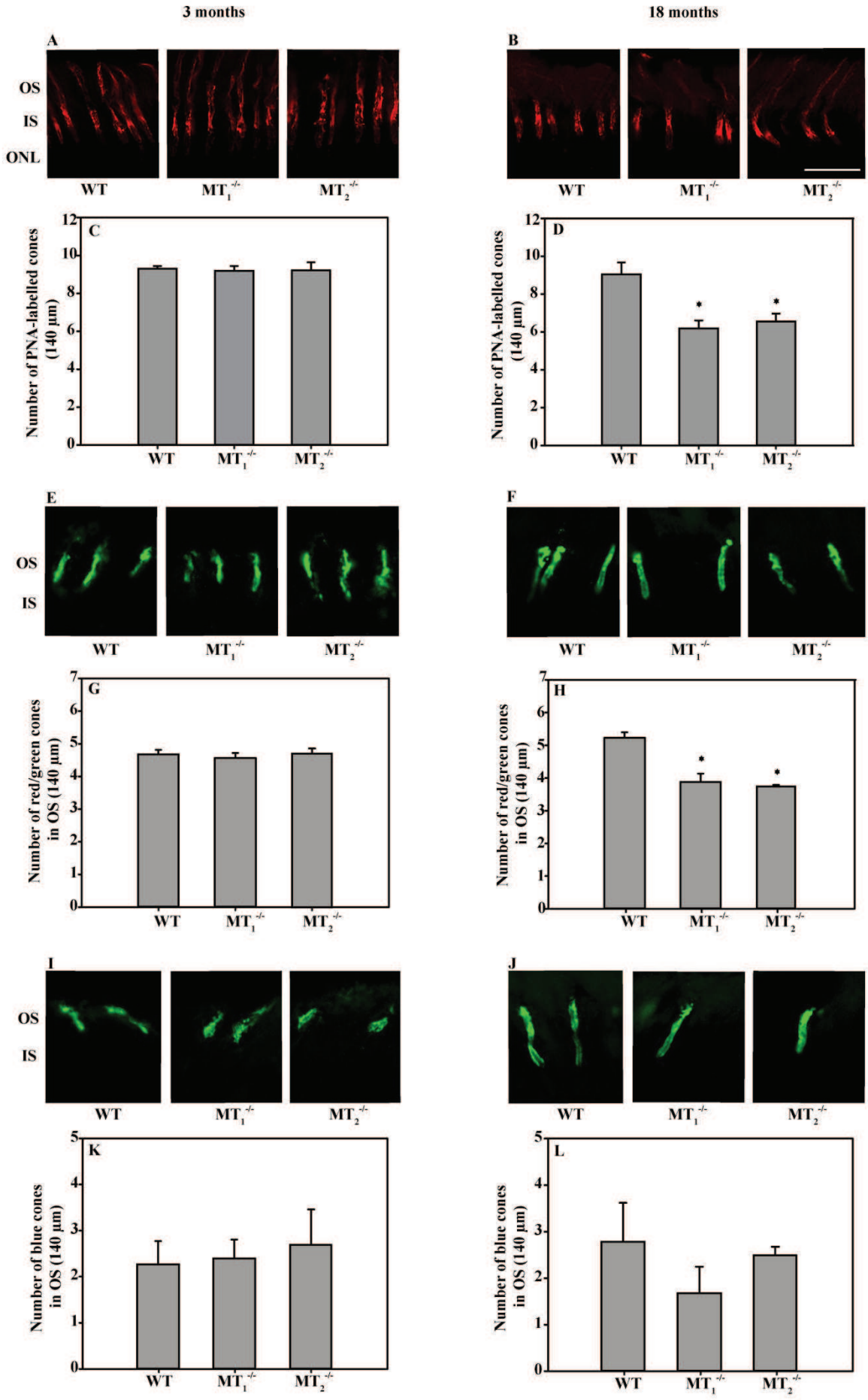
3 months
18 months
A
B
OS
IS
ONL
WT
MT1-/-
MT2-/-
C
D
Number of PNA-labelled cones (140 µm)
E
F
G
H
Number of red/green cones in OS (140 µm)
I
J
K
L
Number of blue cones in OS (140 µm)

Figure 2. MT_1 and MT_2 deletion reduce cone cell viability during aging.

PNA immunoreactivity in the central retina of C3H/$f^{+/+}$, C3H/$f^{+/+}MT_1^{-/-}$ and C3H/$f^{+/+}MT_2^{-/-}$ mice at 3 months **(A)** and 18 months of age **(B)**. Quantification of PNA-labelled cones at the photoreceptor outer segments (OS) level of C3H/$f^{+/+}$, C3H/$f^{+/+}MT_1^{-/-}$ and C3H/$f^{+/+}MT_2^{-/-}$ mice retina at 3 months **(C)** and 18 months of age **(D)**. A significant change in the number of PNA positive cells is observed between C3H/$f^{+/+}$ and C3H/$f^{+/+}MT_1^{-/-}$, C3H/$f^{+/+}MT_2^{-/-}$ at 18 months. Red/green cones (red/green opsin) localization in the central retina of 3 months **(E)** and 18 months **(F)** C3H/$f^{+/+}$, C3H/$f^{+/+}MT_1^{-/-}$ and C3H/$f^{+/+}MT_2^{-/-}$ mice. Quantification of red/green cone positive cells in C3H/$f^{+/+}$, C3H/$f^{+/+}MT_1^{-/-}$ and C3H/$f^{+/+}MT_2^{-/-}$ mice retina at 3 months **(G)** and 18 months of age **(H)**. A significant change in the number of red/green cones occurs between 18 months old C3H/$f^{+/+}$ and C3H/$f^{+/+}MT_1^{-/-}$, C3H/$f^{+/+}MT_2^{-/-}$ mice. Blue cones (blue opsin) staining in the central retina of C3H/$f^{+/+}$, C3H/$f^{+/+}MT_1^{-/-}$ and C3H/$f^{+/+}MT_2^{-/-}$ mice at 3 months **(I)** and 18 months of age **(J)**. Quantification of blue cone positive cells in the retina of the 3 genotypes mice at 3 months **(K)** and 18 months of age **(L)**. The number of blue cones does not change between 18 months old C3H/$f^{+/+}$ and C3H/$f^{+/+}MT_1^{-/-}$, C3H/$f^{+/+}MT_2^{-/-}$ mice. Each bar, the mean ± SEM; n = 3-4. * $P < 0.05$, one-way ANOVA, Holm-Sidak test. Scale bar = 20 µm. Abbreviations as in Figure 1. Additional abbreviations: OS: outer segment of photoreceptors; IS: inner segment of photoreceptors.

Genotypes	Age	PNA			Red/green opsin			Blue opsin		
		Peripheral	Middle	Central	Peripheral	Middle	Central	Peripheral	Middle	Central
WT	**3**	7.56±0.40	9.56±0.32	10.79±0.16	4.38±0.25	4.83±0.08	5±0.31	1.58±0.79	2.08±0.79	2.75±0.50
	18	7.80±0.87	9.11±0.52	10.21±0.65	4.50±0.31	5.92±0.40	5.25±0.40	2.63±0.76	2.67±0.87	3.04±0.96
$MT_1^{-/-}$	**3**	7.56±0.15	9.28±0.33	10.75±0.65	3.53±0.16	4.81±0.34	5.34±0.69	1.59± 0.24	2.47±0.42	3.13±1.04
	18	4.56±0.50*	6.34±0.47*	7.66±0.58*	3.25±0.39	3.97±0.51*	4.41±0.19	1.41±0.39	1.44±0.60	2.19±0.92
$MT_2^{-/-}$	**3**	7.06±0.44	9.75±0.63	10.75±0.42	3.69±0.32	5.25±0.27	5.22±0.37	1.75 0.47	3.03 1.00	3.28 1.01
	18	5.31±0.40*	6.88±0.67	7.47±0.24*	2.53±0.32*	4.34±0.16*	4.34±0.37	1.84±0.22	2.41±0.14	3.22±0.27

Table 1. MT_1 and MT_2 deletion reduce cone cell viability during aging.

Details of the number of PNA, red/green opsin, blue opsin positive cells in the central, middle and peripheral retina of C3H/$f^{+/+}$, C3H/$f^{+/+}MT_1^{-/-}$ and C3H/$f^{+/+}MT_2^{-/-}$ mice at 3 and 18 months of age. Abbreviations as in Figure 1. Mean ± SEM; n = 3-4.*P < 0.05, one-way ANOVA, Holm-Sidak test.

Effects of melatonin signaling removal on the AKT-FOXO1 pathway

To investigate the signaling pathway by which melatonin may affect cone viability, we determined the levels of P-AKT_{Ser473}/AKT and P-AKT_{Thr308}/AKT in the retina of C3H/$f^{+/+}$, C3H/$f^{+/+}MT_1^{-/-}$ and C3H/$f^{+/+}MT_2^{-/-}$ mice over 24 hours. In C3H/$f^{+/+}$ mice, P-AKT_{Ser473}/AKT levels showed significant changes during the light/dark cycle ($P < 0.01$, one-way ANOVA, Holm-Sidak test) with a peak at ZT22 **(Figure 3D)**. P-AKT_{Thr308}/AKT exhibited similar profile over 24 hours ($P < 0.05$, One-way ANOVA, Holm-Sidak test) **(Figure 3J)**. In C3H/$f^{+/+}MT_1^{-/-}$ and C3H/$f^{+/+}MT_2^{-/-}$ mice, P-AKT_{Ser473}/AKT **(Figure 3E, F)** and P-AKT_{Thr308}/AKT **(Figure 3K, L)** levels were not significantly different during the 24 hours period ($P > 0.05$ in each case, one-way ANOVA). We also assayed the P-FOXO1/FOXO1 levels in the retina of the three genotypes **(Figure 4)**. Once more the levels of P-FOXO1/FOXO1 exhibited a significant change in the retina of C3H/$f^{+/+}$ over 24 hours with a peak at ZT22 ($P < 0.05$ one-way ANOVA, Holm-Sidak test; **Figure 4D**). No changes in P-FOXO1/FOXO1 level were observed over the 24 hours in the retinas of C3H/$f^{+/+}MT_1^{-/-}$ and C3H/$f^{+/+}MT_2^{-/-}$ mice ($P > 0.05$ in both case, one-way ANOVA; **Figure 4E, F**).

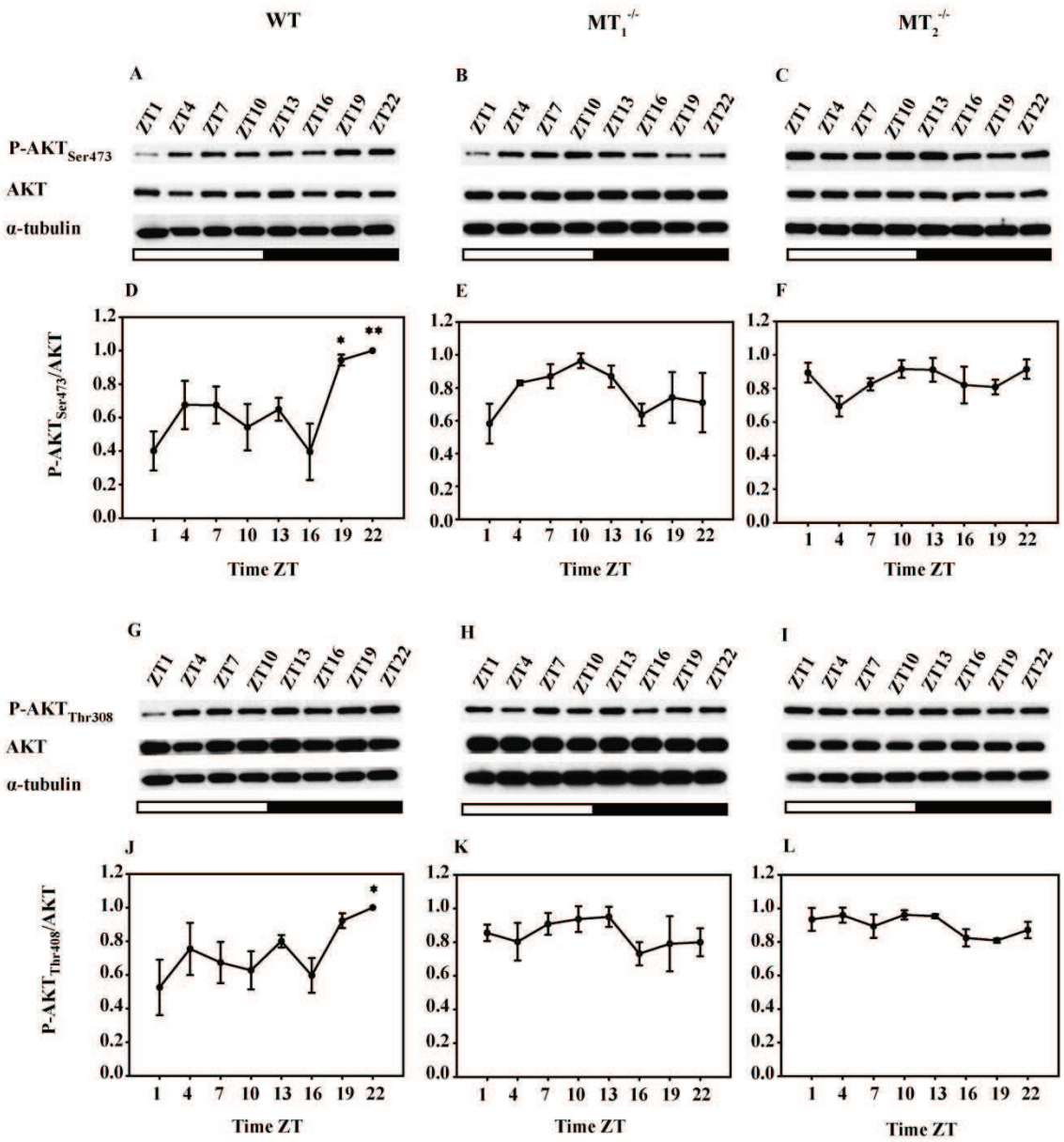

Figure 3. MT_1 and MT_2 deletion have an effect on the P-AKT/AKT level.

Western blotting analysis of P-AKT and AKT (P and UnP) levels in retinas at different Zeitgeber Time (ZT) in 3 months C3H/$f^{+/+}$ **(A, D, G, J)**, C3H/$f^{+/+}MT_1^{-/-}$ **(B, E, H, K)** and C3H/$f^{+/+}MT_2^{-/-}$ mice **(C, F, I, L)**. P-AKT ($_{Thr308}$ and $_{Ser473}$) levels were significantly higher in the late night (ZT19-22; $^{*}P < 0.05$, one-way ANOVA, followed by Holm-Sidak test) in C3H/$f^{+/+}$ but not in C3H/$f^{+/+}$MT1$^{-/-}$ and C3H/$f^{+/+}$MT2$^{-/-}$ mice. Densitometric quantification of P-AKT ($_{Thr308}$ and $_{Ser473}$) and AKT levels were performed on three independent retinal samples for each ZT.

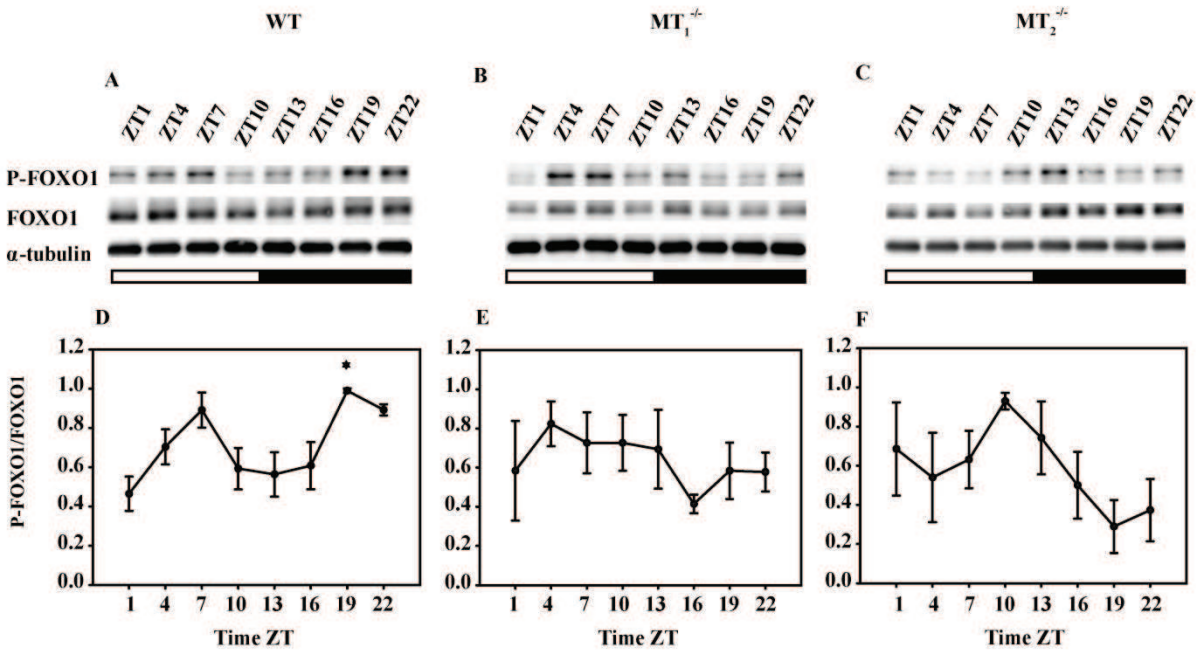

Figure 4. MT_1 and MT_2 deletion have an effect on the P-FOXO1/FOXO1 level.

Western blotting analysis of P-FOXO1 and FOXO1 levels (P and UnP) in retinas at different Zeitgeber Time (ZT) in 3 months old C3H/$f^{+/+}$ **(A and D)**, C3H/$f^{+/+}$MT1$^{-/-}$ **(B and E)** and C3H/$f^{+/+}$MT2$^{-/-}$ mice **(C and F)**. P-FOXO1 levels were significantly higher in the late night in C3H/$f^{+/+}$ (ZT19-22, $^{*}P < 0.05$, one-way ANOVA, followed by Holm-Sidak test) but not in C3H/$f^{+/+}$MT1$^{-/-}$ and C3H/$f^{+/+}$MT2$^{-/-}$ mice. Densitometric quantification of P-FOXO1 and FOXO1 levels were performed on three independent retinal samples for each ZT.

Localization of AKT and FOXO1 in photoreceptors

To localize AKT in the retina of C3H/$f^{+/+}$, C3H/$f^{+/+}MT_1^{-/-}$ and C3H/$f^{+/+}MT_2^{-/-}$ mice we performed immunohistochemistry using antibodies against AKT and P-AKT_{Ser473}, at ZT22 [when the level of phospho-AKT is highest in C3H/$f^{+/+}$ mice **(Figure 3D, J)**] and ZT1 [when the level of P-AKT is lowest in C3H/$f^{+/+}$ mice **(Figure 3D, J)**]. In C3H/$f^{+/+}$, AKT pan was widespread and immunoreactivity was observed in the OS and inner segment (IS) **(Supplemental Figure 1A and A')** as well as in the outer plexiform layer (OPL), inner plexiform layer (IPL) and ganglion cell layer (GCL) **(Supplemental Figure 1A)**. At ZT22, P-AKT_{Ser473} immunoreactivity was localized in OS and GCL of C3H/$f^{+/+}$ **(Figure 5A and A')**, while at ZT1 P-AKT_{Ser473} immunoreactivity was weaker in these locations **(Figure 5B and B')**. In C3H/$f^{+/+}MT_1^{-/-}$ and C3H/$f^{+/+}MT_2^{-/-}$ mice, P-AKT_{Ser473} immunoreactivity was detected in the OS and in GCL at ZT22 **(Figure 5C, E)** and at ZT1 **(Figure 5D, F)**. There were no clear changes in the signal intensity between both time points. We then investigated the cellular localization of P-AKT_{Ser473} in the OS by performing double immunofluorescence with PNA **(Figure 6A')**. In C3H/$f^{+/+}$ mice, P-AKT_{Ser473} immunoreactivity was observed in the OS of cones and rods **(Figure 6A'')**.

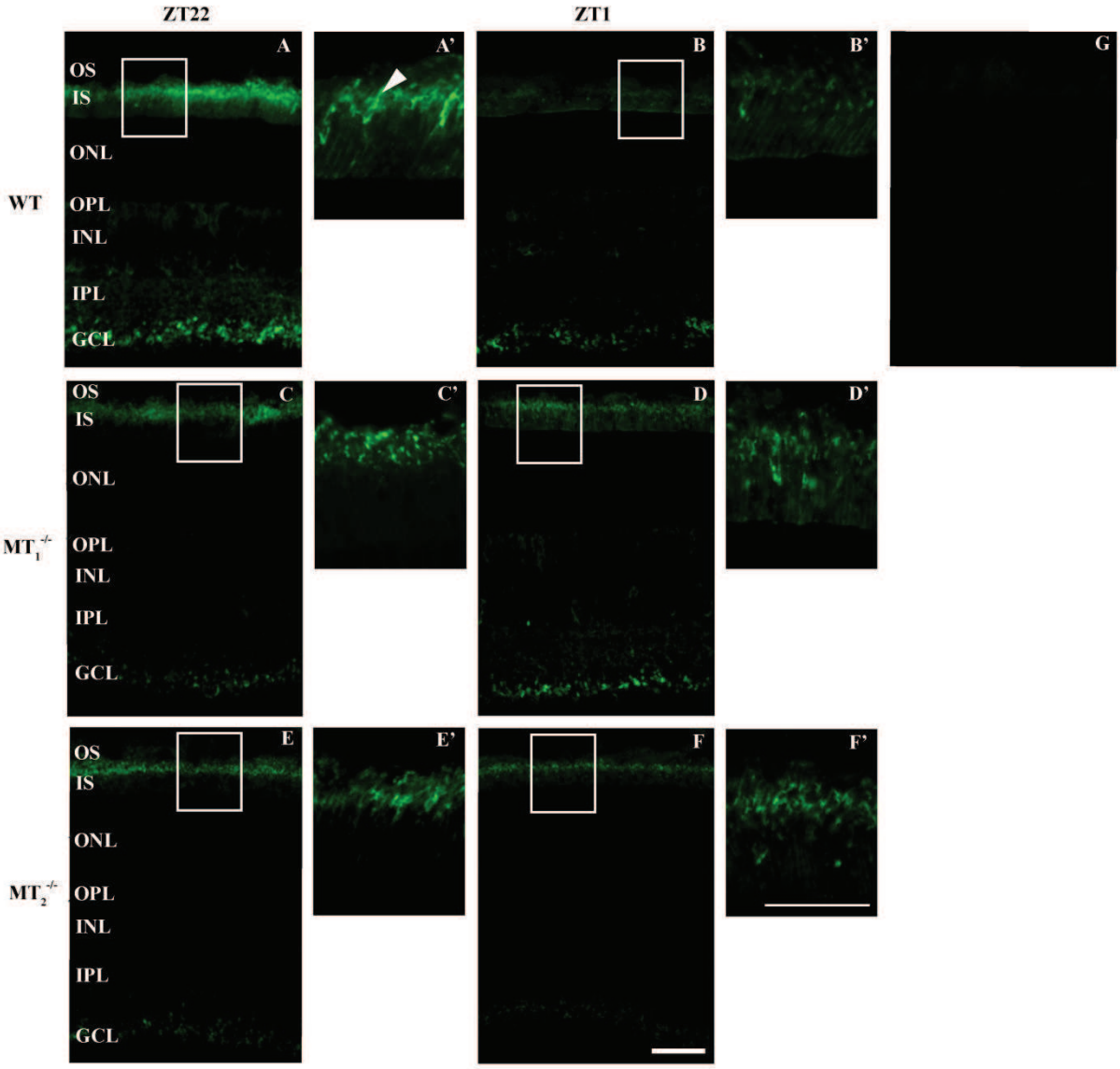

Figure 5. P-AKT is localized within photoreceptors and the GCL.

P-AKT localization by fluorescence immunohistochemistry on the retina sections of 3 months old C3H/$f^{+/+}$, C3H/$f^{+/+}MT_1^{-/-}$ and C3H/$f^{+/+}MT_2^{-/-}$ mice at ZT22 and ZT1. At ZT22 (night time), P-AKT staining is intense in OS and GCL of C3H/$f^{+/+}$ mice **(A)**. P-AKT staining is moderate in OS and GCL of C3H/$f^{+/+}MT_1^{-/-}$ and C3H/$f^{+/+}MT_2^{-/-}$ mice respectively **(C, E)**. Enlargement of boxed area of C3H/$f^{+/+}$ mice at ZT22 **(A')**. Staining is present in one specific structure in OS (arrowhead) **(A')**. Enlargement of boxed area of C3H/$f^{+/+}MT_1^{-/-}$ and C3H/$f^{+/+}MT_2^{-/-}$ mice retinas respectively confirm P-AKT expression in OS **(C', E')**. At ZT1, P-AKT staining is low in OS and GCL of C3H/$f^{+/+}$ **(B)**. P-AKT staining is present in OS and GCL of C3H/$f^{+/+}MT_1^{-/-}$ and C3H/$f^{+/+}MT_2$-/- mice respectively **(D, F)**. Enlargement of boxed area of C3H/$f^{+/+}$ mice retinas at ZT1 confirm low P-AKT staining in OS **(B')**. Enlargement of boxed area of C3H/$f^{+/+}MT_1^{-/-}$and C3H/$f^{+/+}MT_2^{-/-}$ mice retinas respectively show moderate staining in OS **(D', F')**. Control without primary antibody **(G)**. Scale bar = 50 µm for A, B, C, D, E, F, G) and 20 µm for A', B', C', D', E', F', G'. Abbreviations as in Figure 1, 2, S1.

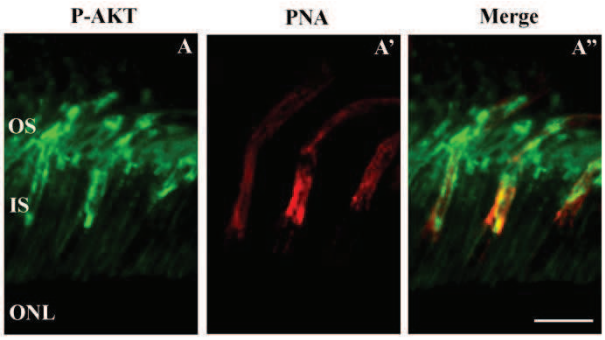

Figure 6. P-AKT is present in cones and rods.

Fluorescence immunohistochemistry of C3H/$f^{+/+}$ mice retinal sections at 3 months. Images were obtained at the level of the OS at ZT22. P-AKT (green) is seen in one specific structure **(A)**. Cones are stained with PNA (red) while rods are unstained and visible as dark profiles **(A')**. In the merge, P-AKT is present in cone and rod OS **(A'')**. Scale bar = 10 µm. Abbreviations as in Figure 1, 2, S1.

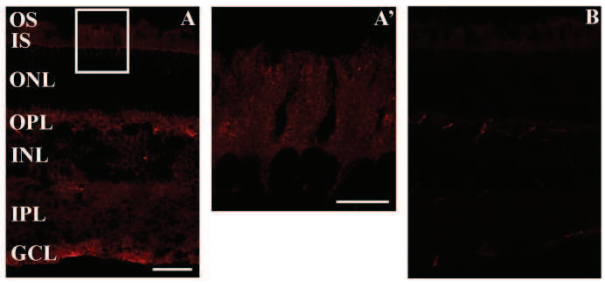

Supplemental Figure 1. AKT immunoreactivity is widespread.

AKT pan (P and UnP) localization by immunofluorescence in transversal retinal section of C3H/$f^{+/+}$ mice at 3 months. At ZT22, AKT staining was visible in OS, IS, OPL, INL, IPL and GCL **(A)**. Enlargement of the box area showing AKT localization in OS and IS **(A')**. The control without primary antibody is presented on panel **(B)**. Scale bar = 50 µm (A, B) and 10 µm (A'). Abbreviations as in Figure 1, 2 and 3. OPL: outer plexiform layer; INL: inner nuclear layer; IPL: inner plexiform layer; GCL: ganglion cell layer.

At ZT22, FOXO1 immunoreactivity was weak and widespread **(Supplemental Figure 2A)**. P-FOXO1 immunoreactivity was localized to the OS, IS and GCL of C3H/$f^{+/+}$ mice at ZT22 **(Figure 7A)**. As for P-AKT, P-FOXO1 signal in the OS and IS was stronger at ZT22 **(Figure 7A')** than at ZT1 **(Figure 7B, B')**. In C3H/$f^{+/+}MT_1^{-/-}$ and C3H/$f^{+/+}MT_2^{-/-}$ mice, P-FOXO1 was weakly detected in OS and IS at ZT22 **(Figure 7C, E)** and ZT1 **(Figure 7D, F)**. The pattern of P-FOXO1 immunoreactivity in OS and IS was similar (slight signal and no difference between ZT22 and ZT1, **Figure 7C', D', E', F'**) in C3H/$f^{+/+}MT_1^{-/-}$ and C3H/$f^{+/+}MT_2^{-/-}$ mice. Also in this case, we performed double immunofluorescence with P-FOXO1 antibody and PNA. P-FOXO1 staining was stronger in the cones, but the signal was also present in rods **(Figure 8A'')**.

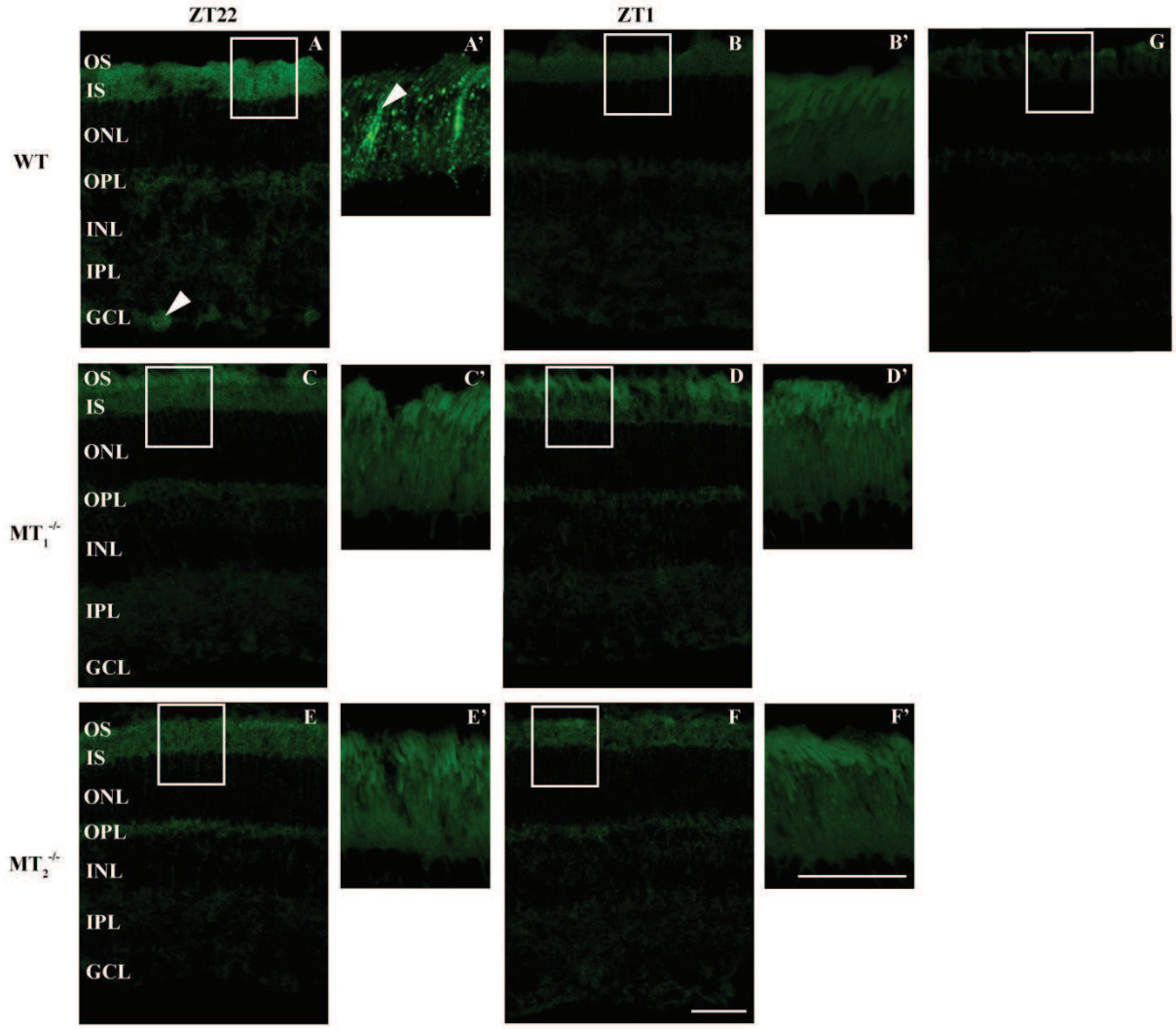

Figure 7. P-FOXO1 is localized within photoreceptors and the GCL.

P-FOXO1 localization by fluorescence immunohistochemistry performed on retinal sections of 3 months old C3H/$f^{+/+}$, C3H/$f^{+/+}MT_1^{-/-}$ and C3H/$f^{+/+}MT_2^{-/-}$ mice at ZT22 and ZT1. At ZT22, P-FOXO1 is localized in OS, IS and GCL (arrowhead) of C3H/$f^{+/+}$ **(A)**. Enlargement of boxed area show the staining mainly in one specific structure in OS and IS (arrowhead) **(A')**. At ZT1, P-FOXO1 is not detected in the retina of C3H/$f^{+/+}$ **(B)**. Enlargement of the boxed area confirms no staining detected in OS and IS of C3H/$f^{+/+}$ **(B')**. P-FOXO1 staining is very weak in OS, IS and GCL of C3H/$f^{+/+}MT_1^{-/-}$ at ZT22 **(C)** and ZT1 **(D)** as in OS, IS and GCL of C3H/$f^{+/+}MT_2^{-/-}$ mice at ZT22 **(E)** and ZT1 **(F)**. Enlargement of boxed area confirms a very low level of P-FOXO1 in OS and IS of C3H/$f^{+/+}$ $MT_1^{-/-}$ and C3H/$f^{+/+}$ $MT_2^{-/-}$ mice **(C', D', E', F')**. Control without primary antibody **(G)**. Scale bar = 50 µm (A, B, C, D, E, F, G) and 20 µm (A', B', C', D', E', F', G'). Abbreviations as in Figure 1, 2, S1.

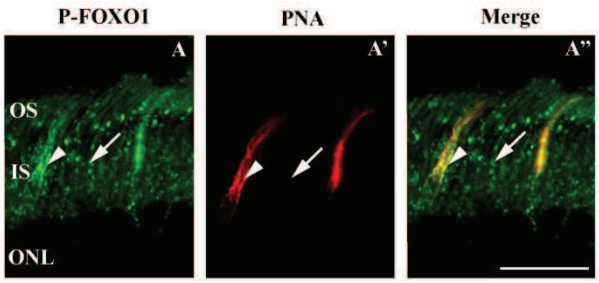

Figure 8. P-FOXO1 is present in rods and strongly in cones.

Fluorescence immunohistochemistry at the level of OS and IS of C3H/$f^{+/+}$mice (3 months old) at ZT22. P-FOXO1 (green) is seen in two structures (arrow, arrowhead) **(A)**. Cones are stained with PNA in red **(A')**. Merged image reveals P-FOXO1 labeling mostly in cone (arrowhead), with weaker staining in the surrounding rod IS (arrow) **(A'')**. Scale bar = 20 µm. Abbreviations as in Figure 1, 2, S1.

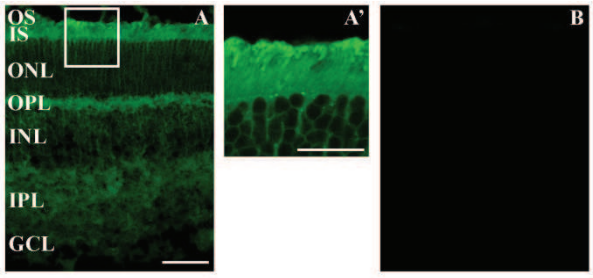

Supplemental Figure 2. FOXO1 immunoreactivity is widespread.

FOXO1 localization (P and UnP) by immunofluorescence in retinal section of C3H/$f^{+/+}$ (3 months old) at ZT22. FOXO1 staining was visible in OS, IS, OPL, IPL. Weak staining was visible in ONL, INL, GCL **(A)**. Enlargement of the box area confirms that FOXO1 is present in OS, IS and ONL **(A')**. Control without primary antibody **(B)**. Scale bar = 50 µm (A, B) and 20 µm (A'). Abbreviations as in Figure 1, 2, S1.

Discussion

The data reported in the present study indicate that melatonin signaling via its G-protein coupled receptors increases photoreceptor viability during aging. C3H/$f^{+/+}MT_1^{-/-}$ and C3H/$f^{+/+}MT_2^{-/-}$ mice lose 20 % of photoreceptors at 18 months compared to C3H/$f^{+/+}$ mice at the same age **(Figure 1)**. The observation that similar results were obtained in C3H/$f^{+/+}MT_1^{-/-}$ and C3H/$f^{+/+}MT_2^{-/-}$ mice suggests that also in this case the action of melatonin is mediated by MT_1/MT_2 heteromers *(Baba et al., 2013)*. We used PNA marker to determine the effect of MT_1 and MT_2 receptor deletion on cone number during aging. In the mouse, cones represent a small percentage (2-3 %) of the total number of photoreceptors with the red/green being the most prevalent type and with a wide distribution within the retina, while the blue cones are low in number and with inferior-superior gradient *(Röhlich et al., 1994; Peichl, 2005; Ait-Hmyed et al., 2013)*. As shown in Table 1 we did not detect significant changes in the number of PNA-labeled cones in C3H/$f^{+/+}$ mice during aging. However removal of melatonin receptors led to a decrease of PNA-labeled cones during aging. To support these observations, the number of red/green cones did not decrease in C3H/$f^{+/+}$ mice during aging while the number of such cells decreased when melatonin receptors were deleted **(Table 1)**. During aging the decline of red/green cones is more pronounced in the middle retina of C3H/$f^{+/+}MT_1^{-/-}$ and C3H/$f^{+/+}MT_2^{-/-}$ mice but also in the peripheral retina of C3H/$f^{+/+}MT_2^{-/-}$ mice **(Table 1)**. We did not detect a significant

change in the number of blue cones in C3H/$f^{+/+}$, C3H/$f^{+/+}MT_1^{-/-}$ and C3H/$f^{+/+}MT_2^{-/-}$ mice **(Table 1)** possibly due to their unequal topography and their low density across the entire retina *(Peichl, 2005)*. We observed a centro-peripheral density gradient of PNA, red/green and blue labeled cones in C3H/$f^{+/+}$, C3H/$f^{+/+}MT_1^{-/-}$ and C3H/$f^{+/+}MT_2^{-/-}$ mice at 3 months and 18 months **(Table 1)**. The highest densities are present in the central retina and lowest densities in the peripheral retina, consistent with previous reports in mammals *(Peichl, 2005)*.

It is here worthwhile to mention that the vast majority of mouse strains are genetically incapable of synthesizing melatonin *(see Tosini et al., 2014 for a discussion on this topic)*. Indeed, most of laboratory strains [eg. C57/BL6, Balb/C, SV129] are considered melatonin-deficient mice whereas only CBA and C3H are considered melatonin-proficient strains. Interestingly melatonin-deficient mice strains also show a significant decrease in cone numbers during aging *(Gresh et al., 2003; Fernandez-Sanchez et al., 2014)*. Such result further supports the notion that melatonin signaling is important for cones viability during aging.

Previous studies have reported that the number of photoreceptors decreases during aging and that rods and cones are both affected *(Curcio et al., 1993; Gresh et al., 2003; Cunea & Jeffery, 2007; Baba et al., 2009)*. Most studies have established that the loss of the rods precedes the loss of cones *(Curcio et al., 1993; Hicks & Sabel, 1999)*, thus suggesting that rods may produce a trophic factor necessary for cone survival *(Mohand-Said et al., 1998; Léveillard et al., 2004)*. However the variability in cone survival patterns in different rod-initiated degenerations suggests this cannot be the only explanation *(Marc et al., 2003)*. Cones may also produce their own survival factor, eg. in cone rich squirrel retinas, the primate macula and in pure-cone foveas of lizards and birds *(Marc et al., 2003)*. A more recent work has suggested that the death of rods leads to development of a hyper-oxygenated micro environment that increases oxidative stress and promotes cone death *(Komeima et al., 2006)*. In our study we detected a reduction in the number of rods **(Figure 1)** and cones **(Figure 2 and Table 1)**. Since MT_1 and MT_2 receptors are localized in both photoreceptor types *(Sengupta et al., 2011; Baba et al., 2013)*, we believe that rods and cones are directly affected by removal of melatonin signaling. Additional studies are required to determine which type of photoreceptor die first in mice lacking melatonin signaling.

Previous studies have also shown that melatonin may affect the phosphatidylinositol 3 kinase (PI3K)-AKT pathway *(reviewed in: Hardeland, 2009)*. AKT plays a critical role in controlling the balance between apoptosis and cell survival in response to extra- and intra-cellular signaling. The principal role of AKT is to facilitate growth factor-mediated cell survival and to block apoptotic cell death, which is achieved by phosphorylating and deactivating pro-apoptotic factors. AKT activity is the result of a balance between two phosphorylation sites on Thr308 and Ser473 *(Beaulieu et al., 2007)*. Several studies have shown that AKT can directly phosphorylate FOXO thus promoting cell survival *(Brunet et al., 1999)*. When AKT is inactive, FOXOs are localized within the nucleus where it induces the expression of *FasL* mRNA *(Brunet et al., 2001)*. On the contrary when AKT is activated it phosphorylates FOXOs. FOXOs are then translocated from the nucleus to the cytoplasm, thus inhibiting the expression of pro-apoptotic genes *(Brunet et al., 2001; Daitoku et al., 2011 for reviews on this topic)*. Experimental evidence indicates that inactivation of AKT-FOXO protein inhibits the survival pathway in the photoreceptors *(Jomary et al., 2006)*.

The results obtained with the Western blotting indicate that melatonin signaling has a significant effect on the P-AKT/AKT and P-FOXO1/FOXO1 levels **(Figure 3 and 4)**. In C3H/$f^{+/+}$ mice the levels of P-

AKT_{Ser473}/AKT, P-AKT_{Thr308}/AKT and P-FOXO1/FOXO1 showed a significant rhythm with a peak at night (ZT22, ie. when melatonin levels are high) **(Figure 3 and 4)**. These results are consistent with previous study showing a circadian regulation of AKT phosphorylation on Thr308 that peaked at night in chick retina *(Ko et al., 2009)*. Indeed PI3K-AKT signaling has been shown to contribute to the circadian phase-dependent modulation of L-type voltage-gated calcium channels (L-VGCCs) in photoreceptors suggesting that PI3K-AKT signaling serves as a circadian output in the retina *(Ko et al., 2009)*. P-AKT_{Ser473}/AKT, P-AKT_{Thr308}/AKT and P-FOXO1/FOXO1 nocturnal peaks were lost in mice lacking melatonin receptors. Such results suggest that melatonin signaling is necessary for the activation of the AKT-FOXO1 pathway at night in the retina. Although the data obtained with Western blot were promising, they did not indicate whether the rhythmic expression in P-AKT/AKT and P-FOXO1/FOXO1 observed in C3H/$f^{+/+}$ was occurring in the photoreceptors or in other parts of the retina. To address this question we decided to investigate the expression of P-AKT and P-FOXO1 in the retina using immunocytochemistry **(Figures 5-8)**. Consistent with previous report *(Reiter et al., 2003; Jomary et al., 2006; Li et al., 2007)* we localized P-AKT and P-FOXO1 within photoreceptors and GCL, and observed that phosphorylated proteins are expressed in cones. Moreover, the pattern of AKT and FOXO1 phosphorylation in the photoreceptors is affected by removal of melatonin signaling **(Figures 5 and 7)** since their rhythms are lost in mice lacking melatonin receptors **(Figures 5 and 7)**. Our data also indicated that FOXO1 activation seems to be stronger in the cones than in the rods **(Figures 6 and 8)** and this further suggests that the melatonin activation of this pathway at night may be important for the cone survival during aging.

In conclusion we believe that melatonin can protect photoreceptors during aging and we propose the following working model to explain the protective action of melatonin on the photoreceptors. In photoreceptors, nocturnal melatonin binds to MT_1/MT_2 heteromers to elicit the recruitment of PI3K to the plasma membrane. The catalytic subunit of PI3K generates the phosphoinositide-phosphates PIP2 and PIP3 which in turn phosphorylate the phosphoinositide-dependent kinase-1 (PDK1). PDK1 activates AKT at Thr308 but AKT can also be phosphorylated at Ser473 by a PDK1 independent mechanism *(Brunet et al., 2001; Franke et al., 2003)*. Once AKT is activated, FOXOs are phosphorylated. 14-3-3 protein binds to FOXO phosphorylated to export it to the cytoplasm. This leads to the suppression of pro-apoptotic genes transcription (*(Brunet et al., 2002)*, **see Figure 9**).

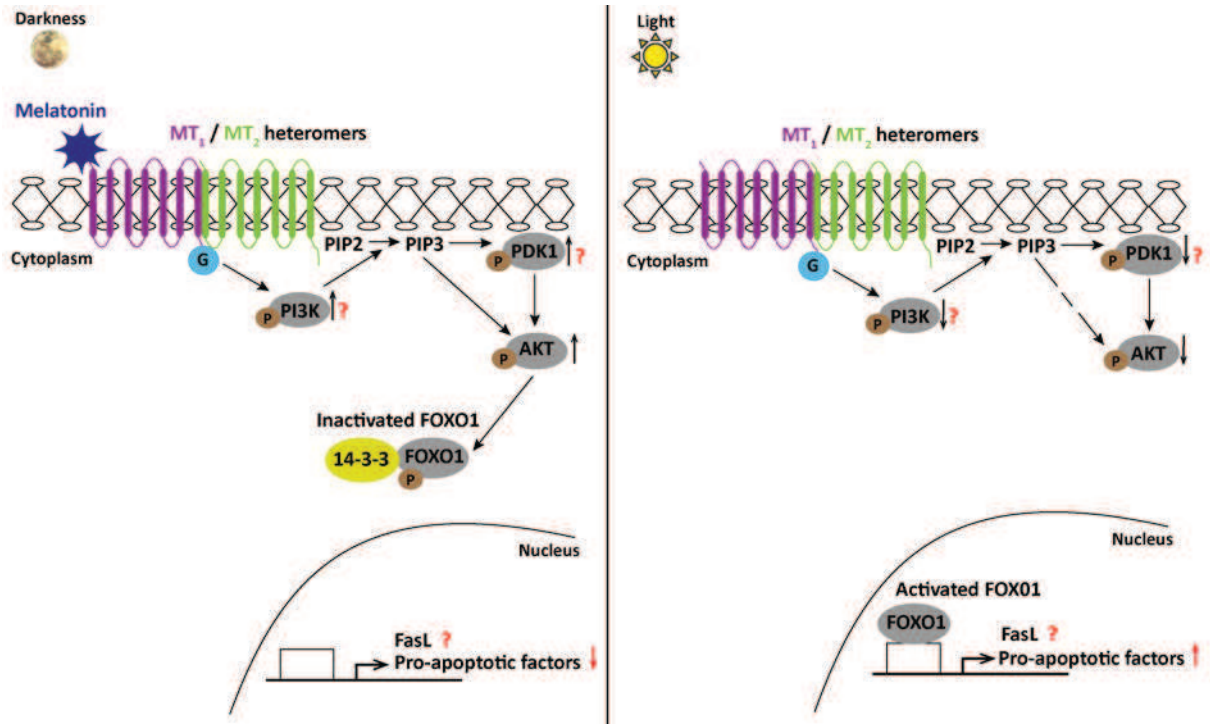

Figure 9. Proposed mechanism to explain the protective action of melatonin on photoreceptors.

Left panel: during the night, once AKT is activated by melatonin signaling, FOXO1 is phosphorylated. 14-3-3 protein bind to FOXO1 phosphorylated and exported it to the cytoplasm. When FOXO1 is localized in the cytoplasm, the transcription of pro-apoptotic genes is suppressed. **Right panel:** in the absence of melatonin signaling AKT is inactive and FOXO1 is localized in the nucleus where it activates the transcription of pro-apoptotic genes. Abbreviations: G: G protein; P: phosphorylated; PIP2: phosphoinositide-phosphates 2; PIP3: phosphoinositide-phosphates 3; PDK1: phosphoinositide-dependent kinase-1; AKT: serine/threonine protein kinase; FOXO1: Forkhead-related family of mammalian transcription factor 1; FasL: Fas ligand.

Acknowledgments

This work was supported by grants from the National Institutes of Health Grants EY022216 and EY020821 to G.T. and by 5U54NS083932, S21MD000101, G12-RR03034, U54RR026137 to Morehouse School of Medicine. We also thank the animal facility of Morehouse School of Medicine for the care and breeding of mice.

References

Ait-Hmyed, O., Felder-Schmittbuhl, M.-P., Garcia-Garrido, M., Beck, S., Seide, C., Sothilingam, V., Tanimoto, N., Seeliger, M., Bennis, M., & Hicks, D. (**2013**) Mice lacking Period 1 and Period 2 circadian clock genes exhibit blue cone photoreceptor defects. *The European journal of neuroscience*, 1–13.

Ayoub, M.A., Couturier, C., Lucas-Meunier, E., Angers, S., Fossier, P., Bouvier, M., & Jockers, R. (**2002**) Monitoring of ligand-independent dimerization and ligand-induced conformational changes of melatonin receptors in living cells by bioluminescence resonance energy transfer. *Journal of Biological Chemistry*, **277**, 21522–21528.

Ayoub, M.A., Levoye, A., Delagrange, P., & Jockers, R. (**2004**) Preferential formation of MT1/MT2 melatonin receptor heterodimers with distinct ligand interaction properties compared with MT2 homodimers. *Molecular pharmacology*, **66**, 312–321.

Baba, K., Benleulmi-Chaachoua, A., Journé, A.-S., Kamal, M., Guillaume, J.-L., Dussaud, S., Gbahou, F., Yettou, K., Liu, C., Contreras-Alcantara, S., Jockers, R., & Tosini, G. (**2013**) Heteromeric MT1/MT2 Melatonin Receptors Modulate Photoreceptor Function. *Science Signaling*, **6**, ra89.

Baba, K., Pozdeyev, N., Mazzoni, F., Contreras-Alcantara, S., Liu, C., Kasamatsu, M., Martinez-Merlos, T., Strettoi, E., Iuvone, P.M., & Tosini, G. (**2009**) Melatonin modulates visual function and cell viability in the mouse retina via the MT1 melatonin receptor. *Proceedings of the National Academy of Sciences of the United States of America*, **106**, 15043–15048.

Beaulieu, J.-M., Tirotta, E., Sotnikova, T.D., Masri, B., Salahpour, A., Gainetdinov, R.R., Borrelli, E., & Caron, M.G. (**2007**) Regulation of Akt signaling by D2 and D3 dopamine receptors in vivo. *The Journal of neuroscience : the official journal of the Society for Neuroscience*, **27**, 881–885.

Brunet, A., Bonni, A., Zigmond, M.J., Lin, M.Z., Juo, P., Hu, L.S., Anderson, M.J., Arden, K.C., Blenis, J., & Greenberg, M.E. (**1999**) Akt Promotes Cell Survival by Phosphorylating and Inhibiting a Forkhead Transcription Factor. *Cell*, **96**, 857–868.

Brunet, A., Datta, S.R., & Greenberg, M.E. (**2001**) Transcription-dependent and -independent control of neuronal survival by the PI3K – Akt signaling pathway. *Current Opinion in Neurobiology*, **11**, 297–305.

Brunet, A., Kanai, F., Stehn, J., Xu, J., Sarbassova, D., Frangioni, J. V, Dalal, S.N., DeCaprio, J. a, Greenberg, M.E., & Yaffe, M.B. (**2002**) 14-3-3 Transits To the Nucleus and Participates in Dynamic Nucleocytoplasmic Transport. *The Journal of cell biology*, **156**, 817–828.

Cahill, G.M. & Besharse, J.C. (**1989**) Retinal melatonin is metabolized within the eye of xenopus laevis. *Proceedings of the National Academy of Sciences of the United States of America*, **86**, 1098–1102.

Cahill, G.M. & Besharse, J.C. (**1993**) Circadian clock functions localized in Xenopus retinal photoreceptors. *Neuron*, **10**, 573–577.

Coleman, H.R., Chan, C.-C., Ferris, F.L., & Chew, E.Y. (**2008**) Age-related macular degeneration. *Lancet*, **372**, 1835–1845.

Cunea, A. & Jeffery, G. (**2007**) The ageing photoreceptor. *Visual neuroscience*, **24**, 151–155.

Curcio, C.A., Millican, C.L., Allen, K. a., & Kalina, R.E. (**1993**) Aging of the human photoreceptor mosaic: Evidence for selective vulnerability of rods in central retina. *Investigative Ophthalmology and Visual Science*, **34**, 3278–3296.

Daitoku, H., Sakamaki, J.I., & Fukamizu, A. (**2011**) Regulation of FoxO transcription factors by acetylation and protein-protein interactions. *Biochimica et Biophysica Acta - Molecular Cell Research*, **1813**, 1954–1960.

Fernandez-Sanchez, L., de Sevilla Muller, L.P., Brecha, N.C., & Cuenca, N. (**2014**) Loss of Outer Retinal Neurons and Circuitry Alterations in the DBA/2J Mouse. *Investigative Ophthalmology & Visual Science*, **55**, 6059–6072.

Franke, T.F., Hornik, C.P., Segev, L., Shostak, G. a, & Sugimoto, C. (**2003**) PI3K/Akt and apoptosis: size matters. *Oncogene*, **22**, 8983–8998.

Fujieda, H., Hamadanizadeh, S. a., Wankiewicz, E., Pang, S.F., & Brown, G.M. (**1999**) Expression of mt1 melatonin receptor in rat retina: Evidence for multiple cell targets for melatonin. *Neuroscience*, **93**, 793–799.

Fukuhara, C., Dirden, J.C., & Tosini, G. (**2001**) Photic regulation of melatonin in rat retina and the role of proteasomal proteolysis. *Neuroreport*, **12**, 3833–3837.

Fukuhara, C., Liu, C., Ivanova, T.N., Chan, G.C.-K., Storm, D.R., Iuvone, P.M., & Tosini, G. (**2004**) Gating of the cAMP signaling cascade and melatonin synthesis by the circadian clock in mammalian retina. *The Journal of neuroscience : the official journal of the Society for Neuroscience*, **24**, 1803–1811.

Gresh, J., Goletz, P.W., Crouch, R.K., & Rohrer, B. (**2003**) Structure-function analysis of rods and cones in juvenile, adult, and aged C57bl/6 and Balb/c mice. *Visual neuroscience*, **20**, 211–220.

Hardeland, R. (**2009**) Melatonin: Signaling mechanisms of a pleiotropic agent. *BioFactors*, **35**, 183–192.

Hicks, D. & Sabel, J. (**1999**) The implications of rod-dependent cone survival for basic and clinical research. *Investigative Ophthalmology and Visual Science*, **40**, 3071–3074.

Hiragaki, S., Baba, K., Coulson, E., Kunst, S., Spessert, R., & Tosini, G. (**2014**) Melatonin Signaling Modulates Clock Genes Expression in the Mouse Retina. *PLoS ONE*, **9**, e106819.

Huang, H., Lee, S.-C., & Yang, X.-L. (**2005**) Modulation by melatonin of glutamatergic synaptic transmission in the carp retina. *The Journal of physiology*, **569**, 857–871.

Iuvone, P.M., Tosini, G., Pozdeyev, N., Haque, R., Klein, D.C., & Chaurasia, S.S. (**2005**) Circadian clocks, clock networks, arylalkylamine N-acetyltransferase, and melatonin in the retina. *Progress in Retinal and Eye Research*, **24**, 433–456.

Jomary, C., Cullen, J., & Jones, S.E. (**2006**) Inactivation of the Akt survival pathway during photoreceptor apoptosis in the retinal degeneration mouse. *Investigative ophthalmology & visual science*, **47**, 1620–1629.

Klein, D.C., Coon, S.L., Roseboom, P.H., Weller, J.L., Bernard, M., Gastel, J.A., Zatz, M., Iuvone, P.M., Rodriguez, I.R., Bégay, V., Falcon, J., Cahill, G.M., Cassone, V.M., & Baler, R. (**1997**) The melatonin rhythm-generating enzyme: molecular regulation of serotonin N-acetyltransferase in the pineal gland. *Recent progress in hormone research*, **52**, 307–357.

Ko, M.L., Jian, K., Shi, L., & Ko, G.Y.-P. (**2009**) Phosphatidylinositol 3 kinase-Akt signaling serves as a circadian output in the retina. *Journal of Neurochemistry*, **108**, 1607–1620.

Komeima, K., Rogers, B.S., Lu, L., & Campochiaro, P. a (**2006**) Antioxidants reduce cone cell death in a model of retinitis pigmentosa. *Proceedings of the National Academy of Sciences of the United States of America*, **103**, 11300–11305.

Léveillard, T., Mohand-Saïd, S., Lorentz, O., Hicks, D., Fintz, A.-C., Clérin, E., Simonutti, M., Forster, V., Cavusoglu, N., Chalmel, F., Dollé, P., Poch, O., Lambrou, G., & Sahel, J.-A. (**2004**) Identification and characterization of rod-derived cone viability factor. *Nature genetics*, **36**, 755–759.

Li, G., Anderson, R.E., Tomita, H., Adler, R., Liu, X., Zack, D.J., & Rajala, R.V.S. (**2007**) Nonredundant role of Akt2 for neuroprotection of rod photoreceptor cells from light-induced cell death. *The Journal of neuroscience : the official journal of the Society for Neuroscience*, **27**, 203–211.

Liang, F.Q., Aleman, T.S., ZaixinYang, Cideciyan, A. V, Jacobson, S.G., & Bennett, J. (**2001**) Melatonin delays photoreceptor degeneration in the rds/rds mouse. *Neuroreport*, **12**, 1011–1014.

Marc, R.E., Jones, B.W., Watt, C.B., & Strettoi, E. (**2003**) Neural remodeling in retinal degeneration. *Progress in Retinal and Eye Research*, **22**, 607–655.

Marchiafava, P.L. & Longoni, B. (**1999**) Melatonin as an antioxidant in retinal photoreceptors. *Journal of pineal research*, **26**, 184–189.

McMahon, D.G., Iuvone, P.M., & Tosini, G. (**2014**) Circadian organization of the mammalian retina: from gene regulation to physiology and diseases. *Progress in retinal and eye research*, **39**, 58–76.

Mohand-Said, S., Deudon-Combe, A., Hicks, D., Simonutti, M., Forster, V., Fintz, A., Léveillard, T., Dreyfus, H., & Sahel, J. (**1998**) Normal retina releases a diffusible factor stimulating cone survival in the retinal degeneration mouse. *Neurobiology*, **95**, 8357–8362.

Peichl, L. (**2005**) Diversity of mammalian photoreceptor properties: Adaptations to habitat and lifestyle? *Anatomical Record - Part A Discoveries in Molecular, Cellular, and Evolutionary Biology*, **287**, 1001–1012.

Ping, Y., Huang, H., Zhang, X.-J., & Yang, X.-L. (**2008**) Melatonin potentiates rod signals to ON type bipolar cells in fish retina. *The Journal of physiology*, **586**, 2683–2694.

Reiter, C.E.N., Sandirasegarane, L., Wolpert, E.B., Klinger, M., Simpson, I.A., Barber, A.J., Antonetti, D.A., Kester, M., Gardner, T.W., & Chad, E.N. (**2003**) Characterization of insulin signaling in rat retina in vivo and ex vivo.

Röhlich, P., Van Veen, T., & Szél, Á. (**1994**) Two different visual pigments in one retinal cone cell. *Neuron*, **13**, 1159–1166.

Rosen, R., Hu, D., Perez, V., Tai, K., Yu, G., Chen, M., Tone, P., Mccormick, S.A., & Walsh, J. (**2009**) Urinary 6-sulfatoxymelatonin level in age-related macular degeneration patients. *Molecular vision*, **15**, 1673–1679.

Savaskan, E., Jockers, R., Ayoub, M., Angeloni, D., Fraschini, F., Flammer, J., Eckert, A., Muller-Spahn, F., & Meyer, P. (**2007**) The MT2 melatonin receptor subtype is present in human retina and decreases in Alzheimer's disease. *Current Alzheimer research*, **4**, 47–51.

Scher, J., Wankiewicz, E., Brown, G.M., & Fujieda, H. (**2002**) MT(1) melatonin receptor in the human retina: expression and localization. *Investigative ophthalmology & visual science*, **43**, 889–897.

Sengupta, A., Baba, K., Mazzoni, F., Pozdeyev, N. V, Strettoi, E., Iuvone, P.M., & Tosini, G. (**2011**) Localization of melatonin receptor 1 in mouse retina and its role in the circadian regulation of the electroretinogram and dopamine levels. *PloS one*, **6**, e24483.

Sugawara, T., Sieving, P. a., Iuvone, P.M., & Bush, R. a. (**1998**) The melatonin antagonist luzindole protects retinal photoreceptors from light damage in the rat. *Investigative Ophthalmology and Visual Science*, **39**, 2458–2465.

Tosini, G., Baba, K., Hwang, C.K., & Iuvone, P.M. (**2012**) Melatonin: An underappreciated player in retinal physiology and pathophysiology. *Experimental eye research*, 1–8.

Tosini, G., Davidson, A.J., Fukuhara, C., Kasamatsu, M., & Castanon-Cervantes, O. (**2007**) Localization of a circadian clock in mammalian photoreceptors. *FASEB journal : official publication of the Federation of American Societies for Experimental Biology*, **21**, 3866–3871.

Tosini, G. & Menaker, M. (**1998**) The clock in the mouse retina: melatonin synthesis and photoreceptor degeneration. *Brain research*, **789**, 221–228.

Tosini, G., Owino, S., Guillaume, J.L., & Jockers, R. (**2014**) Understanding melatonin receptor pharmacology: Latest insights from mouse models, and their relevance to human disease. *BioEssays*, **36**, 778–787.

Wiechmann, A.F. & O'Steen, W.K. (**1992**) Melatonin increases photoreceptor susceptibility to light-induced damage. *Investigative Ophthalmology and Visual Science*, **33**, 1894–1902.

Wiechmann, A.F., Vrieze, M.J., Dighe, R., & Hu, Y. (**2003**) Direct modulation of rod photoreceptor responsiveness through a Mel 1c melatonin receptor in transgenic Xenopus laevis retina. *Investigative Ophthalmology and Visual Science*, **44**, 4522–4531.

Wiechmann, A.F., Yang, X.L., Wu, S.M., & Hollyfield, J.G. (**1988**) Melatonin enhances horizontal cell sensitivity in salamander retina. *Brain research*, **453**, 377–380.

Yi, C., Pan, X., Yan, H., Guo, M., & Pierpaoli, W. (**2005**) Effects of melatonin in age-related macular degeneration. *Annals of the New York Academy of Sciences*, **1057**, 384–392.

Zawilska, J.B. & Iuvone, P.M. (**1992**) Melatonin synthesis in chicken retina: effect of kainic acid-induced lesions on the diurnal rhythm and D2-dopamine receptor-mediated regulation of serotonin N-acetyltransferase activity. *Neuroscience letters*, **135**, 71–74.

DISCUSSION AND PERSPECTIVES

Studies focusing on melatonin synthesis in the pineal gland have established that a variety of strategies have evolved among vertebrates to generate a nocturnal increase in melatonin production *(Klein et al., 1997)*. In the retina, the second major melatonin production site, the hormone production exhibits differences among species **(Introduction Table 1 and Table 2)** suggesting species dependent regulation of melatonin synthesis as well as different functions for the hormone.

This work brings new information about the cellular site of melatonin synthesis as well as melatonin circadian expression with the aim to propose retinal function(s) for melatonin.

I. DIFFERENT SITES OF MELATONIN SYNTHESIS

I.A. AA-NAT expression suggests different sites of melatonin production in *Arvicanthis ansorgei* retina

We provide strong evidence that within the photoreceptors, *aa-nat* expression is exclusively present in cones and not rods. This result is consistent with data from rat retina *(Niki et al., 1998)* **(Chapter 1 Article 1, Supplemental Figure 1)**. In our study the cone-specific localization was facilitated by the abundance of cones in this species (33 %, *(Bobu et al., 2006)*), and their precise alignment in the ONL. The quantification of cones *Aa-nat* mRNA highlighted *aa-nat* circadian rhythm with the highest level during the night. At the opposite, in the GCL we could observe *aa-nat* mRNA circadian variation with expression restricted to the day. Thus *aa-nat* gene seems to display an opposing cyclic expression in cones and GCL of *Arvicanthis ansorgei* retina. A recent study *(Valdez et al., 2012)* described a similar pattern in chicken retina. Indeed, AA-NAT activity in RGCs display its highest level during the day whereas in PRs the level is the highest during the night *(Valdez et al., 2012)*. *Aa-nat* mRNA was also weakly seen in INL of *Arvicanthis ansorgei* with a slight increase at night. *Aa-nat* mRNA distribution in the 3 nuclear layers has also been observed in rat *(Liu et al., 2004)*, monkey *(Coon et al., 2002)* and trout *(Besseau et al., 2006)*.

In addition to mRNA detection, we also addressed the issue of AA-NAT protein localization. Multiple immunohistochemical procedures preceded by antigen retrieval were tested with the aim to make AA-NAT epitopes accessible to antibodies. Indeed AA-NAT is strongly associated with the 14-3-3 chaperone protein which can mask epitopes *(Pozdeyev et al., 2006)*. Optimal results were achieved using immunoperoxidase and DAB detection together with antigen retrieval. This is the first demonstration of AA-NAT cellular protein localization in the retina. Indeed, it was found in cones, cells within the INL and in the majority of neurons within the GCL (RGCs and displaced amacrine cells which constitute ~40 % of neurons in the GCL *(Jeon et al., 1998)*). AA-NAT immunoreactivity in cones, INL and GCL is consistent with the results of *Aa-nat* transcripts. However, mRNA was not seen in the GCL at night when AA-NAT protein is present. A possible explanation is a lower sensitivity of our digoxygenin *in situ* hybridization method compared to immunohistochemistry with DAB detection. Another possibility is that immunohistochemistry with DAB detection give a non specific staining in the GCL at night.

All together these results suggest several possible sources of melatonin secretion.

I.B. HIOMT expression supports melatonin synthesis in cones and ganglion cells of *Arvicanthis ansorgei*

HIOMT represents the ultimate step in melatonin production and is therefore crucial for understanding melatonin synthetic pathway. HIOMT detection has always been complicated because of mRNA and protein low levels, weak sequence homology between species and lack of specific antibodies. HIOMT expression in the retina is even questioned *(Klein, 2004)*. We were able to produce *hiomt* rat riboprobe. To confirm the probe specificity, we performed *in situ* hybridization in both rat and *Arvicanthis ansorgei* pineal gland and retina. The rat riboprobe gave no specific signal in *Arvicanthis ansorgei* pineal gland and retina, whereas it could detect *hiomt* in rat. For the first time, *hiomt* was detected in a mammal retina. Indeed mRNA was localized in GCL, ONL and weakly in INL. At night, *hiomt* expression is present in rare loci along the scleral border of the ONL suggesting a localization in cones since these cells represents 2 % of rat PRs *(Szél & Rohlich, 1992)*. The co-immunostaining with cone arrestin confirmed that *hiomt* is expressed in cones. At night, very low *hiomt* levels are detected in GCL. On the contrary, during the day, *hiomt* is mainly detected in GCL and no more in cones. *Hiomt* expression level in the INL does not seem to vary during the light/dark cycle. These results demonstrate that **like *aa-nat* gene in *Arvicanthis ansorgei* retina, *hiomt* seems to display an opposite cyclic expression in cone and GCL of rat**. Detection of *hiomt* in PR rat retina confirm results obtained in chicken *(Wiechmann & Craft, 1993).* Our results are also consistent with those of trout retina where *hiomt* was detected in ONL, INL and GCL *(Besseau et al., 2006)*. Finally a study in chicken retina suggests that Otx2, a specific transcription factor of PR genes, can activate *hiomt* gene, supporting a probable *hiomt* localization in PRs. *(Dinet et al., 2006)*.

Preliminary results of our team regarding *hiomt* mRNA detection in the different layers of *Arvicanthis ansorgei* retina were achieved by PCR. PR, inner retina (INL, IPL) and GCL layers were isolated by vibratome. *Hiomt* was detected in the different isolated layers.

In the retina of *Arvicanthis*, examination of whole mounted retina confirmed the localization of the enzyme in cones but not rods, as well as in RGC. Our data fit with studies on chicken retina demonstrating the presence of HIOMT in cones and to a lower extent in rods as well as in GCL *(Voisin et al., 2012)*. Our results are also in agreement with HIOMT localization in mammals showing mainly protein in PR and to a lower extent in GCL of rat, as well as in PR of bovine and human *(Wiechmann et al., 1985)*. In the same way, HIOMT was expressed in cones of lizard retina *(Wiechmann et al., 1985)*. HIOMT expression coincides largely with that of AA-NAT. However HIOMT presence was not established in INL of *Arvicanthis ansorgei* retina, probably because it is expressed in very low amount in this layer.

Overall, it appears evident that melatonin is not solely produced by photoreceptors. Indeed *aa-nat* mRNA and melatonin are still rhythmic in the retina of rat lacking photoreceptors *(Sakamoto et al., 2004)*. Moreover *aa-nat* transcripts are detected in the INL and GCL of these rats *(Sakamoto et al., 2004)*.

Finally our work demonstrates that cones and the GCL (probably RGC and displaced amacrine cells) express AA-NAT and HIOMT in *Arvicanthis ansorgei* and rat retina implying the existence of two sources of melatonin production. INL might also produce melatonin but apparent extremely low levels forbid any definite conclusion. Our results suggest at least 2 systems of melatonin production which could allow different functions of melatonin.

II. SPECIFIC TEMPORAL EXPRESSION OF MELATONIN IN *ARVICANTHIS ANSORGEI*

II.A. Is AA-NAT temporal expression controlled by circadian clock and light?

Aa-nat transcripts display a nocturnal peak in *Arvicanthis ansorgei* cones, consistent with the known regulation of *aa-nat* synthesis in the retina of nocturnal rodents *(Sakamoto & Ishida, 1998a, 1998b)* and in the pineal gland of rat and *Arvicanthis ansorgei* *(Garidou et al., 2002)*. Furthermore quantitative PCR detection of *aa-nat* exhibits a rhythmic expression with a peak at night in the retina of *Arvicanthis ansorgei* maintained under LD condition. In DD the peak is reduced, but still present at night whereas in LL, *aa-nat* mRNA exhibits a smaller nocturnal peak *(Bobu et al., 2013)*. These results show that ***aa-nat* mRNA is primarily under the control of a circadian clock** and to a lower extent light-dependent.

The protein expression profile was determined by blotting analyses of AA-NAT expression across the 24 hours. Data obtained from at least 3 independent experiments and 5 animals per time point indicate a variation of AA-NAT expression over 24 hours. Repeated large inter-individual variations rendered statistical analysis non significant. In LD condition, the overall pattern displayed a nocturnal maximum but also sustained expression throughout most of the day except the beginning of the day. No studies have so far reported AA-NAT protein expression across the 24 hours in mammalian retina. In DD condition, AA-NAT presents similar profile than in LD (ie. increase at night and lower expression at the beginning of the day) but surprisingly exhibits a significant peak at the middle of the day (CT7). In the pineal gland and retina of chicken, *Xenopus* and rat it is generally accepted that AA-NAT is under strict circadian and light control resulting in highly predominant nocturnal activity *(Iuvone et al., 2005)*. In *Arvicanthis ansorgei*, the suppression of light input induces an AA-NAT peak during the day suggesting that the control of AA-NAT by the light/dark cycle reduces the diurnal protein level. This phenomenon could be the result of **post-translational modification**. Proteosomic proteolysis of one part of AA-NAT could occur during the light period *(Pozdeyev et al., 2006)*. To conclude, our results suggest that **AA-NAT level is controlled mainly by the light/dark cycle in *Arvicanthis ansogei* retina but it still controlled by the circadian clock**.

In the pineal gland, AA-NAT activity always follows the protein profile. In retina, such phenomenon was described in monkey *(Coon et al., 2002)*. In chicken, AA-NAT activity exhibits a more pronounced day/night difference compared to the protein *(Iuvone et al., 2002)*. In *Arvicanthis ansorgei* retina, AA-NAT activity is constitutively present with a smaller increase at night compared to the protein level. These results suggest that the protein is overall always present and that its activity vary the same way. However these results are obtained in the entire retina and we can speculate that regulation of AA-NAT activation is different between the 2 melatonin production sites.

Future studies should seek for *Arvicanthis* retinal AA-NAT level in LL condition and in animals housed in LD conditions and submitted to light pulse during the night. These experiments could help us understand whether AA-NAT is a direct reflection of photoperiod.

II.B. Control of AA-NAT protein expression by the light/dark cycle

Previous studies in rat retina have proposed that light decreases Ca^{2+} and cAMP levels leading to activation of proteasomal proteolysis *(Fukuhara et al., 2001)*. Studies in chicken have shown that during the day AA-NAT phosphorylation by PKA is decreased, leading to dissociation from the 14-3-3 chaperone and subsequent degradation by the proteasome *(Iuvone et al., 2002; Pozdeyev et al., 2006)*.

Preliminary results in *Arvicanthis ansorgei* retina indicate that P-AA-NAT and 14-3-3 proteins are present throughout the 24 hours with a slight increase at the end of the day and night. These results suggest that both proteins could form a complex to protect AA-NAT from proteosomal proteolysis during the day and the night.

It is evident that remarkable differences among species exist concerning the molecular mechanisms involved in AA-NAT regulation *(Klein et al., 1997)*. In human pineal gland, P-AA-NAT is constitutively present *(Maronde et al., 2011)*. It is speculated that the effect of light on AA-NAT stability is mediated by a mechanism independent of Ca^{2+} or cAMP, possibly involving post-translational modifications.

Another possible explanation for the presence of P-AA-NAT during the day is that cAMP could be present during the day in *Arvicanthis ansorgei* retina. Indeed Garbarino-Pico et al,. reported that melatonin, *aa-nat* mRNA and cAMP peak during the subjective day in chicken RGCs *(Garbarino-Pico et al., 2004)*.

The high level of nocturnal UnP-AA-NAT in *Arvicanthis ansorgei* suggests that the proteasomal proteolysis may also occur at night. Similar hypotheses have been advanced in fish retina where proteasomal proteolysis plays a role in reducing AA-NAT protein at night *(Besseau et al., 2006).* The authors proposed that the effect of light on AA-NAT can be mediated by a mechanism that does not involve Ca^{2+} or cAMP.

To summarize, in *Arvicanthis ansorgei* retina, the presence of P-AA-NAT during the day could be explain by mechanisms dependent of cAMP specific regulation (ie. peak at day) or independent of cAMP **(Figure)**.

In future study it will be interesting to assess the circadian expression of cAMP in *Arvicanthis ansorgei* retina to see whether it fits with AA-NAT protein circadian expression. We could also activate cAMP with forskolin treatment and measure P-AA-NAT level to see whether the protein synthesis is increased and thus driven by a cAMP dependent mechanism.

Finally, to better understand AA-NAT regulation in the diurnal rodent retina, we propose to perform a co-immunoprecipitation experiment in order to determine the P-AA-NAT/14-3-3 complex formation in retinas collected over 24 hours.

It will also be relevant to perform intraocular injection of proteasomal inhibitor (MG132) during the day to *Arvicanthis ansorgei* raised in LD conditions before sacrifice and western blotting analysis of retinal AA-NAT. This experiment could allow us to see if proteasomal proteolysis plays a role in reducing AA-NAT protein amount during the day. The same experiment will be performed with MG132 injection during the night to see if proteasomal proteolysis plays a role in reducing AA-NAT protein level during the night.

II.C. HIOMT expression is low in *Arvicanthis ansorgei* retina

Because of the weak level of HIOMT, only two studies have reported its detection in the retina of rat and hen with a constant expression throughout the 24 hours *(Nowak et al., 1989; Gauer & Craft, 1996)*. In *Arvicanthis ansorgei* retina, HIOMT enzyme displays a fiftyfold lower level of activity compared to AA-NAT. Abundant data have put forward AA-NAT as the rate limiting enzyme for the rhythmic synthesis of melatonin in both pineal gland and retina *(Klein et al., 1997; Tosini & Fukuhara, 2003)*

The profile of melatonin expression was described as rhythmic with a night-time peak in the rat retina *(Pang et al., 1980; do Carmo Buonfiglio et al., 2011)*. In our diurnal model, regulation is clearly different: both AA-NAT and HIOMT are expressed and active throughout the 24 hours period with small increases at the end of the day and night. Melatonin is also produced across the 24 hours with similar small variations. Therefore, **in *Arvicanthis,* retinal melatonin production might be controlled by subtle transcriptional and translational regulation of AA-NAT and HIOMT. Moreover, the regulation might be site (ie. in PRs and RGCs) and time dependent.**

II.D. Comparison with the control mechanism of melatonin synthesis in nocturnal rodents

In *Arvicanthis ansorgei,* as in rat, *aa-nat* mRNA rhythm is driven by the circadian clock (Figure). In addition, **AA-NAT activity is mainly regulated by light in rat retina. Similar mechanism seems to be present in *Arvicanthis ansorgei*** since AA-NAT protein level is mainly controlled by light **(Figure)**.

However, in rat, the changes in mRNA expression are followed by variations in AA-NAT activity and then in melatonin level which is not the case in *Arvicanthis ansorgei*. **Initiation of melatonin synthesis is under transcriptional and post-translational control in rat retina (see Introduction IV.A.2)**. **In *Arvicanthis ansorgei* retina, melatonin synthesis seems to be controlled by post-translational regulation** since melatonin expression follows AA-NAT activity and not the *aa-nat* mRNA profile **(Figure)**. **The post-translational regulation are different in *Arvicanthis ansorgei* retina compared to the one established in the rat** and chicken retina *(Pozdeyev et al., 2006)* **(see Introduction IV.A.2)**. Indeed in *Arvicanthis*, P-AA-NAT and 14-3-3 chaperone proteins are both present during the day suggesting that diurnal AA-NAT is not completely degraded by proteasomal proteolysis **(Figure)**.

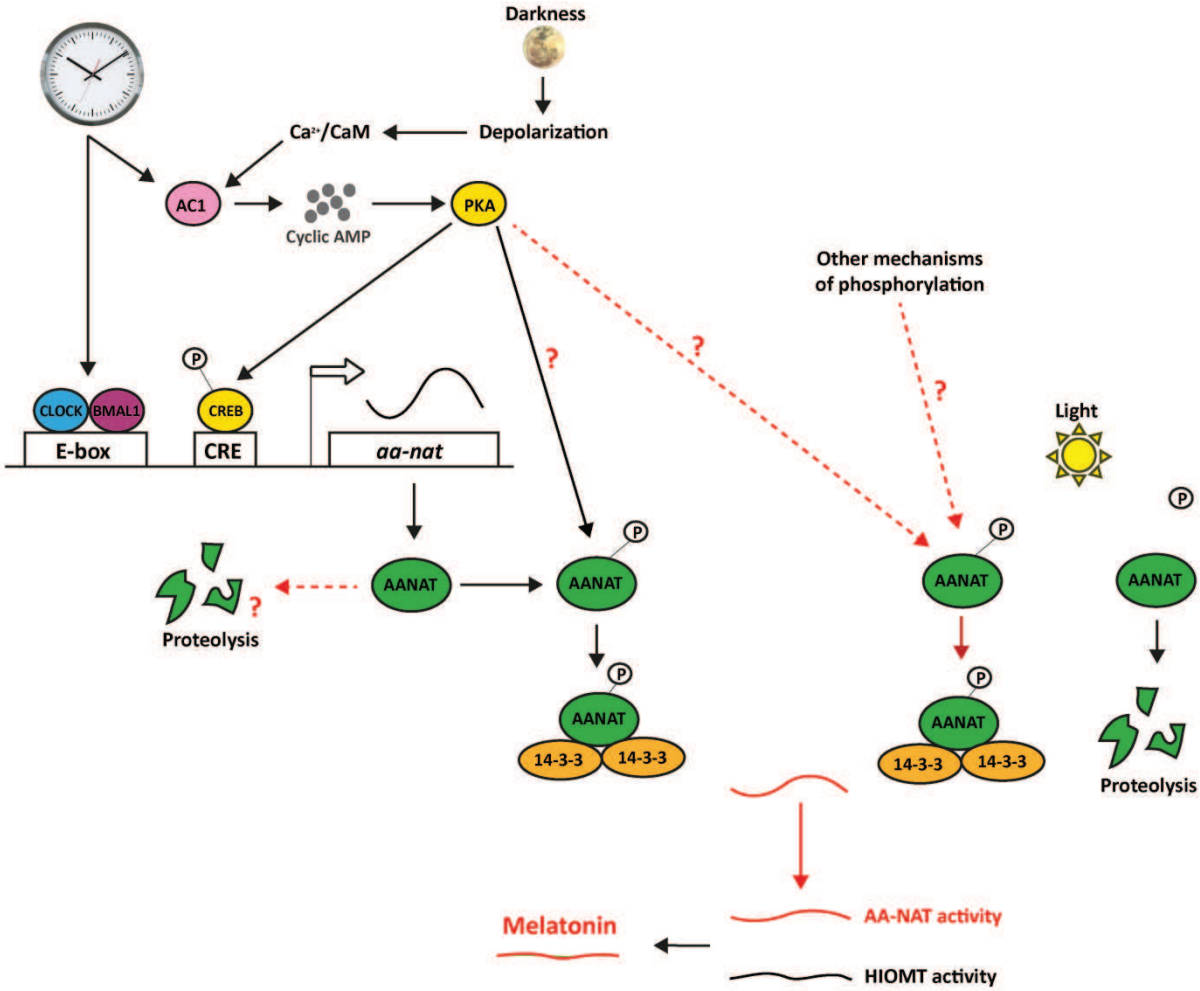

Figure 34. Hypothetical model of melatonin regulation in *Arvicanthis ansorgei* retina.

Initiation of melatonin synthesis is controlled by post-translational regulation. AA-NAT is present under phosphorylated and unphosphorylated forms over the 24 hours. Effect of light on AA-NAT can be mediated by a mechanism that does not involve Ca^{2+} or cAMP. Diagram modified from *(Tosini et al., 2012)* to compare the regulation of retinal melatonin synthesis in the diurnal rodent *Arvicanthis ansorgei* with the accepted pathway in the nocturnal rodent's retina. *Arvicanthis ansorgei* differences are presented in red. Dotted line and question marks present hypothetical mechanisms. P: phosphorylated.

II.E. Does AA-NAT have additional functions?

In *Arvicanthis ansorgei* retina, the high level of AA-NAT activity compared to the low level of HIOMT's suggests another function of AA-NAT besides melatonin synthesis. At least two alternative roles can be proposed for AA-NAT. First, AA-NAT generates NAS, which has recently been shown to exhibit pronounced intrinsic biological activity. Notably, it binds to trkB receptor (BDNF receptor) with high affinity and thereby exert neuroprotective effects *(Jang et al., 2010; Sompol et al., 2011)*. We analyzed retinas of *Arvicanthis ansorgei* by HPLC in order to detect NAS. However we could not detect NAS in the samples probably because its level is low and inferior to the detection threshold of HPLC. AA-NAT higher expression than that of HIOMT does not account for NAS production in *Arvicanthis* retina.

Secondly, AA-NAT is an aryl-alkylamine transferase, which could have a role in detoxification. Cones of *Arvicanthis* contain AA-NAT. In PRs, retinaldehyde (essential for photon capture) are depleted by reacting with arylalkylamines (tyramine, serotonin, tryptamine). This generates toxic-bis-retinyl arylalkylamine (A2AA). AA-NAT prevents A2AA formation by N-acetylating the arylalkylamines and thereby help detoxify the cell *(Klein, 2004).* Previous results from our team showed that *Arvicanthis ansorgei* retinas are highly resistant to intense light damage *(Boudard et al., 2011)*. This phenomenon may represent an adaptation to high ambient light conditions to which *Arvicanthis* is exposed in its natural environment. We can suppose that AA-NAT play a role in cones detoxification in the diurnal rodent retina.

II.F. Does bloodstream and retinal melatonin mixed up?

II.F.1. Does circulating melatonin enter in the retina?

Melatonin produced in the pineal gland is released in the bloodstream and irrigates all the body. Since the retina is highly vascularized, pineal melatonin possibly enter in the retina.

AA-NAT and melatonin day/night expression levels in the pineal gland and the retina of *Arvicanthis ansorgei* are here compared to determine whether pineal melatonin enter in the retina in physiological condition (and *in vivo*). *Arvicanthis ansorgei* pineal gland exhibits a daily profile of *aa-nat* mRNA, AA-NAT activity and melatonin with nocturnal peaks *(Garidou et al., 2002)* **(Table)**. The day-to-night ratio and level of expression observed in the retina is much lower than that in the pineal gland **(Table)**. The comparison between pineal gland and retina values suggests that bloodstream melatonin contributes weakly to the retinal level in *Arvicanthis ansorgei*.

	***Arvicanthis* pineal gland**	***Arvicanthis* retina**
***aa-nat* mRNA**	*(Garidou et al., 2002):* N>D ~250x.	In PR, N>D ~4x; in RGC, D>N by ISH. *(Bobu et al., 2013):* N>D ~20x by qPCR.
AA-NAT protein	Nd	Present at all times except ZT3. N>D ~10x.
AA-NAT activity	*(Garidou et al., 2002):* 1000 pmol/pineal/h. N>D ~10x.	~100 pmol/mg prot/h. Present at all times, small increase at night, ~1.5x.
Melatonin	*(Garidou et al., 2002):* 400 pg/pineal. N>D ~20x.	~18 pg/mg prot. N=D.

Table 10. Circadian variation of AA-NAT and melatonin in the pineal gland and retina *of Arvicanthis ansorgei*.

N: night value; D: day value; ISH: *in sity* hybridization; qPCR: quantitative PCR; nd: not determined.

However it is important to note that pharmacological concentration of melatonin administrated in the circulation reaches the retina. Indeed, in human, daytime oral administration of melatonin (when endogenous level is low) modifies cone ERG, suggesting that bloodstream hormone reaches the eye *(Gagné et al., 2009)*. Similarly, daytime intraperitoneal injection of melatonin in C3H mice (melatonin proficient mice) increases rods light sensitivity *(Baba et al., 2009, 2013)*. Under DD condition, daily intraperitoneal melatonin injections at night in C57black6 mice (melatonin deficient mice) restores retinal melatonin and dopamine rhythmicity *(Doyle et al., 2002)*.

II.F.2. Does retinal melatonin contribute to the bloodstream pool?

Pinealectomy reduces the nocturnal plasma melatonin value by 80 % in chicks. The addition of bilateral enucleation reduces the value off another 9 %. These results suggest that 9 % of the plasma melatonin comes from the eyes, thus retina which is the major melatonin production site in eye *(Reppert & Sagar, 1983)*. The authors conclude that only a minor level of bloodstream melatonin comes from retina. Indeed another study reports that the retinal melatonin production does not seem to contribute significantly to plasma levels *(Vaughan & Reiter, 1986)*. These finding indicate that melatonin is synthesized in the retina principally for local purpose *(Vanecek, 1998)*.

III. MODEL OF MELATONIN SYNTHESIS IN *ARVICANTHIS ANSORGEI* RETINA

III.A. Two systems of melatonin production

Our work identifies at least two main sites of melatonin production: cones and RGCs. AA-NAT and HIOMT expressions were also seen within the INL, but were not further characterized in this layer. We propose the following model **(Figure 35)**. On one hand, AA-NAT mRNA and protein display a rhythmic expression in the photoreceptors with a peak at night **(Chapter I Article I, Figure 1 and 3)**. In addition, *hiomt* mRNA in rat is stronger at ZT23 compared to ZT7 in the photoreceptors. We propose that the increase of melatonin during the night is PR dependent. This hypothesis is consistent with what has been previously described in rat and chicken *(Garbarino-Pico et al., 2004; Liu et al., 2004; Valdez et al., 2012)*. Indeed, rhythmic melatonin production by retinal PRs occurs at night *(Garbarino-Pico et al., 2004; Liu et al., 2004; Valdez et al., 2012)*.

On the other hand, AA-NAT and HIOMT protein are present in RGC during the day. Furthermore, *aa-nat* mRNA is strongly expressed in the GCL of *Arvicanthis ansorgei* retina during the day suggesting a distinct regulation of melatonin production in these cells. In addition, *hiomt* mRNA is strongly detected in the GCL during the day in the rat retina. We hypothesize that the production of melatonin during the day might be controlled by RGCs **(Figure 35)**. This hypothesis is consistent with the study in the chicken retina where they described a daily peak of AA-NAT in RGCs, suggesting a diurnal peak of melatonin *(Garbarino-Pico et al., 2004; Valdez et al., 2012)*. Finally, melatonin profile observed in the entire retina was of a constitutive nature which could reflect the sum of at least two distinctly regulated production sites: one in the cones, the other in the RGCs **(Figure 35)**.

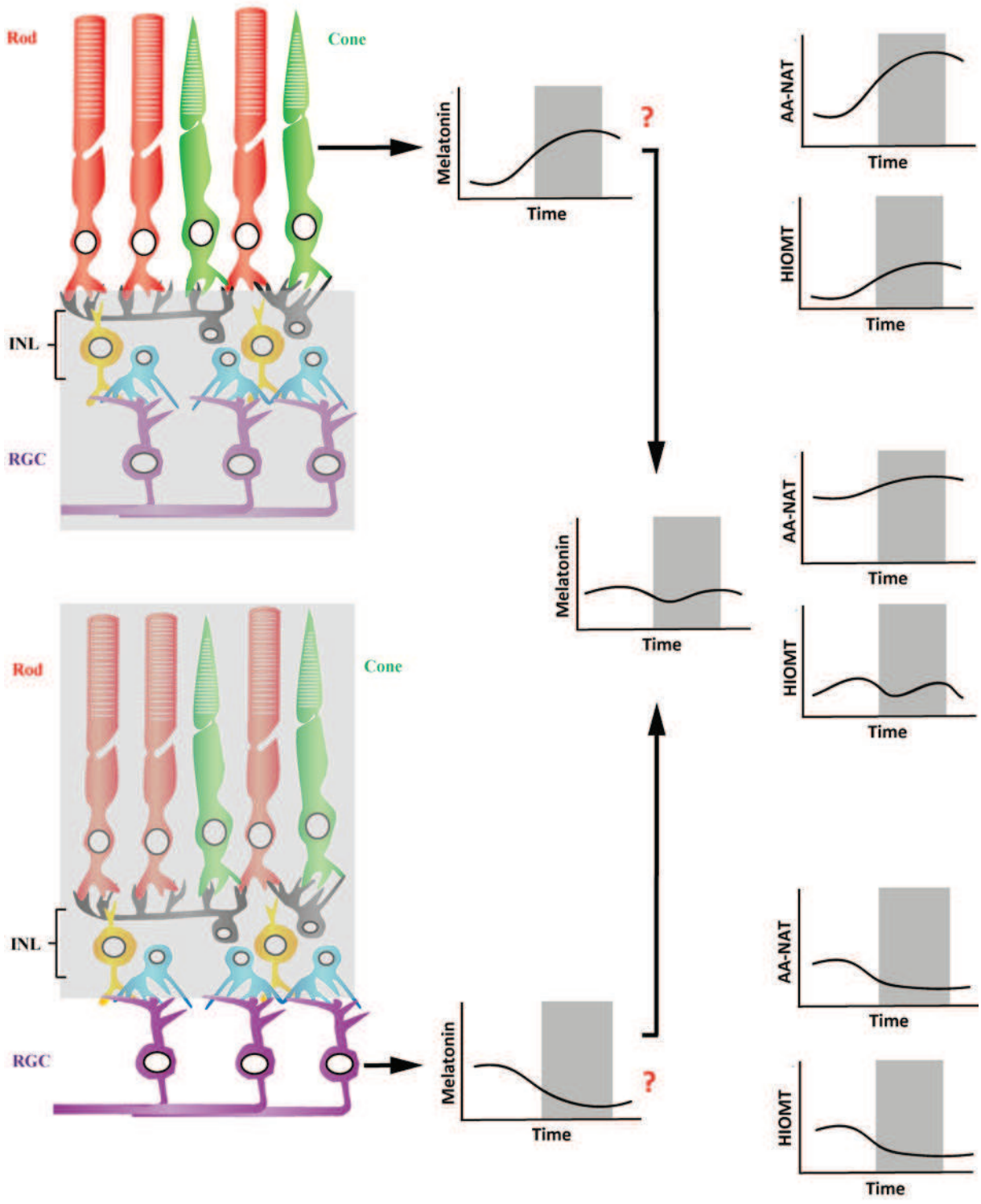

Figure 35. Model of melatonin synthesis in *Arvicanthis ansorgei* retina.

Upper panel: melatonin is produced by cones during the night. **Lower panel:** melatonin is produced by RGCs during the day. Constitutive melatonin level in the retina might be composed of PRs and RGCs melatonin. AA-NAT expression throughout the 24 hours could be the results of the integration of PR nocturnal AA-NAT and RGC daytime AA-NAT productions. The same hypothesis can be proposed for HIOMT.

III.B. Cell-dependent control mechanism of melatonin synthesis?

III.B.1. Does the chicken model explain two mammal systems of melatonin regulation?

The control mechanism of melatonin synthesis in *Arvicanthis ansorgei* **(Figure 36 and Figure 37)** could be similar to the one proposed in chicken retina by Valdez et al. *(Valdez et al., 2012)*.

RGCs probably contain a circadian clock *(Ruan et al., 2006; Liu et al., 2012; Jaeger et al., 2015)* and some of these cells (ipRGCs) are able to receive light information. Valdez et al. have demonstrated that AA-NAT activity rhythm in RGCs of chicken retina is not regulated by light or dopamine *(Valdez et al., 2012)*. Indeed, AA-NAT activity exhibits a peak during the day in LD, DD as well as in LL conditions. A light pulse during the subjective night or day had no effect on AA-NAT activity in RGCs. Finally dopamine injection at night (to mimic light effect) had no effect on AA-NAT level.

On the contrary, PR AA-NAT activity exhibited a nocturnal peak in LD and DD but not in LL condition. A light pulse during the subjective night, as well as dopamine injection at night decrease AA-NAT activity in PRs.

The authors suggest that the regulation of the diurnal AA-NAT increase in RGCs undergoes a different control mechanism that the one in PRs. In PRs, the endogenous clock, light and dopamine control AA-NAT activity whereas only the circadian clock seems to control AA-NAT in RGCs *(Valdez et al., 2012)*.

I propose to isolate *Arvicanthis ansorgei* PR and GCL by vibratome in a way to perform western blotting and enzymatic assay. These experiments should serve to assess AA-NAT protein and activity respectively in each layer. These experiments should take place in LD, DD and LL conditions to test whether the light controls AA-NAT nycthemeral rhythm.

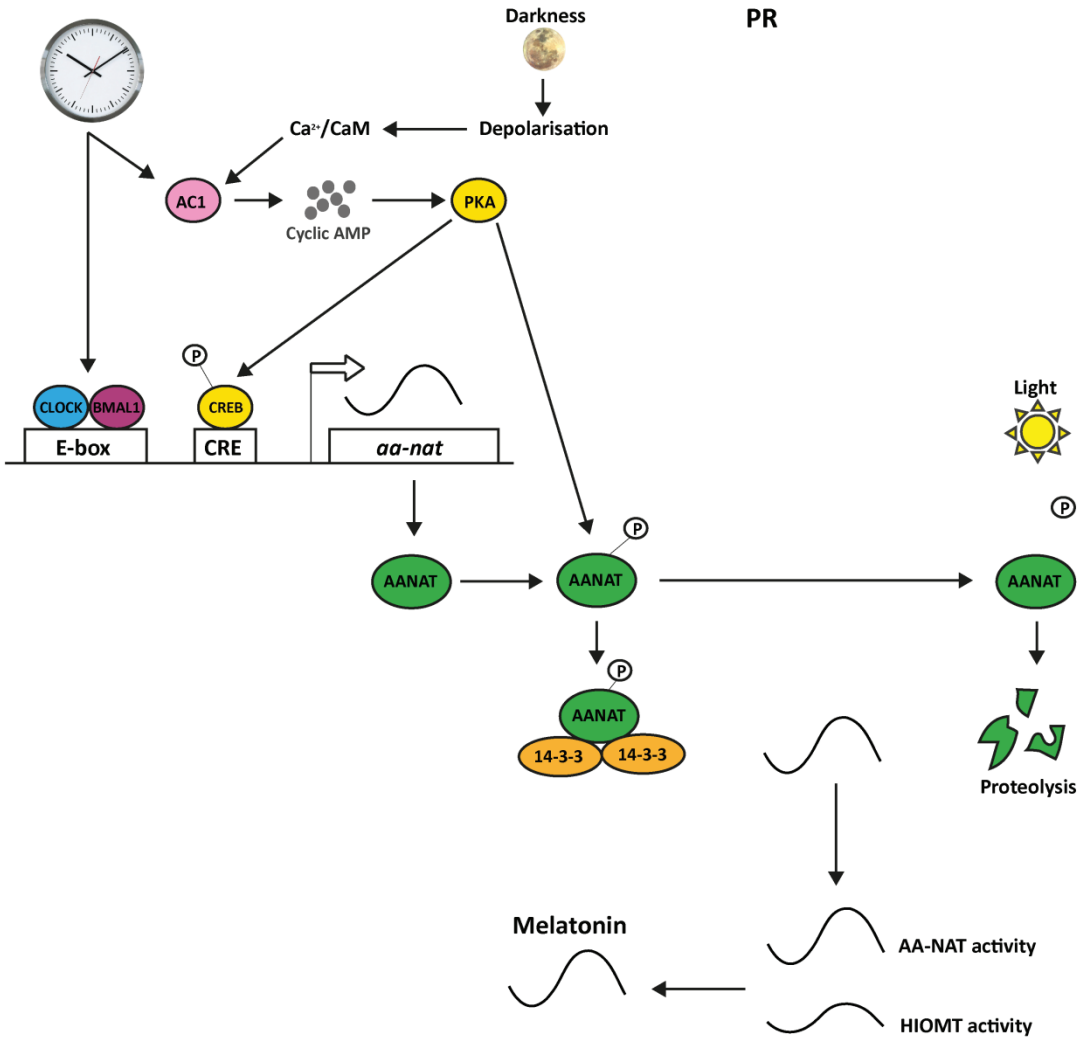

Figure 36. Hypothetical model of melatonin synthesis in PR of *Arvicanthis ansorgei*.

PRs nocturnal melatonin may be under control of the **circadian clock** and the **light**. Modified from *(Tosini et al., 2012)* to allow comparison with the accepted model in the rat retina.

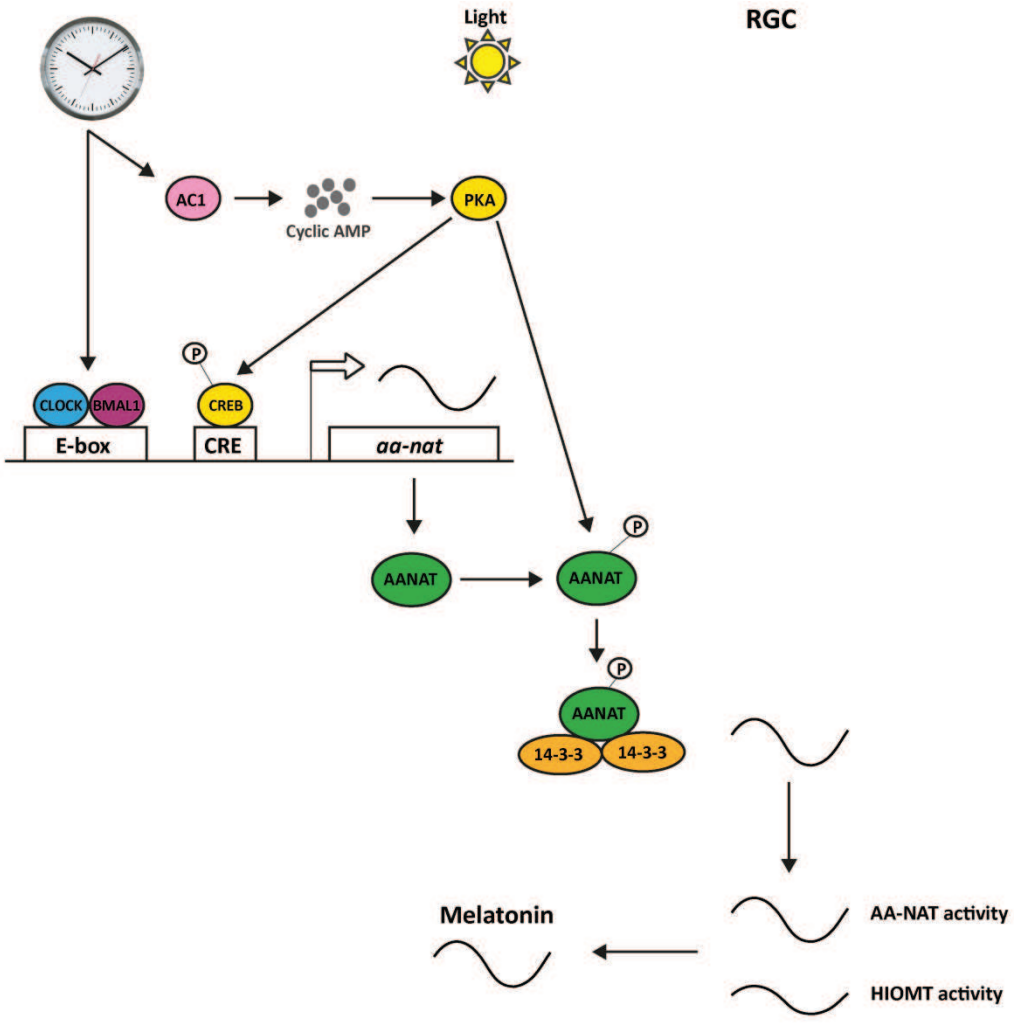

Figure 37. Hypothetical model of melatonin synthesis in RGC of *Arvicanthis ansorgei*.

RGC diurnal melatonin may be under control of the **endogenous clock**. Modified from *(Tosini et al., 2012)*.

IV. CAN SUSTAINED MELATONIN PRODUCTION RESPOND TO PHYSIOLOGICAL NEED IN *ARVICANTHIS* RETINA?

IV.A. Melatonin displays autocrine and paracrine functions in the retina

In our study, melatonin appears constitutively produced according AA-NAT and HIOMT activities. Furthermore the indolamine production coincides with the temporal expression of MT_1 receptors in the rods, INL and GCL **(Chapter I Article I, Figure 6)**. The localization of MT_1 receptors are consistent with results obtained in the mouse retina *(Sengupta et al., 2011)*. **These results suggest that cone melatonin may act as a paracrine messenger binding to its receptors in rods, INL and GCL. RGC melatonin may have autocrine action via MT_1 on RGCs as well as a paracrine role via MT_1 on INL and rods.**

Accordingly, our data support two action modes for melatonin in *Arvicanthis ansorgei* retina via MT_1 receptors.

IV.B. *Arvicanthis ansorgei*: a bimodal rodent

Melatonin is always presented as a nocturnal signal used by the retina to modulate neurotransmitter secretion, neuronal electric activity, photoreceptor phagocytosis or dark adaptation *(Wiechmann & Sherry, 2013)*.

In our study, melatonin appears constitutively produced in agreement with AA-NAT and HIOMT activity. We know that *Arvicanthis ansorgei* exhibits a bimodal locomotor activity with an increase at dawn and dusk *(Katona & Smale, 1997; García-Allegue et al., 1999; Weinert et al., 2007; Cuesta et al., 2009).* These data suggest that *Arvicanthis* need retinal adaptation both to a nocturnal and a diurnal vision as described below.

IV.C. Nighttime melatonin

First, our data may support retina adaptation to darkness through melatonin/dopamine interplay: a fundamental aspect of mammal retina function *(McMahon et al., 2014)*. Indeed, dopamine is the main neurotransmitter activated by light *(Popova, 2014)*. In fact, dopamine inhibits melatonin, and melatonin in turn inhibits dopamine release, forming a mutual inhibition loop *(Dubocovich, 1983; Zawilska & Iuvone, 1992; Boatright et al., 1994; Nguyen-legros et al., 1996; Tosini & Dirden, 2000; Ribelayga et al., 2004)*. In our study dopamine/DOPAC levels rose at ZT7 in the middle of the day and did overlap with the daytime melatonin increase. These results differ from the previously described interplay between both compounds. As dopamine and melatonin are measured in the entire retina, we have not determined the rhythmic profile of dopamine and melatonin in PRs. However it is likely that melatonin peaks during the night in PRs and thereby inhibits the production of dopamine at night. One study in chicken shows that intraocular injection of dopamine during the night presented significant inhibition of AA-NAT activity in PRs showing that the feedback loop between melatonin/dopamine occurs at least in PRs *(Valdez et al., 2012)*.

We know that PRs are coupled one to another via homologous (rod-to-rod, cone-to-cone) as well as heterologous (rod-to-cone) gap junctions. While such coupling may modulate visual acuity, it is also beneficial for retinal signaling. Gap junction conductance is modulated by phosphorylation of the connexins which composed the gap junction. These phoshorylation sites are accessible to PKC and PKA that are integrators of many intracellular cascades *(Völgyi, Kovács-öller, et al., 2013)*. During the day, dopamine activates D2 receptor in PRs and inhibits AC/cAMP/PKA pathway. At night, the low level of dopamine cannot activate the D2 receptor which leads to an increase in PKA level. This induces connexin phosphorylations and an increase of rod-cone gap junction conductance *(Völgyi, Kovács-öller, et al., 2013)*. Indeed recently, Ribeleyga and Mangel have demonstrated that inhibition of D2 receptors increase the rod input to A type horizontal cell by enhancing rod-cone coupling *(Ribelayga & Mangel, 2010)*. In *Arvicanthis ansorgei*, melatonin is produced by cones at night when DOPAC is low and melatonin can binds MT_1 receptor on rods to activate/inhibit intracellular signaling pathway. These results suggest that melatonin can modulate gap junction conductance and be involved in the cross-talk between cones and rods. A recent study proposes that nocturnal melatonin increase rod light sensitivity in the retina of mice via MT_1/MT_2 heteromeres and PLC/PKC pathway *(Baba et al., 2013)*. This pathway leads to an increase of Ca^{2+} intracellular level which is described to reduce gap junction conductance *(Völgyi, Kovács-öller, et al., 2013)*. Gap junction low conductance has been thought to favor the light signal transmission with slow kinetics, which is a characteristic of

single photon evoked response in rod *(Völgyi, Kovács-öller, et al., 2013)*. These elements suggest that **PRs melatonin could be involved in the cross-talk between cones and rods in order to prepare for dark adaptation**.

Alternatively, our finding echoes the prevalence of clock protein expression in cones and ipRGCs of the mouse retina *(Liu et al., 2012)*. A recent study has demonstrated the involvement of ultraviolet sensitive (UVS) cones in ipRGC-SCN dialogue in response to UV light *(Van Oosterhout et al., 2012)*. In addition, it is known that cone signals can be relayed to the SCN via pathways from ipRGCs in order to drive circadian photoentrainment *(Do & Yau, 2010)*. Irradiance at dawn has been shown to provides an important cue for the entrainment of the mammalian circadian clock *(Berson et al., 2002; Do & Yau, 2010)*. Cones could respond to light as a "primary" retina sensor *(Liu et al., 2012)* and subsequently produce a signal that will participate in the ipRGC transmission of information to the SCN. We can speculate that melatonin which is produced at night in the cones of *Arvicanthis ansorgei* retina could be involved in the communication between cones and ipRGCs. Indeed melatonin receptors are expressed in RGCs and INL of *Arvicanthis* retina. **Thus melatonin could be involved in the transmission of light information within the layers of the retina and maybe towards SCN.**

IV.D. Daytime melatonin

The contribution of RGC melatonin to total retinal melatonin appears to be modest, it could be acting locally to regulate the physiology of the inner retinal circuitries during the light period *(Valdez et al., 2012)*.

First, RGCs form gap junction with themselves to correlate their spiking activity with those of their direct neighbors *(Völgyi, Kovács-öller, et al., 2013; Völgyi, Pan, et al., 2013)*. As described previously, RGC gap junction conductance are modulate by AC/cAMP/PKA pathway *(Völgyi, Kovács-öller, et al., 2013)*. In *Arvicanthis ansorgei*, we can speculate that daytime melatonin in RGC binds to MT_1 receptors in these cells to inhibit AC/cAMP/PKA pathway and modulate RGC-RGC gap junction conductance.

Second, melatonin can control the daily rhythms of scotopic and photopic ERG in C3H/$f^{+/+}$ mice whereas the circadian regulation of ERG is abolished in C3H/$MT_2^{-/-}$ and C3H/$MT_1^{-/-}$ *(Baba et al., 2009, 2013)*. Mice lacking melanopsin *(Opn4$^{-/-}$)* exhibit diurnal variation in the cone ERG, ie. amplitude and implicit time (time to peak) circadian rhythm *(Barnard et al., 2006)*. However, the magnitude of these diurnal differences was reduced compared to WT mice. These events inhibit the effect of optimizing photopic vision at a time of day when it is likely to be employed *(Barnard et al., 2006)*. These results suggest that ipRGCs have important function in optimizing classical visual pathways according to the time of the day *(Barnard et al., 2006)*. Authors propose that ipRGCs provide photoentrainment of retinal oscillators and that the loss of melanopsin may result in desynchronization of cellular clocks and abolition of coherent circadian signaling within the retina. We can speculate that RGCs daytime melatonin, as an output of the clock, could act as a time-giver and help synchronizing retinal signaling.

Finally, studies suggest that melatonin increases PRs degeneration of the rat retina exposed to bright light *(Wiechmann & O'Steen, 1992; Sugawara et al., 1998).* However, as described previously in *Arvicanthis ansorgei*, the daytime RGC melatonin is low and probably acts locally. In addition,

Arvicanthis retina is particularly resistant to damage from light *(Boudard et al., 2011)*. Such observations suggest that daytime melatonin level cannot increase the susceptibility of PRs to light damage in *Arvicanthis*. Melatonin could have different functions in the retina of diurnal and nocturnal mammals in order to adapt this sensory organ to the environment.

V. MELATONIN IS INVOLVED IN CELLS VIABILITY DURING AGING

V.A. In nocturnal rodent

V.A.1. Cones viability is affected by removal of MT_1 and MT_2 receptors

In mice, melatonin may increase PRs viability during aging via MT_1 and MT_2 receptors. Indeed interruption of MT_1 and MT_2 receptors reduce PRs viability by 20 % and particularly cones viability by 30 % in 18 months old mice.

The results obtained by counting PNA labeled cones (PNA stains the cones sheath matrix) demonstrated a cone loss in peripheral, middle and central retinal regions of C3H/$f^{+/+}MT_1^{-/-}$ old mice. The cone loss was significant in the peripheral and central retina of C3H/$f^{+/+}MT_2^{-/-}$ old mice. To confirm these results, immunostaining of the cones was performed with anti-red/green and -blue opsins antibodies. The red/green cones number was significantly decreased in the middle retina of C3H/$f^{+/+}MT_1^{-/-}$ and in the middle and peripheral retina of C3H/$f^{+/+}MT_2^{-/-}$ old mice. Intensity of red/green cone loss is different among the retinal regions. The number of blue cones was not significantly reduced in mice without melatonin receptors. This can be explain because of their highly asymmetric distribution and low density throughout the retina *(Peichl, 2005)*. Indeed we performed blue cones immunostaining in transversal section. The number of blue cones varies greatly between sections which result in high standard deviation.

The retinal region specificity of cone loss can be a consequence of melatonin region specific effect or a consequence of our experimental protocol. Future studies should include immunostaining of the cones with PNA and red/green, blue opsins antibodies on whole mounted retina of C3H/$f^{+/+}$, C3H/$f^{+/+}MT_1^{-/-}$ and C3H/$f^{+/+}MT_2^{-/-}$ young and old mice. PNA and red/green opsin positive cells would be counted on three randomly fields. Blue cones positive cells would be counted in 5 high density fields of blue cones covering the ventral hemisphere and the central dorsal hemisphere, and in 12 low density fields in the middle and peripheral dorsal hemispheres *(Ait-Hmyed et al., 2013)*.

V.A.2. How melatonin modulates cones viability?

V.A.2.1. AKT-FOXO1 rhythm is affected by melatonin pathway interruption

The PI3K/AKT signaling pathway plays a critical role in mediating survival signals in a wide range of neuronal cell types. AKT can block cell death machinery and regulates the expression of genes involved in cell death and survival *(Brunet et al., 2001)*. Indeed AKT can promote cell survival by phosphorylating and inhibiting the Forkhead transcription factor (FOXO) *(Brunet et al., 1999)*. This inactivates components of the apoptotic machinery and critical genes for cell death such as the *Fas ligand* (*FasL*) gene *(Brunet et al., 1999)*. Melatonin has been described to activate PI3K/AKT/FOXO

pathway via MT_1 and MT_2 receptors and the βγ dimer release from G_i or G_q protein *(Hardeland, 2009)*.

Measures of P-AKT_{Thr308}, P-AKT_{Ser473} and P-FOXO1 levels by western blotting demonstrate a circadian activation of each protein in WT mice. These result are consistent with study in chick retina showing AKT phosphorylation on Thr308 under circadian control *(Ko et al., 2009)*. The rhythms of P-AKT_{Thr308}, P-AKT_{Ser473} and P-FOXO1 are abolished in C3H/$f^{+/+}MT_1^{-/-}$ and C3H/$f^{+/+}MT_2^{-/-}$ mice suggesting that **melatonin modulates P-AKT and P-FOXO1 rhythms via MT_1 and MT_2 receptors**. As AKT/FOXO1 pathway is known to mediate survival signal we proposed that P-AKT and P-FOXO1 rhythm could be important to maintain cones survival with aging.

V.A.2.2. AKT/FOXO1 pathway is localized in PRs and the GCL

P-AKT and P-FOXO1 were localized in OS and the GCL of C3H/$f^{+/+}$ mice. Immunostaining level increases during the night. P-AKT is also detected in OS and GCL of C3H/$f^{+/+}MT_1^{-/-}$ and C3H/$f^{+/+}MT_2^{-/-}$ mice. However P-AKT level does not increase at night. P-FOXO1 is weakly detected in OS and IS of C3H/$f^{+/+}MT_1^{-/-}$ and C3H/$f^{+/+}MT_2^{-/-}$ mice with no difference between day and night. In conclusion, **AKT and FOXO1 are present in OS and the GCL and seem to exhibit different patterns between WT and C3H/$f^{+/+}MT_1^{-/-}$, C3H/$f^{+/+}MT_2^{-/-}$ mice.**

In future studies, we should quantify P-AKT and P-FOXO1 immunostaining in C3H/$f^{+/+}$, C3H/$f^{+/+}MT_1^{-/-}$ and C3H/$f^{+/+}MT_2^{-/-}$ mice to confirm different expression level between day and night.

These results are consistent with a study showing the expression of P-AKT and P-FOXO1 in OS and the GCL of C57BL/6 mice *(Jomary et al., 2006)*.

P-AKT and P-FOXO1 were shown to be localized in cones but also in rods in C3H/$f^{+/+}$ mice at night, suggesting a **role of the AKT/FOXO1 pathway in cones and rods viability**.

P-AKT and P-FOXO1 were also localized in the GCL, suggesting that **the signaling pathway may also play a role in the GCL viability.** Indeed, study demonstrated a loss of cell in the GCL of C3H/$f^{+/+}MT_1^{-/-}$ old mice compared to C3H/$f^{+/+}$ at the same age *(Baba et al., 2009) (Tosini team communication)*.

V.A.2.3. Model: melatonin modulates cones and rods viability via MT_1/MT_2 heteromers and AKT/FOXO1 pathway

C3H/$f^{+/+}MT_1^{-/-}$ and C3H/$f^{+/+}MT_2^{-/-}$ mice exhibited similar results regarding P-AKT and P-FOXO1 levels and localization. These data suggest the involvement of MT_1/MT_2 heteromers. Indeed, MT_1/MT_2 heteromer was previously localized in PRs to modulate function of these cells *(Baba et al., 2013)*.

We propose that the circadian melatonin expression modulates the rhythmic activation of the survival pathway in cones, rods and the GCL (see mechanism proposed in Chapter II Article II Figure 9 and reported in Figure 38 below). FOXO transcription factor is regulated by reversible phosphorylation and acetylation. FOXO1 acetylation impairs its DNA binding and increases AKT mediated phosphorylation of FOXO1 at Ser253 in the nucleus *(Daitoku et al., 2011)*. P-FOXO1 interacts with 14-3-3 protein in the nucleus. In this complex, 14-3-3 mediates P-FOXO1 export and retention to the cytoplasm *(Brunet et al., 2002; Daitoku et al., 2011)*.

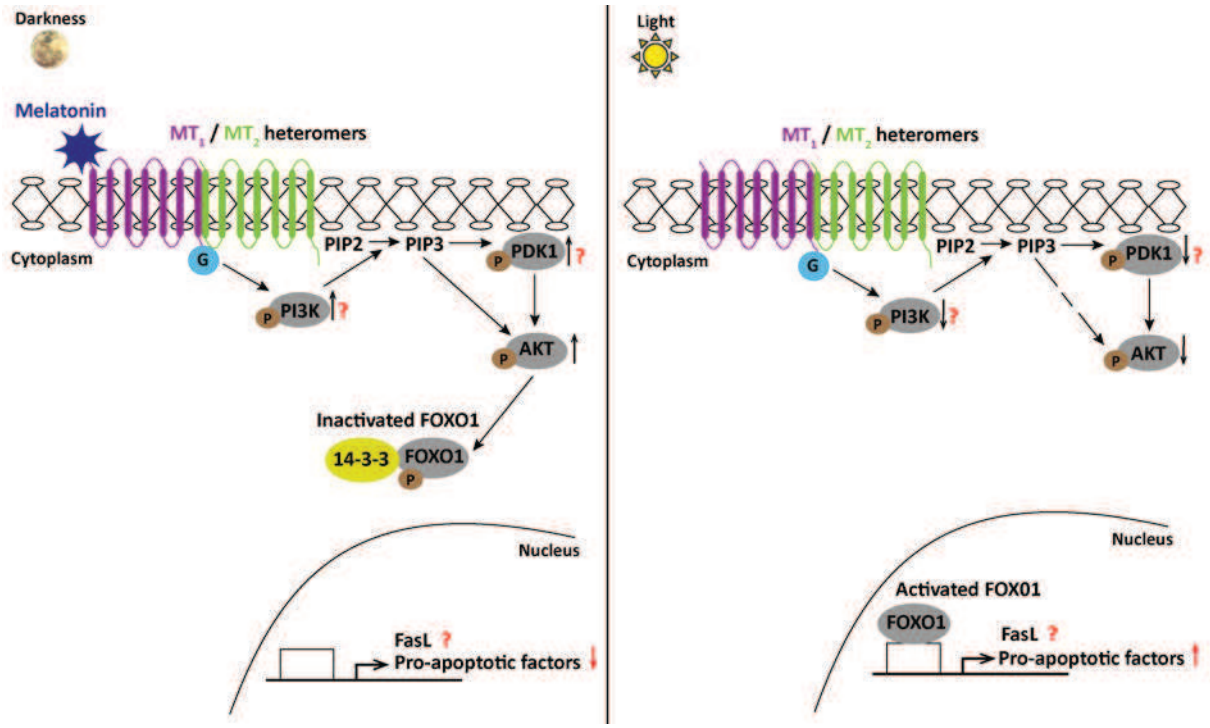

Figure 38. Mechanism by which protective action of melatonin may occur.

Diagram proposed in Chapter II. **Left panel:** during the night, melatonin binds MT_1/MT_2 heteromers and activates AKT. FOXO1 is thus phosphorylated and exported to the cytoplasm by binding to 14-3-3 protein. When FOXO1 is localized in the cytoplasm, the transcription of pro-apoptotic genes is suppressed. **Right panel:** in the absence of melatonin, signaling AKT is inactive and FOXO1 is localized in the nucleus where it activates the transcription of pro-apoptotic genes. Abbreviation: G: G protein; P: phosphorylated.

Future studies should aim to confirm the surviving pathway activation by melatonin via MT_1/MT_2 heteromers. One possible experiment is to measure the production of different components of the signaling pathway after stimulation with melatonin in cone like cells (661w) transfected with vectors containing either MT_1, MT_2 or MT_1/MT_2 receptors.

It will also be necessary to identify the death genes activated by FOXO1 in PRs. Laser micro dissection technique could be used to dissociate PR layers from others. FasL seems to be a good candidate since it was localized in PRs *(Chang et al., 2012)*. FasL by binding to its receptor Fas recruits and activates caspase 8 which in turn directly activates caspase 3 and leads to apoptosis *(Brunet et al., 2001)*. We could measure PRs mRNA levels of *FasL*, *Fas* and *Caspase 3* by quantitative-PCR.

V.A.3. Melatonin and AMD

Our study with $C3H/f^{+/+}MT_1^{-/-}$ and $C3H/f^{+/+}MT_2^{-/-}$ old mice indicate that interruption of MT_1, MT_2 signaling pathway decreases cones viability compared to $C3H/f^{+/+}$ at the same age. It is well established that the number of photoreceptors decreases with aging in human and rodent *(Curcio et al., 1993; Cunea & Jeffery, 2007)*. In addition, melatonin synthesis decreases during aging *(Pulido & Clifford, 1986; Tosini et al., 2006)*. Recent clinical data indicate that melatonin levels are significantly lower in patients affected by AMD with respect to age matched control *(Rosen et al., 2009)* suggesting a possible role of melatonin in the etiology of AMD. In addition daily rhythm of melatonin may be disrupted in AMD patients *(Schmid-Kubista et al., 2009)*. However, one study in human

patient with AMD showed mutation in 19 different genes *(The AMD Gene Consortium, 2013)* but not in MT_1 or MT_2 genes. These results suggest that MT_1 and MT_2 genes are not a direct target to cure AMD. However melatonin could be interesting in complement of other AMD treatments. Indeed melatonin appears to help protecting the retina and delay the progression of AMD *(Yi et al., 2005)*.

V.B. In diurnal rodent

Our results on the retina of *Arvicanthis ansorgei* demonstrates that melatonin is produced by cones at night. It is possible that melatonin binds to its receptors on rods in order to modulate the rhythmic activation of AKT/FOXO1 pathway in rods. This phenomenon could be important to maintain rods survival with aging.

This study also shows that RGCs express MT_1 receptor in *Arvicanthis ansorgei* retina. Furthermore, AKT and FOXO1 are present in the GCL. We can speculate that melatonin produced at night by cones binds to MT_1 receptor in RGCs to synchronize AKT/FOXO1 pathway and protect RGCs from degeneration with aging.

VI. CONCLUSION

By investigating the synthetic pathway and role of melatonin in the retina of rodent my project brings new information regarding melatonin synthesis cellular localization and function in mammals.

In the retina, melatonin appears to be produced not only in PRs but also in RGCs. Moreover melatonin regulation is different in these two production sites. Melatonin synthesis seems to display a circadian rhythm with different acrophases cell-type dependent. Indeed PR melatonin peaks at night while RGC melatonin is maximal during the day.

Melatonin circadian rhythm may modulate different phenomenon in the retina to respond to physiological need. Indeed melatonin via MT_1 and MT_2 receptors appears to synchronize the survival pathway activation in order to improve PRs and RGCs viability during the course of aging.

My work can be summarized in the diagram below.

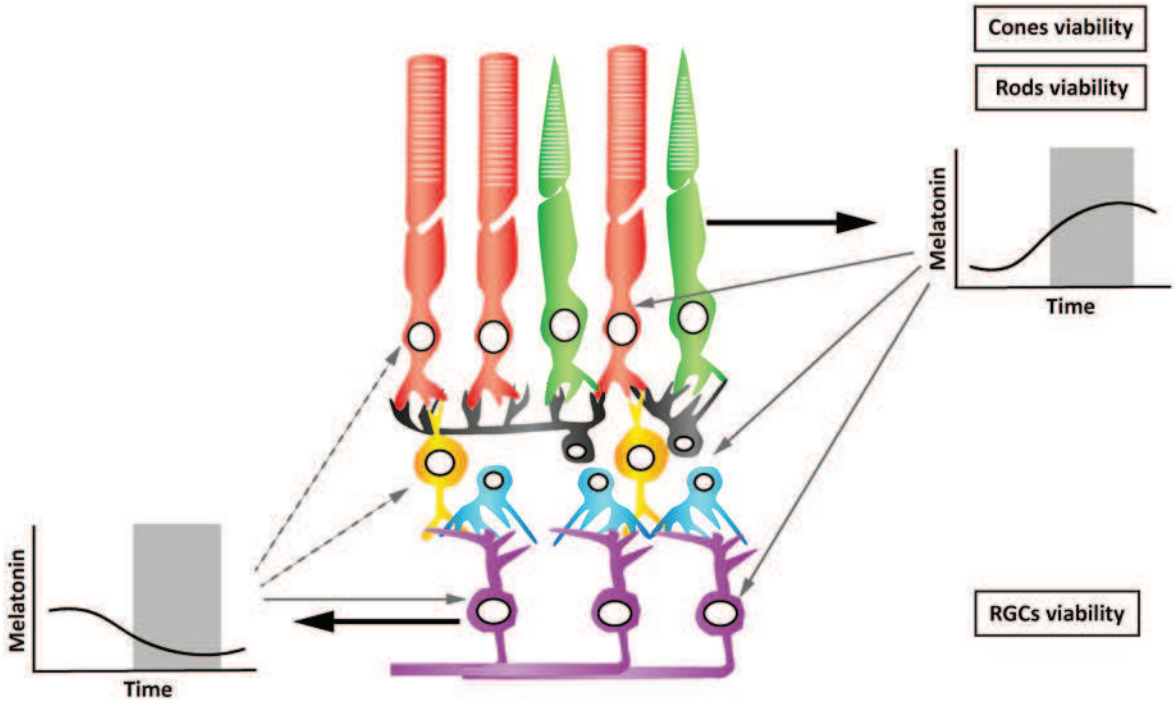

Figure 39. Summary of melatonin production and function demonstrated in my thesis.

Melatonin is produced in cones at night and can bind its receptor on photoreceptors (rods and probably cones), INL and RGCs. Melatonin may improve cones, rods and RGCs viability during the course of aging. Melatonin is also produced in RGCs where the hormone might have autocine affect as well as paracrine effect.

The regulation of melatonin synthesis as well as melatonin function might vary between species in order to adapt the retina to physiological need such as the light/dark cycle, the light intensity irradiance, food search, to avoid predators, ie. between nocturnal and diurnal/bimodal mammals.

BIBLIOGRAPHY

Ait-Hmyed, O., Felder-Schmittbuhl, M.-P., Garcia-Garrido, M., Beck, S., Seide, C., Sothilingam, V., Tanimoto, N., Seeliger, M., Bennis, M., & Hicks, D. (**2013**) Mice lacking Period 1 and Period 2 circadian clock genes exhibit blue cone photoreceptor defects. *The European journal of neuroscience*, 1–13.

Aitken, A. (**2002**) Functional specificity in 14-3-3 isoform interactions through dimer formation and phosphorylation. Chromosome location of mammalian isoforms and variants. *Plant Molecular Biology*, **50**, 993–1010.

Aitken, A. (**2006**) 14-3-3 proteins: A historic overview. *Seminars in Cancer Biology*, **16**, 162–172.

Alarma-Estrany, P., Crooke, A., Mediero, A., Peláez, T., & Pintor, J. (**2008**) Sympathetic nervous system modulates the ocular hypotensive action of MT2-melatonin receptors in normotensive rabbits. *Journal of Pineal Research*, **45**, 468–475.

Alarma-Estrany, P. & Pintor, J. (**2007**) Melatonin receptors in the eye: Location, second messengers and role in ocular physiology. *Pharmacology and Therapeutics*, **113**, 507–522.

Alcantara-Contreras, S., Baba, K., & Tosini, G. (**2011**) Removal of melatonin receptor tye 1 increases intraocular pressure and retinal ganglion cells death in the mouse. *Neuroscience letters*, **494**, 61–64.

Aschoff, J. (**1954**) Zeitgeber des tierischen Tagesperiodik. *Naturwissenschaften*, **41**, 49–56.

Axelrod, J. & Weissbach, H. (**1961**) Purification and Properties of Hydroxyindole- O-methyl Transferase. *The Journal of biological chemistry*, **236**, 211–213.

Ayoub, M.A., Levoye, A., Delagrange, P., & Jockers, R. (**2004**) Preferential formation of MT1/MT2 melatonin receptor heterodimers with distinct ligand interaction properties compared with MT2 homodimers. *Molecular pharmacology*, **66**, 312–321.

Baba, K., Benleulmi-Chaachoua, A., Journé, A.-S., Kamal, M., Guillaume, J.-L., Dussaud, S., Gbahou, F., Yettou, K., Liu, C., Contreras-Alcantara, S., Jockers, R., & Tosini, G. (**2013**) Heteromeric MT1/MT2 Melatonin Receptors Modulate Photoreceptor Function. *Science Signaling*, **6**, ra89.

Baba, K., Pozdeyev, N., Mazzoni, F., Contreras-Alcantara, S., Liu, C., Kasamatsu, M., Martinez-Merlos, T., Strettoi, E., Iuvone, P.M., & Tosini, G. (**2009**) Melatonin modulates visual function and cell viability in the mouse retina via the MT1 melatonin receptor. *Proceedings of the National Academy of Sciences of the United States of America*, **106**, 15043–15048.

Baba, K., Sengupta, A., Tosini, M., Contreras-Alcantara, S., & Tosini, G. (**2010**) Circadian regulation of the PERIOD 2::LUCIFERASE bioluminescence rhythm in the mouse retinal pigment epithelium-choroid. *Molecular vision*, **16**, 2605–2611.

Baler, R., Covington, S., & Klein, D.C. (**1997**) The Rat Arylalkylamine N -Acetyltransferase Gene Promoter. *The Journal of biological chemistry*, **272**, 6979–6985.

Barnard, A.R., Hattar, S., Hankins, M.W., & Lucas, R.J. (**2006**) Melanopsin regulates visual processing in the mouse retina. *Current Biology*, **16**, 389–395.

Barnstable, C.. (**1980**) Monoclonal antibodies which recognize different cell types in the rat retina. *Nature*, **286**, 231–235.

Bégay, V., Falcón, J., Cahill, G.M., Klein, D.C., & Coon, S.L. (**1998**) Transcripts encoding two melatonin synthesis enzymes in the teleost pineal organ: Circadian regulation in pike and zebrafish, but not in trout. *Endocrinology*, **139**, 905–912.

Belforte, N.A., Moreno, M.C., De Zavalía, N., Sande, P.H., Chianelli, M.S., Keller Sarmiento, M.I., & Rosenstein, R.E. (**2010**) Melatonin: A novel neuroprotectant for the treatment of glaucoma. *Journal of Pineal Research*, **48**, 353–364.

Bernard, M., Dinet, V., & Voisin, P. (**2001**) Transcriptional regulation of the chicken hydroxyindole-O-methyltransferase gene by the cone - Rod homeobox-containing protein. *Journal of Neurochemistry*, **79**, 248–257.

Bernard, M., Donohue, S.J., & Klein, D.C. (**1995**) Human hydroxyindole-O-methyltransferase in pineal gland, retina and Y79 retinoblastoma cells. *Brain Research*, **696**, 37–48.

Bernard, M., Guerlotte, J., Cogne, M., Greve, P., Collin, J.P., & Voisin, P. (**1993**) Transcriptional regulation of hydroxyindole O-methyltransferase in the chicken pineal gland: day/night changes and long-term effects of light and darkness. *The Biochemical journal*, **290**, 661–664.

Bernard, M., Iuvone, P.M., Cassone, V.M., Roseboom, P.H., Coon, S.L., & Klein, D.C. (**1997**) Avian melatonin synthesis: photic and circadian regulation of serotonin N-acetyltransferase mRNA in the chicken pineal gland and retina. *Journal of neurochemistry*, **68**, 213–224.

Bernard, M. & Klein, D.C. (**1996**) Retinoic acid increases hydroxyindole-O-methyltransferase

activity and mRNA in human Y-79 retinoblastoma cells. *Journal of neurochemistry*, **67**, 1032–1038.

Berson, D.M., Dunn, F. a, & Takao, M. (**2002**) Phototransduction by retinal ganglion cells that set the circadian clock. *Science (New York, N.Y.)*, **295**, 1070–1073.

Besharse, J.C. & Dunis, D.A. (**1983**) Methoxyindoles and Photoreceptors Metabolism: Activation of Rod Shedding. *Science*, **219**, 1341–1343.

Besharse, J.C. & Hollyfield, J.G. (**1979**) Turnover of mouse photoreceptor outer segments in constant light and darkness. *Investigative ophthalmology & visual science*, **18**, 1019–1024.

Besharse, J.C. & Iuvone, P.M. (**1983**) Circadian clock in Xenopus eye controlling retinal serotonin N-acetyltransferase. *Nature*, **305**, 133–135.

Besseau, L., Benyassi, A., Møller, M., Coon, S.L., Weller, J.L., Boeuf, G., Klein, D.C., & Falcón, J. (**2006**) Melatonin pathway: breaking the "high-at-night" rule in trout retina. *Experimental eye research*, **82**, 620–627.

Boatright, J.H., Rubim, N.M., & Iuvone, P.M. (**1994**) Regulation of endogenous dopamine release in amphibian retina by melatonin: the role of GABA. *Visual neuroscience*, **11**, 1013–1018.

Bobu, C., Craft, C.M., Masson-pevet, M., & Hicks, D. (**2006**) Photoreceptor organization and rhythmic phagocytosis in the Nile rat Arvicanthis ansorgei: a novel diurnal rodent model for the study of cone pathophysiology. *Investigative ophthalmology & visual science*, **47**, 3109–3118.

Bobu, C. & Hicks, D. (**2009**) Regulation of retinal photoreceptor phagocytosis in a diurnal mammal by circadian clocks and ambient lighting. *Investigative ophthalmology & visual science*, **50**, 3495–3502.

Bobu, C., Lahmam, M., Vuillez, P., Ouarour, A., & Hicks, D. (**2008**) Photoreceptor organisation and phenotypic characterization in retinas of two diurnal rodent species: potential use as experimental animal models for human vision research. *Vision research*, **48**, 424–432.

Bobu, C., Sandu, C., Laurent, V., Felder-Schmittbuhl, M.-P., & Hicks, D. (**2013**) Prolonged light exposure induces widespread phase shifting in the circadian clock and visual pigment gene expression of the Arvicanthis ansorgei retina. *Molecular Vision*, **19**, 1060–1073.

Boelen, M.K., Boelen, M.G., & Marshak, D.W. (**1998**) Light-stimulated release of dopamine from the primate retina is blocked by 1-2-amino-4-phosphonobutyric acid (APB). *Visual neuroscience*, **15**, 97–103.

Bonnefond, C., Monnerie, R., Richard, J.P., & Martinet, L. (**1993**) Melatonin and the circadian clock in mink: effects of daily injections of melatonin on circadian rhythm of locomotor activity and autoradiographic localization of melatonin binding sites. *Journal of neuroendocrinology*, **5**, 241–246.

Borjigin, J., Wang, M.M., & Snyder, S.H. (**1995**) Diurnal variation in mRNA encoding serotonin N-acetyltransferase in pineal gland. *Nature*, **378**, 783–785.

Bothorel, B., Barassin, S., Saboureau, M., Perreau, S., Vivien-Roels, B., Malan, A., & Pévet, P. (**2002**) In the rat, exogenous melatonin increases the amplitude of pineal melatonin secretion by a direct action on the circadian clock. *European Journal of Neuroscience*, **16**, 1090–1098.

Botros, H.G., Legrand, P., Pagan, C., Bondet, V., Weber, P., Ben-Abdallah, M., Lemière, N., Huguet, G., Bellalou, J., Maronde, E., Beguin, P., Haouz, A., Shepard, W., & Bourgeron, T. (**2013**) Crystal structure and functional mapping of human ASMT, the last enzyme of the melatonin synthesis pathway. *Journal of Pineal Research*, **54**, 46–57.

Bouatia-Naji, N., Bonnefond, A., Cavalcanti-Proença, C., Sparsø, T., Holmkvist, J., Marchand, M., Delplanque, J., Lobbens, S., Rocheleau, G., Durand, E., De Graeve, F., Chèvre, J.-C., Borch-Johnsen, K., Hartikainen, A.-L., Ruokonen, A., Tichet, J., Marre, M., Weill, J., Heude, B., Tauber, M., Lemaire, K., Schuit, F., Elliott, P., Jørgensen, T., Charpentier, G., Hadjadj, S., Cauchi, S., Vaxillaire, M., Sladek, R., Visvikis-Siest, S., Balkau, B., Lévy-Marchal, C., Pattou, F., Meyre, D., Blakemore, A.I.F., Jarvelin, M.-R., Walley, A.J., Hansen, T., Dina, C., Pedersen, O., & Froguel, P. (**2009**) A variant near MTNR1B is associated with increased fasting plasma glucose levels and type 2 diabetes risk. *Nature genetics*, **41**, 89–94.

Boudard, D.L., Acar, N., Bretillon, L., & Hicks, D. (**2011**) Retinas of the diurnal rodent Arvicanthis ansorgei are highly resistant to experimentally induced stress and degeneration. *Investigative Ophthalmology and Visual Science*, **52**, 8686–8700.

Brunet, A., Bonni, A., Zigmond, M.J., Lin, M.Z., Juo, P., Hu, L.S., Anderson, M.J., Arden, K.C., Blenis, J., & Greenberg, M.E. (**1999**) Akt Promotes Cell Survival by Phosphorylating and Inhibiting a Forkhead Transcription Factor. *Cell*, **96**, 857–868.

Brunet, A., Datta, S.R., & Greenberg, M.E. (**2001**) Transcription-dependent and -independent

control of neuronal survival by the PI3K – Akt signaling pathway. *Current Opinion in Neurobiology*, **11**, 297–305.

Brunet, A., Kanai, F., Stehn, J., Xu, J., Sarbassova, D., Frangioni, J. V, Dalal, S.N., DeCaprio, J. a, Greenberg, M.E., & Yaffe, M.B. (**2002**) 14-3-3 Transits To the Nucleus and Participates in Dynamic Nucleocytoplasmic Transport. *The Journal of cell biology*, **156**, 817–828.

Brydon, L., Roka, F., Petit, L., de Coppet, P., Tissot, M., Barrett, P., Morgan, P.J., Nanoff, C., Strosberg, A.D., & Jockers, R. (**1999**) Dual signaling of human Mel1a melatonin receptors via G(i2), G(i3), and G(q/11) proteins. *Molecular endocrinology (Baltimore, Md.)*, **13**, 2025–2038.

Buonfiglio, D.C., Malan, A., Sandu, C., Jaeger, C., Cipolla-Neto, J., Hicks, D., & Felder-Schmittbuhl, M.-P. (**2014**) Rat retina shows robust circadian expression of clock and clock output genes in explant culture. *Molecular vision*, **20**, 742–752.

Burke, Z., Wells, T., Carter, D., Klein, D., & Baler, R. (**1999**) Genetic targeting: The serotonin N-acetyltransferase promoter imparts circadian expression selectively in the pineal gland and retina of transgenic rats. *Journal of Neurochemistry*, **73**, 1343–1349.

Caldelas, I., Poirel, V.J., Sicard, B., Pévet, P., & Challet, E. (**2003**) Circadian profile and photic regulation of clock genes in the suprachiasmatic nucleus of a diurnal mammal Arvicanthis ansorgei. *Neuroscience*, **116**, 583–591.

Cardinali, D.P., Lynch, H.J., & Wurtman, R.J. (**1972**) Binding of melatonin to human and rat plasma proteins. *Endocrinology*, **91**, 1213–1218.

Cardinali, D.P. & Pévet, P. (**1998**) Basic aspects of melatonin action. *Sleep medicine*, **2**, 175–190.

Cardinali, D.P. & Wurtman, R.J. (**1972**) Hydroxyindole-O-methyl transferases in rat pineal, retina and harderian gland. *Endocrinology*, **91**, 247–252.

Carter-Dawson, L.D., LaVail, M.M., & Sidman, R.L. (**1979**) Differential effect of the rd mutation on rods and cones in the mouse retina. *J Comp Neurol*, **17**, 489–498.

Celebi, S., Dilsiz, N., Yilmaz, T., & Kukner, A.S. (**2002**) Effects of melatonin, vitamin E and octreotide on lipid peroxidation during ischemia-reperfusion in the guinea pig retina. *European journal of ophthalmology*, **12**, 77–83.

Challet, E., Le Maho, Y., Robin, J.P., Malan, a., & Cherel, Y. (**1995**) Involvement of corticosterone in the fasting-induced rise in protein utilization and locomotor activity. *Pharmacology Biochemistry and Behavior*, **50**, 405–412.

Challet, E., Pitrosky, B., Sicard, B., Malan, A., & Pévet, P. (**2002**) Circadian organization in a diurnal rodent, Arvicanthis ansorgei Thomas 1910: chronotypes, responses to constant lighting conditions, and photoperiodic changes. *Journal of biological rhythms*, **17**, 52–64.

Chang, Q., Peter, M.E., & Grassi, M. a (**2012**) Fas ligand-Fas signaling participates in light-induced apoptotic death in photoreceptor cells. *Investigative ophthalmology & visual science*, **53**, 3703–3716.

Chaurasia, S.S., Haque, R., Pozdeyev, N., Jackson, C.R., & Michael, P. (**2006**) Temporal coupling of cyclic AMP and Ca2+/CaM-stimulated adenylyl cyclase to the circadian clock in chick retinal photoreceptor cells. *J Neurochem*, **99**, 1142–1150.

Chen, W. & Baler, R. (**2000**) The rat arylalkylamine N-acetyltransferase E-box: Differential use in a master vs. a slave oscillator. *Molecular Brain Research*, **81**, 43–50.

Chiquet, C., Claustrat, B., Thuret, G., Brun, J., Cooper, H.M., & Denis, P. (**2006**) Melatonin Concentrations in Aqueous Humor of Glaucoma Patients. *American Journal of Ophthalmology*, **142**, 325–328.

Cicerone, C.M. (**1976**) Cones survive rods in the light-damaged eye of the albino rat. *Science (New York, N.Y.)*, **194**, 1183–1185.

Claustrat, B., Geoffriau, M., Brun, J., & Chazot, G. (**1996**) [Melatonin: from hormone to drug?]. *Pathologie-biologie*, **44**, 645–653.

Coleman, A.L., Yu, F., Ensrud, K.E., Stone, K.L., Cauley, J. a., Pedula, K.L., Hochberg, M.C., & Mangione, C.M. (**2010**) Impact of age-related macular degeneration on vision-specific quality of life: Follow-up from the 10-year and 15-year visits of the study of osteoporotic fractures. *American Journal of Ophthalmology*, **150**, 683–691.

Coleman, M.A., Garland, T.J., Marler, C.A., Newton, S.S., Swallow, J.G., & Carter, P. a (**1998**) Glucocorticoid response to forced excercise in laboratory house mice (Musdomesticus). *Physiology and Behavior*, **63**, 279–285.

Conti, A., Conconi, S., Hertens, E., Skwarlo-Sonta, K., Markowska, M., & Maestroni, G.J.M. (**2000**) Evidence for melatonin synthesis in mouse and human bone marrow cells. *Journal of Pineal Research*, **28**, 193–202.

Conti, A. & Maestroni, G.J.M. (**1996**) HPLC validation of a circadian melatonin rhythm in the pineal gland of inbred mice. *Journal of Pineal Research*, **20**, 138–144.

Contin, M.A., Verra, D.M., & Guido, M.E. (**2006**) An invertebrate-like phototransduction cascade mediates light detection in the chicken retinal ganglion cells. *The FASEB journal : official publication of the Federation of American Societies for Experimental Biology*, **20**, 2648–2650.

Coon, S.L., Del Olmo, E., Young, W.S., & Klein, D.C. (**2002**) Melatonin synthesis enzymes in Macaca mulatta: focus on arylalkylamine N-acetyltransferase (EC 2.3.1.87). *The Journal of clinical endocrinology and metabolism*, **87**, 4699–4706.

Coon, S.L., Mazuruk, K., Bernard, M., Roseboom, P.H., Klein, D.C., & Rodriguez, I.R. (**1996**) The human serotonin N-acetyltransferase (EC 2.3.1.87) gene (AANAT): structure, chromosomal localization, and tissue expression. *Genomics*, **34**, 76–84.

Coon, S.L., Roseboom, P.H., Baler, R., Weller, J.L., Namboodiri, M. a, Koonin, E. V, & Klein, D.C. (**1995**) Pineal serotonin N-acetyltransferase: expression cloning and molecular analysis. *Science (New York, N.Y.)*, **270**, 1681–1683.

Craft, C.M., Murage, J., Brown, B., & Zhan-Poe, X. (**1999**) Bovine arylalkylamine N-acetyltransferase activity correlated with mRNA expression in pineal and retina. *Molecular Brain Research*, **65**, 44–51.

Craft, C.M. & Zhan-Poe, X. (**2000**) Identification of specific histidine residues and the carboxyl terminus are essential for serotonin N-acetyltransferase enzymatic activity. *Molecular Brain Research*, **75**, 198–207.

Cuesta, M., Clesse, D., Pévet, P., & Challet, E. (**2009**) From daily behavior to hormonal and neurotransmitters rhythms: Comparison between diurnal and nocturnal rat species. *Hormones and Behavior*, **55**, 338–347.

Cunea, A. & Jeffery, G. (**2007**) The ageing photoreceptor. *Visual neuroscience*, **24**, 151–155.

Curcio, C.A., Allen, K.A., Sloan, K.R., Lerea, C.L., Hurley, J.B., Klock, I.B., & Milam, a H. (**1991**) Distribution and morphology of human cone photoreceptors stained with anti-blue opsin. *The Journal of comparative neurology*, **312**, 610–624.

Curcio, C.A., Millican, C.L., Allen, K. a., & Kalina, R.E. (**1993**) Aging of the human photoreceptor mosaic: Evidence for selective vulnerability of rods in central retina. *Investigative Ophthalmology and Visual Science*, **34**, 3278–3296.

Daitoku, H., Sakamaki, J.I., & Fukamizu, A. (**2011**) Regulation of FoxO transcription factors by acetylation and protein-protein interactions. *Biochimica et Biophysica Acta - Molecular Cell Research*, **1813**, 1954–1960.

Deguchi, T. & Axelrod, J. (**1972a**) Control of Circadian Change of Serotonin N-Acetyltransferase Activity in the Pineal Organ by the beta-adrenergic receptor. *Proceedings of the National Academy of Sciences of the United States of America*, **69**, 2547–2550.

Deguchi, T. & Axelrod, J. (**1972b**) Sensitive assay for serotonin N-Acetyltransferase activity in rat pineal. *Analytical biochemistry*, **50**, 174–179.

Devavry, S., Legros, C., Brasseur, C., Cohen, W., Guenin, S.P., Delagrange, P., Malpaux, B., Ouvry, C., Cogé, F., Nosjean, O., & Boutin, J. a. (**2012**) Molecular pharmacology of the mouse melatonin receptors MT 1 and MT 2. *European Journal of Pharmacology*, **677**, 15–21.

Di Paolo, T., Harnois, C., & Daigle, M. (**1987**) Assay of dopamine and its metabolites in human and rat retina. *Neuroscience letters*, **74**, 250–254.

Dinet, V., Ansari, N., Torres-Farfan, C., & Korf, H.W. (**2007**) Clock gene expression in the retina of melatonin-proficient (C3H) and melatonin-deficient (C57BL) mice. *Journal of Pineal Research*, **42**, 83–91.

Dinet, V., Girard-Naud, N., Voisin, P., & Bernard, M. (**2006**) Melatoninergic differentiation of retinal photoreceptors: Activation of the chicken hydroxyindole-O-methyltransferase promoter requires a homeodomain-binding element that interacts with Otx2. *Experimental Eye Research*, **83**, 276–290.

Dinet, V. & Korf, H.W. (**2007**) Impact of melatonin receptors on pCREB and clock-gene protein levels in the murine retina. *Cell and Tissue Research*, **330**, 29–34.

Djeridane, Y., Pitrosky, B., Vivien-Roels, B., Simonneaux, V., Kirsch, R., & Pévet, P. (**2000**) Long-term daily melatonin infusion induces a large increase in N-acetyltransferase activity, hydroxyindole-O-methyltransferase activity, and melatonin content in the Harderian gland and eye of pinealectomized male Siberian hamsters (Phodopus sungorus). *Journal of pineal research*, **29**, 65–73.

Djeridane, Y., Vivien-Roels, B., Simonneaux, V., Miguez, J.M., & Pévet, P. (**1998**) Evidence for melatonin synthesis in rodent Harderian gland: A dynamic in vitro study. *Journal of Pineal Research*, **25**, 54–64.

Do Carmo Buonfiglio, D., Peliciari-Garcia, R.A., do Amaral, F.G., Peres, R., Nogueira, T.C.A., Afeche, S.C., & Cipolla-Neto, J. (**2011**) Early-stage retinal melatonin synthesis impairment in streptozotocin-induced diabetic wistar rats.

Investigative ophthalmology & visual science, **52**, 7416–7422.

Do, M. & Yau, K. (**2010**) Intrinsically Photosensitive Retinal Ganglion Cells. *Physiological Reviews*, **90**, 1547–1581.

Donohue, S.J., Roseboom, P.H., Illnerova, H., Weller, J.L., & Klein, D.C. (**1993**) Human hydroxyindole-O-methyltransferase: presence of LINE-1 fragment in a cDNA clone and pineal mRNA. *DNA and cell biology*, **12**, 715–727.

Doyle, S.E., Grace, M.S., McIVOR, W., & Menaker, M. (**2002**) Circadian rhythms of dopamine in mouse retina: The role of melatonin. *Visual Neuroscience*, **19**, 593–601.

Drew, J.E., Barrett, P., Williams, L.M., Conway, S., & Morgan, P.J. (**1998**) The ovine melatonin-related receptor: Cloning and preliminary distribution and binding studies. *Journal of Neuroendocrinology*, **10**, 651–661.

Dubocovich, M.L. (**1983**) Melatonin is a potent modulator of dopamine release in the retina. *Nature*, **306**, 782–784.

Dubocovich, M.L. (**1988**) Luzindole (N-0774): A NovelMelatonin Receptor Antagonist '. *the journal of pharmacology and experimental therapeutics*, **246**, 902–910.

Dubocovich, M.L. (**1995**) Melatonin receptors: Are there multiple subtypes? *Trends in Pharmacological Sciences*, **16**, 50–56.

Dubocovich, M.L., Delagrange, P., Krause, D.N., Sugden, D., Cardinali, D.P., & Olcese, J. (**2010**) International Union of Basic and Clinical Pharmacology . LXXV . Nomenclature , Classification , and Pharmacology of G Protein-Coupled Melatonin Receptors. *Pharmacological reviews*, **62**, 343–380.

Dubocovich, M.L., Masana, M.I., Iacob, S., & Sauri, D.M. (**1997**) Melatonin receptor antagonists that differentiate between the human Mel 1a and Mel 1b recombinant subtypes are used to assess the pharmacological profile of the rabbit retina ML 1 presynaptic heteroreceptor. *Naunyn-Schmiedeberg's Archives of Pharmacology*, **355**, 365–375.

Ducroz, J.F., Volobouev, V., & Granjon, L. (**1998**) A molecular perspective on the systematics and evolution of the genus Arvicanthis (Rodentia, Muridae): inferences from complete cytochrome b gene sequences. *Molecular phylogenetics and evolution*, **10**, 104–117.

Dufourny, L., Levasseur, A., Migaud, M., Callebaut, I., Pontarotti, P., Malpaux, B., & Monget, P. (**2008**) GPR50 is the mammalian ortholog of Mel1c: evidence of rapid evolution in mammals. *BMC evolutionary biology*, **8**, 1–14.

Duncan, M.J. (**2007**) Circannual prolactin rhythms: calendar-like timer revealed in the pituitary gland. *Trends in Endocrinology and Metabolism*, **18**, 259–260.

Dyda, F., Klein, D.C., & Hickman, A.B. (**2000**) GCN5-Related N-A cetyltransferases: A Structural Overview. *Annual review of biophysics and biomolecular structure*, **29**, 81–103.

Ebihara, S., Marks, T., Hudson, D.J., & Menaker, M. (**1986**) Genetic Control of Melatonin Synthesis in the Pineal Gland of the Mouse. *Science*, **231**, 491–493.

Eskin, A. (**1979**) Identification and physiology of circadian pacemakers. Introduction. *Federation proceedings*, **38**, 2570–2572.

Faillace, M.P., Cutrera, R., Sarmiento, M.I., & Rosenstein, R.E. (**1995**) Evidence for local synthesis of melatonin in golden hamster retina. *Neuroreport*, **6**, 2093–2095.

Falcón, J. (**1999**) Cellular circadian clocks in the pineal. *Progress in Neurobiology*, **58**, 121–162.

Faria, J.A., Kinote, A., Ignacio-souza, L.M., Araújo, T.M. De, Razolli, D.S., Diego, L., Paschoal, L.B., Lellis-santos, C., Bertolini, G.L., Velloso, L.A., Bordin, S., & Anhe, G.F. (**2013**) Melatonin acts through MT1/MT2 receptors to activate hypothalamic AKT and suppress hepatic gluconeogenesis in rats. *American Journal of Physiology Endocrinology and Metabolism*, **305**, E230–E242.

Fleming, J. V., Barrett, P., Coon, S.L., Klein, D.C., & Morgan, P.J. (**1999**) Ovine arylalkylamine N-acetyltransferase in the pineal and pituitary glands: Differences in function and regulation. *Endocrinology*, **140**, 972–978.

Fontana, J.A. & Lovenberg, W. (**1971**) A cyclic AMP-dependent protein kinase of the bovine pineal gland. *Proceedings of the National Academy of Sciences of the United States of America*, **68**, 2787–2790.

Foster, R.G., Provencio, I., Hudson, D., Fiske, S., De Grip, W., & Menaker, M. (**1991**) Circadian photoreception in the retinally degenerate mouse (rd/rd). *Journal of comparative physiology. A, Sensory, neural, and behavioral physiology*, **169**, 39–50.

Foulkes, N.S. & Sassone-Corsi, P. (**1996**) Transcription factors coupled to the cAMP-signalling pathway. *Biochimica et Biophysica Acta - Reviews on Cancer*, **1288**, F101–F121.

Franze, K., Grosche, J., Skatchkov, S.N., Schinkinger, S., Foja, C., Schild, D., Uckermann, O., Travis, K., Reichenbach, A., & Guck, J. (**2007**) Muller cells are living optical fibers in the vertebrate retina. *Proceedings of the National Academy of Sciences of the United States of America*, **104**, 8287–8292.

Fu, Y. (**2010**) Phototransduction in rods and cones. *Webvision:The organization of the retina and visual system*, 1–47.

Fu, Y., Tang, M., Fan, Y., Zou, H., Sun, X., & Xu, X. (**2012**) Anti-apoptotic effects of melatonin in retinal pigment epithelial cells. *Frontiers in bioscience (Landmark edition)*, **17**, 1461–1468.

Fujieda, H., Hamadanizadeh, S. a., Wankiewicz, E., Pang, S.F., & Brown, G.M. (**1999**) Expression of mt1 melatonin receptor in rat retina: Evidence for multiple cell targets for melatonin. *Neuroscience*, **93**, 793–799.

Fujieda, H., Scher, J., Hamadanizadeh, S. a, Wankiewicz, E., Pang, S.F., & Brown, G.M. (**2000**) Dopaminergic and GABAergic amacrine cells are direct targets of melatonin: immunocytochemical study of mt1 melatonin receptor in guinea pig retina. *Visual neuroscience*, **17**, 63–70.

Fukuhara, C., Dirden, J.C., & Tosini, G. (**2001**) Photic regulation of melatonin in rat retina and the role of proteasomal proteolysis. *Neuroreport*, **12**, 3833–3837.

Fukuhara, C., Liu, C., Ivanova, T.N., Chan, G.C.-K., Storm, D.R., Iuvone, P.M., & Tosini, G. (**2004**) Gating of the cAMP signaling cascade and melatonin synthesis by the circadian clock in mammalian retina. *The Journal of neuroscience : the official journal of the Society for Neuroscience*, **24**, 1803–1811.

Gagné, A.-M., Danilenko, K. V, Rosolen, S.G., & Hébert, M. (**2009**) Impact of oral melatonin on the electroretinogram cone response. *Journal of circadian rhythms*, **7**, 1–7.

Ganguly, S., Coon, S.L., & Klein, D.C. (**2002**) Control of melatonin synthesis in the mammalian pineal gland: the critical role of serotonin acetylation. *Cell and tissue research*, **309**, 127–137.

Ganguly, S., Gastel, J. a, Weller, J.L., Schwartz, C., Jaffe, H., Namboodiri, M. a, Coon, S.L., Hickman, a B., Rollag, M., Obsil, T., Beauverger, P., Ferry, G., Boutin, J. a, & Klein, D.C. (**2001**) Role of a pineal cAMP-operated arylalkylamine N-acetyltransferase/14-3-3-binding switch in melatonin synthesis. *Proceedings of the National Academy of Sciences of the United States of America*, **98**, 8083–8088.

Ganguly, S., Weller, J.L., Ho, A., Chemineau, P., Malpaux, B., & Klein, D.C. (**2005**) Melatonin synthesis: 14-3-3-dependent activation and inhibition of arylalkylamine N-acetyltransferase mediated by phosphoserine-205. *Proceedings of the National Academy of Sciences of the United States of America*, **102**, 1222–1227.

Garbarino-Pico, E., Carpentieri, A.R., Contin, M. a, Sarmiento, M.I.K., Brocco, M. a, Panzetta, P., Rosenstein, R.E., Caputto, B.L., & Guido, M.E. (**2004**) Retinal ganglion cells are autonomous circadian oscillators synthesizing N-acetylserotonin during the day. *The Journal of biological chemistry*, **279**, 51172–51181.

García-Allegue, R., Lax, P., Madariaga, A.M., & Madrid, J.A. (**1999**) Locomotor and feeding activity rhythms in a light-entrained diurnal rodent, Octodon degus. *The American journal of physiology*, **277**, R523–R531.

García-Allegue, R., Madrid, J. a, & Sánchez-Vázquez, F.J. (**2001**) Melatonin rhythms in European sea bass plasma and eye: influence of seasonal photoperiod and water temperature. *Journal of pineal research*, **31**, 68–75.

Garidou, M.L., Bartol, I., Calgari, C., Pévet, P., & Simonneaux, V. (**2001**) In vivo observation of a non-noradrenergic regulation of arylalkylamine N-acetyltransferase gene expression in the rat pineal complex. *Neuroscience*, **105**, 721–729.

Garidou, M.-L., Gauer, F., Vivien-Roels, B., Sicard, B., Pevet, P., & Simonneaux, V. (**2002**) Pineal arylalkylamine N-acetyltransferase gene expression is highly stimulated at night in the diurnal rodent, Arvicanthis ansorgei. *European Journal of Neuroscience*, **15**, 1632–1640.

Gauer, F. & Craft, C.M. (**1996**) Circadian regulation of hydroxyindole-O-methyltransferase mRNA levels in rat pineal and retina. *Brain research*, **737**, 99–109.

Gibson, C.J. (**1988**) Diurnal alterations in retinal tyrosine level and dopamine turnover in diabetic rats. *Brain research*, **454**, 60–66.

Gillette, M.U. & Mitchell, J.W. (**2002**) Signaling in the suprachiasmatic nucleus: Selectively responsive and integrative. *Cell and Tissue Research*, **309**, 99–107.

Gómez-Corvera, A., Cerrillo, I., Molinero, P., Naranjo, M.C., Lardone, P.J., Sanchez-Hidalgo, M., Carrascosa-Salmoral, M.P., Medrano-Campillo, P., Guerrero, J.M., & Rubio, A. (**2009**) Evidence of immune system melatonin production by two pineal melatonin deficient mice, C57BL/6 and Swiss strains. *Journal of pineal research*, **47**, 15–22.

Goto, M., Oshima, I., Tomita, T., & Ebihara, S. (**1989**) Melatonin Content of the Pineal Gland in Different Mouse Strains. *Journal of Pineal Research*, **7**, 195–204.

Grace, M.S., Chiba, A., & Menaker, M. (**1999**) Circadian control of photoreceptor outer

segment membrane turnover in mice genetically incapable of melatonin synthesis. *Visual neuroscience*, **16**, 909–918.

Green, C.B. & Besharse, J.C. (**2004**) Retinal circadian clocks and control of retinal physiology. *Journal of biological rhythms*, **19**, 91–102.

Grota, L.J., Holloway, W.R., & Brown, G. (**1982**) 24-Hour Rhythm of Hypothalamic Melatonin Immunofluorescence Correlates with Serum and Retinal Melatonin Rhythms. *Neuroendocrinology*, **34**, 363–368.

Guajardo, M.H., Terrasa, A.M., & Catalá, A. (**2003**) Protective effect of indoleamines on in vitro ascorbate-Fe2+ dependent lipid peroxidation of rod outer segment membranes of bovine retina. *Journal of pineal research*, **35**, 276–282.

Guillaume, J.L., Daulat, A.M., Maurice, P., Levoye, A., Migaud, M., Brydon, L., Malpaux, B., Borg-Capra, C., & Jockers, R. (**2008**) The PDZ protein Mupp1 promotes Gi coupling and signaling of the Mt1 melatonin receptor. *Journal of Biological Chemistry*, **283**, 16762–16771.

Ha, E., Yim, S.V., Chung, J.H., Yoon, K.S., Kang, I., Yong, H.C., & Baik, H.H. (**2006**) Melatonin stimulates glucose transport via insulin receptor substrate-1/phosphatidylinositol 3-kinase pathway in C2C12 murine skeletal muscle cells. *Journal of Pineal Research*, **41**, 67–72.

Hall, F., Tengerdy, C., Morita, M., & Pautler, E. (**1985**) Determination of bovine retinal melatonin with HPLC-EC. *Current eye research*, **4**, 847–850.

Hamada, T., Ootomi, M., Horikawa, K., Niki, T., Wakamatu, H., & Ishida, N. (**1999**) The expression of the melatonin synthesis enzyme: arylalkylamine N-acetyltransferase in the suprachiasmatic nucleus of rat brain. *Biochemical and biophysical research communications*, **258**, 772–777.

Hamm, H.E. & Menaker, M. (**1980**) Retinal rhythms in chicks: circadian variation in melatonin and serotonin N-acetyltransferase activity. *Proceedings of the National Academy of Sciences of the United States of America*, **77**, 4998–5002.

Hannibal, J. (**2002**) Neurotransmitters of the retino-hypothalamic tract. *Cell and Tissue Research*, **309**, 73–88.

Hardeland R (**2005**) Antioxidative Protection by Melatonin. *Endocrine*, **27**, 119–130.

Hardeland, R. (**2009**) Melatonin: Signaling mechanisms of a pleiotropic agent. *BioFactors*, **35**, 183–192.

Herrmann, R., Heflin, S.J., Hammond, T., Lee, B., Wang, J., Gainetdinov, R.R., Caron, M.G., Eggers, E.D., Frishman, L.J., McCall, M. a., & Arshavsky, V.Y. (**2011**) Rod Vision Is Controlled by Dopamine-Dependent Sensitization of Rod Bipolar Cells by GABA. *Neuron*, **72**, 101–110.

Hickman, A.B., Klein, D.C., & Dyda, F. (**1999**) Melatonin biosynthesis: The structure of serotonin N-acetyltransferase at 2.5 A resolution suggests a catalytic mechanism. *Molecular Cell*, **3**, 23–32.

Hickman, A.B., Namboodiri, M.A., Klein, D.C., & Dyda, F. (**1999**) The structural basis of ordered substrate binding by serotonin N-acetyltransferase: enzyme complex at 1.8 A resolution with a bisubstrate analog. *Cell*, **97**, 361–369.

Hiragaki, S., Baba, K., Coulson, E., Kunst, S., Spessert, R., & Tosini, G. (**2014**) Melatonin Signaling Modulates Clock Genes Expression in the Mouse Retina. *PLoS ONE*, **9**, e106819.

Ho, A.K., Thomas, T.P., Chikll, C.L., Anderson, W.B., & Klein, D.C. (**1988**) Protein Kinase C : Subcellular Redistribution by Increased Ca2 + Influx SU. *The Journal of biological chemistry*, **263**, 9292–9297.

Huang, H., Lee, S.-C., & Yang, X.-L. (**2005**) Modulation by melatonin of glutamatergic synaptic transmission in the carp retina. *The Journal of physiology*, **569**, 857–871.

Ishida, I., Obinata, M., & Deguchi, T. (**1987**) Molecular Cloning and Nucleotide Sequence of cDNA Encoding Hydroxyindole 0-Methyltransferase of Bovine Pineal Glands *. *The Journal of biological chemistry*, **262**, 2895–2899.

Itoh, M.T., Ishizuka, B., Kudo, Y., Fusama, S., Amemiya, A., & Sumi, Y. (**1997**) Detection of melatonin and serotonin N-acetyltransferase and hydroxyindole-O-methyltransferase activities in rat ovary. *Molecular and Cellular Endocrinology*, **136**, 7–13.

Iuvone, P.M. & Besharse, J.C. (**1983**) Regulation of indoleamine N-acetyltransferase activity in the retina: effects of light and dark, protein synthesis inhibitors and cyclic nucleotide analogs. *Brain research*, **273**, 111–119.

Iuvone, P.M., Brown, A.D., Haque, R., Weller, J., Zawilska, J.B., Chaurasia, S.S., Ma, M., & Klein, D.C. (**2002**) Retinal Melatonin Production : Role of Proteasomal Proteolysis in Circadian and Photic Control of Arylalkylamine N - Acetyltransferase. *Investigative ophthalmology & visual science*, **43**, 564–572.

Iuvone, P.M. & Gan, J. (**1994**) Melatonin receptor-mediated inhibition of cyclic AMP

accumulation in chick retinal cell cultures. *Journal of neurochemistry*, **63**, 118–124.

Iuvone, P.M., Tigges, M., Stone, R. a., Lambert, S., & Laties, a. M. (**1991**) Effects of apomorphine, a dopamine receptor agonist, on ocular refraction and axial elongation in a primate model of myopia. *Investigative Ophthalmology and Visual Science*, **32**, 1674–1677.

Iuvone, P.M., Tosini, G., Pozdeyev, N., Haque, R., Klein, D.C., & Chaurasia, S.S. (**2005**) Circadian clocks, clock networks, arylalkylamine N-acetyltransferase, and melatonin in the retina. *Progress in Retinal and Eye Research*, **24**, 433–456.

Ivanova, E. a, Bechtold, D. a, Dupré, S.M., Brennand, J., Barrett, P., Luckman, S.M., & Loudon, A.S.I. (**2008**) Altered metabolism in the melatonin-related receptor (GPR50) knockout mouse. *American journal of physiology. Endocrinology and metabolism*, **294**, E176–E182.

Ivanova, T.N. & Iuvone, P.M. (**2003**) Circadian rhythm and photic control of cAMP level in chick retinal cell cultures: A mechanism for coupling the circadian oscillator to the melatonin-synthesizing enzyme, arylalkylamine N-acetyltransferase, in photoreceptor cells. *Brain Research*, **991**, 96–103.

Jackson, C.R., Chaurasia, S.S., Hwang, C.K., & Iuvone, P.M. (**2011**) Dopamine D4 receptor activation controls circadian timing of the adenylyl cyclase 1/cyclic AMP signaling system in mouse retina. *European Journal of Neuroscience*, **34**, 57–64.

Jacobs, G.H. (**1998**) A perspective on color vision in platyrrhine monkeys. *Vision Research*, **38**, 3307–3313.

Jaeger, C., Sandu, C., Mellac, K., & Hicks, D. (**2015**) Circadian organization of the rodent retina involves strongly coupled, layer-specific oscillators. *FASEB*, **29**, 1–12.

Jang, S.-W., Liu, X., Pradoldej, S., Tosini, G., Chang, Q., Iuvone, P.M., & Ye, K. (**2010**) N-acetylserotonin activates TrkB receptor in a circadian rhythm. *Proceedings of the National Academy of Sciences of the United States of America*, **107**, 3876–3881.

Jeon, C.J., Strettoi, E., & Masland, R.H. (**1998**) The major cell populations of the mouse retina. *The Journal of neuroscience : the official journal of the Society for Neuroscience*, **18**, 8936–8946.

Jiang, T., Chang, Q., Zhao, Z., Yan, S., Wang, L., Cai, J., & Xu, G. (2012) Melatonin-Mediated Cytoprotection against Hyperglycemic Injury in Müller Cells. *PLoS ONE*, **7**, 1–8.

Jiménez, A.-J., Garcia-Fernandez, J.-M., González, B., & Foster, R.G. (**1996**) The spatio-temporal pattern of photoreceptor degeneration in the aged rd / rd mouse retina. *Cell and Tissue Research*, **284**, 193–202.

Jin, X., Gall, C. Von, Pieschl, R.L., Gribkoff, V.K., Stehle, J.H., Reppert, S.M., & Weaver, D.R. (**2003**) Targeted Disruption of the Mouse Mel 1b Melatonin Receptor. *molecular and cellular biology*, **23**, 1054–1060.

Jin, X., Shearman, L.P., Weaver, D.R., Zylka, M.J., Vries, G.J. De, & Reppert, S.M. (**1999**) A molecular mechanism regulating rhythmic output from the Suprachiasmatic Circadian Clock. *Cell*, **96**, 57–68.

Jockers, R., Petit, L., Lacroix, I., Coppet, P. De, Barrett, P., Morgan, P.J., Guardiola, B., Delagrange, P., Marullo, S., & Strosberg, a D. (**1997**) Novel Isoforms of Mel 1c Melatonin Receptors intracellular Cyclic Guanosine3',5' - Monophosphate Levels. *Molecular Endocrinology*, **11**, 1070–1081.

Jomary, C., Cullen, J., & Jones, S.E. (**2006**) Inactivation of the Akt survival pathway during photoreceptor apoptosis in the retinal degeneration mouse. *Investigative ophthalmology & visual science*, **47**, 1620–1629.

Kappers, J.A. (**1960**) The development, topographical relations and innervation of the epiphysis cerebri in the albino rat. *Zeitschrift fur Zellforschung und mikroskopische Anatomie (Vienna, Austria : 1948)*, **52**, 163–215.

Karin, M. & Smeal, T. (**1992**) Control of transcription factors by signal transduction pathways: the beginning of the end. *Trends in biochemical sciences*, **17**, 418–422.

Karsch, F.J., Malpaux, B., Wayne, N.L., & Robinson, J.E. (**1988**) Characteristics of the melatonin signal that provide the photoperiodic code for timing seasonal reproduction in the ewe. *reproduction nutrition development*, **28**, 459–472.

Kasahara, T., Abe, K., Mekada, K., Yoshiki, A., & Kato, T. (**2010**) Genetic variation of melatonin productivity in laboratory mice under domestication. *Proceedings of the National Academy of Sciences of the United States of America*, **107**, 6412–6417.

Katona, C. & Smale, L. (**1997**) Wheel-running rhythms in Arvicanthis niloticus. *Physiology & behavior*, **61**, 365–372.

Kennaway, D.J., Voultsios, a, Varcoe, T.J., & Moyer, R.W. (**2002**) Melatonin in mice: rhythms,

response to light, adrenergic stimulation, and metabolism. *American journal of physiology. Regulatory, integrative and comparative physiology*, **282**, R358–R365.

Klein, D.C. (**2004**) The 2004 Aschoff/Pittendrigh lecture: Theory of the origin of the pineal gland--a tale of conflict and resolution. *Journal of biological rhythms*, **19**, 264–279.

Klein, D.C., Coon, S.L., Roseboom, P.H., Weller, J.L., Bernard, M., Gastel, J.A., Zatz, M., Iuvone, P.M., Rodriguez, I.R., Bégay, V., Falcon, J., Cahill, G.M., Cassone, V.M., & Baler, R. (**1997**) The melatonin rhythm-generating enzyme: molecular regulation of serotonin N-acetyltransferase in the pineal gland. *Recent progress in hormone research*, **52**, 307–357.

Klein, D.C., Ganguly, S., Coon, S., Weller, J.L., Obsil, T., Hickman, a, & Dyda, F. (**2002**) 14-3-3 Proteins and photoneuroendocrine transduction: role in controlling the daily rhythm in melatonin. *Biochemical Society transactions*, **30**, 365–373.

Klein, D.C., Roseboom, P.H., & Coon, S.L. (**1996**) New light is shining on the melatonin rhythm enzyme the first postcloning view. *Trends in Endocrinology and Metabolism*, **7**, 106–112.

Klein, D.C. & Weller, J.L. (**1970**) Indole metabolism in the pineal gland: a circadian rhythm in N-acetyltransferase. *Science (New York, N.Y.)*, **169**, 1093–1095.

Ko, M.L., Jian, K., Shi, L., & Ko, G.Y.-P. (**2009**) Phosphatidylinositol 3 kinase-Akt signaling serves as a circadian output in the retina. *Journal of Neurochemistry*, **108**, 1607–1620.

Kolb, H. (**2005**) Simple Anatomy of the Retina. *Webvision: the organization of the retina and visual system*, 1–26.

Konturek, S.J., Konturek, P.C., & Brzozowski, T. (**2006**) Melatonin in gastroprotection against stress-induced acute gastric lesions and in headling of chronic gastric ulcers. *Journal of Physiology and Pharmacology*, **57**, 51–66.

Kuwano, R., Iwanaga, T., Nakajima, T., Masuda, T., & Takahashi, Y. (**1983**) Immunocytochemical demonstration of hydroxyindole O-methyltransferase (HIOMT), neuron-specific enolase (NSE) and S-100 protein in the bovine pineal gland. *Brain research*, **274**, 171–175.

La Cour, M. & Ehinger, B. (**2005**) *The Biology of the Eye*, Advances in Organ Biology. Elsevier.

Larsen, P.J., Enquist, L.W., & Card, J.P. (**1998**) Characterization of the multisynaptic neuronal control of the rat pineal gland using viral transneuronal tracing. *European Journal of Neuroscience*, **10**, 128–145.

LaVail, M.M. (**1976**) Rod outer segment disk shedding in rat retina: relationship to cyclic lighting. *Science (New York, N.Y.)*, **194**, 1071–1074.

Legros, C., Devavry, S., Caignard, S., Tessier, C., Delagrange, P., Ouvry, C., Boutin, J. a., & Nosjean, O. (**2014**) Melatonin MT1 and MT2 receptors display different molecular pharmacologies only in the G-protein coupled state. *British Journal of Pharmacology*, **171**, 186–201.

Lem, J., Flannery, J.G., Li, T., Applebury, M.L., Farber, D.B., & Simon, M.I. (**1992**) Retinal degeneration is rescued in transgenic rd mice by expression of the cGMP phosphodiesterase beta subunit. *Proceedings of the National Academy of Sciences of the United States of America*, **89**, 4422–4426.

Lerner, A.B., Case, J.D., & Takahashi, Y. (**1960**) Isolation of melatonin and 5-Methoxyindole-3-acetic acid from bovine pineal gland. *The journal of biolo*, **235**, 1992–1997.

Levoye, A., Dam, J., Ayoub, M. a, Guillaume, J.-L., Couturier, C., Delagrange, P., & Jockers, R. (**2006**) The orphan GPR50 receptor specifically inhibits MT1 melatonin receptor function through heterodimerization. *The EMBO journal*, **25**, 3012–3023.

Li, G., Anderson, R.E., Tomita, H., Adler, R., Liu, X., Zack, D.J., & Rajala, R.V.S. (**2007**) Nonredundant role of Akt2 for neuroprotection of rod photoreceptor cells from light-induced cell death. *The Journal of neuroscience : the official journal of the Society for Neuroscience*, **27**, 203–211.

Li, X., Chen, S., Wang, Q., Zack, D.J., Snyder, S.H., & Borjigin, J. (**1998**) A pineal regulatory element (PIRE) mediates transactivation by the pineal/retina-specific transcription factor CRX. *Proceedings of the National Academy of Sciences of the United States of America*, **95**, 1876–1881.

Liang, F.Q., Aleman, T.S., ZaixinYang, Cideciyan, A. V, Jacobson, S.G., & Bennett, J. (**2001**) Melatonin delays photoreceptor degeneration in the rds/rds mouse. *Neuroreport*, **12**, 1011–1014.

Liang, F.-Q., Green, L., Wang, C., Alssadi, R., & Godley, B.F. (**2004**) Melatonin protects human retinal pigment epithelial (RPE) cells against oxidative stress. *Experimental eye research*, **78**, 1069–1075.

Liu, C., Fukuhara, C., Wessel, J.H., Iuvone, P.M., & Tosini, G. (**2004**) Localization of Aa-nat mRNA in the rat retina by fluorescence in situ hybridization and laser capture microdissection. *Cell and tissue research*, **315**, 197–201.

Liu, C., Weaver, D.R., Jin, X., Shearman, L.P., Pieschl, R.L., Gribkoff, V.K., & Reppert, S.M. (**1997**) Molecular dissection of two distinct actions of melatonin on the suprachiasmatic circadian clock. *Neuron*, **19**, 91–102.

Liu, X., Zhang, Z., & Ribelayga, C.P. (**2012**) Heterogeneous expression of the core circadian clock proteins among neuronal cell types in mouse retina. *PloS one*, **7**, e50602.

Lowry, O.H., Rosebrough, N.J., Lewis Farr, A., & Randall, R.J. (**1951**) Protein measurement with the folin phenol reagent. *Journal of Biological Chemistry*, **193**, 265–275.

Lu, J., Zoran, M.J., & Cassone, V.M. (**1995**) Daily and circadian variation in the electroretinogram of the domestic fowl: effects of melatonin. *Journal of comparative physiology. A, Sensory, neural, and behavioral physiology*, **177**, 299–306.

Lukáts, Á., Szabó, A., Röhlich, P., Vígh, B., & Szél, Á. (**2005**) Photopigment coexpression in mammals: Comparative and developmental aspects. *Histology and Histopathology*, **20**, 551–574.

Lundmark, P.O., Pandi-Perumal, S.R., Srinivasan, V., Cardinali, D.P., & Rosenstein, R.E. (**2007**) Melatonin in the eye: implications for glaucoma. *Experimental eye research*, **84**, 1021–1030.

Ma, X., Chen, C., Krausz, K.W., Idle, J.R., & Gonzalez, F.J. (**2008**) A metabolomic perspective of melatonin metabolism in the mouse. *Endocrinology*, **149**, 1869–1879.

Malpaux, B., Thiéry, J.C., & Chemineau, P. (**1999**) Melatonin and the seasonal control of reproduction. *Reproduction, nutrition, development*, **39**, 355–366.

Marchiafava, P.L. & Longoni, B. (**1999**) Melatonin as an antioxidant in retinal photoreceptors. *Journal of pineal research*, **26**, 184–189.

Maronde, E., Saade, A., Ackermann, K., Goubran-Botros, H., Pagan, C., Bux, R., Bourgeron, T., Dehghani, F., & Stehle, J.H. (**2011**) Dynamics in enzymatic protein complexes offer a novel principle for the regulation of melatonin synthesis in the human pineal gland. *Journal of pineal research*, **51**, 145–155.

Martin, M.T., Azpiroz, F., & Malagelada, J.R. (**1998**) Melatonin and the gastrointestinal tract. *Therapie*, **53**, 453–458.

Martin, X.D., Malina, H.Z., Brennan, M.C., Hendrickson, P.H., & Lichter, P.R. (**1992**) The ciliary body--the third organ found to synthesize indoleamines in humans. *European journal of ophthalmology*, **2**, 67–72.

Masana, M.I., Doolen, S., Ersahin, C., Al-Ghoul, W.M., Duckles, S.P., Dubocovich, M.L., & Krause, D.N. (**2002**) MT(2) melatonin receptors are present and functional in rat caudal artery. *The Journal of pharmacology and experimental therapeutics*, **302**, 1295–1302.

Masri, H., Goureau, O., Hecquet, C., Simon, A., & Nguyen-Legros, J. (**1996**) [Dopamine slows phagocytosis of rods from bovine pigment epithelium in vitro trough D1 receptor]. *Comptes rendus de l'Academie des sciences. Serie III, Sciences de la vie*, **319**, 687–691.

Maurice, P., Daulat, A.M., Turecek, R., Ivankova-Susankova, K., Zamponi, F., Kamal, M., Clement, N., Guillaume, J.-L., Bettler, B., Galès, C., Delagrange, P., & Jockers, R. (**2010**) Molecular organization and dynamics of the melatonin MT_1 receptor/RGS20/G(i) protein complex reveal asymmetry of receptor dimers for RGS and G(i) coupling. *The EMBO journal*, **29**, 3646–3659.

McArthur, A.J., Gillette, M.U., & Prosser, R.A. (**1991**) Melatonin directly resets the rat suprachiasmatic circadian clock in vitro. *Brain research*, **565**, 158–161.

McGoogan, J.M. & Cassone, V.M. (**1999**) Circadian regulation of chick electroretinogram: effects of pinealectomy and exogenous melatonin. *The American journal of physiology*, **277**, R1418–R1427.

McMahon, D.G., Iuvone, P.M., & Tosini, G. (**2014**) Circadian organization of the mammalian retina: from gene regulation to physiology and diseases. *Progress in retinal and eye research*, **39**, 58–76.

Melamed, E., Frucht, Y., Lemor, M., Uzzan, a, & Rosenthal, Y. (**1984**) Dopamine turnover in rat retina: a 24-hour light-dependent rhythm. *Brain research*, **305**, 148–151.

Menendez-Pelaez, A. & Reiter, R.J. (**1993**) Distribution of melatonin in mammalian tissues: the relative importance of nuclear versus cytosolic localization. *Journal of pineal research*, **15**, 59–69.

Meyer, P., Pache, M., Loeffler, K.U., Brydon, L., Jockers, R., Flammer, J., Wirz-Justice, a, & Savaskan, E. (**2002**) Melatonin MT-1-receptor immunoreactivity in the human eye. *The British journal of ophthalmology*, **86**, 1053–1057.

Modis, Y. & Wierenga, R. (**1998**) Two crystal structures of N-acetyltransferases reveal a new fold for CoA-dependent enzymes. *Structure (London, England : 1993)*, **6**, 1345–1350.

Møller, M. & Baeres, F.M. (**2002**) The anatomy and innervation of the mammalian pineal gland. *Cell and Tissue Research*, **309**, 139–150.

Morton, D.J. (**1986**) Methoxyindole production by the pineal gland appears to be dependent on the concentration of hydroxy precursors and their affinity for hydroxyindole-O-methyltransferase. *Journal of Endocrinology*, **111**, 133–136.

Morton, D.J. (**1987**) Hydroxyindole-O-methyltransferase catalyses production of methoxyindoles in rat pineal gland dependent on the concentration of hydroxy precursors and their affinity for the enzyme. *The Journal of endocrinology*, **115**, 455–458.

Nader, N., Chrousos, G. p, & Kino, T. (**2012**) Interactions of the circadian CLOCK system and the HPA axis. *Trends in Endocrinology and Metabolism*, **21**, 277–286.

Nakane, M., Yokoyama, E., & Deguchi, T. (**1983**) Species heterogeneity of pineal hydroxyindole-O-methyltransferase. *Journal of neurochemistry*, **40**, 790–796.

Namboodiri, M. a, Nakai, C., & Klein, D.C. (**1979**) Effects of selected treatments on stability and activity of pineal serotonin N-acetyltransferase. *Journal of neurochemistry*, **33**, 807–810.

Nash, M.S. & Osborne, N.N. (**1995**) Pertussis Toxin-Sensitive Melatonin Receptors Negatively Coupled to Adenylate Cyclase Associated With Cultured Human and Rat Retinal Pigment Epithelial Cells. *Investigative ophthalmology & visual science*, **36**, 95–102.

Natesan, A.K. & Cassone, V.M. (**2002**) Melatonin receptor mRNA localization and rhythmicity in the retina of the domestic chick, Gallus domesticus. *Visual neuroscience*, **19**, 265–274.

Nathans, J., Thomas, D., & Hogness, D.S. (**1986**) Molecular Genetics of Human Color Vision: The Genes Encoding Blue, Green, and Red Pigments. *Science*, **232**, 193–202.

Nguyen-legros, J., Chanut, E., Versaux-botteri, C., Simon, A., & Trouvin, J. (**1996**) Dopamine Inhibits Melatonin Synthesis in Photoreceptor Cells Through a D -Like Receptor Subtype in the Rat Retina : Biochemical and Histochemical Evidence. *Journal of neurochemistry*, **67**, 2514–2520.

Niki, T., Hamada, T., Ohtomi, M., Sakamoto, K., Suzuki, S., Kako, K., Hosoya, Y., Horikawa, K., & Ishida, N. (**1998**) The Localization of the Site of Arylalkylamine N -Acetyltransferase Circadian Expression in the Photoreceptor Cells of Mammalian Retina. *Biochemical and biophysical research communications*, **248**, 115–120.

Nir, I., Haque, R., & Iuvone, P.M. (**2000**) Diurnal metabolism of dopamine in dystrophic retinas of homozygous and heterozygous retinal degeneration slow (rds) mice. *Brain Research*, **884**, 13–22.

Nosjean, O., Ferro, M., Cogé, F., Beauverger, P., Henlin, J.M., Lefoulon, F., Fauche, J.L., Delagrange, P., Canet, E., & Boutin, J. a. (**2000**) Identification of the melatonin-binding site MT3 as the quinone reductase 2. *Journal of Biological Chemistry*, **275**, 31311–31317.

Nowak, J.Z., Szymańska, B., Zawilska, J.B., & Białek, B. (**1993**) Hydroxyindole-O-methyltransferase activity in ocular and brain structures of rabbit and hen. *Journal of pineal research*, **15**, 35–42.

Nowak, J.Z. & Zurawska, E. (**1989**) Dopamine in the rabbit retina and striatum: diurnal rhythm and effect of light stimulation. *Journal of neural transmission*, **75**, 201–212.

Nowak, J.Z., Zurawska, E., & Zawilska, J. (**1989**) Melatonin and its generating system in vertebrate retina: circadian rhythm, effect of environmental lighting and interaction with dopamine. *Neurochemistry international*, **14**, 397–406.

Ogilvie, J.M. & Speck, J.D. (**2002**) Dopamine has a critical role in photoreceptor degeneration in the rd mouse. *Neurobiology of disease*, **10**, 33–40.

Olcese, J. & Møller, M. (**1989**) Characterization of serotonin N-acetyltransferase activity in the retina of the Mongolian gerbil, Meriones unguiculates. *Neuroscience letters*, **102**, 235–240.

Osborne, N.N., Nash, M.S., & Wood, J.P. (**1998**) Melatonin counteracts ischemia-induced apoptosis in human retinal pigment epithelial cells. *Investigative ophthalmology & visual science*, **39**, 2374–2383.

Pang, S.F., Yu, H.S., Suen, H.C., & Brown, G.M. (**1980**) Melatonin in the retina of rats: a diurnal rhythm. *J.Endocr*, **87**, 89–93.

Parfitt, A., Weller, J.L., Klein, D.C., Sakai, K.K., & Marks, B.H. (**1975**) Blockade by ouabain or elevated potassium ion concentration of the adrenergic and adenosine cyclic 3',5'-monophosphate-induced stimulation of pineal serotonin N-acetyltransferase activity. *Molecular pharmacology*, **11**, 241–255.

Park, S.-W., Lee, H.-S., Sung, M.-S., & Kim, S.-J. (**2012**) The effect of melatonin on retinal ganglion cell survival in ischemic retina. *Chonnam medical journal*, **48**, 116–122.

Peichl, L. (**2005**) Diversity of mammalian photoreceptor properties: Adaptations to habitat and lifestyle? *Anatomical Record - Part A Discoveries in Molecular, Cellular, and Evolutionary Biology*, **287**, 1001–1012.

Petit, L., Lacroix, I., Coppet, P. De, Strosberg, a D., & Jockers, R. (**1999**) Differential Signaling of Human Mel1a and Mel1b Melatonin Receptors through the Cyclic Guanosine 3'-5 '-Monophosphate Pathway. *Biochemical pharmacology*, **58**, 633–639.

Pévet, P., Agez, L., Bothorel, B., Saboureau, M., Gauer, F., Laurent, V., & Masson-Pévet, M. (**2006**) Melatonin in the multi-oscillatory mammalian circadian world. *Chronobiology international*, **23**, 39–51.

Pévet, P., Balemans, M.G.., Legerstee, W.C., & Vivien-Roels, B. (**1980**) Circadian Rhythmicity of the Activity of Hydroxyindole-O-Methyl Transferase (HIOMT) in the Formation of Melatonin and 5-Methoxytryptophol in the Pineal, Retina and Harderian Gland of the Golden Hamster. *Journal of neural transmission*, **49**, 229–245.

Pevet, P. & Challet, E. (**2011**) Melatonin: Both master clock output and internal time-giver in the circadian clocks network. *Journal of Physiology Paris*, **105**, 170–182.

Ping, Y., Huang, H., Zhang, X.-J., & Yang, X.-L. (**2008**) Melatonin potentiates rod signals to ON type bipolar cells in fish retina. *The Journal of physiology*, **586**, 2683–2694.

Pintor, J., Martin, L., Pelaez, T., Hoyle, C., & Peral, A. (**2001**) Involvement of melatonin MT 3 receptors in the regulation of intraocular pressure in rabbits. *European Journal of Pharmacology*, **416**, 251–254.

Pitrosky, B., Masson-Pevet, M., Kirsch, R., Vivien-Roels, B., Canguilhem, B., & Pévet, P. (**1991**) Effects of different doses and durations of melatonin infusions on plasma melatonin concentrations in pinealectomized Syrian hamsters: consequences at the level of sexual activity. *Journal of pineal research*, **11**, 149–155.

Pittendrigh, C.S. (**1960**) Circadian rhythms and the circadian organization of living systems. *Cold Spring Harbor symposia on quantitative biology*, **25**, 159–184.

Poché, R.A., Furuta, Y., Chaboissier, M.C., Schedl, A., & Behringer, R.R. (**2008**) Sox9 is expressed in mouse multipotent retinal progenitor cells and functions in Müller Glial cell development. *Journal of Comparative Neurology*, **510**, 237–250.

Popova, E. (**2014**) Role of dopamine in distal retina. *Journal of comparative physiology. A, Neuroethology, sensory, neural, and behavioral physiology*, **200**, 333–358.

Pozdeyev, N., Taylor, C., Haque, R., Chaurasia, S.S., Visser, A., Thazyeen, A., Du, Y., Fu, H., Weller, J., Klein, D.C., & Iuvone, P.M. (**2006**) Photic regulation of arylalkylamine N-acetyltransferase binding to 14-3-3 proteins in retinal photoreceptor cells. *The Journal of neuroscience : the official journal of the Society for Neuroscience*, **26**, 9153–9161.

Pozdeyev, N., Tosini, G., Li, L., Ali, F., Rozov, S., Rehwa, H., & Iuvone, P.M. (**2008**) Dopamine modulates diurnal and circadian rhythms of protein phosphorylation in photoreceptor cells of mouse retina. *European Journal of Neuroscience*, **27**, 2691–2700.

Pozdeyev, N. V & Lavrikova, E. V (**2000**) Diurnal changes of tyrosine, dopamine, and dopamine metabolites content in the retina of rats maintained at different lighting conditions. *Journal of molecular neuroscience : MN*, **15**, 1–9.

Privat, K., Ravault, J.-P., Chesneau, D., & M, F. (**1999**) Day / night variation of tryptophan hydroxylase and serotonin N-acetyltransferase mRNA levels in the ovine pineal gland and retina. *Journal of Pineal Research Pineal Research*, **26**, 193–203.

Pulido, O. & Clifford, J. (**1986**) Age associated changes in the circadian rhythm of retinal N-acetylserotonin and melatonin in rats with pigmented eyes. *Experimental Gerontology,* **21**, 23–30.

Rada, J.A.S. & Wiechmann, A.F. (**2006**) Melatonin receptors in chick ocular tissues: implications for a role of melatonin in ocular growth regulation. *Investigative ophthalmology & visual science*, **47**, 25–33.

Redman, J., Armstrong, S., & Ng, K.T. (**1983**) Free-running activity rhythms in the rat: entrainment by melatonin. *Science (New York, N.Y.)*, **219**, 1089–1091.

Refinetti, R. & Menaker, M. (**1992**) The Circadian Rhythm of Body Temperature. *Physiology & behavior*, **51**, 613–637.

Reiter, C.E.N., Sandirasegarane, L., Wolpert, E.B., Klinger, M., Simpson, I.A., Barber, A.J., Antonetti, D.A., Kester, M., Gardner, T.W., & Chad, E.N. (**2003**) Characterization of insulin signaling in rat retina in vivo and ex vivo.

Reiter, J., Richardson, B.A., Matthews, S.A., Lane, S.J., & Ferguson, B.N. (**1983**) Rhythms in immunoreactive melatonin in the retina and hardarian gland of rats: persistence after pinealectomy. *Life Sciences*, **32**, 1229–1236.

Reppert, S.M. (**1997**) Melatonin receptors: molecular biology of a new family of G protein-coupled receptors. *Journal of biological rhythms*, **12**, 528–531.

Reppert, S.M., Godson, C., Mahle, C.D., Weaver, D.R., Slaugenhaupt, S. a, & Gusella, J.F. **(1995)** Molecular characterization of a second

melatonin receptor expressed in human retina and brain: the Mel1b melatonin receptor. *Proceedings of the National Academy of Sciences of the United States of America*, **92**, 8734–8738.

Reppert, S.M. & Sagar, S.M. (**1983**) Characterization of the day-night variation of retinal melatonin content in the chick. *Investigative Ophthalmology and Visual Science*, **24**, 294–300.

Reppert, S.M. & Weaver, D.R. (**1995**) Melatonin madness. *Cell*, **83**, 1059–1062.

Reppert, S.M., Weaver, D.R., & Ebisawa, T. (**1994**) Cloning and characterization of a mamalian melatonin receptor that mediates reproductive and circadian responses. *Neuron*, **13**, 1177–1185.

Reppert, S.M., Weaver, D.R., Ebisawa, T., Mahle, C.D., & Kolakowski, L.F. (**1996**) Cloning of a melatonin-related receptor from human pituitary. *FEBS Letters*, **386**, 219–224.

Ribelayga, C., Cao, Y., & Mangel, S.C. (**2008**) The circadian clock in the retina controls rod-cone coupling. *Neuron*, **59**, 790–801.

Ribelayga, C., Garidou, M.L., Malan, a, Gauer, F., Calgari, C., Pévet, P., & Simonneaux, V. (**1999**) Photoperiodic control of the rat pineal arylalkylamine-N-acetyltransferase and hydroxyindole-O-methyltransferase gene expression and its effect on melatonin synthesis. *Journal of biological rhythms*, **14**, 105–115.

Ribelayga, C., Gauer, F., Calgari, C., Pevet, P., & Simonneaux, V. (**1999**) Photoneural Regulation of Rat Pineal Hydroxyindole- O -Methyltransferase (HIOMT) Messenger Ribonucleic Acid Expression : An Analysis of Its Complex Relationship with HIOMT Activity *. *Endocrinology*, **140**.

Ribelayga, C. & Mangel, S.C. (**2010**) Identification of a circadian clock-controlled neural pathway in the rabbit retina. *PLoS ONE*, **5**, e11020.

Ribelayga, C., Pevet, P., & Simonneaux, V. (**1997**) Adrenergic and peptidergic regulations of hydroxyindole- O -methyltransferase activity in rat pineal gland. *Brain Research*, **777**, 247–250.

Ribelayga, C., Pévet, P., & Simonneaux, V. (**1998**) Possible involvement of neuropeptide Y in the seasonal control of hydroxyindole-O-methyltransferase activity in the pineal gland of the European hamster (Cricetus cricetus). *Brain Research*, **801**, 137–142.

Ribelayga, C., Wang, Y., & Mangel, S.C. (**2004**) A circadian clock in the fish retina regulates dopamine release via activation of melatonin receptors. *The Journal of physiology*, **554**, 467–482.

Roca, A.L., Godson, C., Weaver, D.R., & Reppert, S.M. (**1996**) Structure, characterization, and expression of the gene encoding the mouse Mel1a melatonin receptor. *Endocrinology*, **137**, 3469–3477.

Rodieck, B.Y.R.W. & Rushton, W.A.H. (**1976**) Cancellation of rods signals by cones, and cone signals by rods in the cat retina. *The Journal of physiology*, **254**, 775–785.

Rodriguez, I.., Mazuruk, K., Schoen, T.., & Chader, G.. (**1994**) Structural analysis of the human hydroxyindole-O-methyltransferase gene. *The Journal of biological chemistry*, **269**, 31969–31977.

Röhlich, P., Van Veen, T., & Szél, Á. (**1994**) Two different visual pigments in one retinal cone cell. *Neuron*, **13**, 1159–1166.

Roseboom, P.H., Coon, S.L., Baler, R., McCune, S.K., Weller, J.L., & Klein, D.C. (**1996**) Melatonin synthesis: analysis of the more than 150-fold nocturnal increase in serotonin N-acetyltransferase messenger ribonucleic acid in the rat pineal gland. *Endocrinology*, **137**, 3033–3045.

Roseboom, P.H., Namboodiri, M.A., Zimonjic, D.B., Popescu, N.C., Rodriguez, I.R., Gastel, J.A., & Klein, D.C. (**1998**) Natural melatonin " knockdown " in C57BL/6J mice : rare mechanism truncates serotonin N-acetyltransferase. *Molecular Brain Research*, **63**, 189–197.

Rosen, R., Hu, D., Perez, V., Tai, K., Yu, G., Chen, M., Tone, P., Mccormick, S.A., & Walsh, J. (**2009**) Urinary 6-sulfatoxymelatonin level in age-related macular degeneration patients. *Molecular vision*, **15**, 1673–1679.

Ruan, G.X., Allen, G.C., Yamazaki, S., & McMahon, D.G. (**2008**) An autonomous circadian clock in the inner mouse retina regulated by dopamine and GABA. *PLoS Biology*, **6**, 2248–2265.

Ruan, G.-X., Zhang, D.-Q., Zhou, T., Yamazaki, S., & McMahon, D.G. (**2006**) Circadian organization of the mammalian retina. *Proceedings of the National Academy of Sciences of the United States of America*, **103**, 9703–9708.

Sakamoto, K. & Ishida, N. (**1998a**) Circadian expression of serotonin N-acetyltransferase mRNA in the rat retina. *Neuroscience Letters*, **245**, 113–116.

Sakamoto, K. & Ishida, N. (**1998b**) Molecular cloning of serotonin N-acetyltransferase gene from the mouse and its daily expression in the retina. *Neuroscience letters*, **250**, 181–184.

Sakamoto, K., Liu, C., Kasamatsu, M., Iuvone, P.M., & Tosini, G. (**2006**) Intraocular injection of kainic acid does not abolish the circadian rhythm of arylalkylamine N-acetyltransferase mRNA in rat photoreceptors. *Molecular vision*, **12**, 117–124.

Sakamoto, K., Liu, C., Kasamatsu, M., Pozdeyev, N. V., Iuvone, P.M., & Tosini, G. (**2005**) Dopamine regulates melanopsin mRNA expression in intrinsically photosensitive retinal ganglion cells. *European Journal of Neuroscience*, **22**, 3129–3136.

Sakamoto, K., Liu, C., & Tosini, G. (**2004**) Circadian rhythms in the retina of rats with photoreceptor degeneration. *Journal of Neurochemistry*, **90**, 1019–1024.

Sakamoto, K., Oishi, K., Shiraishi, M., Hamano, S., Otsuka, H., Miyake, Y., & Ishida, N. (**2000**) Two circadian oscillatory mechanisms in the mammalian retina. *Neuroreport*, **11**, 3995–3997.

Samples, J., Krause, G., & AJ, L. (**1988**) Effect of melatonin on intraocular pressure. *Current eye research*, **7**, 649–653.

Savaskan, E., Jockers, R., Ayoub, M., Angeloni, D., Fraschini, F., Flammer, J., Eckert, A., Muller-Spahn, F., & Meyer, P. (**2007**) The MT2 melatonin receptor subtype is present in human retina and decreases in Alzheimer's disease. *Current Alzheimer research*, **4**, 47–51.

Savaskan, E., Wirz-Justice, A., Olivieri, G., Pache, M., Kräuchi, K., Brydon, L., Jockers, R., Müller-Spahn, F., & Meyer, P. (**2002**) Distribution of melatonin MT1 receptor immunoreactivity in human retina. *The journal of histochemistry and cytochemistry : official journal of the Histochemistry Society*, **50**, 519–526.

Scher, J., Wankiewicz, E., Brown, G.M., & Fujieda, H. (**2002**) MT(1) melatonin receptor in the human retina: expression and localization. *Investigative ophthalmology & visual science*, **43**, 889–897.

Scher, J., Wankiewicz, E., Brown, G.M., & Fujieda, H. (**2003**) AII amacrine cells express the MT1 melatonin receptor in human and macaque retina. *Experimental Eye Research*, **77**, 375–382.

Schmid-Kubista, K.E., Glittenberg, C.G., Cezanne, M., Holzmann, K., Neumaier-Ammerer, B., & Binder, S. (**2009**) Daytime levels of melatonin in patients with age-related macular degeneration. *Acta ophthalmologica*, **87**, 89–93.

Sengupta, A., Baba, K., Mazzoni, F., Pozdeyev, N. V, Strettoi, E., Iuvone, P.M., & Tosini, G. (**2011**) Localization of melatonin receptor 1 in mouse retina and its role in the circadian regulation of the electroretinogram and dopamine levels. *PloS one*, **6**, e24483.

Serle, J.B., Wang, R.-F., Peterson, W.M., Plourde, R., & Yerxa, B.R. (**2004**) Effect of 5-MCA-NAT, a putative melatonin MT3 receptor agonist, on intraocular pressure in glaucomatous monkey eyes. *Journal of glaucoma*, **13**, 385–388.

Sheng, W.-L., Chen, W.-Y., Yang, X.-L., Zhong, Y.-M., & Weng, S.-J. (**2015**) Co-Expression of Two Subtypes of Melatonin Receptor on Rat M1-Type Intrinsically Photosensitive Retinal Ganglion Cells. *Plos One*, **10**, e0117967.

Silver, R. & Kriegsfeld, L.J. (**2014**) Circadian rhythms have broad implications for understanding brain and behavior. *European Journal of Neuroscience*, **39**, 1866–1880.

Simonneaux, V. (**2011**) Naughty melatonin: how mothers tick off their fetus. *Endocrinology*, **152**, 1734–1738.

Siu, A.W., Reiter, R.J., & To, C.H. (**1999**) Pineal indoleamines and vitamin E reduce nitric oxide-induced lipid peroxidation in rat retinal hoogenates. *Journal of Pineal Research*, **27**, 122–128.

Skene, D.J. & Arendt, J. (**2007**) Circadian rhythm sleep disorders in the blind and their treatment with melatonin. *Sleep Medicine*, **8**, 651–655.

Slaugenhaupt, S.A., Roca, A.L., Liebert, C.B., Altherr, M.R., Gusella, J.F., & Reppert, S.M. (**1995**) Mapping of the gene for the Mel1a melatonin receptor to human chromosome 4 (MTNR1A) and mouse chromosome 8 (Mtnr1a). *Genomics*, **27**, 355–357.

Slominski, A., Pisarchik, A., Semak, I., Sweatman, T., & Wortsman, J. (**2003**) Characterization of the serotoninergic system in the C57BL/6 mouse skin. *European Journal of Biochemistry*, **270**, 3335–3344.

Sompol, P., Liu, X., Baba, K., Paul, K.N., Tosini, G., Iuvone, P.M., & Ye, K. (**2011**) N-acetylserotonin promotes hippocampal neuroprogenitor cell proliferation in sleep-deprived mice. *Proceedings of the National Academy of Sciences of the United States of America*, **108**, 8844–8849.

Stefulj, J., Hörtner, M., Ghosh, M., Schauenstein, K., Rinner, I., Wölfler, a, Semmler, J., & Liebmann, P.M. (**2001**) Gene expression of the key enzymes of melatonin synthesis in extrapineal tissues of the rat. *Journal of pineal research*, **30**, 243–247.

Stehle, J.H., Foulkes, N.S., Molina, C.A., Simonneaux, V., Pévet, P., & Sassone-Corsi, P. (**1993**) Adrenergic signals direct rhythmc expression of transcriptional repressor CREM in the pineal gland. *Nature*, **363**, 314–320.

Stehle, J.H., von Gall, C., Schomerus, C., & Korf, H.W. (**2001**) Of rodents and ungulates and melatonin: creating a uniform code for darkness by different signaling mechanisms. *Journal of biological rhythms*, **16**, 312–325.

Storch, K.-F., Paz, C., Signorovitch, J., Raviola, E., Pawlyk, B., Li, T., & Weitz, C.J. (**2007**) Intrinsic circadian clock of the mammalian retina: importance for retinal processing of visual information. *Cell*, **130**, 730–741.

Strada, S.J., Klein, D.C., Weller, J., & Weiss, B. (**1972**) Effect of norepinephrine on the concentration of adenosine 3',5'-monophosphate of rat pineal gland in organ culture. *Endocrinology*, **90**, 1470–1475.

Strauss, O. (**2005**) The Retinal Pigment Epithelium in Visual Function. *Physiological Reviews*, **85**, 845–881.

Sugawara, T., Sieving, P. a., Iuvone, P.M., & Bush, R. a. (**1998**) The melatonin antagonist luzindole protects retinal photoreceptors from light damage in the rat. *Investigative Ophthalmology and Visual Science*, **39**, 2458–2465.

Sugden, D., Yeh, L.K., & Teh, M.T. (**1999**) Design of subtype selective melatonin receptor agonists and antagonists. *Reproduction, nutrition, development*, **39**, 335–344.

Sugita, Y. & Tasaki, K. (**1988**) The activation of cones in scotopic and rods in photopic vision. *The Tohoku journal of experimental medicine*, **156**, 311–317.

Szél, A. & Rohlich, P. (**1992**) Two Cone Types of Rat Retina Detected by Anti-visual Pigment Antibodies. *Exp.Eye Res.*, **55**, 47–52.

Szel, A., Rohlich, P., Caffe, A.R., Juliusson, B., Aguirre, G., & Van Veen, T. (**1992**) Unique topographic separation of two spectral classes of cones in the mouse retina. *The Journal of comparative neurology*, **325**, 327–342.

Takahashi, J.S., Hong, H.-K., Ko, C.H., & McDearmon, E.L. (**2008**) The genetics of mammalian circadian order and disorder: implications for physiology and disease. *Nature reviews genetics*, **9**, 764–775.

Teirstein, P.S., Goldman, A.I., & Brien, O. (**1980**) Evidence for both local and central Regulation of Rat Rod Outer Segment Disc Shedding. *Investigative ophthalmology & visual science*, **19**, 1268–1273.

Tetsuo, M., Markey, S.P., & Kopin, I.J. (**1980**) Measurement of 6-hydroxymelatonin in human urine and its diurnal variations. *Life Sciences*, **27**, 105–109.

The AMD Gene Consortium (**2013**) Seven New Loci Associated with Age-Related Macular Degeneration. *Nature Genetics*, **45**, 433–439e2.

Tosini, G., Baba, K., Hwang, C.K., & Iuvone, P.M. (**2012**) Melatonin: An underappreciated player in retinal physiology and pathophysiology. *Experimental eye research*, 1–8.

Tosini, G., Chaurasia, S.S., & Michael Iuvone, P. (**2006**) Regulation of arylalkylamine N-acetyltransferase (AANAT) in the retina. *Chronobiology international*, **23**, 381–391.

Tosini, G. & Dirden, J.C. (**2000**) Dopamine inhibits melatonin release in the mammalian retina: In vitro evidence. *Neuroscience Letters*, **286**, 119–122.

Tosini, G. & Fukuhara, C. (**2003**) Photic and circadian regulation of retinal melatonin in mammals. *Journal of neuroendocrinology*, **15**, 364–369.

Tosini, G. & Menaker, M. (**1996**) Circadian rhythms in cultured mammalian retina. *Science (New York, N.Y.)*, **272**, 419–421.

Tosini, G. & Menaker, M. (**1998**) The clock in the mouse retina: melatonin synthesis and photoreceptor degeneration. *Brain research*, **789**, 221–228.

Tosini, G., Owino, S., Guillaume, J.L., & Jockers, R. (**2014**) Understanding melatonin receptor pharmacology: Latest insights from mouse models, and their relevance to human disease. *BioEssays*, **36**, 778–787.

Tosini, G., Pozdeyev, N., Sakamoto, K., & Iuvone, P.M. (**2008**) The circadian clock system in the mammalian retina. *BioEssays : news and reviews in molecular, cellular and developmental biology*, **30**, 624–633.

Tzavara, E.T.H., Pouille, Y., Defer, N., & Hanoune, J. (**1996**) Diurnal variation of the Adenylyl Cyclase Type 1 in the rat pineal gland. *Proceedings of the National Academy of Sciences of the United States of America Natl. Acad. Sci*, **93**, 11208–11212.

Uz, T. & Manev, H. (**1999**) Chronic fluoxetine administration increases the serotonin N-acetyltransferase messenger RNA content in rat hippocampus. *Biological Psychiatry*, **45**, 175–179.

Uz, T., Qu, T., Sugaya, K., & Manev, H. (**2002**) Neuronal expression of arylalkylamine N-acetyltransferase (AANAT) mRNA in the rat brain. *Neuroscience Research*, **42**, 309–316.

Valdez, D.J., Garbarino-Pico, E., Díaz, N.M., Silvestre, D.C., & Guido, M.E. (**2012**) Differential regulation of arylalkylamine N-acetyltransferase activity in chicken retinal ganglion cells by light and circadian clock. *Chronobiology international*, **29**, 1011–1020.

Van Hook, M.J., Wong, K.Y., & Berson, D.M. (**2012**) Dopaminergic modulation of ganglion-cell photoreceptors. *European Journal of Neuroscience*, **35**, 507–518.

Van Oosterhout, F., Fisher, S.P., Van Diepen, H.C., Watson, T.S., Houben, T., Vanderleest, H.T., Thompson, S., Peirson, S.N., Foster, R.G., & Meijer, J.H. (**2012**) Ultraviolet light provides a major input to non-image-forming light detection in mice. *Current Biology*, **22**, 1397–1402.

Vanecek, J. (**1998**) Cellular mechanisms of melatonin action. *Physiological reviews*, **78**, 687–721.

Vanecek, J., Sugden, D., Weller, J., & Klein, D.C. (**1985**) Atypical synergistic alpha 1- and beta-adrenergic regulation of adenosine 3',5'-monophosphate and guanosine 3',5'-monophosphate in rat pinealocytes. *Endocrinology*, **116**, 2167–2173.

Vaughan, G.M. & Reiter, R.J. (**1986**) Pineal dependence of the Syrian hamster's nocturnal serum melatonin surge. *Journal of pineal research*, **3**, 9–14.

Vella, F., Ferry, G., Delagrange, P., & Boutin, J. a. (**2005**) NRH:quinone reductase 2: An enzyme of surprises and mysteries. *Biochemical Pharmacology*, **71**, 1–12.

Verhagen, L.A.W., Pévet, P., Saboureau, M., Sicard, B., Nesme, B., Claustrat, B., Buijs, R.M., & Kalsbeek, A. (**2004**) Temporal organization of the 24-h corticosterone rhythm in the diurnal murid rodent Arvicanthis ansorgei Thomas 1910. *Brain Research*, **995**, 197–204.

Vijayalaxmi, Reiter, R.J., Tan, D.X., Herman, T.S., & Thomas, C.R. (**2004**) Melatonin as a radioprotective agent: A review. *International Journal of Radiation Oncology Biology Physics*, **59**, 639–653.

Vivien-Roels, B., Malan, a., Rettori, M.-C., Delagrange, P., Jeanniot, J.-P., & Pevet, P. (**1998**) Daily Variations in Pineal Melatonin Concentrations in Inbred and Outbred Mice. *Journal of Biological Rhythms*, **13**, 403–409.

Voisin, P., Cailleau, V., Naud, N., Cantereau, a, & Bernard, M. (**2012**) Visual photoreceptor subtypes in the chicken retina: melatonin-synthesizing activity and in vitro differentiation. *Cell and tissue research*, **348**, 417–427.

Voisin, P., Guerlotté, J., Bernard, M., Collin, J.-P., & Cogné, M. (**1992**) Molecular cloning and nucleotide sequence of a cDNA encoding hydroxyindole O-methyltransferase from chicken pineal gland. *Biochemical journal*, **282**, 571–576.

Völgyi, B., Kovács-öller, T., Atlasz, T., Wilhelm, M., & Gábriel, R. (**2013**) Gap junctional coupling in the vertebrate retina: Variations on one theme? *Progress in Retinal and Eye Research*, **34**, 1–18.

Völgyi, B., Pan, F., Paul, D.L., Wang, J.T., Huberman, A.D., & Bloomfield, S. a. (**2013**) Gap Junctions Are Essential for Generating the Correlated Spike Activity of Neighboring Retinal Ganglion Cells. *PLoS ONE*, **8**, e69426.

Von Gall, C., Garabette, M.L., Kell, C. a, Frenzel, S., Dehghani, F., Schumm-Draeger, P.-M., Weaver, D.R., Korf, H.-W., Hastings, M.H., & Stehle, J.H. (**2002**) Rhythmic gene expression in pituitary depends on heterologous sensitization by the neurohormone melatonin. *Nature neuroscience*, **5**, 234–238.

Von Schantz, M., Lucas, R.J., & Foster, R.G. (**1999**) Circadian oscillation of photopigment transcript levels in the mouse retina. *Molecular Brain Research*, **72**, 108–114.

Waldhauser, F., Waldhauser, M., Lieberman, H.R., Deng, M.-H., Lynch, H.J., & Wurtman, R.J. (**1984**) Bioavailability of oral melatonin in humans. *Neuroendocrinology*, **39**, 307–313.

Weinert, D., Weinandy, R., & Gattermann, R. (**2007**) Photic and non-photic effects on the daily activity pattern of Mongolian gerbils. *Physiology and Behavior*, **90**, 325–333.

White, B.H., Sekura, R.D., & Rollag, M.D. (**1987**) Pertussis toxin blocks melatonin-induced pigment aggregation in Xenopus dermal melanophores. *Journal of comparative physiology. B, Biochemical, systemic, and environmental physiology*, **157**, 153–159.

White, M.P. & Fisher, L.J. (**1989**) Effects of exogenous melatonin on circadian disc shedding in the albino rat retina. *Vision research*, **29**, 167–179.

Wiechmann, A.F. (**1986**) Melatonin: parallels in pineal gland and retina. *Experimental eye research*, **42**, 507–527.

Wiechmann, A.F., Bok, D., & Horwitz, J. (**1985**) Localization of hydroxyindole-O-methyltransferase in the mammalian pineal gland and retina. *Investigative Ophthalmology and Visual Science*, **26**, 253–265.

Wiechmann, A.F. & Craft, C.M. (**1993**) Localization of mRNA encoding the indolamine synthesizing enzyme, hydroxyindole-O-methyltransferase, in chicken pineal gland and retina by in situ hybridization. *Neuroscience Letters*, **150**, 207–211.

Wiechmann, A.F. & O'Steen, W.K. (**1992**) Melatonin increases photoreceptor susceptibility to light-induced damage. *Investigative*

Ophthalmology and Visual Science, **33**, 1894–1902.

Wiechmann, A.F. & Sherry, D.M. (**2013**) *Role of Melatonin and Its Receptors in the Vertebrate Retina.*, International review of cell and molecular biology. Elsevier.

Wiechmann, A.F. & Smith, A.R. (**2001**) Melatonin receptor RNA is expressed in photoreceptors and displays a diurnal rhythm in Xenopus retina. *Molecular Brain Research*, **91**, 104–111.

Wiechmann, A.F., Udin, S.B., & Summers Rada, J. a (**2004**) Localization of Mel1b melatonin receptor-like immunoreactivity in ocular tissues of Xenopus laevis. *Experimental eye research*, **79**, 585–594.

Wiechmann, A.F., Vrieze, M.J., Dighe, R., & Hu, Y. (**2003**) Direct modulation of rod photoreceptor responsiveness through a Mel 1c melatonin receptor in transgenic Xenopus laevis retina. *Investigative Ophthalmology and Visual Science*, **44**, 4522–4531.

Wiechmann, A.F. & Wirsig-Wiechmann, C.R. (**2001**) Melatonin receptor mRNA and protein expression in Xenopus laevis nonpigmented ciliary epithelial cells. *Experimental eye research*, **73**, 617–623.

Witkovsky, P. (**2004**) Dopamine and retinal function. *Documenta Ophthalmologica*, **108**, 17–40.

Wong, W.L., Su, X., Li, X., Cheung, C.M.G., Klein, R., Cheng, C.Y., & Wong, T.Y. (**2014**) Global prevalence of age-related macular degeneration and disease burden projection for 2020 and 2040: A systematic review and meta-analysis. *The Lancet Global Health*, **2**, e106–e116.

Wulle, I., Kirsch, M., & Wagner, H.J. (**1990**) Cyclic changes in dopamine and DOPAC content, and tyrosine hydroxylase activity in the retina of a cichlid fish. *Brain research*, **515**, 163–167.

Xiang, M., Zhou, L., Peng, Y.W., Eddy, R.L., Shows, T.B., & Nathans, J. (**1993**) Brn-3b: a POU domain gene expressed in a subset of retinal ganglion cells. *Neuron*, **11**, 689–701.

Yamajuku, D., Shibata, Y., Kitazawa, M., Katakura, T., Urata, H., Kojima, T., Takayasu, S., Nakata, O., & Hashimoto, S. (**2011**) Cellular DBP and E4BP4 proteins are critical for determining the period length of the circadian oscillator. *FEBS Letters*, **585**, 2217–2222.

Yi, C., Pan, X., Yan, H., Guo, M., & Pierpaoli, W. (**2005**) Effects of melatonin in age-related macular degeneration. *Annals of the New York Academy of Sciences*, **1057**, 384–392.

Yoo, S.-H., Ko, C.H., Lowrey, P.L., Buhr, E.D., Song, E., Chang, S., Yoo, O.J., Yamazaki, S., Lee, C., & Takahashi, J.S. (2005) A noncanonical E-box enhancer drives mouse Period2 circadian oscillations in vivo. *Proceedings of the National Academy of Sciences of the United States of America*, **102**, 2608–2613.

Yoshimura, T., Nagabukuro, A., Matsuda, Y., Suzuki, T., Kuroiwa, A., Iigo, M., Namikawa, T., & Ebihara, S. (**1997**) Chromosomal mapping of the gene encoding serotonin N-acetyltransferase to rat chromosome 10q32.3 and mouse chromosome 11E2. *Cytogenetics and cell genetics*, **79**, 172–175.

Young, I.M., Leone, R.M., Francis, P., Stovell, P., & Silman, R.E. (**1985**) Melatonin is metabolized to N-acetyl serotonin and 6-hydroxymelatonin in man. *Journal of Clinical Endocrinology and Metabolism*, **60**, 114–119.

Yu, H.S., Pang, S.F., & Tang, P.L. (**1981**) Increase in the level of retinal melatonin and persistence of its diurnal rhythm in rats after pinealectomy. *Journal of Endocrinology*, **91**, 477–481.

Zawilska, J.B. & Iuvone, P.M. (**1992**) Melatonin synthesis in chicken retina: effect of kainic acid-induced lesions on the diurnal rhythm and D2-dopamine receptor-mediated regulation of serotonin N-acetyltransferase activity. *Neuroscience letters*, **135**, 71–74.

Zhao, W., Zhang, M., Miao, Y., Yang, X., & Wang, Z. (**2010**) Melatonin potentiates glycine currents through a PLC / PKC signalling pathway in rat retinal ganglion cells. *The Journal of physiology*, **588**, 2605–2619.

Zheng, W., Schwarzer, D., LeBeau, A., Weller, J.L., Klein, D.C., & Cole, P. a. (**2005**) Cellular stability of serotonin N-acetyltransferase conferred by phosphonodifluoromethylene alanine (Pfa) substitution for Ser-205. *Journal of Biological Chemistry*, **280**, 10462–10467.

Zheng, W., Zhang, Z., Ganguly, S., Weller, J.L., Klein, D.C., & Cole, P. a (**2003**) Cellular stabilization of the melatonin rhythm enzyme induced by nonhydrolyzable phosphonate incorporation. *Nature structural biology*, **10**, 1054–1057.

Coralie GIANESINI

Synthesis and role of melatonin in the retina of rodents

Résumé

La mélatonine, hormone "donneuse de temps de l'organisme", en plus de sa synthèse principale dans la glande pinéale est produite dans la rétine où sa régulation et ses fonctions restent partiellement connues chez les mammifères. **Le but de mon projet a été de caractériser l'expression temporelle et spatiale de la mélatonine et d'examiner son rôle potentiel dans la physiopathologie rétinienne.** Une première partie a révélé au moins deux sites de production de la mélatonine dans la rétine : une synthèse nocturne de l'hormone dans les photorécepteurs de type cône ainsi qu'une production diurne dans les cellules ganglionnaires. Nos résultats ont démontré que la mélatonine peut agir par l'intermédiaire de son récepteur nommé MT_1, localisés dans chacune des trois couches rétiniennes. Une seconde partie a mis en évidence que la mélatonine augmente la survie des photorécepteurs chez les rongeurs âgés en modulant l'activation de la voie de survie cellulaire via ses récepteurs MT_1 et MT_2.

Mots clefs

Mélatonine, rétine, photorécepteur, cône, rongeur, diurne.

Summary

Melatonin, a major hormonal "Zeitgeber" in the body, is produced in the pineal gland as well as the retina. In mammals its regulation and functions in this tissue are only partially understood. **The aim of my project was to characterize the temporal and spatial expressions of melatonin as well as its potential roles in retinal physiopathology.** In the first part**,** we identified the timing and sites of melatonin production. Notably, nocturnal synthesis occurs in the cones while diurnal production is seen in the ganglion cells. Our work also establishes that melatonin can act via its MT_1-type receptors localized in the three retinal nuclear layers. The second axis demonstrated that melatonin increases photoreceptors viability via its receptors during the course of aging by modulating activation of an intracellular survival pathway.

Keywords

Melatonin, retina, photoreceptor, cone, rodent, diurnal.